# Environmental variability and energetic adaptability of the great scallop, *Pecten maximus*, facing climate change

Promotors: Dr. F. Jean
Pr. S.A.L.M. Kooijman
Dr. Ø. Strand
Co-promotor: Dr. J. Flye-Sainte-Marie

The research presented in this thesis was carried out at the Laboratory of Marine Environmental Sciences, University of Western Brittany (Plouzané, France), at the Department of Theoretical Biology, Vrije Universiteit Amsterdam (The Netherlands) and at the Institute of Marine Research (Bergen, Norway).

# Contents

# Chapter 1

# Introduction

## 1.1 Linkage between environment and organisms

The relationship between environmental conditions and life history have intrigued biologists for centuries. Individuals can present strong differences in the variability of life-history traits, which can be attributed either to external factors, such as the environment they are living in, or to internal factors, i.e. their genetic background. It is, in fact, a combination of the two, interacting to produce a phenotype, which determines the observed life traits patterns. Phenotype is, thus, the result of a dynamic equilibrium between environmental and intrinsic forcing.

The study of life history traits along environmental gradients has received increased interest in the last decades (Angilletta et al., 2004). First, because the description of biological patterns at a large geographical scale allows one to deal with both ecological theories (through hypotheses explaining the interaction between life traits and environmental parameters) and evolutionary concepts (plasticity, adaptation, speciation), which should contribute to the integration of our knowledge in these two disciplines (Peters, 1986). Furthermore we still find difficulties in explaining how environment can drive the physiology of organisms (Schmidt-Nielsen, 1997; Clarke, 2003). Except for temperature which effect on metabolic rates is rather described and accepted (Kooijman, 2010), part of the mystery remains in many other interactions: the understanding of evolutionary temperature adaptation (Clarke, 2003), the extremely extended lifespan of few species in bleak environments (Ropes and Murawski, 1983), the body size and temperature relationship (Thiel et al., 1996; Angilletta et al., 2004), light influence on biological cycles (Pittendrigh, 1993).

Latitudinal, bathymetric, and any other physico-chemical gradients may induce physiological changes within species. The description and understanding of physiological and metabolic processes leading to variable life-history traits is crucial to better understanding inter-individual variability in the physiological response of organisms to changing conditions. Several terms are used to

describe the various levels of differentiation within species, ranging from phenotypic flexibility (reversible plasticity within individuals; Piersma and Drent, 2003), phenotypic plasticity (capacity of a single genotype to exhibit variable phenotypes in different environments; Whitman and Agrawal, 2009), local individual adaptation (genetic mechanisms allowing an individual to overcome an environmental constraint) to population adaptation (West-Eberhard, 2003) and speciation. These different steps in adaptation are driven by natural selection, in response to environmental conditions. The dynamic equilibrium between biotic and abiotic factors of the environment and the physiological response of individuals might be understood through intra-specific comparisons under different conditions to establish the phenotypic range of responses (Bayne et al., 1983; Calow, 1983).

In this context, the present work focuses on the environmental forcing on life history of a species that lives in contrasting conditions: the great scallop, *Pecten maximus*. The description of the energy fluxes within individuals is used as a mean to investigate the complex linkages between the organism and its surroundings. A particular attention is paid to feeding, which is a crucial biological function in dynamic ecosystems. A combination of modeling tools and environmental monitoring will be used to study the tight relationship between life history traits and the environment.

## 1.2 The great scallop, *Pecten maximus*

### 1.2.1 Ecology

The great scallop (also named king scallop), *Pecten maximus* (Linnaeus, 1758), is a molluscan bivalve species of the Pectinid family. In 2011, 63 702 t were harvested worldwide and it is a particularly economically important species in the UK, France and Spain, where it is considered as a high value product (Brand, 2006b). The exploitation of this species mainly relies on dredge fishing and to a lesser extent on diving collection, sea ranching and aquaculture which benefited from developments in Norway, Scotland and also in France (Norman et al., 2006; Strand and Parsons, 2006).

Its distribution, although limited to the North-East Atlantic, covers a wide range of latitudes and depths (Fig. 1.1). It is observed from northern Norway (Lofoten Islands) south to the Iberian Peninsula (Tebble, 1966; Høisæter, 1986). The species has also been reported as far south as Canary Islands, off Africa's west coast, and at the entry of Mediterranean sea (Bellon-Humbert, 1972; Mason, 1983; Ansell et al., 1991; Peña, 2001), where it encroaches upon *P. jacobeus*' (Linnaeus, 1758) distribution range. It can be found from just below the water mark in coastal waters to the edge of the continental shelf, which corresponds to a depth gradient of about 200 m (Antoine, 1979; Brand, 2006a). *P. maximus* lives in shallow depressions on the seabed consisting of firm sand, shell sand, fine or sandy gravel, sometimes with an admixture of

mud (Brand, 2006a and references therein). The oldest individual ever reported was 20 years old (Tang, 1941) and the biggest one reached a size of 23 cm (A. Jolivet, pers. comm., individual belonging to the EVECOS data collection maintained by "Observatoire Marin de l'IUEM, INSU, Plouzané").

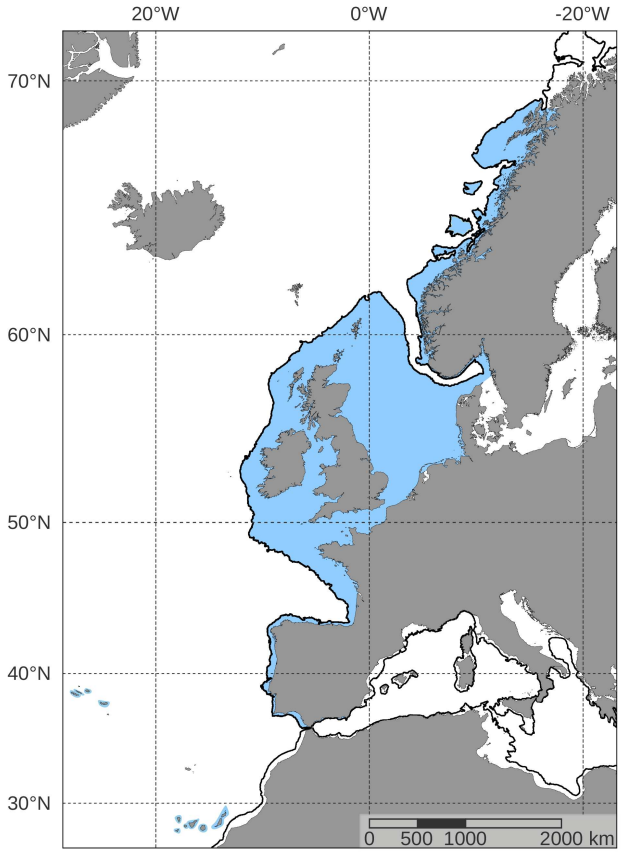


**Figure 1.1:** Distribution map of *P. maximus* (blue area). The edge of the continental shelf (200 m) is represented by the dark line. Combined sources: FAO, Mason (1983) and Brand (2006a).

### 1.2.2 Life cycle

*P. maximus* has a meroplanktonic life cycle (Fig. 1.2), which means that part of its development takes place in the water column while the rest of its life is spent on the sea floor (Le Pennec et al., 2003). Eggs hatch after two days of development and larvae have a pelagic life that last between 24 and 32 days (Gruffydd and Beaumont, 1972; Samain et al., 1986; Casse, 1995),

depending on temperature and food availability conditions. Then the larva sinks and settles on the sediment where it fixes to complete its metamorphosis (Buestel et al., 1982; Paulet et al., 1988; Le Pennec et al., 2003). This event consists of a major reorganization of all the tissues that will allow the young scallop to shift to a benthic life. The animal is transformed into a post-larva that will complete the development of its newly organized body while fixed to the substrate. The juvenile scallop then looks like a small adult and pursues its development for approximately one year. The reproductive activity of the great scallop starts during the second year (Tang, 1941; Mason, 1958). Maturity may be maintained almost all life along with a probable decrease in gamete production and release in older age-classes, like in other bivalve species (Vahl, 1985; Bricelj and Krause, 1992; Walker and Heffernan, 1996), which is likely due to disease/parasites (Ø. Strand pers. comm.). *P. maximus* is an asynchronous hermaphrodite spawner releasing between 4 and 20 billion spermatozoa and from 3 to 80 million oocytes in each spawning event (Paulet and Fifas, 1989; Paulet et al., 1997; Andersen et al., 2011; Suquet et al., 2012). There is considerable variation in the reproductive cycle of this species (Mason, 1958; Comely, 1974; Lubet et al., 1987; Paulet et al., 1988; Strand and Nylund, 1991; Mackie and Ansell, 1993; Hold et al., 2013). Both external (temperature, food density, photoperiod, etc.) and internal (genetic) factors seem to be controlling certain features of the reproductive activity (Brand, 2006a). Even at a regional scale major discrepancies in the spawning strategy (number of spawnings, onset of gametogenesis) are observed (Paulet et al., 1988, 1995).

### 1.2.3 Feeding

Scallops are suspension-feeding organisms. They use their ctenidium (gill), composed of hundreds of narrow filaments, to mechanically sieve surrounding water from which nutrient rich micro-particles are retained while non elusive material is expelled as pseudo-faeces. The epithelium of the gill filaments is covered with three types of ciliary tracts: (1) frontal tracts on the outer surface of the filaments which cilia generate a water current, measured as the filtration (or clearance) rate; (2) lateral tracts on the surfaces facing other filaments which cilia move food particles (trapped in mucus) anteriorly to the mouth; (3) laterofrontal tracts, located across the entrance to interfilamentary spaces, are sometimes attributed a particular role in particle selection (Møhlenberg and Riisgård, 1978; Shumway et al., 1985; Ward et al., 1998; Ward and Shumway, 2004; MacDonald et al., 2006; Ward and Kach, 2009). Trapped and rubbed into mucus strings produced by mucocystes (Dufour and Beninger, 2001), food particles are then transported to the aboral side of the gills where labial palps, acting as a conveyor belt, sort and reject or bring food pellets to the mouth for ingestion. In *P. maximus* the filtration efficiency is typically low for a particle size under 5 µm (Møhlenberg and Riisgård, 1978; MacDonald et al., 2006). Pico- and nano-particles (under this threshold of 5 µm) may be ingested when aggregated or stuck on bigger ones (Ward and

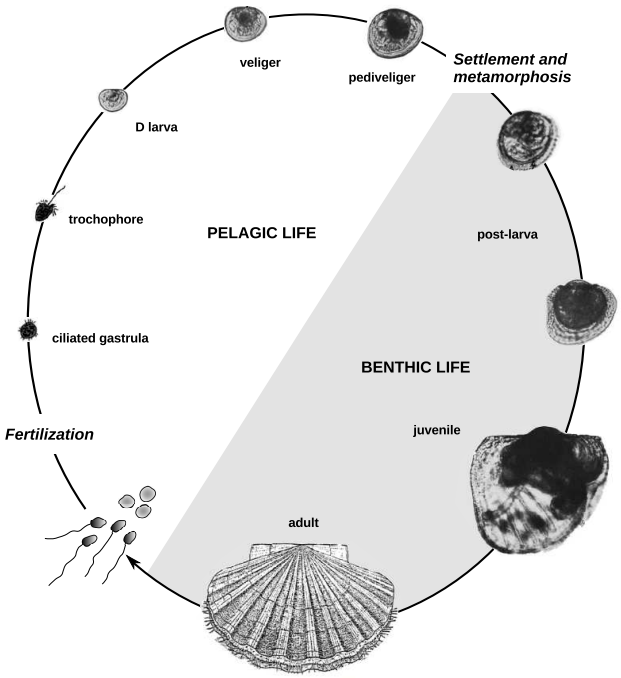


**Figure 1.2:** Biological cycle of *P. maximus*, modified from Le Pennec et al. (2003).

Shumway, 2004). Suspensivorous bivalves are known to feed upon various trophic sources including pelagic phytoplankton, microphytobenthos, detrital material, nanoplankton, bacteria, zooplankton and macro-algae detritus (see e.g. Heral, 1989; Langdon and Newell, 1990; Kamermans, 1994; Alber and Valiela, 1996; Chauvaud et al., 2001; MacDonald et al., 2006; Bachok et al., 2009; Yokoyama et al., 2009; Cranford et al., 2011; Nerot et al., 2012). They are subsequently able to develop a plastic trophic niche, variable in space and time as an adaptation/acclimation to the available trophic resources and depending on their developmental stage (Rossi et al., 2004; Marín Leal et al., 2008). Finally, great scallops, as other bivalves, are able to select and sort incoming particles in order to retain the more edible and essential nutrients (Møhlenberg and Riisgård, 1978; Stuart and Klumpp, 1984; Shumway et al., 1985; Ward et al., 1997; Bacon et al., 1998; Levinton et al., 2002; Beninger et al., 2004; Ward and Shumway, 2004; MacDonald et al., 2006; Ward and Kach, 2009). Three levels of sorting have been described and rely on size, chemotactism and electrical charge criteria (Rubenstein and Koehl, 1977; Jørgensen, 1983; LaBarbera, 1984; Silvester and Sleigh, 1984; Espinosa et al., 2010; Rosa et al., 2013). Filtration selectivity is the first step of food particle sorting, which depends mainly on the particle size when sieved by the gill (Riisgård, 2001; Strohmeier et al., 2012). Moreover, the role of ctenidial filaments (ciliated structures of the gill) in particle sorting has been shown in oysters (Ward et al., 1998). The second site of pre-ingestive selection is the labial palps, where non-nutritive particles are rejected as pseudo-faeces prior to ingestion (Ward and Shumway, 2004). A differential utilization of various algal species has been reported to be achieved by labial palps (Peirson, 1983; Ward et al., 1998; Beninger et al., 2004). Finally, an intern sorting has been reported inside the digestive gland (Cucci et al., 1985; Shumway et al., 1985; MacDonald et al., 2006), where differential digestion and assimilation of food passing through the gut is known. In *P. maximus*, as in some other Pectinids, the gonad is traversed by an intestinal loop (Le Pennec et al., 2003). Ultrastructural studies have showed a transfer of metabolites from the intestine epithelial cells to the surrounding gonadal tissue (Beninger et al., 2003; Le Pennec et al., 2003).

### 1.2.4 Genetics

Previous work about the genetic structuration of *P. maximus* populations are rather controversial, varying according to the method used and the populations studied. On one hand, the investigation of polymorphic allozyme loci of scallops from the UK and France did not demonstrate the existence of sub-populations between these locations (Beaumont et al., 1993; Wilding et al., 1998). On the other hand, the use of RFLP (Restriction Fragment Length Polymorphism) and RAPDs (Random Amplified Polymorphic DNA) techniques on mitochondrial DNA markers revealed a genetic isolation of the Mulroy Bay population in Ireland (Wilding et al., 1997; Heipel et al., 1998).

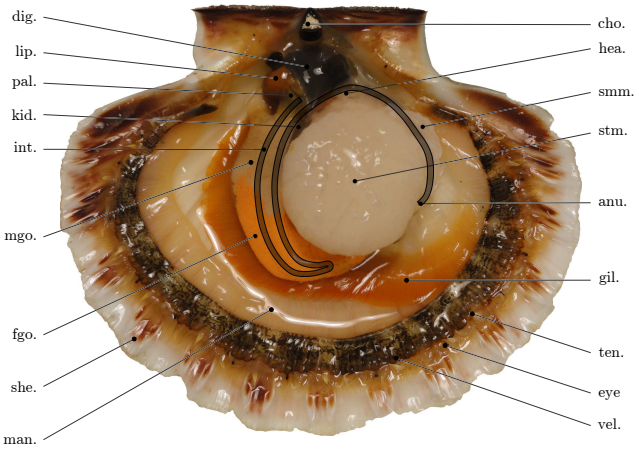


**Figure 1.3:** Photograph of the anatomy of the great scallop with left shell valve, left mantle fold and left gill removed. *anu.*: anus; *cho.*: chondrophore (ligament); *dig.*: digestive gland; *fgo.*: female gonad; *gil.*: gill (right fold); *hea.*: heart; *int.*: intestine (not seen, drawn); *kid.*: kidney; *lip.*: lips; *pal.*: labial palps; *man.*: mantle (right fold); *mgo.*: male gonad; *she.*: shell (right valve); *smm.*: smooth adductor muscle; *ten.*: sensory tentacle; *stm.*: striated adductor muscle; *vel.*: velum.

Moreover, it seems that the study of haplotype frequencies would set the Norwegian populations apart from the rest of Europe (Beaumont, 2006). Studies are being carried out on neutral markers (micro-satellites) at the distribution range scale. As these genetic markers are not subject to any selection pressure, they might help to clarify the current knowledge on the presence or absence of differentiated populations within the species.

### 1.2.5 Sclerochronology

The shell of mollusks is formed by the precipitation of calcium carbonate present in the surrounding environment. The calcification of carbonated skeletons is a sequential and discontinuous mechanism. Growth increment width rely on the variation of carbonate accretion rate. During winter, *P. maximus* experiences a reduction of growth close to a cessation (Mason, 1957) that results in the impression of a thick easily identifiable ring, which can be used to estimate the age of the animal. As in other organisms (Neville, 1967), the growth rhythm of the great scallop's shell follows a circadian cycle that induces the formation of daily micro-striae (Clark, 1968; Antoine, 1978; Chauvaud et al., 1998; Clark, 2005). This phenomenon has been extensively studied: incremental width is mainly controlled by temperature (Chauvaud et al., 1998) and food conditions (Chauvaud et al., 1998; Laing, 2000) but rapid changes

of growth rate have also been suspected to be caused by salinity variations (Laing, 2002) and algae blooms (Chauvaud et al., 1998; Lorrain et al., 2000; Liu et al., 2008). The daily periodicity of growth has been exploited to use the shell as a biological archive for many different purposes including physiology (Lorrain et al., 2000), paleoclimate reconstructions through sclerochronology (Chauvaud et al., 2005), the study of growth influencing factors (Chauvaud et al., 1998; Laing, 2000, 2002) and elemental concentrations investigation (Barats et al., 2008a,b, 2009; Thébault and Chauvaud, 2013).

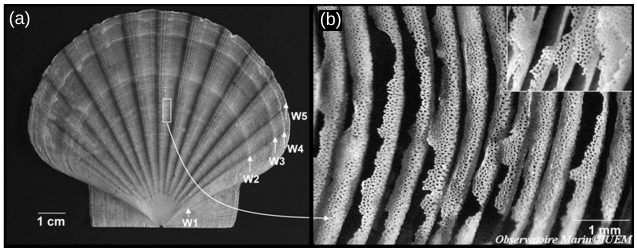


**Figure 1.4:** Upper surface of the left valve of *P. maximus* shell. "Winter marks" (W1 to W5) deposited during spring growth restart are macroscopically visible in all individuals, allowing an unambiguous aging. (b) In this species, daily growth increments can be observed without any treatment aside from surface cleaning. Modified from Chauvaud et al. (2005).

## 1.3 Environmental variability and climate change

Due to its broad distribution range, the great scallop lives in very contrasting environments: Norwegian waters are cold and oligotrophic with a high variability in food availability (Erga, 1989; Strand and Brynjeldsen, 2003; Aure et al., 2007; Strohmeier, 2009). Warmer waters of the English Channel provide large amount of food and other particulate organic matter (POM). Finally, in the cold deep waters of the continental shelf, environmental condition are very stable (less than one degree of thermal amplitude throughout the year; Lazure et al., 2009) and food availability only rely on sedimentation from upper water layers (McCave, 1975; Oliver, 1979; Allen, 1983). Therefore, understanding of the variability in life-history patterns of *P. maximus* requires a good knowledge of its environment. Coastal temperate environments are interface zones where seasonal variations can be more important than in deep waters in terms of hydrological and productivity parameters (Bunt, 1975). This may allow for a greater diversity of physiological patterns between populations (MacDonald et al., 2006; Patry, 2009; Nerot et al., 2012).

In the past decades, many concerns and questions have been raised by the consequences of climate change on marine communities. The latest report from the International Panel on Climate Change (IPCC, 2013) confirms the

impacts of increasing amount of carbon dioxide ($CO_2$) in the atmosphere. Four scenarios of prediction have been reported, which all converge to a more or less important rise in surface and sub-surface oceanic temperatures within the century. The modification of physico-chemical parameters in marine ecosystems leads to biological responses which can vary at various spatiotemporal scales (Lett et al., 2010; Lefort et al., 2013; Woodin et al., 2013). Temperature has a fundamental impact on all physiological processes as it influences essential metabolic activities such as enzymatic reactions and cell membrane permeability (Hochachka and Somero, 2002). It has also been shown that the ability to acclimatize to changing thermal conditions was greatest among species exposed to moderately variable environments (Tomanek, 2010). As *P. maximus* lives in very contrasting environments, one could ask how southern populations would respond to these changes compared to northern ones (Artigaud et al., subm.).

At the base of marine food webs sits the primary production, mainly relying on phytoplankton. In coastal environments terrestrial inputs can contribute significantly to this production. Temperature, together with light and nutrient availability, controls phytoplankton development, which afterwards sustains superior trophic levels. As seawater temperature will increase, the temporal dynamics of phytoplankton is very likely to change (Polovina et al., 2008; Doney et al., 2009). While this might be profitable to consumer growth it should also have critical drawbacks. Indeed, phytoplankton dynamics are characterized by extremely fast events of biomass explosion and brutal collapsing of the community. Many studies have pointed out the tight relationship and synchronism of bivalve reproduction with environmental variables (Olive et al., 1990; Lawrence and Soame, 2004; Toupoint et al., 2012), often described by the theory of match/mismatch (Cushing, 1990). Thus, newly born larvae have to hatch when trophic conditions are suitable to have a chance of survival (Paulet et al., 1988). While some studies have predicted an enhancement of recruitment with increasing temperatures (Shephard et al., 2010), the modification of seston quality and seasonality could dramatically alter *P. maximus* recruitment (Thouzeau, 1991).

With increasing uptake of carbon from the atmosphere, the chemical equilibrium of oceans also tends towards the formation of carbonic acid, leading to an acidification of seawater (Caldeira and Wickett, 2003). Several experimental studies conducted over the last decade have shown negative (yet variable) effects of ocean acidification, especially on calcifying organisms (Fabry et al., 2008; Doney et al., 2009; Kroeker et al., 2010). Most studies have shown decrease in survival, shell growth, normal larval development (Gazeau et al., 2011; Andersen et al., 2013), on shell thickness and strength (Chaparro et al., 2009; Gaylord et al., 2011; Welladsen et al., 2010) and calcification/dissolution equilibrium (Fabry et al., 2008; Ries et al., 2009).

Finally, climate change may eventually increase ecosystem natural variability, disturbing even more the response of organisms to changing environments.

## 1.4 Bioenergetics

### 1.4.1 Environmental effect on metabolism

Metabolism is defined as all the biological processes implied in the use or production of energy, provided by resources from the environment. Organisms convert them into other forms within their bodies, allocate them to the fitness-enhancing processes of survival, growth, and reproduction, and excrete altered forms back into the environment. Energy allocation is a complex result of all these metabolic requirements, which is to be considered as a dynamic process. Indeed, organisms are open thermodynamic systems that develop through interactions with their environment. The study of the influence of environmental factors (mainly temperature, food availability) on energy flow and allocation of energy within individuals is crucial to better understand observed life history traits and particular features within a species. In the Pectinidae family, growth and reproductive cycles have long been studied owing to their importance for fisheries management and aquaculture developments (Thompson and MacDonald, 2006). The mechanisms behind observed patterns in growth and reproduction in *P. maximus* are subject to many hypotheses (Comely, 1974; Strand and Nylund, 1991; Pazos et al., 1997; Chauvaud et al., 1998; Lorrain et al., 2002; Paulet et al., 2006; Guarini et al., 2011) which have not been fully validated. Bioenergetics study have also improved the comprehension of *P. maximus* physiology (Comely, 1974; Pazos et al., 1997; Strohmeier et al., 2000; Lorrain et al., 2002; Paulet et al., 2006). Basically, energy stored as glycogen in the adductor muscle and principally as lipids in the digestive gland during spring and summer is used to sustain reproductive effort and maintenance during winter (López-Benito, 1956; Comely, 1974; Lucas, 1993; Soudant et al., 1996; Pazos et al., 1997; Saout, 2000; Strohmeier et al., 2000; Lorrain et al., 2002; Paulet et al., 2006). In spring and summer, somatic and reproductive production are directly fueled by the abundant food. From November to April, energy transfers from somatic to reproductive tissues have been described. From April to May, a transitory period occurs, with simultaneous production of somatic and reproductive tissues mainly relying on food. From June to October, major energetic fluxes originating from food are used for reserve building (Paulet et al., 1988; Saout et al., 1999; Saout, 2000; Strohmeier et al., 2000; Lorrain et al., 2002; Paulet et al., 2006).

### 1.4.2 Modeling of bivalve bioenergetics

Modeling is a useful approach for the comprehension and the description of mechanisms and rules behind these energy exchanges. Bioenergetic models are developed to define the energy balance relationship between the amount of food consumed by an organism and its use in somatic growth, reproductive effort, maintenance requirements and products (Brandt and Hartman, 1993). The applications of such an approach are diverse: some studies seek the funda-

mentals of physiological activity (Hawkins et al., 2002; MacDonald and Ward, 2009), while others are trying to identify energy sources (Dowd, 1997; Bernard et al., 2011; this study: Chap. 2) and some attempt to examine energy dynamics in the context of aquaculture (Grant, 1996; Grant and Bacher, 2001; Grant et al., 2007; Filgueira et al., 2010; Sarà et al., 2012). Physiology modeling is a rather complicated task for suspension-feeding shellfish are highly responsive to fluctuations in the quantity and quality of food (Hawkins et al., 2002), which frequently occur in nearshore environments.

Bioenergetic models have been generally used to estimate or describe growth patterns in bivalve mollusks and often in relation to commercial exploitation and production yields. The firsts attempts to model growth in bivalves were based on growth theories from Gompertz and von Bertalanffy (Ricker, 1975; Cloern and Nichols, 1978; Bayne and Worrall, 1980). And these approaches are still used to estimate and manage natural stocks of marine species (Fifas, 1993; Aguire, 2010; Van Wynsberge et al., 2013). In a comparison of these growth equations, Theisen (1973) concluded that the sigmoidal Gompertz curve described the growth of *Mytilus edulis* from Greenland to about half the maximum shell length, whereas the von Bertalanffy equation was valid for sizes larger than one-third the maximum length. These growth models have the advantage of facilitating comparisons between populations (Bayne and Worrall, 1980). However, they fail to integrate environmental variability and different life stages when critical changes occur in the life history of an organism (Kooijman, 2010).

In most of bioenergetic studies, the energy transfers are simulated in net production models, also known as "scope for growth" (SFG) models (Warren and Davies, 1967; Bayne, 1976; Bayne and Worrall, 1980; Bayne and Newell, 1983). They assume that resource allocation relies on empirical allometric relationships. Assimilated energy is immediately available for maintenance, the rest is used for other metabolic processes: growth, development and reproduction (Pouvreau et al., 2006). Such models have been applied to *Ostrea edulis* (Buxton et al., 1981), *Placopecten magellanicus* (MacDonald and Thompson, 1986), *Crassostrea virginica* (Powell et al., 1992), *M. edulis* (Cranford and Hill, 1999), *Argopecten purpuratus* (Navarro et al., 2000), *Pinctada marguaritifera* (Pouvreau et al., 2000), *Ruditapes philippinarum* (Solidoro et al., 2000; Flye-Sainte-Marie et al., 2007) and to *Crassostrea gigas* (Guzmán-Agüero et al., 2012). SFG models are often used to investigate the dynamic interaction between bivalves and their environment in studies determining the carrying capacity of coastal ecosystems (Grant et al., 1993; Grant, 1996; Bacher et al., 1997; Dowd, 1997; Smaal et al., 1997). A study based on the description of the energy budget by Lucas (1993) was conducted by Fouillaron (2001) on *P. maximus*, in which energy fluxes between the different compartments of the great scallop were modeled. This study was essentially based on specific allometric relations of modeled fluxes, leading to a specific model hardly applicable to other species.

However, although these models can be very good descriptors of a species' biology in a particular environment, they present several drawbacks: (1) they do not allow for inter-specific comparison as they use species specific sets of equations; (2) these methods have fundamental limitations when applied to predicting the behaviour of populations in a dynamically varying environment; (3) or when considering different life stages; (4) none of them can link different levels of biological organization (Ross and Nisbet, 1990; Nisbet et al., 2000); (5) they usually require a very large number of parameters; (6) the relative role of diverse environmental factors are generally very subjective (e.g. Barillé et al., 1997; Hawkins et al., 2014). Nisbet et al. (2000) called for more cohesive and generic approaches providing comparative tools between species and environments. The emergence of mechanistic models allows a deep understanding of metabolic processes as they are deterministic and able to quantitatively follow energy flows.

### 1.4.3 Dynamic Energy Budget theory

#### A mechanistic approach of energy flux quantification

The Dynamic Energy Budget (DEB) theory does provide a mechanistic approach for mass and energy budgets in relation to environmental conditions (Kooijman, 2010). Based on simple and sound principles of thermodynamics, this theoretical framework describes quantitatively energy flow and its allocation to growth development, reproduction and maintenance. It has been successfully applied to more than 300 species from fungi to mammals (Kooijman, subm.) and especially to bivalve species such as *C. gigas* in the same taxonomic order (Pouvreau et al., 2006; Cardoso et al., 2006; Bourlès et al., 2009; Alunno-Bruscia et al., 2011; Bernard et al., 2011), *M. edulis* (Cardoso et al., 2006; Rosland et al., 2009; Troost et al., 2010; Saraiva et al., 2011b), *Ruditapes philippinarum* (Flye-Sainte-Marie et al., 2009), *Perna canaliculus* (Ren and Ross, 2005), *Cerastoderma edule* (Cardoso et al., 2006; Troost et al., 2010; Wijsman and Smaal, 2013), *Macoma baltica*, *Mya arenaria* (Freitas et al., 2009) and *Pinctada margaritifera* (on the larval stage; Thomas et al., 2011a). These models are now more and more used to describe, for instance, the physiological response of organisms to their changing environment (Ren and Ross, 2005; Maury et al., 2007; Alunno-Bruscia et al., 2011), their feeding ecology (Bourlès et al., 2009), the impact of toxins on their fitness (Jager et al., 2006), isotopic ecology (Emmery et al., 2011) or population dynamics (Diekmann and Metz, 2010). Moreover, compared to other approaches, DEB models have always been found to be more reliable (Nisbet et al., 2000; Bacher and Gangnery, 2006; Filgueira et al., 2011; Larsen et al., 2014).

#### Environmental forcing

Standard DEB models are driven by two inputs: the temperature and a food availability proxy. Temperature is a crucial parameter in the study of energy

fluxes as it affects all metabolic rates, particularly in ectotherms. For a specific range of temperatures, the description proposed by Arrhenius (1889) is usually adopted:

$$\dot{k}(T) = \dot{k}_1 \exp\left(\frac{T_A}{T_1} - \frac{T_A}{T}\right)$$

with $T$ the absolute temperature (in Kelvin), $T_1$ a chosen reference temperature, the Arrhenius temperature parameter $T_A$, $\dot{k}$ a metabolic rate and $\dot{k}_1$ its value at the temperature $T_1$. In ectotherms, temperature play a key role in the energy budget (Grant and Porter, 1992), especially for sessile aquatic animals such as *P. maximus* which have to cope with the fluctuation of the environment.

While the main source of energy for the great scallop is likely to remain phytoplankton according to MacDonald et al. (2006), *P. maximus* should, nevertheless, be able to use various food sources (e.g. MacDonald et al., 2006; Bachok et al., 2009; Cranford et al., 2011; Nerot et al., 2012), which makes it complex to determine accurate proxies of energy inputs. In previous bioenergetics modeling studies on suspension-feeding bivalves, chlorophyll-*a* concentrations, the main photosynthetic pigment found in every algae, has been commonly used as food descriptor (e.g. Pouvreau et al., 2006; Rosland et al., 2009; Dabrowski et al., 2012). However, Bourlès et al. (2009) noted many sources of discrepancies when using chlorophyll-*a* to estimate available phytoplankton biomass: (1) the variability in chlorophyll-*a* content of microalgae cells, which depends on the physiological state of phytoplankton and the period of the year (Llewellyn et al., 2005); (2) the presence of chlorophyll-*a* in certain algae class known to be avoided by scallops due to their toxicity and/or poor energetic value (Barillé et al., 1993; Dupuy et al., 2000; Hégaret et al., 2007). Bourlès et al. (2009) thus investigated different food indicators that could be used in a DEB model for *C. gigas*. They concluded that the number of cells of particular phytoplankton species was a better proxy of the energy availability, providing quantitative as well as qualitative information.

## 1.5 Objectives and thesis outline

To develop the best scientific understanding of ecological processes, pluridisciplinarity research is vital (McCarthy et al., 2012; Mueller et al., 2014). It has become increasingly evident in recent years that integrated studies are needed to encapsulate field observations, controlled experiments and modeling tools development. Observation is the core and the basis of every scientific study, allowing the description of phenomena and collecting real data over time. For example, the collection of climatic monitoring acquired since the first measurements from 1850s allows us to see the actual trend of global warming (Smith et al., 1996; Smith and Reynolds, 2003). Experimentation permits us to look at the effect of one or several factors on a phenomena in control conditions,

providing evidence of poorly understood processes in the natural environment. Finally, modeling is an unavoidable tool if we want to understand and accurately predict how ecosystems may cope with global change. Moreover, modeling allows integration of various level of organization (Angilletta and Sears, 2011).

The following doctorate work fits into the context of trophic and bioenergetics studies, with the general aim to understand the effect of the environment on the life history traits and the metabolism of the great scallop *Pecten maximus*. To this end, different approaches were considered by combining in situ observations and theoretical thinking to investigate the following questions:

- How does environmental variability affect *P. maximus* bioenergetics?
- Can energy allocation modeling help understanding growth and reproduction variability at a regional scale and in the distribution range ?
- What are the feeding dynamics of the great scallop?
- Can we use modeling to infer energy inputs from growth patterns?

In the first part of this thesis I present the work initiated to develop an individual bioenergetic model based on the concepts of dynamic energy budgets (Chapter 2). A first set of DEB parameters is estimated for *P. maximus* according to the covariation method for the estimation of DEB parameters (Lika et al., 2011a). Following previous studies' recommendations (Bourlès et al., 2009; Troost et al., 2010; Saraiva et al., 2011a), the model was implemented using the concept of synthesizing units of Kooijman (2010) in order to cope with several food inputs. The rationale behind this was to test the hypothesis of selection between two food sources: phytoplankton cells and the rest of the particulate organic matter.

In the second part, the individual bioenergetic model is coupled to a hydrodynamical model, a 3D-biogeochemical model and a population dynamic model in order to assess the distribution of *P. maximus* in the English Channel (Chapter 3). This is a first step into the population modeling of scallop stocks, using the DEB model as an individual physiological model to infer the state and dynamics of the English Channel population.

A key feature of the ecology of suspension-feeding bivalves is their ability to deal with various foraging sources (e.g. Shumway et al., 1987; Kang et al., 1999; MacDonald et al., 2006; Ward and Kach, 2009). Moreover, it is of high importance to accurately identify and quantify the energy sources of an organism in order to model its bioenergetics. With the aim of improving the knowledge of the dynamics of *P. maximus*' diet, a study of the seasonal feeding ecology based on the use of trophic biomarkers (lipids and pigments) is presented in Chapter 4.

In the last two chapters, a very promising tool, based on the use of growth trajectories to reconstruct temporal physiological history has been developed. In Chapter 5 the method is first described and then investigated through

theoretical tests. Both modeling biologists and ecologists should find interest in this approach, as (1) it is the first genuine DEB model inversion implemented; (2) exciting perspectives of paleoenvironment reconstruction arise through the coupling of this method to the geochemical study of the shell.

Chapter 6 finally shows an application of the reconstruction procedure with the study of a collection of data set from various environments along the distribution area of the great scallop. This allows the study of bioenergetic patterns along two gradients (latitudinal and bathymetric), and more particularly to understand the key process of assimilation in contrasting environments.

Finally, Chapter 7 gathers concluding remarks and perspectives opened up through this thesis work.

# Chapter 2

# A DEB model for the great scallop

**Feeding and energetics of the great scallop, *Pecten maximus*, through a DEB model**

*Journal of Sea Research (2013) In Press*

**Romain Lavaud**, Jonathan Flye-Sainte-Marie, Fred Jean, Antoine Emmery, Øivind Strand and Sebastiaan A.L.M. Kooijman.

**Abstract**
We developed a full life-cycle bioenergetic model for the great scallop *P. maximus* relying on the concepts of the Dynamic Energy Budget (DEB) theory. The covariation method was implemented to estimate the parameters of a standard DEB model. Such models are able to predict various metabolic processes from a food availability marker and temperature in the environment. However, suspension-feeders are likely to feed on various trophic sources, from microalgae cells to detritus. They are also able to sort and select food particles very efficiently, depending on their size, energetic value or quality. The present model includes a mechanistic description of the feeding processes, based on Kooijman's Synthesizing Unit principle which allow one to deal with several food sources. Moreover we tested the hypothesis of a differential selectivity between two potential substrates (phytoplankton cell and the remaining particulate organic matter). Simulations of shell length, daily shell growth rate, dry weight and gonado-somatic index (GSI) variations were carried out and compared to field data from a monitoring conducted in the Bay of Brest (Brittany, France) for six years. The model showed its capacity to efficiently

reproduce all life history traits of the wild great scallops. Predicted length data were estimated to the nearest millimeter. The fit of simulated weights to observed data was very satisfactory. GSI predictions were also in accordance with observations but improvements are required to better capture the sharp increase of gametogenesis at the beginning of the year. Finally, results bring evidences that *P. maximus* is actually preferentially feeding on living algae cells rather than on the rest of organic particles.

**Keywords:** *Pecten maximus*; DEB theory; synthesizing units; phytoplankton; feeding process; Bay of Brest

## 2.1 Introduction

The great scallop *Pecten maximus* (Linnaeus, 1758) is a bivalve mollusk living in coastal environments of North-Western Atlantic, commercially important for fisheries and sea ranching. A large number of studies has long explored the physiological and ecological traits of this animal, both in controlled environment and in the wild (e.g. Mason, 1957; Antoine et al., 1979; Paulet et al., 1997; Saout et al., 1999; Laing, 2000; Chauvaud et al., 2001; Laing, 2002; Strohmeier et al., 2009; Chauvaud et al., 2012). Its broad latitudinal and bathymetric distribution results in a variability of life history traits with a large ultimate size in northern environments and small size in southern areas and deep locations (Chauvaud et al., 2012). Known to feed mainly on phytoplankton and microphytobenthos (Robert et al., 1994; Chauvaud et al., 2001), its diet has also been reported to include bacteria and nanoplankton as well (Heral, 1989; Langdon and Newell, 1990; MacDonald et al., 2006; Nerot et al., 2012), but in proportion that still need to be assessed. These two aspects of *P. maximus* biology (growth and feeding) are key processes for a better comprehension of the physiology of this species.

Within the French project COMANCHE, we are trying to combine various scientific and economic approaches around the biology and exploitation of *P. maximus* in the English Channel region. The development of a bioenergetic individual-based model is a crucial step to combine hydrodynamic, larval development and dispersion models with population dynamic modeling. Thus we were motivated to set up a mechanistic model capable, with as few variables as possible, to simulate the evolution through time of diverse physiological traits that would serve as basis for fishery management.

We tried to combine knowledge accumulated about this species in a model for metabolic processes, which can give reliable insights on the physiological evolution of the organism and thus capture the variability observed in biological pattern. Dynamic Energy Budget theory (DEB; Kooijman, 2010) provides such a generalized, individual-based, bioenergetic framework suitable for linking levels of metabolic organization through a mechanistic model. It has been successfully applied to 240 species from fungi to mammals (Kooijman, subm.) and especially to bivalves species closely related to *P. maximus* such as *Cras-*

*sostrea gigas* in the same taxonomic order (Pouvreau et al., 2006; Cardoso et al., 2006; Bourlès et al., 2009; Alunno-Bruscia et al., 2011; Bernard et al., 2011), *Mytilus edulis* (Cardoso et al., 2006; Rosland et al., 2009; Troost et al., 2010; Saraiva et al., 2011b), *Ruditapes philippinarum* (Flye-Sainte-Marie et al., 2007), *Perna canaliculus* (Ren and Ross, 2005), *Cerastoderma edule* (Cardoso et al., 2006; Troost et al., 2010; Wijsman and Smaal, 2013), *Macoma baltica*, *Mya arenaria* (Freitas et al., 2009) and *Pinctada margaritifera* (on the larval stage; Thomas et al., 2011b).

In this study we aim at developing the first DEB model for a member of the pectinid family, *P. maximus*. Using literature data we estimated the standard DEB parameters and built our model with the Synthesizing Units concept (Kooijman, 2010). The inter-annual variability of several physiological processes of adult scallops was studied and compared to monitoring data gathered over six years in the Bay of Brest (Brittany, France). An innovative aspect of this work is the implementation of the hypothesis of a differential selectivity in food sources, tested using the Synthesizing Units principle from Kooijman (2010).

## 2.2 Material and methods

### 2.2.1 Model formulation

The model developed in this study is based on the Dynamic Energy Budget theory (Kooijman, 2010). According to DEB theory the energetics of an organism can be described by the dynamics of three state variables: (1) the structural volume $V$ (somatic tissue excluding reserves), (2) the reserves $E$ and (3) the energy allocated to maturity and reproduction $E_R$. Trophic resource provides energy that fuels the reserve compartment. A fixed fraction ($\kappa$) of energy flux from reserve is then allocated to somatic growth plus its maintenance, with a priority given to maintenance. The remaining fraction (1-$\kappa$) is used for maturity maintenance, maturation (in embryos and juveniles) and reproduction (i.e. gamete production in adults). A conceptual scheme, illustrating the modeled energy flows through the scallop, is given in Fig. 2.1. Notation of the variables and parameters is from Kooijman (2010) (Table 2.1).

In this study, we paid a particular attention to the feeding process, which is rather complex in suspension-feeders (Ward and Shumway, 2004; Cranford et al., 2011). Briefly, the filtering process in bivalves can be described as follows. A water current is generated through the pallial cavity by ciliary activity of the gills. Water is then sieved by the gills, the amount of water totally cleared of its particles per unit of time is denoted as clearance (or filtration) rate $\dot{F}_X$. For each food particle present in the surrounding water, with a density $X$, the flux of particles extracted from the environment, known as consumption rate, can be assessed by $X\dot{F}_X$. Rubbed into mucus strings, food particles are then transported to the aboral side of the gills where labial palps sort and bring food pellets to the mouth for ingestion ; this ingestion rate

**Table 2.1:** Equations for the implementation of energy fluxes in the DEB model for *P. maximus*.

| *Name of the variable* | *Symbol* | *Unit* | *Equation* |
|---|---|---|---|
| Reserve density | $[E]$ | $\mathrm{J\,cm^{-3}}$ | $= \dfrac{E}{V}$ |
| Assimilation rate | $\dot{p}_A$ | $\mathrm{J\,d^{-1}}$ | $= \dot{J}_{EA}\,\mu_E\,V^{2/3}$ |
| Mobilization rate | $\dot{p}_C$ | $\mathrm{J\,d^{-1}}$ | $= \dfrac{[E]}{[E_G]+\kappa[E]}\left(\dfrac{E_G\,\dot{v}}{V^{1/3}}+[\dot{p}_M]\right)$ |
| Somatic maintenance | $\dot{p}_M$ | $\mathrm{J\,d^{-1}}$ | $= [\dot{p}_M]\,V$ |
| Maturity maintenance coefficient | $\dot{p}_J$ | $\mathrm{J\,d^{-1}}$ | $= E_H\,k_J$ |
| Structural growth | $\dot{p}_G$ | $\mathrm{J\,d^{-1}}$ | $= max(0, \kappa\,\dot{p}_C - \dot{p}_M)$ |
| Allocation to reproduction buffer | $\dot{p}_R$ | $\mathrm{J\,d^{-1}}$ | $= max(0, (1-\kappa)\,\dot{p}_C - \dot{p}_J)$ |
| Shrink to pay somatic maintenance | $\dot{p}_{S1}$ | $\mathrm{J\,d^{-1}}$ | $= max(0, \dot{p}_M - \kappa\,\dot{p}_C)$ |
| Shrink to pay maturity maintenance | $\dot{p}_{S2}$ | $\mathrm{J\,d^{-1}}$ | $= max(0, \dot{p}_J - (1-\kappa)\,\dot{p}_C)$ |
| Resorption of gonad | $\dot{p}_{RS}$ | $\mathrm{J\,d^{-1}}$ | $= \dfrac{\dot{p}_R\,\kappa_R + E_R\,\dfrac{1}{dt}}{\kappa_R}$ |
| Lysis of structure | $\dot{p}_{VS}$ | $\mathrm{J\,d^{-1}}$ | $= \dfrac{(\dot{p}_{S1}+\dot{p}_{S2}) - \dot{p}_{RS}\,\kappa_R)\,d_{Vd}}{\kappa_R\,\mu_E)}$ |

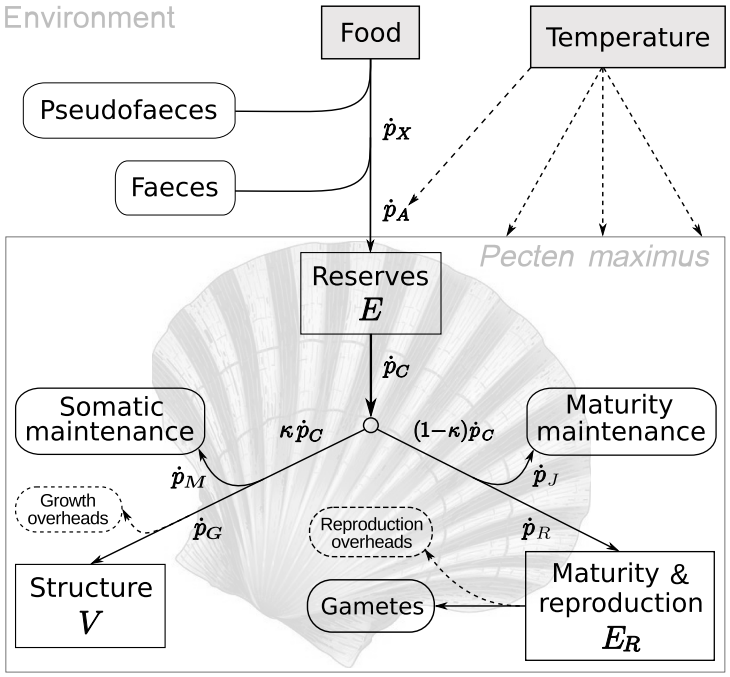


**Figure 2.1:** Conceptual scheme of the DEB model applied to the scallop *P. maximus*. Forcing variables (food and temperature) are in gray; state variables are Reserves($E$), Structure ($V$) and Maturity & reproduction ($E_R$), in white boxes. Dark arrows are energy fluxes and dotted ones show temperature influence on these rates.

is denoted as $\dot{J}_{Xm}$. Suspension-feeding bivalves are known to feed upon various trophic sources (see e.g. Kamermans, 1994; Chauvaud et al., 2001; MacDonald et al., 2006; Bachok et al., 2009; Yokoyama et al., 2009; Nerot et al., 2012) and they are subsequently able to develop a plastic trophic niche, variable in space and time as an adaptation/acclimation to available trophic resources and depending on their development stage (Rossi et al., 2004; Marín Leal et al., 2008). Filtration, ingestion and assimilation processes are characterized by a capacity to select and sort potential food particles, via gill crossing retention, labial palps selectivity, inner digestive gland sorting, differential assimilation rates. Moreover, many studies focusing on modeling the energy dynamics of filter feeders have reported the need (Alunno-Bruscia et al., 2011; Bernard et al., 2011) and the benefit (Troost et al., 2010; Saraiva et al., 2011a) of adding a second food source to forcing variables to improve the food proxy . Thus, to model energy acquisition and afterwards its dynamics in *P. maximus* we focused on two concepts: (1) the processing of two types of food substrates and (2) the selectivity of food particles of different origins and energetic values.

In order to address these issues we chose to work with the concept of Synthetizing Units (SUs; Kooijman, 1998, 2006, 2010; Saraiva et al., 2011a), considered as generalized enzymes that transform an arrival flux of substrates into a production flux of products. Here food particles are considered as substrates and reserves as products. During the processing (handling time), no substrate particles are accepted by the SU, i.e. while handling, the binding probability for each arriving substrate will be null. SUs allow one to deal with different types of food to test some patterns in feeding such as selectivity of substrates. We used two potential trophic sources markers: algal cell counts and the rest of particulate organic matter (POM, i.e. non algal organic particles). Substrates were respectively called $S_X$ for cell counts and $S_Y$ for POM. The arrival flux of food particles was taken to be proportional to the density in spatially homogeneous environments (Kooijman, 2010), which is the case in aquatic environments. We worked with interacting substitutable substrates that are bound in a sequential fashion (Fig. 2.2).

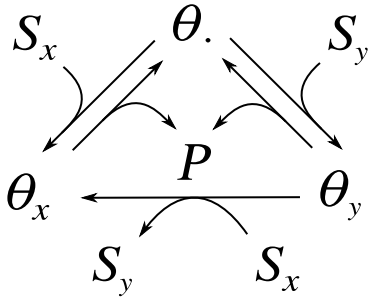


**Figure 2.2:** Graphical representation of the preferential interaction between substrates in the Synthetizing Unit concept (Kooijman, 2010), that allows the substitution of one substrate type to another. $S_X$ is the substrate corresponding to the microalgal cells and $S_Y$ the one for remaining POM. $\theta.$ represents a free SU fraction while $\theta_X$ and $\theta_Y$ are SU fractions bound respectively to a X-type food particle and a Y-type food particle. $P$ stands for the product released after transformation of the substrate.

This scheme illustrates the possibility for a free SU ($\theta.$) to bind to either a substrate particle from type $S_X$ or $S_Y$ to form a SU-$S_X$ complex ($\theta_X$) or a SU-$S_Y$ complex ($\theta_X$) respectively. Moreover, a substrate $S_X$ can replace a $S_Y$ in a SU-$S_Y$ complex ($\theta_Y$) to form a SU-$S_X$ complex ($\theta_X$), releasing an untransformed substrate $S_Y$. Each food type contributes to the production of reserves, specified in yield coefficients ($y_{EX}$ and $y_{EY}$) that were here treated as constant. Given the dissociation rate parameters $\dot{k}_X$ and $\dot{k}_Y$, the binding

parameters $\dot{b}_X$ and $\dot{b}_Y$ and the interaction affinities $\dot{b}_{XY}$ and $\dot{b}_{YX}$, the change in binding fractions for substrates X and Y are:

$$\frac{d}{dt}\theta_\cdot = \dot{k}_X\theta_X + \dot{k}_Y\theta_Y - (\dot{b}_X X + \dot{b}_Y Y)\theta_\cdot \tag{2.1a}$$

$$\frac{d}{dt}\theta_X = -\dot{k}_X\theta_X + \dot{b}_X X\theta_\cdot - \dot{b}_{YX} Y\theta_X + \dot{b}_{XY} X\theta_Y \tag{2.1b}$$

$$\frac{d}{dt}\theta_X = -\dot{k}_X\theta_X + \dot{b}_X X\theta_\cdot - \dot{b}_{YX} Y\theta_X + \dot{b}_{XY} X\theta_Y \tag{2.1c}$$

$$\frac{d}{dt}\theta_Y = -\dot{k}_Y\theta_Y + \dot{b}_Y Y\theta_\cdot + \dot{b}_{YX} Y\theta_X - \dot{b}_{XY} X\theta_Y \tag{2.1d}$$

with $1 = \theta_\cdot + \theta_X + \theta_Y$ and X and Y stand for the densities of substrates $S_X$ and $S_Y$ in a number of particle per liter. The pseudo steady state fractions are:

$$\theta_X^* = \frac{\alpha_Y \dot{b}_X X - \beta_X \dot{b}_Y Y}{\alpha_X \alpha_Y - \beta_X \beta_Y}; \qquad \theta_Y^* = \frac{\alpha_X \dot{b}_Y Y - \beta_Y \dot{b}_X X}{\alpha_X \alpha_Y - \beta_X \beta_Y} \tag{2.2}$$

with

$$\alpha_X = \dot{k}_X + \dot{b}_X X + \dot{b}_{YX} Y; \qquad \alpha_Y = \dot{k}_Y + \dot{b}_Y Y + \dot{b}_{XY} X; \tag{2.3a}$$

$$\beta_X = \dot{b}_X X - \dot{b}_{XY} X; \qquad \beta_Y = \dot{b}_Y Y - \dot{b}_{YX} Y \tag{2.3b}$$

The preference hypothesis is transcribed into the model by changing $\dot{b}_{XY}$ and $\dot{b}_{YX}$, in such a way that the SU would be able to change from substrate X to substrate Y, i.e. setting one probability superior to the other. $\dot{b}_{XY}$ and $\dot{b}_{YX}$ were first turned into $\left\{\dot{b}_{XY}\right\} = \frac{\dot{b}_{XY}}{L^2}$ and $\left\{\dot{b}_{YX}\right\} = \frac{\dot{b}_{YX}}{L^2}$, to get rid of size dependency. $\left\{\dot{b}_{YX}\right\}$ was set at 0 and $\left\{\dot{b}_{XY}\right\}$ was taken equal to the maximum specific filtration rate for $X$-type substrate, $\left\{\dot{F}_{Xm}\right\}$. In this case a change in the substrate to process may occur in one direction only. When both substrates are available, this rule leads to an automatic substitution of the counter-selected substrate (POM particle), already bound to a SU, by the preferred food type (here algae cells). Dissociation rates relate to the maximum specific feeding rates as $\dot{k}_X = \left\{\dot{h}_{XAm}\right\} L^2$ and $\dot{k}_Y = \left\{\dot{h}_{YAm}\right\} L^2$, where $L$ is

the structural length and $\left\{\dot{h}_{XAm}\right\}$ and $\left\{\dot{h}_{YAm}\right\}$ are the maximum specific feeding rates (# $\mathrm{d}^{-1}\,\mathrm{cm}^{-2}$), given by:

$$\left\{\dot{h}_{XAm}\right\} = \frac{\left\{\dot{J}_{XAm}\right\}}{M_X} \quad \text{with} \quad \left\{\dot{J}_{XAm}\right\} = \frac{\{\dot{p}_{Am}\}}{(\mu_E\, y_{EX})} \tag{2.4a}$$

$$\left\{\dot{h}_{YAm}\right\} = \frac{\left\{\dot{J}_{YAm}\right\}}{M_Y} \quad \text{with} \quad \left\{\dot{J}_{YAm}\right\} = \frac{\{\dot{p}_{Am}\}}{(\mu_E\, y_{EY})} \tag{2.4b}$$

where $\left\{\dot{J}_{XAm}\right\}$ and $\left\{\dot{J}_{YAm}\right\}$ are the maximum specific ingestion rates for substrates X and Y (mol $\mathrm{d}^{-1}\,\mathrm{cm}^{-2}$), $\{\dot{p}_{Am}\}$ is the maximum specific assimilation rate (J $\mathrm{d}^{-1}\,\mathrm{cm}^{-2}$), $\mu_E$ is the chemical potential of reserve (J $\mathrm{mol}^{-1}$) and $y_{EX}$ and $y_{EY}$ are the yields of reserve on compound X and Y respectively (mol $\mathrm{mol}^{-1}$).

Finally, the association rates relate to the maximum specific searching rates as $\dot{b}_X = \left\{\dot{F}_{Xm}\right\} L^2$ and $\dot{b}_Y = \left\{\dot{F}_{Ym}\right\} L^2$. Thus the specific assimilation rate for reserve can be written as:

$$\dot{J}_{EA} = y_{EX} \left\{\dot{J}_{XAm}\right\} f_X + y_{EY} \left\{\dot{J}_{YAm}\right\} f_Y \tag{2.5}$$

with

$$f_X = \frac{\alpha_Y \left\{\dot{F}_{Xm}\right\} X - \beta_X \dot{b}_Y Y}{\alpha_X \alpha_Y - \beta_X \beta_Y}; \qquad f_Y = \frac{\alpha_X \left\{\dot{F}_{Ym}\right\} Y - \beta_Y \dot{b}_X X}{\alpha_X \alpha_Y - \beta_X \beta_Y} \tag{2.6a}$$

$$\alpha_X = \left\{\dot{h}_{XAm}\right\} + \left\{\dot{F}_{Xm}\right\} X + \left\{\dot{b}_{YX}\right\} Y; \quad \alpha_Y = \left\{\dot{h}_{YAm}\right\} + \left\{\dot{F}_{Ym}\right\} Y + \left\{\dot{b}_{XY}\right\} X \tag{2.6b}$$

$$\beta_X = \left\{\dot{F}_{Xm}\right\} X - \left\{\dot{b}_{XY}\right\} X; \qquad \beta_Y = \left\{\dot{F}_{Ym}\right\} Y - \left\{\dot{b}_{YX}\right\} Y \tag{2.6c}$$

In order to test the hypothesis of a selectivity in feeding in *P. maximus*, a classical functional response was also calculated, using only one food source (phytoplankton cells). This response to food density variations is based on the Holling type II functional response (Kooijman, 2010) : $f = \dfrac{X}{X + X_K}$, with $X$ the algae cell concentration (# $\mathrm{L}^{-1}$) and $X_K$ the half-saturation coefficient (# $\mathrm{L}^{-1}$). The value of this parameter was calibrated for each year.

Once assimilation has been implemented, reserves dynamics can be treated. Energy conservation law implies that reserves dynamics amounts to the difference between the assimilation rate $\dot{p}_A$ and the utilization rate of reserves $\dot{p}_C$. The structural growth is provided with a fraction $\kappa$ of this mobilized energy from which somatic maintenance requirements are first paid. The rest of energy flux from the reserve compound is allocated in priority to maturity

maintenance and then to the reproduction buffer $E_R$. During periods of low food availability or prolonged starvation (especially in winter), *P. maximus* is known to undergo a sharp decrease in flesh weight (Comely, 1974; Pazos et al., 1997). In fact, the flux of energy coming from reserves is not sufficient to "pay" maintenance costs (both $\dot{p}_M$ and $\dot{p}_J$). The energy that has to be mobilized to pay somatic maintenance ($\dot{p}_{S1}$) and maturity maintenance ($\dot{p}_{S2}$) is taken from the reproduction buffer (resorption of gonad, $\dot{p}_{RS}$) and if the reproduction buffer is empty, maintenance costs are "paid" from the structural volume (lysis of structure, $\dot{p}_{VS}$).

The dependency of physiological rates on body temperature in ectotherms (in which body temperature equals external temperature) has been described by the Arrhenius relationship within a species-specific tolerance range of temperature (Kooijman, 2010). The following relationship was used to correct all model fluxes for temperature:

$$\dot{k}(T) = \dot{k}_1 T_C \quad \text{with} \quad T_C = \frac{\exp\left(\frac{T_A}{T_1} - \frac{T_A}{T}\right)\left(1 + \exp\left\{\frac{T_{AL}}{T_1} - \frac{T_{AL}}{T_L}\right\}\right)}{1 + \exp\left(\frac{T_{AL}}{T} - \frac{T_{AL}}{T_L}\right)} \tag{2.7}$$

where $\dot{k}(T)$ is the value of the physiological rate at temperature $T$, $\dot{k}_1$ is the physiological rate at the reference temperature $T_1$, $T_A$ is the Arrhenius temperature, $T_L$ is the lower boundary of the tolerance range, and $T_{AL}$ is the Arrhenius temperature for the rate of decrease at the lower boundary. All temperatures are expressed in Kelvin (K).

### 2.2.2 Parameter estimation

The Arrhenius temperature was estimated by fitting the previous equation in a composite data set relating physiological rates (respiration, growth, filtration, assimilation) to temperature, constructed from data available in literature (Laing, 2000, 2002, 2004) and from unpublished studies in the Bay of Brest (Chauvaud and Paulet, unpublished data). A reference temperature ($T_1$) of 288 K was chosen. We applied the covariation method for parameter estimation according to the procedure described by Lika et al. (2011a) that allow one to estimate all parameters of the standard DEB model from empirical datasets of the literature (Table 2.4). Part of these observed data consists of single values, named zero-variate data, such as age, weight and size at the larval stage (Gruffydd and Beaumont, 1972; Buestel et al., 1982; Samain et al., 1986; Shumway and Parsons, 2006), at puberty (Shumway and Parsons, 2006) and for the adult period (Paulet and Fifas, 1989; Paulet et al., 1997; Le Pennec et al., 2003; Shumway and Parsons, 2006). The other type of observations used for parameter calibration is a data set of 288 shell length over age values (EVECOS data base provided by "Observatoire Marin de l'IUEM, INSU,

Plouzané"). The covariation method is a single-step procedure based on the simultaneous minimization of the weighted sum of squared deviations between all observation data sets and model predictions. Weight coefficients can be applied to zero-variate data, in order to quantify the certainty of life history traits gathered from literature (on the basis of their reliability and occurrence). Therefore, little less weight was given to puberty data as the timing of this maturity threshold is rather imprecise. Likewise, as ultimate length is an empirical measurement, hardly reproducible, a lower weight coefficient was also applied to this value. The relevance of the parameter set was assessed by a mean relative error calculation (mre).

### 2.2.3 Study site, forcing and calibration data

To test the estimated parameters we used a data set of a monthly monitoring of *P. maximus* bank located in the Roscanvel site, in the central area of the Bay of Brest (Fig. 2.3). This location is a coastal semi enclosed area located in west France. It is under the influence of high tides and freshwater inputs from two rivers and is connected to the open ocean by a narrow strait (2 km wide). Biometry measurements of scallops from the Roscanvel bank (48°20'N, 4°30'W) has been monitored during several decades (1977 to 2004) and provides a large data set, also including environmental variables. Twenty scallops from the three-year age cohort (2.5 to 3.5 years old) have been collected twice a month (EVECOS data base provided by "Observatoire Marin de l'IUEM, INSU, Plouzané").

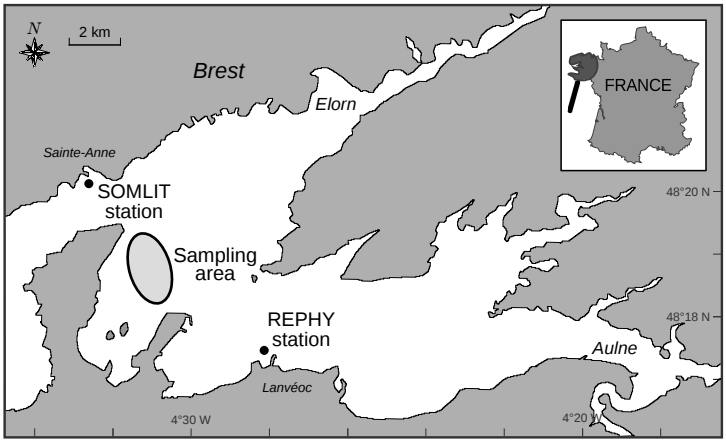


**Figure 2.3:** Map of the Bay of Brest with the location of the sampling area for monthly monitoring of great scallops (indicated in gray), named Roscanvel and the two environmental monitoring sites: the REPHY station at Lanvéoc and the SOMLIT station at Sainte-Anne.

Dry weight of each organ, shell height and gonado-somatic index (gonad dry weight over total body dry weight) were measured on these individuals. In order to compare weight values obtained for different size animals, dry weights were corrected for size differences between individuals following the formula of Bayne et al. (1987):

$$W_r = \left(\frac{L_r}{L_m}\right)^3 W_m \tag{2.8}$$

where $W_r$ is the recalculated weight of an individual of standard shell height $L_r$ and $W_m$ is the measured weight for an individual of measured shell height $L_m$. Length were estimated after measuring the mean daily shell growth rate (DSGR) over an entire growth season using the method proposed by Chauvaud et al. (2012). Each year, five individuals were sampled in December, i.e. after the growth cessation, to capture the entire growth season. Five other individuals harvested in August were used to assign calendar dates to each increment, by knowing the sampling date of the last formed increment. A synchronization procedure was used between the individual growth trajectories within each pool by minimizing the sum of the differences between individual series considered two-by-two. Growth trajectories from the summer pool and the winter pool were finally adjusted in the same way to assign calendar dates to the full year data set.

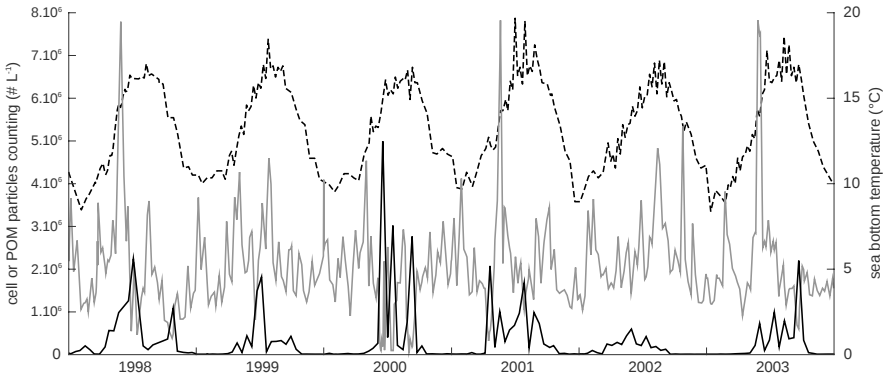


**Figure 2.4:** Environmental forcing variables monitored in the Bay of Brest between 1998 and 2003. Sea bottom temperature were measured on the Roscanvel bank (doted line, in celsius degrees). Phytoplankton enumeration (dark line, in cells per liter) come from the REPHY monitoring station (PHYtoplankton and PHYcotoxins monitoring NEtwork, Ifremer) in Lanvéoc. Particulate Organic Matter to which cell counts have been deducted (gray line, in particles per liter) were measured by the SOMLIT monitoring station in Sainte-Anne (data provided by "Service d'Observation en Milieu Littoral, INSU-CNRS, Brest").

Fig. 2.4 shows the environmental parameters used as forcing variables in the model. Daily temperature has been measured at the water-sediment interface in the Roscanvel bank from 1998 until 2000. A linear regression between registered temperature at Roscanvel and those from the SOMLIT probe in Sainte-Anne (data provided by "Service d'Observation en Milieu Littoral, INSU-CNRS, Brest"), allowed the reconstruction of bottom temperature in Roscanvel between 2001 and 2003. Two food proxies have been monitored: the particulate organic matter (POM, in $\mathrm{mg\,L^{-1}}$) and the phytoplankton concentration (in cell $\mathrm{L^{-1}}$). These data come from an instrumented site which is monitored by the REPHY network (PHYtoplankton and PHYcotoxins monitoring NEtwork, Ifremer). POM data in $\mathrm{mg\,L^{-1}}$ were transformed into a number of particles per liter by considering an average particle diameter of 30 µm (weight of $1.4 \times 10^{-5}$ g for a density of 1) per POM particle. Environmental measurements were linearly interpolated to fit the time step of the simulations.

### 2.2.4 Model simulations

Simulations were performed using GNU Octave software (Eaton et al., 2008; Octave community, 2012). Initial state variables values are obtained from observed measurements in the first sampling of the year (Table 2.2). A Eulerian integration method was used to study the dynamics of each state variable in time. As the individuals are three-year-old and fully mature (Antoine et al., 1979), the initial amount of maturity is taken to be equal to the maturity at puberty (supposed to be maintained during the adult stage; Kooijman, 2010). Using the DEB model developed for *P. maximus* we simulated the body dry weight, the shell height, the DSGR and the gonado-somatic index between 1998 and 2003. The evolution of shell height over time has been simulated from the relationship: $V = (\delta_{\mathcal{M}}\, L_{Obs})^3$, where $L_{Obs}$ is in cm. The gonado-somatic index (GSI) was calculated as a ratio between the wet weight of reserves allocated to reproduction ($W_{E_R}$) and the cubic shell length. Total body dry weight and GSI were calculated according to the formulas:

$$W = V d_{Vd} + \left[ (E + E_R) \frac{w_E}{\mu_E} \right] \tag{2.9}$$

$$GSI = \frac{W_{E_R}}{Ls^3}\, 1000 \quad \text{with} \quad W_{E_R} = \frac{E_R \dfrac{w_E}{\mu_E}}{d_{Vd}} \tag{2.10}$$

where $w_E$ is the molar weight of reserve ($\mathrm{g\,mol^{-1}}$), $\mu_E$ is the energy content of one gram of reserve ($\mathrm{J\,mol^{-1}}$) and $d_{Vd}$ is the wet weight to dry weight ratio.

In DEB theory, strategies for handling the reproduction buffer and spawning are species-specific. In *P. maximus*, gamete releasing is asynchronous, partial and has been reportedto be influenced by four parameters: tempera-

**Table 2.2:** Initial value calculation of the state variables in the DEB model of *P. maximus*.

| | |
|---|---|
| $L_i$ | Observed measurements in the first sampling of the year |
| $W_i$ | |
| $V_i = (L_i\ \delta_{\mathcal{M}})^3$ | |
| $E_i = \frac{\{\dot{p}_{Am}\}}{\dot{\upsilon}}\ V_i$ | |
| $E_{Ri} = \left(W_i - V_i\ k_w - \left\{E_i\ \frac{w_E}{\mu_E}\right\}\right)\ \left(\frac{\mu_E}{w_E}\right)$ | |
| $E_{Hi} = E_H^p$ | |

ture, food density, a minimal GSI and photoperiod (Paulet et al., 1997; Saout et al., 1999; Barber and Blake, 2006). Sharp decreases observed in measured GSI can be correlated to spawning events. The model was then calibrated to fit GSI observations by taking into account the influence of these forcing variables. The first spawning event of the year in the Bay of Brest is usually synchronous with the first spring bloom (Paulet et al., 1997), thus a threshold in food density was set at $3 \times 10^5$ cells $L^{-1}$ (average value corresponding to a substantial resumption of primary production in spring) under which no spawning is possible. As for many bivalve species, temperature has a crucial influence on gametogenesis but also on the releasing of gametes. We decided to apply the day-degree concept as a trigger for spawning. Once the seawater has reached a threshold of 12 ℃, daily cumulative degrees above this limit were counted and a value of 75 degree-days was found to be required to reach a condition ready for spawning. Then, a minimum GSI of 7 was put at the third trigger for spawning, accounting for a minimal advancement in gametogenesis. The reproduction buffer was then half emptied and the degree-days counter reseted. The last parameter, the photoperiod, is a key parameter that blocks the release of gamete so that after the fall equinox no spawning is ever possible (Devauchelle and Mingant, 1991; Duinker et al., 1999; Saout et al., 1999).

## 2.3 Results

### 2.3.1 DEB Parameters estimates

The DEB parameters estimated for *P. maximus* through the covariation method are presented in Table 2.3. The overall goodness of fit of model prediction to data on the great scallop's life history traits (Table 2.4) was evaluated at 8.72 over 10, with fit = 10 × (1 - mre). The only pattern not very well captured is

the age at metamorphosis, known to be between 20 and 30 days and which is estimated in our model at about 10 days. An other evidence that there is a satisfactory correspondence between the simulations and the observations is to use a full life-cycle growth data set (Fig. 2.5), which shows the good prediction of the model. Primary parameters of the DEB model for a given organism always correspond to those of an embryo and for the majority of species do not vary during life span. Nevertheless, some taxa, including *P. maximus*, experience a metabolic acceleration after metamorphosis causing a change in the value of some parameters. The maximum surface-specific assimilation rate $\{\dot{p}_{Am}\}$ and the energy conductance $\dot{v}$ would respectively increase to $282\,\mathrm{J\,d^{-1}\,cm^{-2}}$ and $0.063\,\mathrm{cm\,d^{-1}}$ at this stage transition. As three-year-old individuals are modeled here, values after metamorphosis have been used for the following simulations.

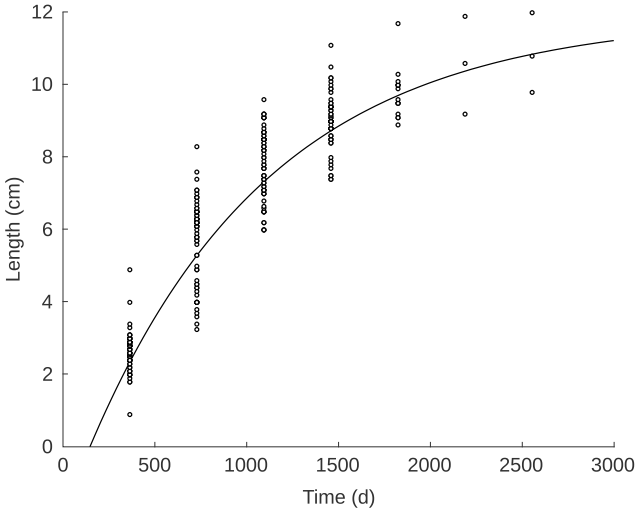


**Figure 2.5:** Simulation of *P. maximus* shell length over a full life-cycle using the primary parameters of the DEB model (dark line). Dots are a collection of shell length data collected over decades in the bay of Brest and archived in the EVECOS time series (EVECOS data base provided by "Observatoire Marin de l'IUEM, INSU, Plouzané").

### 2.3.2 Environmental forcing variables

Temperature monitored during a study period of six years follow a rather constant annual cycle (Fig. 2.4) with common winter values between 8 and 12 °C from December to February and from 15 to 19 °C during summer (July to September). Noticeable peaks occurred in summer 2001 reaching a temperature of 19.7 °C as well as sharp drops until 8.4 °C during January 2003.

**Table 2.3:** List of the parameters implemented in the DEB model of *P. maximus*. * denote estimated parameters using the coveriation method (Lika et al., 2011a), other parameters have been calculated or fixed.

| *Description* | *Symbol* | *Value* | *Unit* |
|---|---|---|---|
| *Feeding process* | | | |
| Number of moles per one $X$-type food particle | $M_X$ | $1.05 \times 10^{-10}$ | mol |
| Number of moles per one $Y$-type food particle | $M_Y$ | $2.49 \times 10^{-9}$ | mol |
| Maximum specific filtration rate of $X$-type particle | $F_X m$ | 25–100 | $\mathrm{L\,d^{-1}\,cm^{-2}}$ |
| Maximum specific filtration rate of $Y$-type particle | $F_Y m$ | 2–4 | $\mathrm{L\,d^{-1}\,cm^{-2}}$ |
| Binding rate of $X$-type particle | $\dot{b}_{XY}$ | $= F_X m$ | $\mathrm{L\,d^{-1}\,cm^{-2}}$ |
| Binding rate of $Y$-type particle | $\dot{b}_{YX}$ | 0 | $\mathrm{L\,d^{-1}\,cm^{-2}}$ |
| Yield of reserve on $X$-type particle | $y_{EX}$ | 0.7 | $\mathrm{mol\,mol^{-1}}$ |
| Yield of reserve on $Y$-type particle | $y_{EY}$ | 0.4 | $\mathrm{mol\,mol^{-1}}$ |
| *Primary parameters* | | | |
| Shape coefficient* | $\delta_{\mathcal{M}}$ | 0.36 | – |
| Fraction of mobilised reserve allocated to soma* | $\kappa$ | 0.86 | – |
| Fraction of reproduction energy fixed in eggs* | $\kappa_R$ | 0.95 | – |
| Energy conductance* | $\dot{v}$ | 0.021 | $\mathrm{cm\,d^{-1}}$ |
| Volume–specific maintenance costs* | $[\dot{p}_M]$ | 33.52 | $\mathrm{J\,cm^{-3}}$ |
| Volume–specific costs for structure* | $[E_G]$ | 2959 | $\mathrm{J\,cm^{-3}}$ |
| Maximum surface–specific assimilation rate* | $\{\dot{p}_{Am}\}$ | 94 | $\mathrm{J\,d^{-1}\,cm^{-2}}$ |
| Maturity maintenance coefficient | $k_J$ | 0.002 | $\mathrm{d^{-1}}$ |
| Maturity at birth* | $E_H{}^b$ | 0.000 28 | J |
| Maturity at metamorphosis* | $E_H{}^m$ | 0.0078 | J |
| Maturity at puberty* | $E_H{}^p$ | 3000 | J |
| *Compound parameters* | | | |
| Maximum reserve density | $[E_m]$ | 4483 | $\mathrm{J\,cm^{-3}}$ |
| Chemical potential of reserve | $\mu_E$ | 474 400 | $\mathrm{J\,mol^{-1}}$ |
| Molecular weight of reserve | $w_E$ | 23.9 | $\mathrm{g\,mol^{-1}}$ |
| Wet weight to dry weight ratio | $d_{Vd}$ | 0.12 | – |
| *Arrhenius temperature* | | | |
| Reference temperature (arbitrary) | $T_1$ | 293 | K |
| Arrhenius temperature | $T_A$ | 8990 | K |
| Lower boundary of tolerance range | $T_L$ | 273 | K |
| Rate of decrease at lower boundary | $T_{AL}$ | 50 000 | K |

**Table 2.4:** Compilation of life-cycle data from the literature used to estimate the model parameters, using the covariation method of Lika et al. (2011a). Values predicted from the estimated parameters are also presented for comparison. Literature references : [1] Gruffydd and Beaumont (1972), [2] Paulet et al. (1988), [3] Mason (1958), [4] Pazos et al. (1997), [5] Chauvaud et al. (1998), [6] Faure (1956), [7] Samain et al. (1986), [8] Christophersen (2000), [9] Fifas (2004), [10] Paulet et al. (1997).

| *Data* | *Literature value* | *Predicted value* | *References* |
|---|---|---|---|
| age at birth | 2 d | 1.795 d | [1] |
| age at metamorphosis | 25 d | 9.563 d | [1], [2] |
| age at puberty | during the second year | 464.3 d | [1], [3], [4], [5] |
| physical length at birth | 0.008 cm | 0.007 313 cm | [1], [2] |
| physical length at metamorphosis | 0.024 cm | 0.028 67 cm | [1], [2], [5] |
| physical length at puberty | 4 cm | 4.426 cm | [1], [5] |
| ultimate physical length | 12 cm | 11.9 cm | [6] |
| dry weight at birth | $10^{-7}$ g | $1.452 \times 10^{-7}$ g | [7] |
| dry weight at metamorphosis | $3 \times 10^{-6}$ g | $4.030 \times 10^{-6}$ g | [8] |
| dry weight at puberty | 1 g | 1.022 g | Chauvaud, pers. comm. |
| ultimate dry weight | 20 g | 19.85 g | [9] |
| maximum reproduction rate | $5.753 \times 10^4$ eggs per day | $4.227 \times 10^4$ | [10] |

POM concentration in the water column is very variable and no clear pattern is identified during the year. Still, tremendous peaks can be seen in May of the years 1998, 2001 and 2003 with values up to almost $8 \times 10^6$ particles per liter, contrasting with the range of variation observed during the rest of the year (between 1 and $3 \times 10^6$ particles per liter). The curve presented here is the result of the deduction of algal cell counts from the total POM measured by the SOMLIT station, thus strong decreases are also observable when phytoplankton blooms occur (e.g. in June, July and December 2000 or in August 2003). Finally, Fig. 2.4 shows a relatively high inter- and intra-annual variability in the number of algal cells along the studied period. The lowest values are recorded in winter with values under $10^4$ every year and the first bloom appears in a very irregular way. Indeed, in 1998, 2001 and 2002 the first phytoplanktonic bloom event occurred in late February-early March whereas in other years it is delayed and only occurs between mid-April and June (in 2000). An other interesting feature is the yearly average of phytoplankton cells concentration, allowing to distinguish highly productive years from unfruitful ones. It appears that 2002 would therefore have been the worst year with only 143 759 cells $L^{-1}$ followed by 1999 and 2003 with respectively 239 305 and 262 260 cells $L^{-1}$. Then come the more productive years, 2001, 1998 with respectively 392 150 and 439 278 cells $L^{-1}$ and eventually, 2000, the most productive year in terms of phytoplankton cell concentration with about 504 592 cells $L^{-1}$.

### 2.3.3 Feeding and food sources

Fig. 2.6 shows the functional responses $f_X$ and $f_Y$, of the two food types respectively and the total $f$ as the overall functional response of the scallop to the food supply. It pictures the alternation between the two food types available according to the period of the year. Phytoplanktonic concentration are very low until the end of winter and after mid fall (Fig. 2.4) whereas POM is present almost all the time. This results into a more elevated $f_Y$ at the beginning and the end of the year which falls under 0.1 the rest of time, when phytoplankton cells are more present. The functional response to POM concentration never reaches levels above 0.5 and are mostly fluctuating between 0 and 0.4. In 1998, it was never over 0.2 and reached a maximum in October 2002. To the contrary, the $f_X$ reaches high values almost all years during phytoplanktonic blooms, from 0.8 in June 2002 to May 0.99 in 2000 but is almost null in winter.

The two calibrated parameters in the simulations using the preference module were the maximum specific filtration rates $F_{Xm}$ and $F_{Ym}$. They account for the amount of water cleared when food particles of each type are in the environment. $F_{Xm}$ varied between $50\,L\,d^{-1}\,cm^{-2}$, in 2001 and $100\,L\,d^{-1}\,cm^{-2}$, in 2000 and $F_{Ym}$ from $2\,L\,d^{-1}\,cm^{-2}$, in 1998 to $4\,L\,d^{-1}\,cm^{-2}$, in 1999. Most of the $F_{Xm}$ were set around $50\,L\,d^{-1}\,cm^{-2}$ and most of the $F_{Ym}$ around $2\,L\,d^{-1}\,cm^{-2}$. No clear relationship is found between values of $F_{Xm}$ and $F_{Ym}$ and the phy-

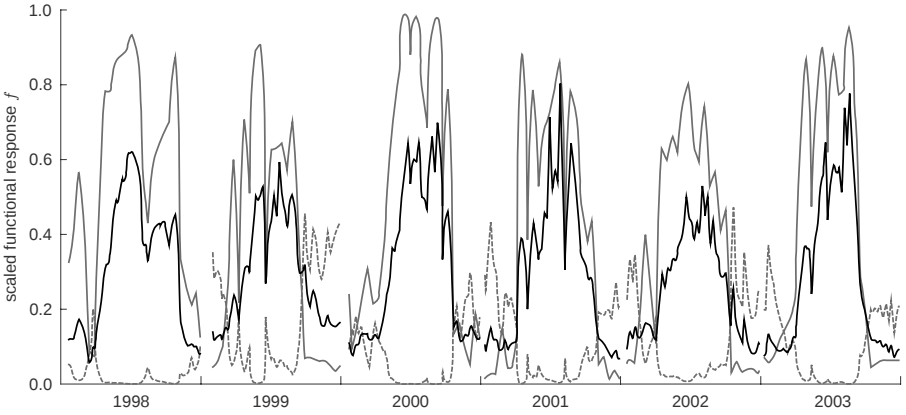


**Figure 2.6:** Scaled functional responses for the different food proxies in simulations of three-year-old *P. maximus* in the Bay of Brest between 1998 and 2003. The doted line represents the scaled functional response $f_Y$ for POM food type, the gray line is for scaled functional response $f_X$ for the microalgae food type and the resulting total scaled functional response $f$ is plotted by the dark line.

toplankton or POM concentration in the water. As for the value of $X_K$ in the simulations using only phytoplankton, it ranged from 40 000 # $L^{-1}$ in 2000 to 160 000 # $L^{-1}$ in 1998 and 2001.

### 2.3.4 Model simulation

Several physiological processes and life traits of three-year-old scallops were simulated using the DEB model from 1998 to 2003 in the Bay of Brest. Simulations of dry flesh weight are presented in Fig. 2.7. The model successfully captured the variations of dry weight along the seasons. Modeled weights using only one food proxy are less accurate than weight estimations resulting from the two-food-type assimilation module. The general pattern observed when the model is fed with one food source is an over-estimation in spring and autumn whereas at the end of the year, simulations often decrease too much compared to observations. Now concerning the simulations when both cell counts and POM are taken into account, a slight over-estimation in winter 1998 and 2000 is to be noticed, and a small under-estimation during winter 1999 too. The brutal weight losses that can be seen along the simulations account for spawning events which seem to have a rather low impact on the total body dry weight. Flesh growth is variable from one year to another but very similar between observed and simulated data: during year 2000, scallop dry weight increased of 4 g dry mass (5 g according to simulations) whereas in 2002 the gain in mass was only of 1.7 g dry weight (1.8 g according to sim-

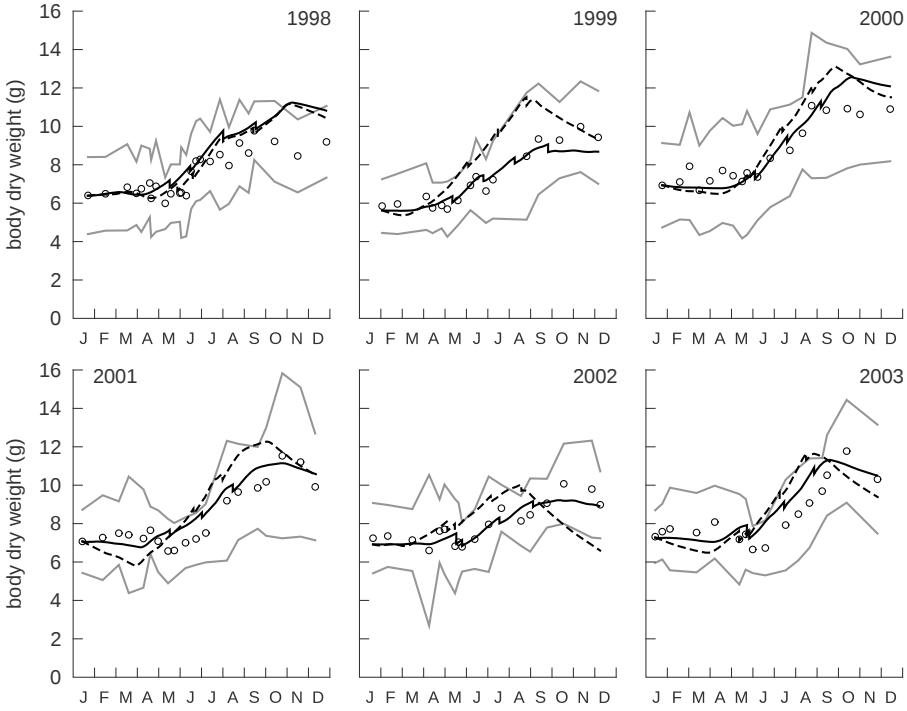


**Figure 2.7:** Simulated flesh dry weight (in g) of an average three-year-old individual of *P. maximus* in the Bay of Brest between 1998 and 2003, using phytoplankton counts (dashed dark line) and using POM as a supplementary food source (strait dark line). Dots are observed mean flesh dry weights (average on 20 individuals) of three-year-old great scallops collected in the Bay of Brest between 1998 and 2003 (EVECOS data base provided by "Observatoire Marin de l'IUEM, INSU, Plouzané"). Gray curves are upper and lower limits of the confidence interval ($p = 0.05$) for measurements.

ulations). The highest discrepancy between observed and simulated data is reached in 1998 as the model predicts a final dry weight 1.6 g heavier than the observations. That year, during the last months of growth, the observed weight loss (down to 8.5 g) was not reproduced as the model predicted a rather strong peak (11.2 g) in November. At the end of winter, scallops sometimes do not have enough energy in reserves and maintenance has to be paid from structural volume. The flesh dry weight can then loose few it is milligrams as observed between January and March 2001 and 2003 with a loss of 0.3 and 0.2 g dry weight respectively. The acceleration of growth rate from spring to mid-autumn is well reproduced every year, after which a decrease in the first months of winter is well simulated.

Shell growth was investigated in two complementary ways: (1) by examining the daily shell growth rate and (2) by looking at the cumulated growth in length. Fig. 2.8 shows the simulated DSGR for the six studied years. The observed data correspond to the cumulated average of DSGR measured on a sample of ten individuals of the three-year age cohort of the studied year. The lowest measured DSGR was $20.3\,\mu m\,d^{-1}$ (in 2001) and the highest was $156.2\,\mu m\,d^{-1}$ (in 2003) whereas the simulated DSGR ranges from 1 to $91.7\,\mu m\,d^{-1}$. Peaks of growth rate are hardly predicted but the simulated DSGR is still in the order of magnitude of the observations, except in 1998 and 2002 where a low growth is observed. Regarding the duration of the growing season, the simulations are in accordance with the observations. The resumption of shell growth is precisely captured by the model with an average time lag less than a week. An odd feature is observed during the first months of winter 1998, 1999, 2002 and 2003 where the model predicts a tiny growth in length ($<10\,\mu m\,d^{-1}$) at a moment of dormancy for *P. maximus*.

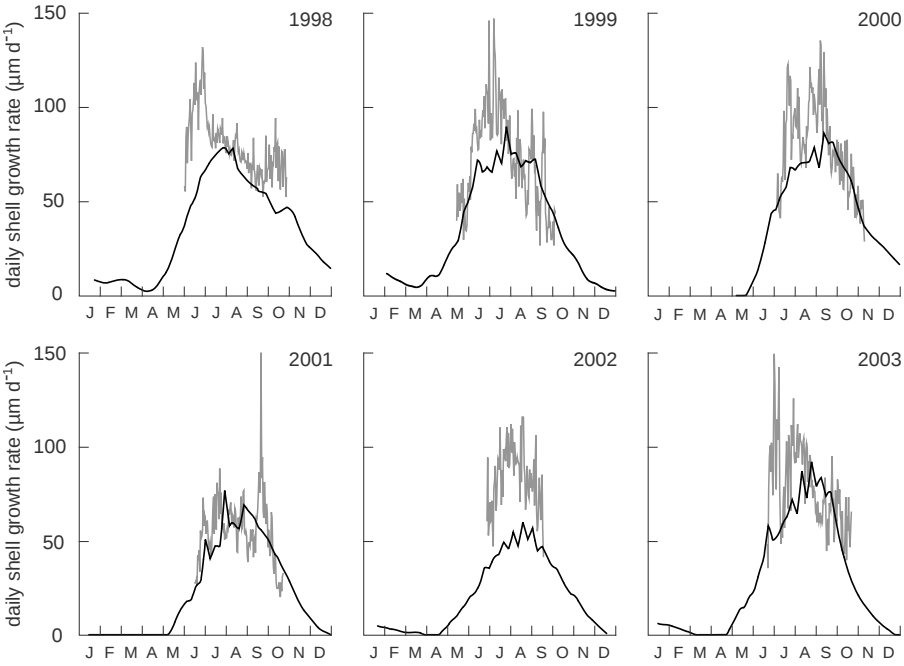


**Figure 2.8:** Simulated (dark line) daily shell growth rate (DSGR, in $\mu m\,d^{-1}$) of an average three-year-old individual of *P. maximus* and mean DSGR (gray line) calculated on ten individuals of three-year-old great scallops collected in the Bay of Brest between 1998 and 2003 (EVECOS data base provided by "Observatoire Marin de l'IUEM, INSU, Plouzané").

The shell lengths presented in Fig. 2.9 correspond to the cumulated growth in length. Simulated growth can here be compared to the observations with an emphasis on the final size of the animal at the end of the growing season. Here again simulated shell length using phytoplankton only are less relevant than those using algae plus POM. Growth always seems to start earlier in simulated data than in observed ones, which relates to the precocious low DSGR observed previously at the beginning of the year (see Fig. 2.8) and not taken into account in the observed data. The total increase in shell length (the shell length produced during the year) is very well modeled, with a slightly longer distance in the predicted data (still less than 100 µm), ranging from 0.05 mm in 2003 to 1.5 mm in 1999 or 2001. Except for the year 2002, the slope of the predicted growth curve is extremely similar to the observed one.

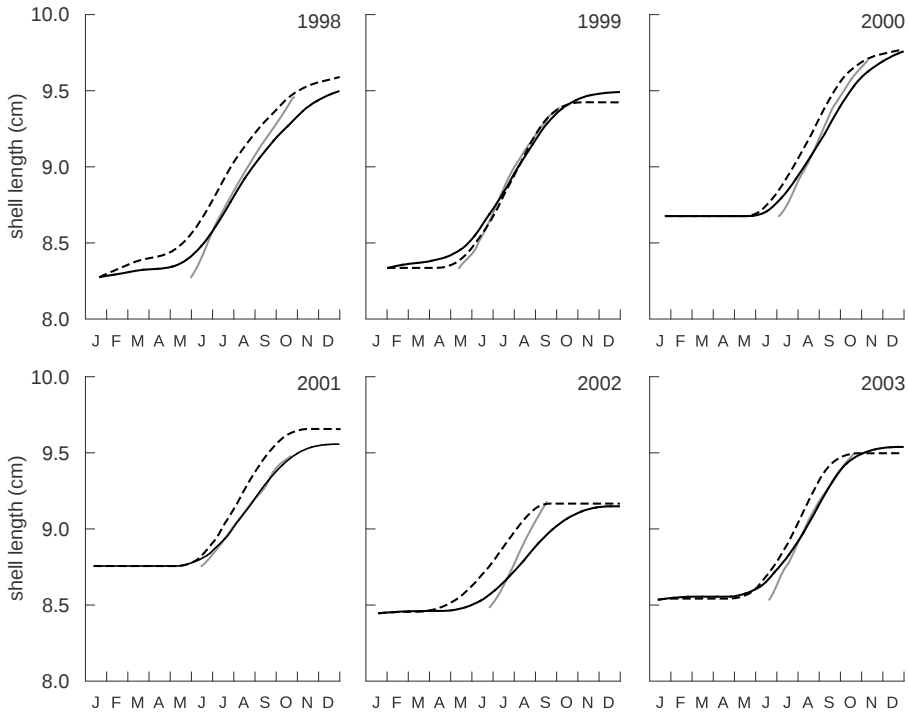


**Figure 2.9:** Simulated shell length (in cm) of an average three-year-old individual of *P. maximus* in the Bay of Brest between 1998 and 2003, using phytoplankton counts (dashed dark line) and using POM as a supplementary food source (strait dark line). Gray line is the observed mean shell length, measured on ten individuals of three-year-old great scallops collected in the Bay of Brest between 1998 and 2003 (EVECOS data base provided by "Observatoire Marin de l'IUEM, INSU, Plouzané").

The last biological trait studied is the gonado-somatic index (GSI), displayed in Fig. 2.10. *P. maximus* from the Bay of Brest are known to spawn in a very variable way, regarding the intensity, the number and the timing of spawning events between individuals and years. Except the slight overestimation at the end of years 1998 and 2001, the ratio of reproduction buffer over structure is rather well described by the model when the two food descriptors are taken into account. If only phytoplankton is considered, more decreasing periods are observed like in spring 1999, 2001 or autumn 2002, which does not match the observed data at these moments.

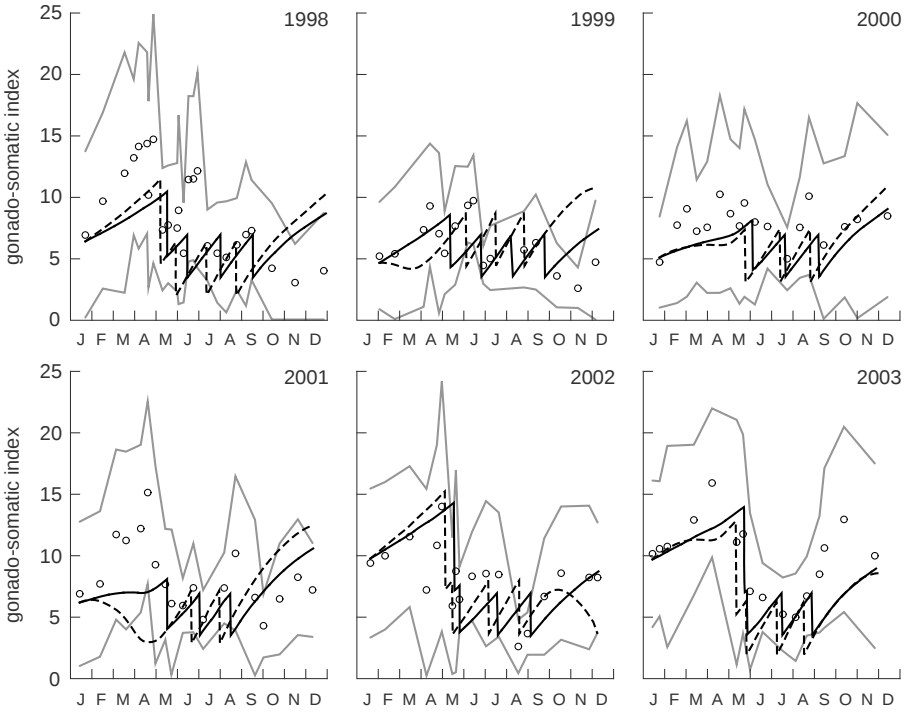


**Figure 2.10:** Simulated gonado-somatic index (GSI, in g) of an average three-year-old individual of *P. maximus* in the Bay of Brest between 1998 and 2003, using phytoplankton counts (dashed dark line) and using POM as a supplementary food source (strait dark line). Dots are observed mean GSI (average on 20 individuals) of three-year-old great scallops collected in the Bay of Brest between 1998 and 2003 (EVECOS data base provided by "Observatoire Marin de l'IUEM, INSU, Plouzané"). Gray curves are upper and lower limits of the confidence interval ($p = 0.05$) for measurements.

The timing of the first spawning event is accurately reproduced in the simulation (a little less when using only one food proxy). The spawning efficiency parameter set at 0.5, meaning that the gonad is half-flushed during spawning,

seems to be a relevant value since the simulated GSI do not fall below the lower bound observed.

The model response was also tested by the simulation of an average individual from its birth until several years of growth along the study period. Fig. 2.11 presents the growth curve of a great scallop born in June 1998 that lived five years in the Bay of Brest (environmental variables were the same as those used in previous simulations). Predictions made by the model are very realistic, producing a five-year-old scallop of 11 cm with a very low growth rate at this age, which closely matches observations. Finally, a last property of the model was highlighted by plotting DSGR data both observed and simulated against environmental variables to look at the effects of forcing parameters on growth. Fig. 2.12 shows for years 1999 and 2001 that simulated DSGR is strongly forced by bottom temperature. Functional response and thus food availability have minor effect on the modeled growth while it appears to be more determining when looking at the measured DSGR. This particularly holds true when the feeding response shows sharp decreases like in June 1999 or late August 2001.

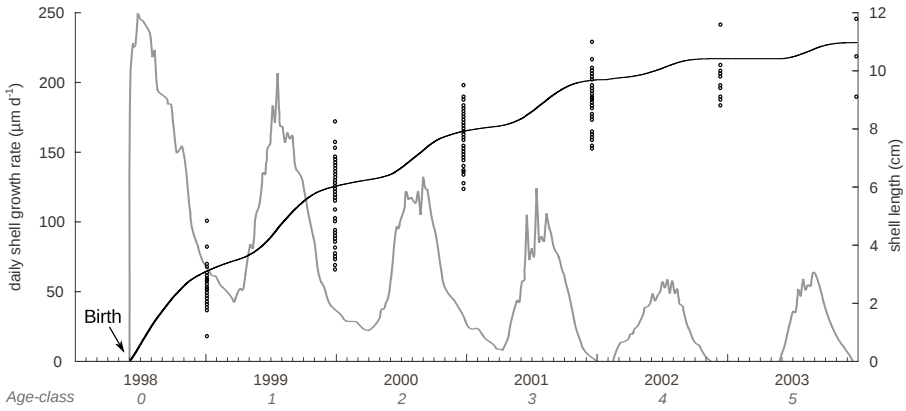


**Figure 2.11:** Simulated growth of an average individual of *P. maximus* in the Bay of Brest, from its birth in June 1998 until 2003. Shell length (dark line, in cm) is compared to the collection of shell length data (dots), gathered over decades in the Bay of Brest and archived in the EVECOS time series (EVECOS data base provided by "Observatoire Marin de l'IUEM, INSU, Plouzané"). Daily shell growth rate (in $\mu m\, d^{-1}$) is the gray line. Environmental variables (temperature and food markers) are the same as those used in simulations of three-year-old scallops.

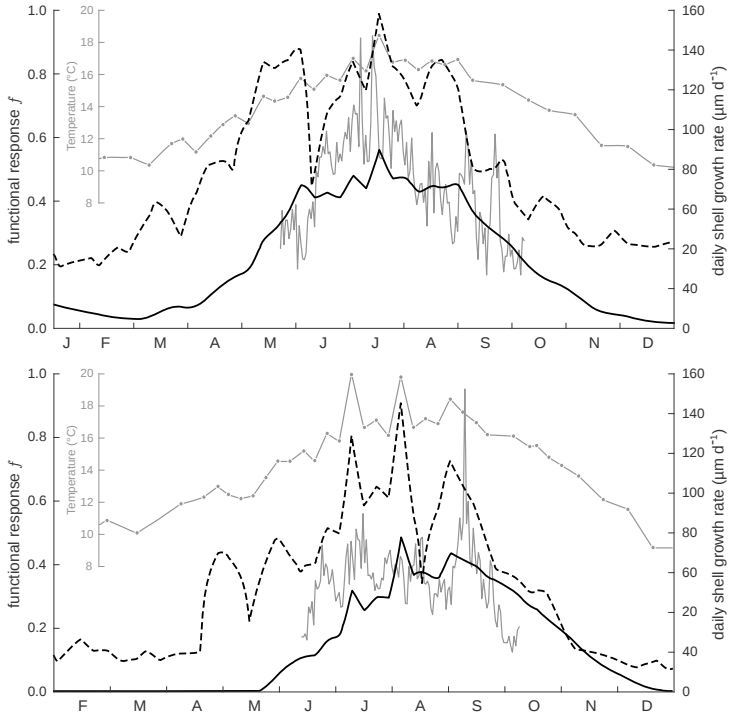


**Figure 2.12:** Simulated (dark line) daily shell growth rate (DSGR, in $\mu m\, d^{-1}$) of an average three-year-old individual of *P. maximus* and observed mean DSGR (gray line), calculated on ten individuals of three-year-old great scallops collected in the Bay of Brest (EVECOS data base provided by "Observatoire Marin de l'IUEM, INSU, Plouzané") in 1999 (a) and 2001 (b). Sea bottom temperature (gray line with dots, in Celsius degrees) and the total functional response $f$ (dotted dark line) are also plotted.

## 2.4 Discussion

### 2.4.1 Modeling the life-cycle of *P. maximus*

In this study, we used DEB theory to build a mechanistic bioenergetic model for *Pecten maximus* in the Bay of Brest, including a detailed formulation of the ingestion and food handling processes through the SU concept. The set of estimated parameters allowed us to reproduce the growth of an average great scallop individual during its entire life-cycle with a satisfying accuracy (Fig. 2.5). The age at metamorphosis was the only life trait that did not fit very well (Table 2.4), despite the addition of the acceleration module (Kooijman et al., 2011) to the standard DEB model. It may be linked to the low accuracy of the determination of age, size and weight at sexual maturity. This maturity

level is reported through the literature to be reached during the second year of life (Mason, 1957; Pazos et al., 1997; Chauvaud et al., 1998). A more precise knowledge of the timing of this critical life trait would certainly allow us to capture more efficiently the characteristics of other development stages.

The model was tested in the well studied environment of the Bay of Brest during six years of environmental monitoring and scallop sampling. Model predictions sometimes showed less good correspondence with measured data, like in 2002 when DSGR was hardly simulated, or at the end of the year 1998 when an over-estimation of dry weight is detected. It has to be noted that daily increments under 50 µm are very difficult to measure under binocular magnifier which tend to reduce the observed number of truly formed increments and the minimal size of striae observed. The model sometimes predicted slightly longer shell height which can easily be explain by the fact that archived shells have been manipulated many times causing damages to the ventral margin of the shell, i.e. the latest increments formed, which can have been abraded. But in a general way, the various physiological traits simulated in three-year-old individuals in the Bay of Brest were very similar to the observations made on wild population during this period.

All simulations presented here were made over one year and for individuals that belong to three-year age cohort, which correspond to an age between 2.5 and 3.5 years old. An interesting question is how the model behave in the long term, when scallops are grown from the egg to an advanced age. Fig. 2.11 shows that when the simulated animal reaches three years old in 2001 it can be compared to observations made this year on scallops of the same year-class (Fig. 2.8 and 2.9). Here again we see that this long term simulation is in accordance with observations.

### 2.4.2 Growth and feeding

An interesting pattern is that simulated DSGR is strongly impacted by bottom temperature, as shown in Fig. 2.12. This is in accordance with works of Chauvaud et al. (1998) who highlighted the major role of thermal conditions in normal growth variations (95 % of the variability explained by this factor). It is also in accordance with DEB theory and more generally with the Arrhenius relationship. This law states that all physiological rates, including the energy flux allocation from reserve to shell production (i.e. structure), are impacted by temperature. Concerning growth anomalies and short term variations in shell growth, it has been established that food was one the most triggering factor (Chauvaud et al., 1998; Lorrain et al., 2000). This pattern was not very well captured by the model compared to measured DSGR (Fig. 2.12). In 1999, scallops showed a daily growth divided in three periods: (1) a low start around 50 µm per day during few weeks, (2) then a sharp increase to more elevated values close to 90 µm per day with two peaks reaching 140 µm per day and (3) a progressive decrease punctuated with small and short peaks until a definitive stop in early October. The same profile was observed on one-year-old scallops

by Lorrain et al. (2000) for the same year. To the contrary, the model predicts a rather smoother growth along the growing period (which has still the same duration and timing), with a DSGR rapidly reaching a plateau around 70 µm and starting to decrease two months later than the observations but at a faster rhythm.

One objective of this work was to test the hypothesis of a selective ingestion of *P. maximus* between two substrates. When looking at the functional responses of the modeled individuals (Fig. 2.6), we see that $f_X$ reaches high values almost all years during phytoplanktonic blooms. To the contrary, $f_Y$ is rather low all along the year, which tends to confirm our guess. The maximum specific filtration rate for phytoplankton cells ($F_{Xm}$), which was calibrated to fit the observed data, varied between 25 and 100 $\mathrm{L\,d^{-1}\,cm^{-2}}$ respectively. This corresponds to values of 11 and 44 $\mathrm{L\,h^{-1}}$ per individual, which is in accordance with literature values (Shumway and Parsons, 2006; Strohmeier et al., 2009; Cranford et al., 2011). On the other hand, $F_{Ym}$ varies at a far more lower level, between 2 and 4 $\mathrm{L\,d^{-1}\,cm^{-2}}$. This clearly indicates that substrate X (phytoplankton cells) is positively selected compared to substrate Y (rest of POM), which confirms our hypothesis. It is relatively easy to understand this when considering the high energetic quality of fresh phytoplankton cells compared to suspended matter, which includes organic debris (Alber and Valiela, 1996). The use of the POM proxy as a second food source, yet under-selected, showed its benefits compared to simple diet simulations. POM seems to be an additional food source allowing scallops to compensate phytoplankton limitation between algae blooms. Indeed some studies already brang evidences of organic aggregates and flocs assimilation in scallops, although less efficiently than phytoplankton (Alber and Valiela, 1996; MacDonald et al., 2006).

Even if the maximum specific filtration rate is in compliance with already reported data, one can see that its variation range is rather large. Although the model is entirely deterministic, we still face the fact that the filtration rate is obtained by calibration, as it used to be the case with the half-saturation constant in previous DEB models. Possible reasons for such differences among years might rely on the inter-individual variability. Indeed, animals collected at the very same moment and selected in the same year class showed considerable heterogeneity in biometric measurements (see the confidence intervals of observed data on Fig. 2.7 and 2.10). Moreover, consequent amounts of inorganic particles from riverine inputs are discharged in the Bay of Brest and could also cause annual variations in the mean filtration rate. Indeed, filtration rates of filter feeding bivalves are negatively impacted by these non-edible particles inputs, which compete with food particles (Kooijman, 2006; Saraiva et al., 2011a). To improve the determinism in the maximum specific filtration rate estimation and avoid calibration steps two conditions are required: (1) integrate the effect of non-edible particles via a third substrate for SUs as done by Saraiva et al. (2011a), (2) include feeding experiment data into the parameter estimation procedure to better determine filtration and ingestion rates parameters.

A recurrent issue in individual bioenergetic modeling is the choice of a good food proxy. Some studies relying on DEB theory to model bivalve bioenergetics have already raised this problem (Pouvreau et al., 2006; Bourlès et al., 2009; Rosland et al., 2009). Bourlès et al. (2009) tested different types of trophic markers like particulate organic matter, particulate organic carbon, chlorophyll-*a* concentration and phytoplankton enumeration. It came out that chlorophyll-*a* concentration, albeit being easily monitored, was not sufficient to capture all the variations observed in the physiological processes studied. On the other hand, they showed that microalgae expressed in cell number per liter should be considered as a better food marker. This approach worked efficiently for *C. gigas* and also seems to be relevant for *P. maximus*. Fig. 2.12 also shows that the simulated ingestion represented by the functional response is in accordance with the observed DSGR, except in early August 2001 when no growth increase is observed whereas the model shows a rather high ingestion.

Deviations between the model and data that might be addressed by a better descriptor of the trophic source that would integrate food quality. Indeed, Lorrain et al. (2000) have shown that the DSGR of one-year-old scallops in the Bay of Brest could be negatively impacted by the presence of some phytoplanktonic species such as diatoms *Ceratolina pelagica* or *Rhizosolenia delicatula*, responsible of short drops in the daily growth of these animals in early May 1998 and 1999. However, since we used individuals from the three-year age cohort who started their shell growth later in the year due to their age (late May and June respectively), we did not observed such effects. Moreover, DSGR of three-year-old scallops is two times lower than in younger individuals. It is thus difficult to see the variation of ingestion according to food biomass from the DSGR profiles in our study. A perspective to the present study could consist in testing differential ingestion rates for *P. maximus* when the phytoplanktonic biomass is dominated by some algae species during crucial period of the growing season (e.g. when the great scallop is also about to start to reproduce and complete its gamete maturation).

### 2.4.3 Reproduction

Modeling reproductive activity is not a simple task, especially for *P. maximus*, an asynchronous spawner that only flush partially its gonad during highly variable spawning events. DEB theory do not specify how to handle reproductive effort in a general way, each species needs a specific implementation. In our model, spawning triggering requires data that are already necessary to run a DEB model (temperature and food) plus a photoperiod signal. It is well known that parameters potentially bringing about gamete release in scallops are numerous, including temperature, food availability, photoperiod but also lunar phase, salinity, dissolved oxygen, pH, mechanical shocks and ectocrines (Barber and Blake, 2006). Therefore, we were motivated to take into account the most recognized factors. The resulted simulated GSI is acceptable as it

reproduces the general pattern of gonad dynamics (Fig. 2.10). The predicted start of gametogenesis in winter matches the observed data, except in 1998 and 2001, where the increase of the simulated index is not as sharp as in the observations. During winter, energy stored in the reproduction buffer $E_R$ is not only used to produce gametes but also to meet maintenance requirements if reserves are not sufficient to do so under seasonal starvation. The fact that this energy would be used for two different processes during the same period (Mason, 1957; Lorrain et al., 2002) might explain the general under-estimation observed at the beginning of the winter. A study of the biological cycles of *P. maximus* carried out by Paulet et al. (1997) brings another look on the mechanisms involved in the compartment dynamics. Paulet and co-workers described the complex evolution of the gonad in relation to somatic tissues along the year. They showed that gametogenesis presented a stop in October and November, another one at the end of the winter and a maximum gametic production period in April and May. This is consistent with our results except for the late autumn stop. As non-emitted gametes during spawning events are resorbed and eliminated during fall, they provide energy to other tissues thanks to atresia (Le Pennec et al., 1991). Exploring this phenomenon in more details could improve the simulation of reproductive effort of *P. maximus* at the end and the beginning of the year (but at the expense of the model simplicity). Eventually, the mismatch between simulated and observed data in early 1998 and 2001 might also suffer from a rather elevated value of$\kappa$ (0.86) compared to other bivalve species such as the Pacific oyster (0.45 in van der Veer et al., 2006) or the blue mussel (0.67 in Saraiva et al., 2011b; 0.45 in Rosland et al., 2009).

Bernard et al. (2011) tried to improve the implementation of the reproductive effort in the DEB model of *C. gigas* in relation to environmental conditions. They adopted an approach involving the creation of a new state variable (the gonad structure) plus three additional parameters, while using derivatives of temperature as signals to begin and end the gametogenesis. However, those manipulations did not significantly addressed the bad fit of simulated gamete releases compared to observed data. Moreover they reported only one spawning event for *C. gigas* whereas several ones are clearly identified in *P. maximus* biological cycle, which may reduce the difficulty to accurately simulate it. One of their conclusion was to put more emphasis on the intake of energy rather than on the reproductive activity. But eventually, when looking at both studies, one focusing on the modeling of reproductive effort and ours on ingestion modeling, results are very similar.

To finish, one step not yet reached by this model is the simulation of the number of gametes emitted. In the current state, our model considers that the flux of reserve $\dot{p}_R$ is used either for maturation (when in the juvenile stage) or to fuel the reproduction buffer (after reaching the adult stage) from which gamete production is accomplished. Modeled reserves in the reproduction buffer are not necessarily used immediately for gamete production. This has a repercussion in the simulation of this index, which can show a too great increase at the end

of the year (especially in 1998 and 2001) compared to the field data. This could be explained by two means. First, it is possible that a very late spawning event occurred, outside the generally expected period in this location (from May to July; Paulet et al., 1997). Incidentally, this late spawning would probably not be significant for the population growth, since larvae hatching at this period of the year would hardly survive to bad food condition of autumn. The second possible cause relies on the already invoked atresia hypothesis. This phenomenon is not integrated into the model and would require additional parameters. In order to keep a relatively low complexity level of the model and because this physiological process was already rather well simulated (our estimations are still in the confidence range of the data variability) we did not implemented this pattern into the model.

### 2.4.4 Conclusions and perspectives

In this study we implemented a DEB model for the great scallop, *P. maximus*, in the Bay of Brest using the Synthesizing units concept to model energy acquisition. Primary parameters were obtained by the covariation method for parameters estimation (Lika et al., 2011a), producing estimates able to reproduce life-cycle history traits with still a slight underestimation of the age at metamorphosis. Various physiological processes such as growth in weight, shell growth or reproductive activity were accurately modeled and successfully matched observation data over a six-years study. To complete the validation of this model we need to test the set of parameters on an other population living in a relatively different environment such as the cold and eutrophic fjords of Norway for instance.

Results of this work showed that assimilation even if well implemented in the model still requires some improvement and a deeper reflection, especially concerning the trophic input. We did not addressed the issue of the determinism of energy input as the maximum filtration rate still requires a calibration. However we brought tools to develop and improve the way feeding of filter feeders is formalized within DEB theory. Saraiva et al. (2011a) went further deep into the description of filtration, ingestion and assimilation processes in mussels *M. edulis*. By taking into account silts as an other potential substrate for SU, they were able to describe these processes through a DEB model, considering the effect of non-edible particles on energy allocation. As the Bay of Brest receives high riverine inputs from two rivers and underwent a recent invasion by the slipper limpet *Crepidula fornicata* causing a significant silting up of the bay's sea-floor (Thouzeau et al., 2002), it would be interesting to look at the response of the model when fueled by both organic and inorganic matter.

It has long been suspected that filter feeders and especially *P. maximus* could be able to select algae cell types according to their chemotactile attractiveness, size or shape (Raby et al., 1997; Ward and Shumway, 2004). The state of freshness of phytoplankton cells might also be critical so efforts should

be deployed to find food markers able to describe the quality of the trophic resource. Moreover, recent works have reaffirmed through isotopic analysis the presence in *P. maximus*'s diet of bacteria (Nerot et al., 2012). It must also be interesting to look at this feature but certainly much more difficult to assess the bacterial biomass in the environment.

## Acknowledgements

We would like to thank the "Service d'Observation en Milieu Littoral, INSU-CNRS, Brest" and the REPHY network (PHYtoplankton and PHYcotoxins monitoring NEtwork, Ifremer) for providing the environmental data. The authors also recognize A. Jolivet for the great help in shell growth analysis and the proofreading of this paper. Part of the funding of this work was provided by the COMANCHE ANR program (ANR-2010-STRA-010).

# Chapter 3

# An application of the DEB model to define scallop habitat

**Modeling the distribution of the Great scallop *Pecten maximus* in the English Channel: linking physical and biological processes to define scallop habitat**

*Manuscript in preparation for submission in Journal of Marine Systems*

Clément Le Goff, **Romain Lavaud**, Philippe Cugier, Jonathan Flye-Sainte-Marie, Eric Foucher and Fred Jean.

**Abstract**
The great scallop *Pecten maximus* is currently the most important species in landings (as well in tons as in value) for the French inshore fleet of the English Channel. A modeling approach has been proposed in order to better understand the determinism of the distribution of the great scallop, integrating both physical and trophic constraints. A 3D bio-hydrodynamical model (ECO-MARS-3D developed at Ifremer) providing environmental conditions has been coupled to a population dynamics model and an individual bioenergetic model, based on the Dynamic Energy Budget (DEB) theory. The population model describes the whole life cycle of the great scallop (planktonic and benthic stages) and is structured in age classes. The steady state is reached after approximately 30 years and some features of *P. maximus* distribution are reproduced and compared with in-situ data. The individual DEB model, allows

the calculation of a growth potential in each part of the English Channel. This approach provides a spatialization of environmental conditions that are favorable enough to allow the survival of *P. maximus* individuals. It also gives information about adult's fecundity (intensity and distribution) that are used in the population dynamic model. This study contributes to the understanding of the biogeographical distribution of the great scallop and especially enlightens the respective role of biological or physical factors in defining its habitat in the English Channel.

**Keywords:** *Pecten maximus*; Dynamic Energy Budget; modeling; population dynamics; English Channel

## 3.1 Introduction

*Pecten maximus* (L.) is exploited all along its latitudinal range, from Norway to Portugal and is an economically important species particularly in the English Channel where it represents the first species in landings (as well in tons as in value) for the French inshore fleet of this area. In addition to its broad distribution and its high economic value, the biology and ecology of this species have been widely studied (Mason, 1957, 1958; Antoine, 1979; Paulet et al., 1988; Chauvaud et al., 1998; Laing, 2000; Le Pennec et al., 2003; Brand, 2006a; Cragg, 2006; Thompson and MacDonald, 2006; Nerot et al., 2012). However, except for few locations such as the Bay of Seine and the Bay of Saint-Brieuc (the two main French fisheries), its distribution and its abundance at the regional scale is still poorly known, only presence/absence data are available. This constitutes a primordial point of interest for ecological scientific reasons as well as for fisheries management issues.

Benthic marine species distribution is driven by many biotic (ecological interactions with competitors and predators, food availability) and/or abiotic factors (temperature, depth availability, substrate type, water currents, turbidity, oxygen concentration and salinity). There have been very few experimental studies carried out under controlled conditions to determine the effects of any of these factors on scallop growth, reproduction or survival (Laing, 2000, 2002, 2004), so it is generally difficult to assess the ecological significance of particular factor (Brand, 2006a). The different life stages have to be taken into account, especially in the case of a meroplanktonic species like *P. maximus*, spending part of its development in the pelagic domain (as a larvae) and the rest of its life on the bottom of the ocean. The mechanisms providing suitable environmental conditions for the settlement and the development of such organisms have thus to be considered simultaneously in order to determine the potential of survival and growth of the individuals in one particular habitat.

Numerical models appear to be powerful tools to integrate processes of such different nature and time scales (local/regional, individual, population and ecosystem levels) and investigate variable environmental conditions and different individual responses. Moreover, the coupling of environmental mod-

els to individual models allows one to deal with these different scales and specific constraints. Several authors have dynamically coupled biogeochemical model to physiological models in order to study the interaction between marine invertebrates and their environment. Eulerian models have been often used to model hydrodynamical variables inside fixed volumes of space, within which nutrients and primary production were subsequently implemented (e.g. Batchelder et al., 2002; Savina and Ménesguen, 2008; Huret et al., 2010; Ibarra et al., 2014). Various approaches have been developed concerning the physiological modeling of bivalves and a particular interest have been shown in coupling these models to other models describing the environmental dynamics in order to studying the carrying capacity of ecosystems. Cugier et al. (2010) assessed the role of benthic filter feeders on phytoplankton production in a shellfish farming site through an physiological framework integrated in a 2D biogeochemical model. Grant and Bacher (2001) and Grant et al. (2008) used scope for growth models in the study of flow and seston modification respectively in suspended mussels aquaculture. Less empirical approaches made use of Dynamic Energy Budget (DEB) theory to model individual physiology (Maar et al., 2009; Grangeré et al., 2010; Guyondet et al., 2010). Finally, Dabrowski et al. (2012) developed a modeling system coupling a DEB model for the blue mussel, a NPZD model and a high resolution 3D numerical model of south-west Ireland featuring an intensive bivalve aquaculture activity.

The aim of this study is to better understand the distribution of the great scallop in the English Channel using a modeling approach. Linking physical and biological processes was achieved by coupling four models: a hydrodynamic model linked with a primary production one, a population dynamic model and an individual bioenergetic model. We analyzed the physiological capacities of sub-populations in relation to environmental conditions and compare the modeled dispersion to the actual knowledge of the distribution of the great scallop in the English Channel.

## 3.2 Material and methods

### 3.2.1 Hydrodynamical and biogeochemical models

The three-dimensional (3D) hydrodynamic model MARS (Model for Applications at Regional Scale; Lazure and Dumas, 2008) was used to simulate the circulation in the study area (Fig. 3.1). It is a finite difference, mode splitting model in a sigma-coordinate framework. The MARS-3D model has been validated in the Bay of Biscay from survey data and satellite observations of currents, salinity, and temperature (Lazure and Dumas, 2008). It was here applied to the English Channel, from 47°88'N to 51°15'N in latitude and from −7°03'W to 3°0'W in longitude (Fig. 3.2). The study area grid was divided in 2 per 2 km meshes with a vertical resolution of ten sigma layers. Currents velocity, temperature and salinity fields were computed here.

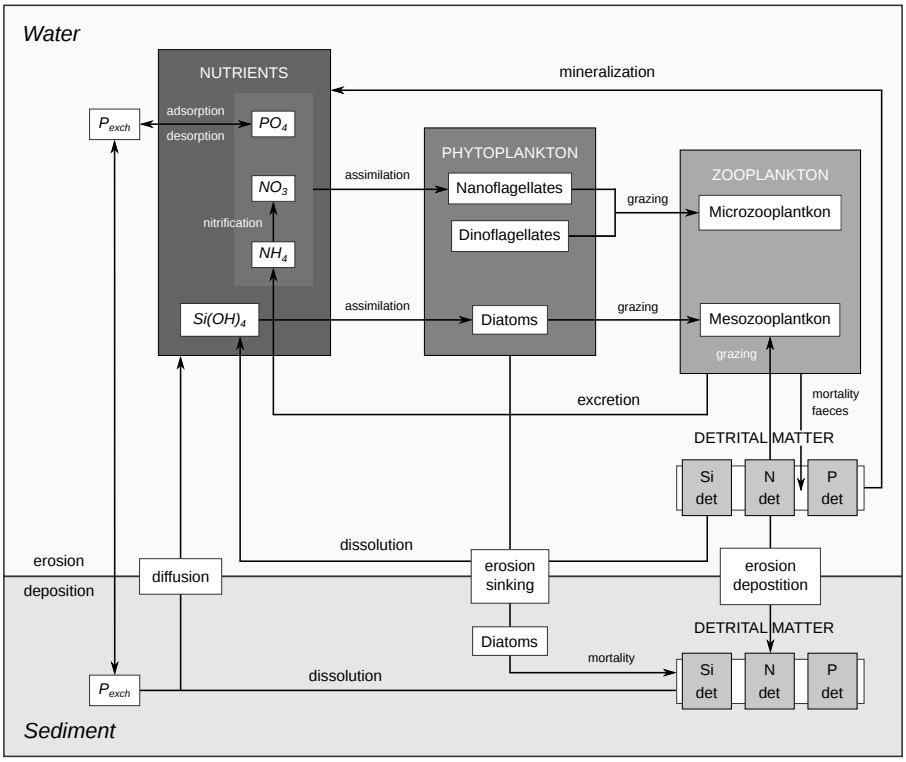


**Figure 3.1:** Scheme of the ECO-MARS-3D model. Nutrient, phytoplankton and zooplankton are modeled to calculate primary production.

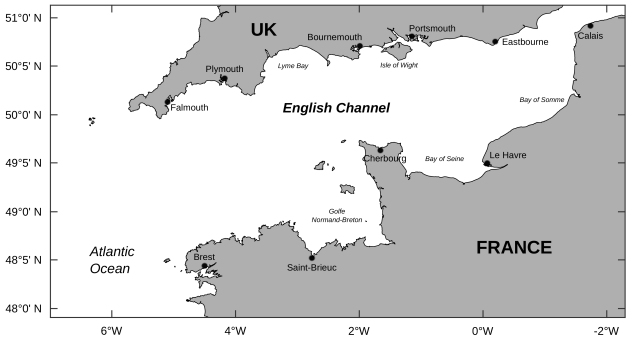


**Figure 3.2:** Simulated area in the English Channel. The horizontal resolution is 2 km and the vertical one is based on 10 sigma layers.

The type of sediment is indirectly taken into account through current modeling, which rely on tide and geographical position. High speed currents are found on coarse sand, gravels and rocky substrates whereas low speed currents are found on muddy flats and fine grain sandy beds.

The primary production model ECO-MARS-3D was used to get a trophic source proxy for the following individual model. It is the result of a coupling between a NPZD-type biogeochemical module and the MARS-3D model (Huret et al., 2010). Nutrients and phytoplankton concentrations dynamics were predicted on the basis of the nitrogen, phosphorus and silica cycles. The Phytoplankton compartment is represented by three variables: diatoms, dinoflagellates and nanoflagellates. Both of them are originally expressed in the form of their nitrogen content. The three variables were combined into a single one which was then expressed in chlorophyll-*a* concentration.

### 3.2.2 The population dynamic model

As for most bivalve species, the development of *P. maximus* takes place in the water column during the larval stage. After a pelagic dispersal period of 30 days in average, larvae settle on the substrate and achieve metamorphosis (Gruffydd and Beaumont, 1972; Le Pennec et al., 2003). Scallops spend the rest of their life on sea bottom. The modeling of population dynamics was inspired by the works of Savina and Ménesguen (2008) on *Paphia rhomboïdes*. The larval pelagic life duration was split into ten age classes, respectively described by the larval abundance in the water column ($\#\ m^{-3}$). Aging of individuals, i.e. the transition from one age class to the next one, was operated every three days (Fig. 3.3). The abundance was computed as the result of three processes: (1) recruitment of individuals from the previous age class (including the arrival of freshly spawned larvae), (2) mortality (taken to be constant during this life stage with a value of $0.5\,d^{-1}$) and (3) aging (i.e. transfer of individuals to the next age class). Abundance also depends on spatial fluxes

**Table 3.1:** List of the DEB parameters used in the individual physiological model of *P. maximus* (from Lavaud et al., 2013).

| *Description* | *Symbol* | *Value* | *Unit* |
|---|---|---|---|
| *Primary parameters* | | | |
| shape coefficient | $\delta_{\mathcal{M}}$ | 0.36 | – |
| fraction of mobilised reserve allocated to soma | $\kappa$ | 0.86 | – |
| energy conductance | $\dot{v}$ | 0.021 | $\mathrm{cm\,d^{-1}}$ |
| volume–specific maintenance costs | $[\dot{p}_M]$ | 33.52 | $\mathrm{J\,cm^{-3}}$ |
| volume–specific costs for structure | $[E_G]$ | 2959 | $\mathrm{J\,cm^{-3}}$ |
| maximum surface–specific assimilation rate | $\{\dot{p}_{Am}\}$ | 94 | $\mathrm{J\,d^{-1}\,cm^{-3}}$ |
| maturity maintenance coefficient | $k_J$ | 0.002 | $\mathrm{d^{-1}}$ |
| maturity at birth | ${E_H}^b$ | 0.000 28 | J |
| maturity at metamorphosis | ${E_H}^m$ | 0.0078 | J |
| maturity at puberty | ${E_H}^p$ | 3000 | J |
| maximum reproduction rate | $R_i$ | $4.227 \times 10^4$ | eggs per day |

of larvae between boxes of the model: horizontal advection and dispersion as well as vertical diffusion and sedimentation (leading to settlement) were driven by the current modeling within the hydrodynamical MARS-3D model.

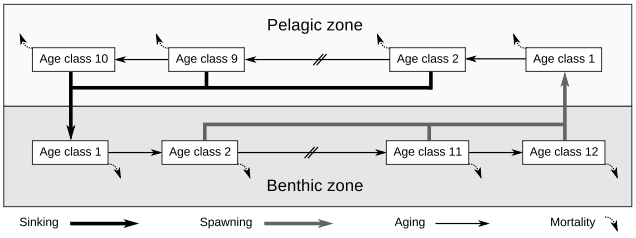


**Figure 3.3:** Structure of the population dynamic model, divided into two compartments: the pelagic zone where *P. maximus* hatches and lives during 30 days as a larva (sub-divided into 10 age classes) before to settle on the sea bottom, i.e. the benthic zone where *P. maximus* spend the rest of its life (sub-divided into 12 age classes.

The adult benthic compartment was split into 12 annual age classes, each being described by its abundance. The abundance was computed as the result of the same three processes: recruitment (including the arrival of young adults from the oldest larval age class), mortality (exponential law) and aging (transfer of individuals to the next age class every year). Spawning is modeled using a Gaussian laws and the amount of egg released was first determined as a mean according to *P. maximus*' reproduction rate (Table. 3.1; Lavaud et al., 2013).

### 3.2.3 The individual physiological model

#### Basic concepts

The third model is an individual bioenergetic model based on Kooijman's Dynamic Energy Budget Theory (Kooijman, 2010) and developed for the great scallop by Lavaud et al. (2013, see Chapter 2). DEB theory defines a mechanistic framework that quantifies energy fluxes to predict growth, reproduction, maintenance from a species specific set of parameters and an environmental forcing including temperature and a food proxy (Fig.3.4). The individual biomass is divided in two compartments: structure and reserve, distinguished by their dynamics. The state variables of the model are $E$, the amount of energy in reserve (J), $V$, the volume of structural mass ($cm^3$) and $E_R$, the reproduction buffer (J), corresponding to the fraction of reserve allocated to reproduction. Energy assimilated from food is converted with a constant efficiency into a reserve pool from which it is mobilized to the various metabolic processes. Reserve dynamics is computed as the difference between assimilation flux and mobilization flux. A fixed proportion $\kappa$ of this mobilization flux is allocated to somatic growth plus its maintenance with priority to maintenance and the remaining fraction (1-$\kappa$) is spent on maturity (maturation, maturity maintenance and reproduction). Temperature controls every rate as a consequence of the Arrhenius law. Detailed equations of fluxes have been described by Lavaud et al. (2013).

#### Feeding

Energy that fuels all processes in the organism is taken from food provided by the environment. This forcing variable in our study was obtained from the biogeochemical model ECO-MARS-3D under the form of chlorophyll-*a* concentrations. Food intake was converted to an assimilation flux via a Holling type II functional response $f$ written as: $f = \dfrac{X}{X_K + X}$, where $X$ is the food density in the environment and $X_K$ the half-saturation coefficient. This constant is known to be site-specific in the Pacific oyster (Pouvreau et al., 2006). Alunno-Bruscia et al. (2011) reported a significant linear relationship between $X_K$ and the mean annual concentration of phytoplankton of 11 sites along French coasts ($X_K = 1.05$ [Chl-$a$] + 163.48 with $R^2 = 0.77$; n = 11). We used this equation to calibrate the $X_K$ value in the very well known location of the Bay of Saint-Brieuc, which was then applied to every point of the study area and kept unchanged for the whole duration of the simulation. The assimilation rate $\dot{p}_A$ (J) is then calculated by: $\dot{p}_A = \{\dot{p}_{Am}\} f V^{(2/3)}$, where $\{\dot{p}_{Am}\}$ is the maximum surface-specific assimilation rate ($J\,d^{-1}\,cm^{-2}$).

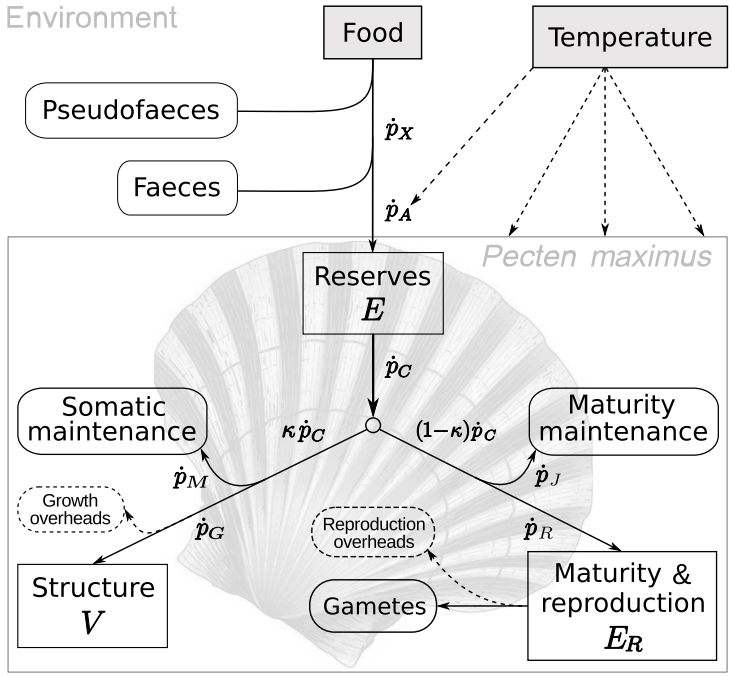


**Figure 3.4:** Conceptual scheme of the DEB model applied to the scallop *P. maximus*. Food and temperature are the forcing variables (in gray) and reserves ($E$), structure ($V$) and maturity/reproduction ($E_R$), are the state variables (in white boxes). Dark arrows show energy fluxes and dotted arrows indicate temperature's influence on these rates.

### 3.2.4 Coupling of the models

#### Population dynamic model and MARS-3D

In a first step we coupled the hydrodynamic model to the population dynamic model by inserting variables such as concentration of larvae and density of adults. We used very basic biological parameters such as the same numbers of eggs spawned by every age class and a mortality scheme only depending on the age and the density of *P. maximus*. This basic coupling allowed us to know the impact of larvae dispersion (hydrodynamic aspect) in the establishment of the population of *P. maximus* in the English Channel without the influence of food availability and temperature.

#### DEB and ECO-MARS-3D

Further, we used the outputs of the NPZD model (ECO-MARS-3D) previously mentioned as food (chlorophyll-$a$) and temperature inputs for the DEB

model. In each cell of the grid we simulated the life of *P. maximus* from birth during seven years (from 2000 to 2006). We calculated the dynamic evolution of weight, growth in length and the number of eggs produced of an average individual in each cell. Hence, we obtained an approximation of the spatialized potential growth in the English channel and the spatialized production of eggs for each age class. The simulations started with newly hatched larvae of 80 µm, $1 \times 10^{-7}$ g DW and a reserve compound filled at its maximum. The number of eggs spawned by individuals over seven years old was set to the number of eggs spawned in the seventh year of life. The number of eggs spawned for each point and for each age class was taken to be constant from year to year.

### Coupling the four models

Finally, we coupled the four approaches. We again used the exponential mortality laws and the mortality density dependence but we used the spatialized production of eggs for the entry of new individuals in the population. Simulations were compared to data gathered from the literature (Mason, 1983; Abbes, 1991; Pitel et al., 2001; Tully et al., 2006), scientific cruises reports (SHP Cruise, NBN Gateway), technical reports of scientific institution which monitor fishing resources in the English Channel about the distribution of the great scallop (SPUE Devon, Ifremer, CEFAS) and unpublished literature (Bay stocks, Fishermen and divers).

## 3.3 Results

### 3.3.1 Hydrodynamical stabilization

The simulations presented in Fig. 3.5a were conducted with the hydrodynamical model coupled to the population model. It shows the distribution of the scallop population thanks to larvae transport without any constraint from other factors except hydrodynamism. High abundance were observed along the British coasts, in the Golfe Normano-Breton, in the Bay of Seine and in the oriental part of the English Channel. Lower densities were modeled in the center of the studied area and in the occidental region as well as along Brittany's coasts. Highest number of scallops were found in the bays such as the Mont-Saint-Michel Bay, the Bay of Seine, Falmouth Bay, Lyme Bay and around the Isle of Wight.

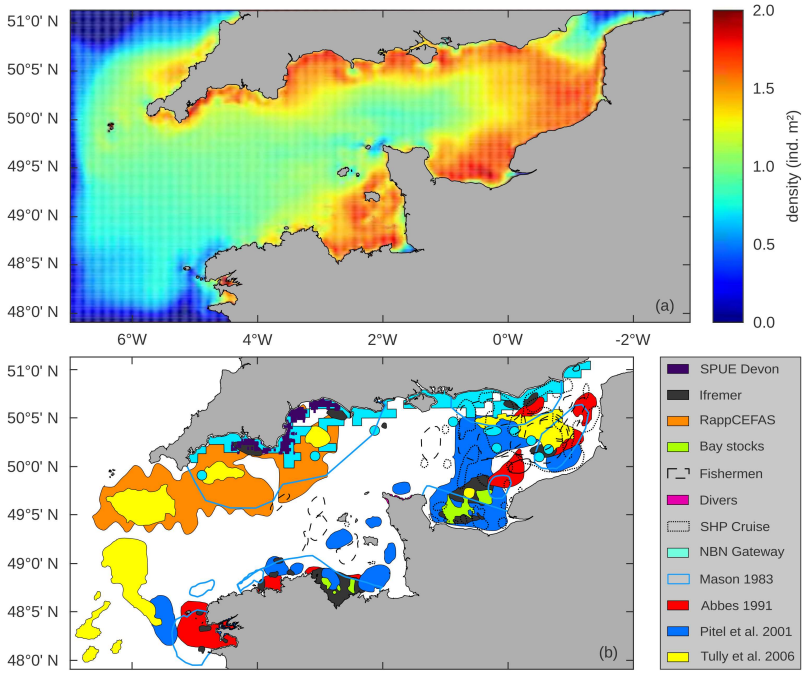


**Figure 3.5:** (a) Distribution map of *P. maximus* population (in number of individuals per squared meter) after 27 years of simulations coupling the hydrodynamical with the population dynamics models. No influence of other environmental factor than hydrodynamism explains the dispersion. (b) Distribution map by presence/absence of *P. maximus* in the English Channel from various information sources (scientific articles, scientific cruises reports and technical reports, see detail in the text).

When compared to the map of presence/absence of the great scallops according to the literature (Fig. 3.5b), occurrence patterns are rather well respected. However the density level seems very high, with more than 0.75 scallops per $m^2$ in the whole studied area.

### 3.3.2 Physiological performances

The individual bioenergetic model (DEB model) was then coupled to the biogeochemical model in order to picture the physiological potential of scallops according to the environmental in each point of the grid. Fig. 3.6 shows the predicted shell length of an average individual in each cell of the grid after a simulation over seven years. The average height of the shell in the whole studied area was around 11 cm and increased up to 15 at the head of the Bay of Seine, the Bay of Somme and in the strait between the Isle of Wight and England. In the eastern half, it increased up to 12–13 cm along the coast. In the occidental part of the English Channel, the size after seven years did not reach 10 cm. A similar pattern was observed concerning in simulations of the dry weight (3.7), with an averaged flesh mass of 40 g DW and individuals weighting up to 55 g in the Golfe Normano-Breton and at the mouth of the Seine and the Somme rivers.

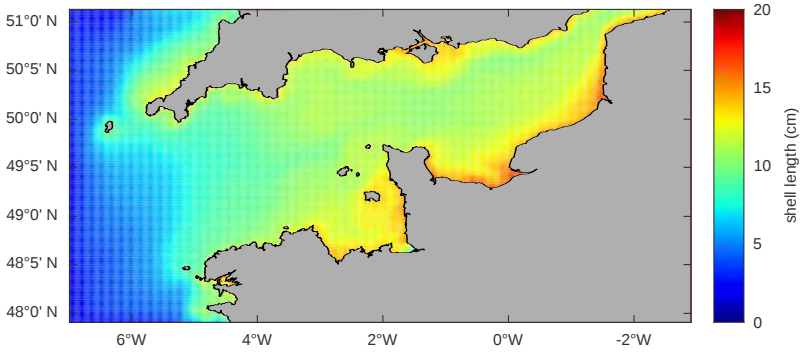


**Figure 3.6:** Structural length in cm of an average individual of *P. maximus* in each grid cell, predicted by the DEB model forced by environmental data (ECO-MARS-3D) after 7 years of simulation.

Regarding the reproduction activity, two patterns were observed. First, the cumulated number of eggs released by each age class during one given year (Fig. 3.8) shows that although individuals start reproducing during their second year of life, the quantity of eggs spawned by two-year-old scallops was very low (less than $0.2 \times 10^6$ eggs $y^{-1}$). A little discrepancy was simulated between the amount of eggs spawned by six- and seven-year-old individuals (less than $0.2 \times 10^6$ eggs $y^{-1}$), indicating the expected stabilization of reproductive effort

when reaching 7 years old. Second, Fig. 3.9 presents a comparison over the seven years of simulation. The inter-annual variability in cumulated amount of eggs released by all individuals is very low as for the seasonality of reproductive activity which is very constant between years. The average total number of eggs spawned per year was $1.03 \times 10^7$.

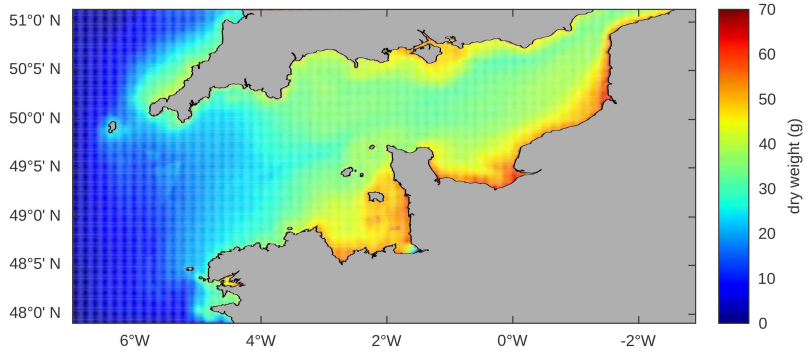


**Figure 3.7:** Dry weight of flesh in g of an average individual of *P. maximus* in each grid cell, predicted by the DEB model forced by environmental data (ECO-MARS-3D) after 7 years of simulation.

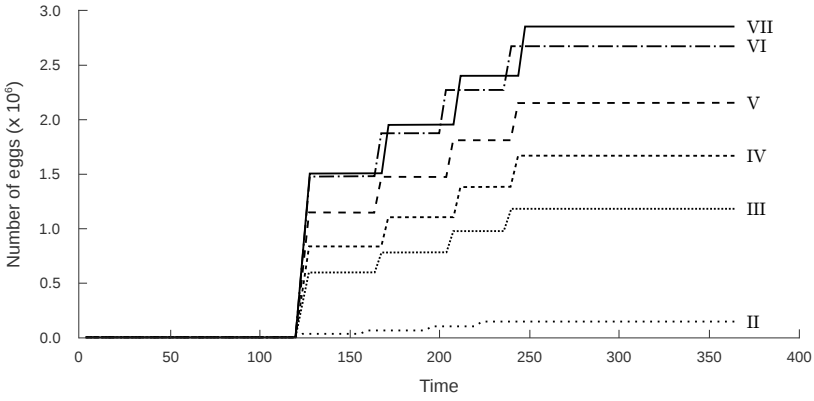


**Figure 3.8:** Cumulative number of eggs spawned by each cohort (II to VII) in one grid cell during one year. This example is from the Bay of Seine. Reproductive activity is computed from the individual DEB model, forced by environmental data (ECO-MARS-3D).

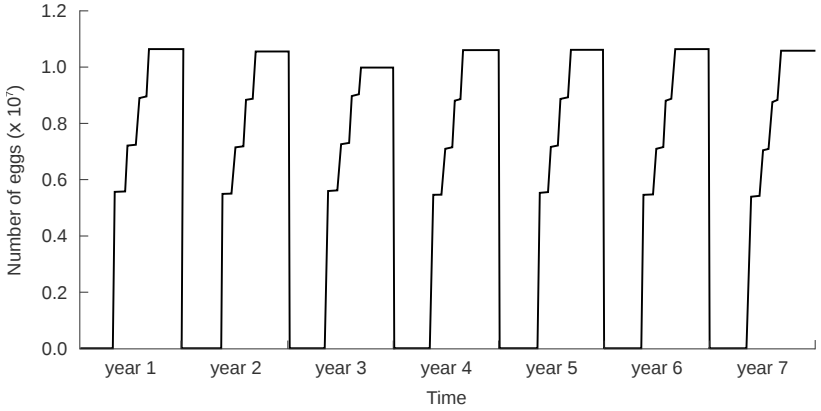


**Figure 3.9:** Cumulative number of eggs spawned by all age classes in the English channel during a 7-year long simulation. Reproductive activity is computed from the individual DEB model, forced by environmental data (ECO-MARS-3D).

### 3.3.3 Coupling the four models

Finally, the coupling of the four models allowed to picture the physiological state of the great scallop individuals in the English Channel. The DEB model allowed us to better constrain the dispersal of individual, as the reproductive activity was then dependent on the environmental conditions (Fig. 3.10). The distribution of great scallops after thirty years as predicted by the modeling system is shown in Fig. 3.11a. It is generally well in accordance with the presence/absence map (Fig. 3.11b). A slight under-estimation of scallop density is possible at the center of the oriental side, given the number of study that reported its presence in this area. However it is very difficult to compare the modeled abundance to this map as it does not account for any quantification of the presence of *P. maximus*. When looking at the representation of the number of eggs spawned for any particular year of the simulation, one can see that there are more eggs released in the eastern English Channel than in the western part. Moreover, very low amount of eggs were simulated in the deepest part of the studied area, i.e. the Celtic Sea.

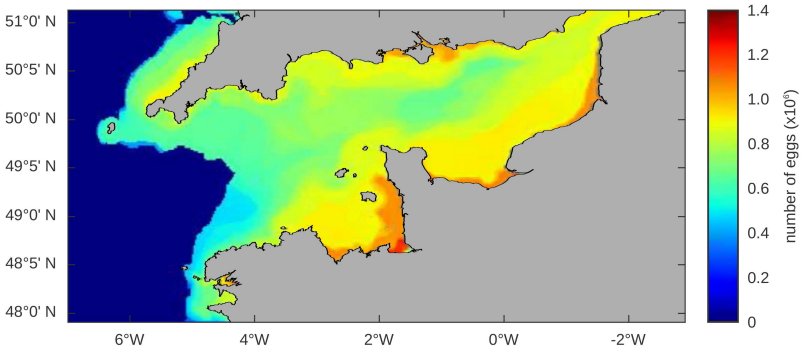


**Figure 3.10:** Spatialized reproductive activity expressed as the number of eggs spawned by all mature cohorts in each grid cell for a particular year.

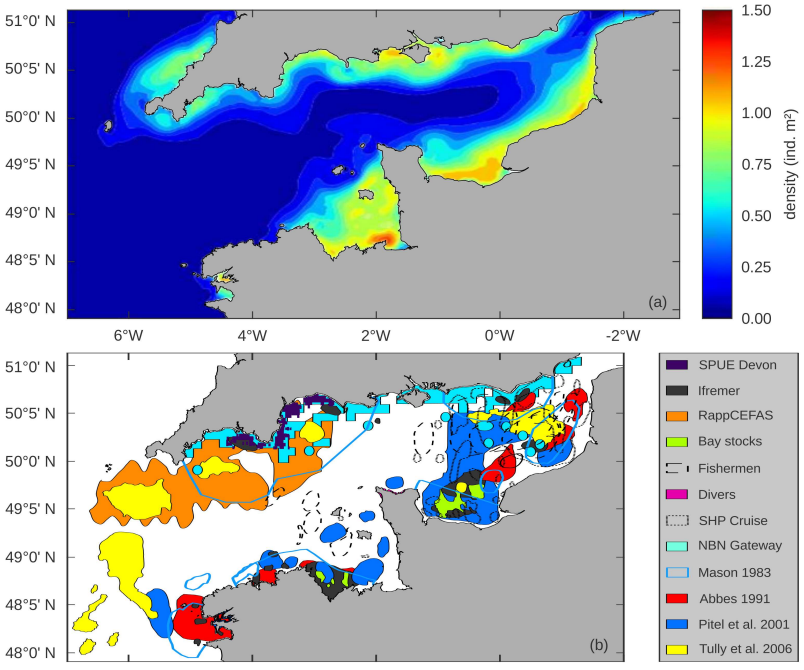


**Figure 3.11:** (a) Distribution map of *P. maximus* population (in number of individuals per squared meter) after 27 years of simulations coupling the DEB model, the population dynamics model and the ECO-MARS-3D model. (b) Distribution map by presence/absence of *P. maximus* in the English Channel from various information sources (scientific articles, scientific cruises reports and technical reports, see detail in the text).

## 3.4 Discussion

This study is first to ever report simulations of the distribution of the great scallop, *Pecten maximus*, in the English Channel. Savina and Ménesguen (2008) developed a similar approach with the banded carpet shell, *Paphia rhomboïdes*. While they were working with a 71 box divided map, they stressed that the use of fine-gridded 3D hydrodynamic and biogeochemical model should be considered, which is the case in this study.

In the first step, we only coupled the hydrodynamical model to the population dynamics model to look at the potential establishment of the population of *P. maximus* through dispersion of larvae. A recent study conducted by Nicolle et al. (2013) on the modeling of *P. maximus* larval dispersion in the English Channel brought new insights on the potential connectivity between the different grounds. They showed that, depending on the meteorological and tidal conditions during spawning, a significant part of the larvae born within two dense populations of scallop along French coast (the Bay of Saint-Brieuc and the Bay of Seine) were retained into these area and subjected to limited transport. We typically observed this retention pattern in our simulations. Moreover, high density were recorded in other semi-enclosed area such as the Lyme Bay, both east and west to the Isle of Wight and also in the Bay of Somme and near Falmouth. Nonetheless, the coupling of individual physiological model with ECO-MARS-3D model revealed that the Bay of Saint-Brieuc, the Bay of Seine, the Bay of Somme and the area around the Isle of Wight were the most productive locations in terms of egg releasing. In their work, Nicolle et al. (2013) highlighted the crucial role of certain subpopulations from these bays in the connectivity between stocks of the English Channel. Thus, locations identified as being favorable for egg production may provide large amount of larvae to other stocks of *P. maximus* in this region.

The physiological performances observed through the coupling of the individual bioenergetic model with the ECO-MARS-3D model are likely to reflect the food availability in the different parts of the English Channel. Indeed, while temperature would explain the growth rates of physiological variables, food concentration is though to influence the ultimate length (and weight) of individuals according to DEB theory (Kooijman, 2010). After seven years of growth, the scallop populations in this region are close to their maximum length (Fifas, 2004; Chauvaud et al., 2012).

The limited distribution of the abundance of released egg to a coastal strip wider in the eastern part of the English Channel than in the western part reveal the potential amount of energy dedicated to reproduction. Because $\kappa$, the coefficient of partitioning of mobilized energy between somatic growth and reproduction buffer, is the same for all the individual of the same species (Kooijman, 2010), the discrepancy in the number of spawned eggs is a result of the amount of energy coming out of the reserve compartment. Therefore, in the deepest locations of the western area, the low to null number of eggs released during one year of the simulation would be explained by the dynamics

of reserve. In this area, where depth typically exceeds 100 m, the low and strong seasonal pattern of food availability, exclusively relying on sedimenting organic particles (McCave, 1975; Bienfang, 1981; Smetacek, 1985), is likely to explain a relatively low amount of reserves compared to enriched coastal areas.

As there is no density data for the great scallop in the English Channel, we could only compare the results of the simulations to presence/absence data. As mentioned by Brand (2006a), it is likely that there are limited number of major areas within the geographical range of scallop species where the population is sufficiently abundant to support a commercial fishery. Such areas, often referred to as grounds are usually widely separated by areas that are environmentally unsuitable for the species (Brand, 2006a). Our results slightly differ from the collection of data gathered here. The eastern part of the English Channel might hold a more dense population than modeled, according to the high number of studies reporting the presence of *P. maximus* in this region. Some studies have also reported its presence south to the west extremity of the UK, while our results reveal only low densities in this area. Nevertheless, the nonexistence of accurate abundance data about this species limits the conclusions of this comparison.

The present approach uses an individual DEB model to simulate growth and reproduction of average individuals in each cell of the ECO-MARS-3D modeling system. For this reason, the computation time was rather long (five days for thirty years of simulation). We may improve both time required and the quality of the simulation by taking inspiration from recent work relying on coupling individual DEB model with Individual Based Models (IBM; Martin, 2013). Actually, it has already been explored by Bacher and Gangnery (2006), who showed that IBM offered a powerful alternative to continuous equations when several physiological variables are involved.

While more accuracy in the simulations (especially from the physiological model) is possible and might be wanted, it is limited by computation time requirements. We worked with a simpler version of the individual DEB model as compared to the original model developed in Lavaud et al. (2013). Nonetheless, there may be an opportunity for improvement through the approach recently adopted by Ibarra et al. (2014), in a study of the production carrying capacity of mussel farm in a Canadian fjord. They developed a coupled Eulerian/IBM hybrid modeling system that allow one to get rid of these computational constraints by computing ecophysiological equations at some discrete locations instead of in every grid cell within the domain. Although their approach requires a large number of parameters (as in many IBM models), trials should be carried out with this assumption of reduced range of computation in order to compare the two approaches.

This study offers great perspectives for regional modeling. The particular interest of our approach relies on the use of a DEB model applied at the individual scale and used to assess patterns at the population level. In fact, DEB theory provides a conceptual framework that allow one to quantitatively implement almost every metabolic processes, given a set of estimated parameters for

a species. Thus, it would be possible to look at various physiological responses aside from growth and reproduction. For instance, an interesting development would be to better assess mortality, on the basis of the state of reserves in the contrasting environments of the English Channel. This could enable us to model the potential survival of different stocks each year. One could also focus on the filtration activity in relation to the environmental food conditions to assess the carrying capacity of potential aquaculture sites. Sensibility analysis should be conducted in order to look at the importance of each parameter of the simulations. A validation of the modeling system can be achieved by comparing growth rates and length simulations to real measurements in exploited areas, which might help in predicting stock evolution.

## 3.5 Conclusions

We developed a coupled modeling system constituted of four independent models, linked together in a dynamic input/output interaction. An Eulerian 3D model (MARS-3D) of hydrodynamics was first coupled to a biogeochemical model, providing an environmental framework of the study area. An individual physiological model based on DEB theory was implemented behind the environmental forcing module. Finally, a population dynamics model was implemented to simulate the evolution of the distribution of *P. maximus* in the English Channel.

Compared to the available information on the distribution of the great scallop at this regional scale, our modeling system successfully achieved to simulate the dispersion patterns of this species. We believe that if applied to a smaller space scale (bays, fjords, pounds, lagoons, etc.) this approach could be even more efficient as the dynamics of environmental conditions and the physiological variables would be simulated faster, which would allow one to detail the great capacity of the physiological module, i.e. taking into account silt effect on feeding in coastal areas (Saraiva et al., 2011a; Lavaud et al., 2013). The transition from individual to population level can also be handled through DEB theory. It would be interesting to compare such an approach to ours in further investigations, which might bring more insights on the distribution patterns of this species.

## Acknowledgements

This study was funded by the COMANCHE ANR program (ANR-2010-STRA-010). The authors acknowledge A. Foveau for the collection of literature data used to map the distribution of the great scallop. We deeply acknowledge Ewan Harney for correction of English writing.

# Chapter 4

# Trophic sources of the great scallop

**New insights of the seasonal feeding ecology of *Pecten maximus* using pigments, fatty acids and sterols analyses**

*Manuscript submitted to Comparative Biochemistry and Physiology - Part B*

**Romain Lavaud**, Sébastien Artigaud, Anne Donval, Fabienne Le Grand, Philippe Soudant, Tore Strohmeier, Øivind Strand, Jonathan Flye-Sainte-Marie and Fred Jean.

**Abstract**
In the present study we combined the use of pigments, fatty acids and sterols as biomarkers to determine the seasonal variation in food sources of a marine suspension-feeding bivalve, the great scallop *P. maximus*. From March to October 2011, a biweekly to twice-weekly sampling was conducted in the Bay of Brest (Brittany, France). Filtrations of seawater samples from the water column (two meters below the surface) and the water-sediment interface were carried out and scallops were collected. Pigment compositions in the seawater and in the stomach and rectum content of the scallops were analyzed by HPLC. Fatty acids and total sterols from seawater filters and digestive gland (DG) tissue were analyzed by gas chromatography. Feeding activity, assessed by the total amount of pigments in the stomach content, seemed to be correlated with phytoplankton dynamics of the water column rather than the water-sediment interface. Fucoxanthin, used as a Bacillariophyceae (diatom) marker, dominated the pigment concentration detected in the gut of *P. maximus*. Peridinin, characterizing Dinophyceae, occurred in high proportions in

the gut, as compared to the low ambient concentration, suggesting a selection of this microalgae group by the scallop. The proportions of fucoxanthin and peridinin in the stomach and rectum content alternated in time. This switch of feeding was confirmed by the proportions in the DG of 20:5(n-3), 16:1(n-7) and 24 methylene cholesterol (marking diatoms) and 22:6(n-3), 18:5(n-3) and brassicasterol (tracing dinoflagellates). Chlorophyceae and green macroalgae, traced by chlorophyll-*b*, 18:2(n-6) and 18:3(n-3) were found in low proportions, suggesting they were not actually ingested. Markers of Prymnesiophyceae (19'hexanoyloxyfucoxanthin and 18:4(n-3)) were also observed at significant levels. Zeaxanthin, used as a cyanobacteria tracer showed that this microalgae class was not ingested by the scallops during the monitoring but may be of higher importance during winter. The proportion of iso 17:0, characteristic of bacteria, was higher in March and October in the DG of scallops. Although at low proportions, microorganisms may represent a nutritious food source during the bleak season. The concentration of degraded pigments (phaeophorbid-*a*, phaeophytin-*a*) from the gut of *P. maximus* increased during low ingestion periods, just before or just after high feeding activity. Switches from one food source to another as well as the selectivity in feeding are discussed relative to the season.

**Keywords:** food sources; pigments; fatty acids; sterols; trophic marker; phytoplankton; *Pecten maximus*

## 4.1 Introduction

Scallops, such as *Pecten maximus* (Linnaeus, 1758), are sessile suspension-feeding animals living half-buried on the sea floor. They rely on the availability of the trophic resources in the nearby water to obtain their food. In coastal environments, temperature, light, riverine inputs, salinity, tide, currents, etc. influence seawater primary production. The availability of food depends on the strong seasonality of these hydrological and biochemical conditions. Therefore, suspension-feeding bivalves must have evolved to develop a plastic trophic niche (Rossi et al., 2004; Nerot et al., 2012). Scallops may thus feed on pelagic and benthic microalgae, protozoans, zooplankton, dissolved organic carbon and detrital organic matter (Shumway et al., 1987; Kang et al., 1999; Roditi et al., 2000; Raikow and Hamilton, 2001; Lorrain et al., 2002; Richard, 2005; MacDonald et al., 2006). Recent studies have confirmed this diversified diet (Nerot et al., 2012), yet only qualitatively.

Studies of trophic sources makes use of various chemical, biological, biochemical or physiological indicators to identify the origin of the food for an organism. Among these markers, stable isotopes are often used (Rossi et al., 2004; Bode et al., 2006; Marín Leal et al., 2008). Although they are able to discriminate between taxa at different trophic position, they have not been reported to be good indicators of different classes of organisms at the same trophic level. Pigments and lipids (fatty acids and sterols), on the other hand,

have long been used to characterize classes, gender and even species of microalgae (Jeffrey, 1968, 1974, 1997; Pastoureaud et al., 1995; Loret et al., 2000; Louda et al., 2008 for pigments; Parrish et al., 1995; Soudant et al., 1996; Bachok et al., 2003, 2009 for fatty acids and Volkman, 1986; Napolitano et al., 1993; Soudant et al., 1998a for sterols). These biomarkers have been extensively used in foraging ecology and food webs studies. Statistical methods are in development to assess the contribution of different food sources in the diet, e.g. Chemtax for pigment (Mackey et al., 1996) and FA analysis (Dijkman and Kromkamp, 2006) or QFASA (Quantitative Fatty Acid Signature Analysis) in FA studies (Iverson et al., 2004). To our knowledge, however, pigment and lipid compositions of tissues have not been coupled to assess seasonal variability of food sources.

Bioenergetics studies require precise knowledge about the energy entry in the organism, which is necessary to complete physiological processes and metabolism work. This energy may come from one or several substrates depending on the ecological position of the species and its feeding strategies. The determination of its trophic sources is essential to better understand the energy intake dynamics and furthermore the variability of any physiological function, such as growth, reproductive effort, etc.

In this study the objective was to describe the temporal qualitative and quantitative variations in trophic sources foraged by *P. maximus*, in an innovative approach combining three well established trophic markers: pigments, fatty acids and sterols, in the digestive gland and gut contents.

## 4.2 Material and methods

The study was conducted in the Bay of Brest (Brittany, France), where *P. maximus* were dredged in the bay in November 2010 and then placed in the location of Lanvéoc (48°17'N, 4°27'W, average depth of 12 m). From March 14$^{th}$ 2011 until October 24$^{th}$ 2011, three individuals were collected by scuba-diving every two weeks. During April and May, corresponding to a period of high phytoplankton productivity, scallops were sampled twice a week. Only animals over three years old, identified by yearly shell growth rings (Mason, 1957), and thus fully mature, were selected for this study. The stomach content was collected in 2 mL Eppendorf tubes by squeezing the digestive gland (DG). In the same way, the gut content was obtained from pressing the rectum. Stomach fraction was used as a proxy of ingested food and rectum fraction was considered as the digested part of food that was not assimilated. Two aliquots of DG tissue were encapsulated into aluminium cups. DG content and tissue samples were frozen in liquid nitrogen and stored in −80 °C until sample treatment.

Seawater was also sampled using a five liter Niskin bottle at two meters below the surface during the entire study period. Sampling of the water-sediment interface was carried out from early May using a 450 mL syringe. Phytoplankton species composition and abundance was determined in samples both in

the water column and at the water-sediment interface. A volume of 250 mL of each sample was fixed with acetic Lugol's. Quantitative and qualitative analyses were carried out from settled cells using an inverted phase microscope. Vacuum filtration of seawater was conducted on GF/F filters (0.7 µm) previously heated for 6 h at 450 °C. Between 500 mL and 1.5 L of sub-surface seawater were filtered at each sampling time. The volume of filtered bottom water ranged from 50 to 150 mL, depending on filter clogging. Two filtrations were carried out for both water column and water-sediment interface samples. Filtrates were stored in sealed aluminium folds at −80 °C until sample treatment. Simultaneous analyses of pigment composition of the seston from the water column and from the water-sediment interface were conducted whenever possible as they are not available for the two first months of the study. Nevertheless, the occurrence, timing and intensity of spring phytoplankton at the bottom are well documented in a previous study carried out at the same time scale and at the very same location (Chatterjee et al., 2013). Pigment and lipid composition of all samples (DG content, DG tissue of scallops and filtrates) were analyzed as described hereafter.

### 4.2.1 Pigment analysis

The procedure used to identify and quantify pigments in the filters and in the DG contents is the method described by Claustre and Ras (2009). The extraction of pigments was achieved from 200 mL of stomach content, 50 mg of rectum content and seawater filtrates from the two depths, in 100 % methanol enriched with vitamin E acetate (used as internal standard, Sigma-Aldrich). To improve extraction yield, samples were disrupted by sonication using a S-4000 sonicator (Misonix Inc.) and stored at −20 °C. Sonication was repeated after two and four hours of extraction. Samples were centrifugated for 10 min at 3000 rpm (4 °C) and passed through 13 mm syringe filters (Puradisc, 0.2 µm, PTFE, Fischer). Pigment analyses were carried out on a complete Agilent Technologies 1200 series HPLC system, equipped with a ZORBAX Eclipse XDB-$C_8$ silica column (3 mm × 150 mm, 3.5 mm particle size) and a diode array detector, which permits automatic pigment identification based on absorption spectra. The elution was run at a flow rate of 0.55 mL $min^{-1}$ using solvent A (tetrabutylammonium acetate and methanol, 30:70 v/v) and solvent B (methanol) in the following elution procedure (min, solv. A, solv. B): (0, 90, 10), (22, 5, 95), (27, 5, 95), (28, 90, 10) and (33, 90, 10). Pigments optical densities were monitored at 450 nm (chloropigments and carotenoids) and at 667 nm (chlorophyll-*a* and derived pigments), automatically compared to the retention times of 15 pigment standards (DHI and Sigma-Aldrich) previously calibrated. The injection precision of the method is estimated at 0.4 %, and the effective limits of quantification for most pigments are rather low: $2.89 \times 10^{-5}$ µg $mL^{-1}$ for chlorophyll-*a* and $3.98 \times 10^{-5}$ µg $mL^{-1}$ for carotenoids. Chemstation software was used for verification and eventual correction of the peak integrations in each chromatogram.

### 4.2.2 Lipid analysis

#### Chemicals

High performance liquid chromatography (HPLC) grade solvents were purchased from VWR International. Boron trifluoride (BF3, 14 % by weight in methanol), tricosanoic acid (C23:0), cholestane and 37-component Fatty Acid Methyl Ester (FAME) mix were obtained from Sigma-Aldrich. Silica gel 60 (63–230 µm mesh) was purchased from Merck. Gas chromatography (GC) capillary column was a DBWAX (30 m × 0.25 mm i.d.; 0.25 µm thickness) for FAME analysis and a Rtx65 (15 m × 0.25 mm i.d.; 0.25 µm thickness) for sterol analysis and were respectively obtained from Agilent and Restek.

#### Lipid extraction

Lipid extraction was conducted by resuspension of the filtrates or of 200 mg aliquots of digestive gland (DG) previously grounded by ball milling under liquid nitrogen. Samples were then put in glass tubes containing 6 mL of chloroform-methanol (2:1, v/v) and stored at −20 °C before analysis.

#### Separation

After centrifugation (2 min, 1000 rpm), lipid analyses were carried out on 1 mL of DG lipid extracts and on 5 mL of filtrate lipid extracts (due to the small amount of material in the seawater when compared to the DG). Lipid extracts were then evaporated to dryness under nitrogen, recovered with three chloroform-methanol (98:2, v/v) washings of 500 µL each and deposited at the top of a silica gel microcolumn (Pasteur pipette of 5 mm inner diameter, plugged with glass wool and filled with silica gel 60 both previously heated for 6 h at 450 °C and deactivated with 6 % water by weight). Neutral lipids (NL), including triglycerides, free fatty acids and sterols, were eluted with 10 mL of chloroform-methanol (98:2 v/v) and polar lipids (PL), containing glycolipids and phospholipids, were eluted with 20 mL of methanol, and were both collected in 20 mL vials.

#### Transesterification

After evaporation to dryness under nitrogen, PL and NL fractions were recovered and transferred in 8 mL vials with three chloroform-methanol (98:2, v/v) washings of 1 mL each. The NL fraction was then equally divided into two vials. The totality of the PL fraction and half of NL fraction were dedicated to fatty acid (FA) analysis whereas the other part of the NL fraction was dedicated to sterol analysis. As internal standards, 2.3 µg of C23:0 was added to the FA vials and 2.5 µg of cholestane was added to the sterols vials. After evaporation to dryness under nitrogen, Fatty Acid Methyl Esters (FAMEs) were obtained by adding 800 µL of methanol-BF3 to FA vials, vortexing and heating for 10 min at 100 °C. For sterol analysis, 2 mL of a sodium methoxyde

solution (NaOH, 27 µg µL$^{-1}$ in methanol) was added to the sterol vials, which were maintained under agitation for 90 min at room temperature. Before GC analysis, organic phases containing FAME or sterols were washed three times with 1 mL of distilled water and 800 µL of hexane and centrifuged (1 min at 1000 rpm) before eliminating the aqueous phase each time. Finally organic phases were transfered into tapering vials and stored at −20 °C.

**Gas chromatography analysis**

FAME were analyzed in a Agilent 6890 gas chromatograph equipped with an on-column injector and a flame-ionization detector, with hydrogen as carrier gas. They were identified by their retention times with reference to those of a standard 37-component FAME mix and other known standard mixtures from marine bivalves (Soudant et al., 1995) and designated following the formula C:X(n-Y) where C is the number of carbon atoms, X is the number of double bonds and Y is the position of the first double bond counted from the CH terminal. The sterols were separated by gas chromatography, in a Chrompack 9002 equipped with an on-column injector and a flame-ionization detector, with hydrogen as carrier gas. Sterols were identified by comparison of their retention time with standards as described in Soudant et al. (1998a).

## 4.3 Results

First of all, the GC analysis of fatty acids (FA) and sterols in the seawater filters revealed extremely low quantities in the samples. Only the most prominent FA could be detected, showing only small peaks which could not be accurately quantified. Several trials to concentrate the samples did not solve this detection threshold issue.

### 4.3.1 Seston pigment concentration and composition

The general pattern of phytoplankton primary production during the season can be seen in Fig. 4.1, showing the dynamics of chlorophyll-*a* concentration in the seston from the water column as well as in the water-sediment interface. The first sign of primary production recovery after winter in the whole water column occurred at the end of March. But the first significant phytoplankton bloom was observed at the water-sediment interface in mid-April. Then, microalgae grew in the water column in early May. In June, another bloom occurred in the water column while pigment concentrations in the bottom water decreased. During the summer few blooms were recorded in the water column while low pigment amounts were found at the bottom. In the autumn period, a renewal of primary production was monitored both at the water-sediment interface and in the water column. The pelagic pigment concentration seemed to crash down in August, while bottom production reached high levels in September, comparable to spring time. As chlorophyll-*a* is present in all marine algae

species and because the goal of this study was to identify specific patterns in the dynamics of several algae classes, chlorophyll-*a* was removed from the total amount of pigments and each pigment quantity was therefore expressed as its contribution to the total amount of pigment without chlorophyll-*a*.

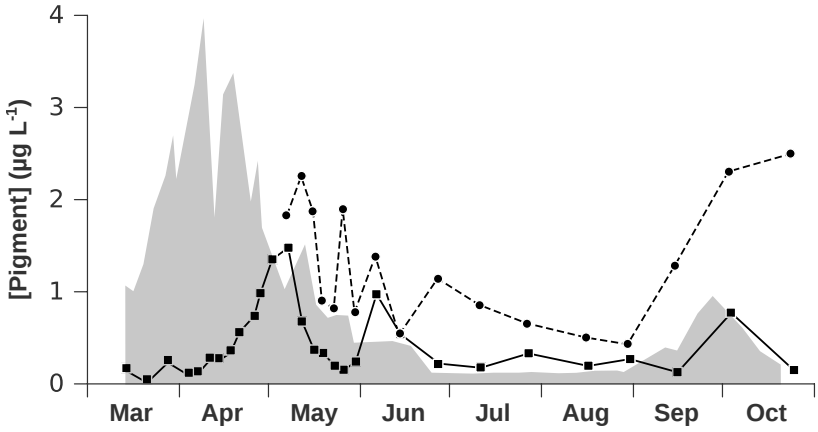


**Figure 4.1:** Chlorophyll-*a* concentration in the water column (solid line, full squares) and in the water-sediment interface (dashed line, full dots) in the Bay of Brest during year 2011. Additional data of chlorophyll-*a* concentration (gray area) at the sea floor are from Chatterjee et al. (2013).

Detailed phytoplankton composition can be assessed by the study of secondary pigments measured in the seston (Fig. 4.2). The first small increase of primary production observed at the end of March was synchronous with an elevation of alloxanthin and peridinin in the water column, associated with the observation of Cryptophyceae and Dinophyceae (*Heterocapsa triquetra* and *Gyrodinium flagellare*; Chatterjee, 2014). Then, the critical peak of chlorophyll-*a* in the water-sediment interface in April was synchronous with blooms of the Bacillariophyceae (diatoms) *Navicula sp.* and *Fragillaria sp.* (Chatterjee, 2014). Chlorophyll-*a* concentration in the water column and at the water-sediment interface both increased in late April, mainly due to blooms of diatoms from the genus *Chaetoceros*, *Cerataulina* and *Pseudo-Nitzschia* and Chryptophyceae (Chatterjee, 2014). Pigment composition of seston in April also showed increasing proportions of 19'hexanoyloxyfucoxanthin (19'HF) and 19'betanoyloxyfucoxanthine (19'BF), up to 15 and 10 % respectively in the water column. Fucoxanthin was at its highest level in early May in the water column, contributing 77 % of the total pigments, when blooms of diatom species (*Chaetoceros sp.*, *Cerataulina pelagica* and *Dactiliosolen fragilissima*) were registered (Chatterjee, 2014). Almost all pigments presented an increase during this bloom, except for peridinin, which only showed short peaks (around 10 % of the total pigment) along the study period. The second high pigment

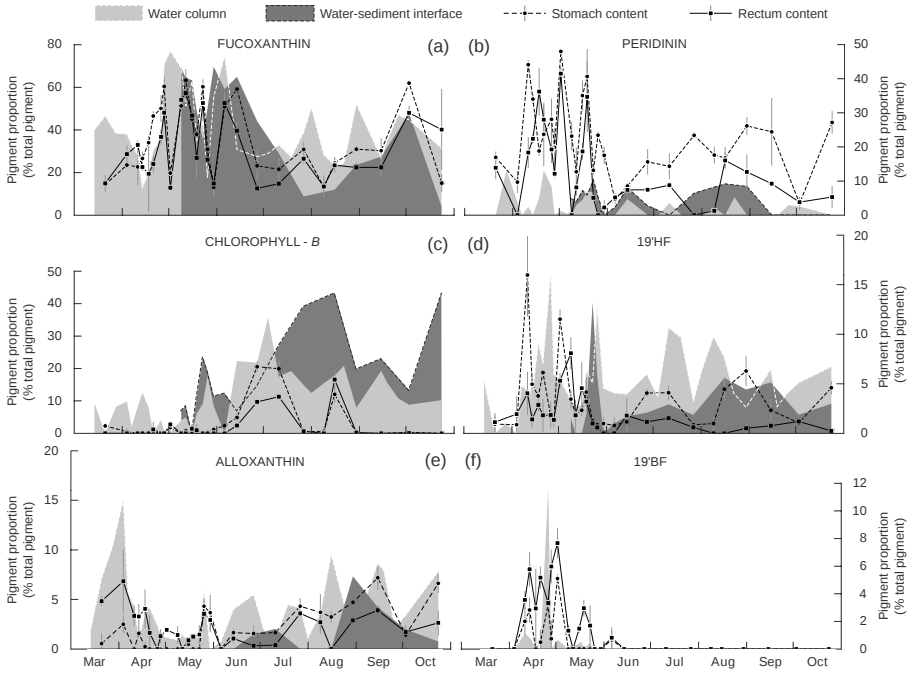


**Figure 4.2:** Proportions of fucoxanthin (a), peridinin (b), chlorophyll-*b* (c), 19'HF (d), alloxanthin (e) and 19'BF (f) in the water column (light gray area) and at the water-sediment interface (dark gray area) and in the stomach (dashed dark line, full dots) and the rectum content (solid dark line, full squares) of *P. maximus* in the Bay of Brest during year 2011. Standard deviations are presented as vertical gray lines.

concentration event was measured in early June and was caused by an increase in fucoxanthin concentration from 0.1 to 0.8 µg $L^{-1}$. This bloom was mainly constituted of the same diatom species that caused May's bloom. From there, fucoxanthin concentrations remained at lower levels both in the water column and at the water-sediment interface, whereas the proportion of chlorophyll-*b* started to increase from about 10 % to more than 20 % in June for the water column. The same occurred at the bottom from July, also accompanied by a similar increase of peridinin and zeaxanthin concentrations (Table 4.1). Alloxanthin and 19'HF remained at 5 % from mid-summer until the end of the study. Finally, in October, seston pigment composition was dominated by fucoxanthin (up to 40 %) and chlorophyll-*b* (50 %).

**Table 4.1:** Pigments proportion (expressed as pigment percentage of total) in the stomach and the rectum of *P. maximus* in the Bay of Brest during year 2011. PHB: Pheophorbid-*a*, PER: Peridinin, BFU: 19'BF, FUC: Fucoxanthin, HFU: 19'HF, ALO: Alloxanthin, ZEA: Zeaxanthin, LUT: Lutein, CHB: Chlorophyll-*b*, PHT: Phaeophytin-*a*. Standard deviations are in brackets.

| *Date* | *PHB* | *PER* | *BFU* | *FUC* | *HFU* | *ALO* | *ZEA* | *LUT* | *CHB* | *PHT* |
|---|---|---|---|---|---|---|---|---|---|---|
| *Stomach* | | | | | | | | | | |
| 21/03 | 18.7 (4.6) | 16.9 (1.6) | 0.0 (0.0) | 14.4 (1.4) | 0.9 (0.8) | 0.7 (1.2) | 2.7 (1.6) | 1.5 (0.7) | 2.3 (0.3) | 27.1 (3.3) |
| 04/04 | 31.1 (7.2) | 9.7 (3.1) | 0.0 (0.0) | 23.6 (0.8) | 0.9 (1.5) | 3.1 (1.0) | 0.0 (0.0) | 0.0 (0.1) | 0.5 (0.9) | 23.1 (6.3) |
| 11/04 | 0.0 (0.0) | 44.1 (1.2) | 2.0 (1.0) | 22.7 (8.4) | 16.0 (4.5) | 0.0 (0.0) | 0.0 (0.0) | 0.0 (0.0) | 0.0 (0.0) | 0.0 (0.0) |
| 18/04 | 7.9 (1.1) | 18.8 (1.3) | 0.0 (0.0) | 34.0 (0.4) | 3.8 (0.4) | 0.3 (0.5) | 0.0 (0.1) | 0.1 (0.2) | 0.3 (0.5) | 28.9 (1.3) |
| 26/04 | 5.2 (1.1) | 28.1 (5.9) | 3.2 (0.5) | 50.1 (6.0) | 1.7 (0.6) | 0.0 (0.0) | 0.0 (0.0) | 0.0 (0.0) | 0.0 (0.0) | 5.1 (1.6) |
| 28/04 | 0.0 (0.0) | 19.8 (5.4) | 0.7 (1.3) | 60.4 (5.0) | 1.3 (0.3) | 0.0 (0.0) | 0.0 (0.0) | 0.0 (0.0) | 0.0 (0.0) | 9.1 (0.9) |
| 02/05 | 0.0 (0.0) | 48.0 (0.1) | 5.1 (0.3) | 19.8 (2.2) | 11.5 (1.0) | 0.0 (0.0) | 0.0 (0.0) | 0.0 (0.0) | 1.8 (1.8) | 0.2 (0.3) |
| 09/05 | 0.0 (0.5) | 25.6 (4.1) | 0.0 (0.0) | 56.6 (4.5) | 3.8 (0.9) | 0.0 (0.0) | 0.0 (0.0) | 0.0 (0.0) | 0.0 (0.0) | 4.2 (1.2) |
| 12/05 | 0.0 (0.9) | 13.3 (6.9) | 0.0 (0.0) | 66.0 (5.0) | 2.0 (0.7) | 0.0 (0.0) | 0.1 (0.1) | 0.0 (0.0) | 0.8 (0.8) | 1.8 (1.7) |
| 16/05 | 0.0 (0.0) | 35.0 (4.3) | 0.0 (0.0) | 45.1 (3.1) | 2.3 (0.6) | 0.6 (0.1) | 0.0 (0.0) | 0.0 (0.0) | 0.4 (0.7) | 3.9 (0.5) |
| 19/05 | 0.0 (0.0) | 40.7 (7.9) | 0.0 (0.0) | 37.9 (6.2) | 4.2 (1.5) | 0.0 (0.0) | 0.0 (0.0) | 0.0 (0.0) | 0.0 (0.0) | 6.9 (2.2) |
| 23/05 | 0.8 (1.2) | 13.2 (1.2) | 0.0 (0.0) | 60.3 (3.2) | 1.3 (0.4) | 0.0 (0.0) | 0.0 (0.0) | 0.0 (0.0) | 0.0 (0.0) | 4.7 (0.1) |
| 26/05 | 22.7 (1.2) | 23.4 (0.9) | 0.0 (0.0) | 30.9 (3.2) | 0.9 (0.0) | 5.4 (0.9) | 0.2 (0.1) | 0.4 (0.2) | 0.3 (0.3) | 3.9 (0.9) |
| 30/05 | 41.1 (2.0) | 17.5 (2.4) | 0.0 (0.0) | 13.2 (2.0) | 1.0 (0.6) | 4.6 (2.2) | 0.0 (0.0) | 0.0 (0.0) | 1.2 (1.0) | 15.5 (3.6) |
| 06/06 | 0.0 (0.0) | 4.6 (1.3) | 0.7 (0.6) | 50.9 (3.4) | 0.8 (0.8) | 0.0 (0.0) | 0.0 (0.0) | 0.4 (0.4) | 2.4 (0.6) | 26.0 (6.7) |
| 14/06 | 2.4 (2.5) | 8.5 (0.3) | 0.0 (0.0) | 59.2 (2.4) | 1.2 (1.1) | 2.1 (0.5) | 0.0 (0.0) | 0.1 (0.1) | 4.9 (1.2) | 5.7 (1.7) |
| 27/06 | 5.7 (1.9) | 15.6 (3.6) | 0.0 (0.0) | 23.2 (7.0) | 4.1 (0.3) | 2.0 (0.9) | 0.0 (0.0) | 2.1 (0.6) | 20.6 (1.5) | 14.0 (3.6) |
| 11/07 | 5.9 (0.8) | 14.3 (3.7) | 0.0 (0.0) | 21.6 (5.2) | 4.1 (0.7) | 2.1 (0.2) | 0.0 (0.0) | 2.5 (0.2) | 19.9 (2.5) | 16.0 (3.7) |
| 27/07 | 22.7 (1.3) | 23.4 (0.9) | 0.0 (0.0) | 30.9 (3.2) | 0.9 (0.0) | 5.4 (1.0) | 0.2 (0.1) | 0.4 (0.2) | 0.5 (0.1) | 3.9 (0.9) |
| 16/08 | 29.1 (3.0) | 19.1 (3.0) | 0.0 (0.0) | 27.8 (2.5) | 5.0 (1.1) | 4.6 (0.6) | 0.0 (0.0) | 3.8 (0.4) | 0.0 (2.4) | 5.4 (0.9) |
| 30/08 | 8.2 (1.2) | 26.2 (2.5) | 0.0 (0.0) | 31.0 (0.5) | 6.3 (1.5) | 5.9 (1.1) | 0.0 (0.0) | 3.7 (1.5) | 0.0 (0.0) | 28.3 (1.8) |
| 15/09 | 10.2 (9.5) | 24.4 (9.7) | 0.0 (0.0) | 30.3 (5.7) | 2.3 (1.1) | 9.0 (1.4) | 0.0 (0.0) | 4.3 (0.3) | 0.0 (0.0) | 5.8 (5.1) |
| 03/10 | 4.3 (2.6) | 3.4 (1.8) | 0.0 (0.0) | 62.0 (1.1) | 1.1 (0.4) | 1.8 (0.2) | 0.1 (0.0) | 0.0 (0.1) | 0.3 (0.6) | 9.5 (4.4) |
| 24/10 | 18.7 (1.2) | 27.2 (3.2) | 0.0 (0.0) | 15.1 (4.0) | 4.6 (0.6) | 8.3 (1.2) | 0.0 (0.0) | 0.3 (0.0) | 0.0 (0.0) | 6.0 (0.2) |
| *Rectum* | | | | | | | | | | |
| 21/03 | 31.4 (8.8) | 13.9 (3.2) | 0.0 (0.0) | 15.0 (3.7) | 1.1 (2.0) | 6.0 (0.6) | 1.1 (0.4) | 1.2 (0.8) | 0.0 (0.0) | 14.2 (0.8) |
| 04/04 | 31.1 (8.1) | 0.0 (0.0) | 0.0 (0.0) | 28.7 (3.8) | 1.9 (3.4) | 8.6 (4.0) | 0.4 (0.2) | 0.6 (0.3) | 0.0 (0.0) | 11.0 (1.9) |
| 11/04 | 6.5 (2.1) | 18.4 (4.4) | 3.6 (0.6) | 33.0 (2.0) | 4.0 (2.1) | 4.2 (1.2) | 0.0 (0.0) | 0.0 (0.0) | 0.0 (0.0) | 10.8 (0.8) |
| 18/04 | 0.0 (0.0) | 36.2 (6.9) | 2.9 (2.8) | 19.5 (17.5) | 2.9 (0.6) | 5.1 (2.4) | 0.3 (0.3) | 1.4 (0.8) | 0.0 (0.0) | 7.9 (7.7) |
| 26/04 | 15.5 (1.4) | 19.3 (3.8) | 3.3 (1.0) | 36.8 (3.5) | 1.9 (1.3) | 0.0 (0.0) | 0.2 (0.2) | 0.1 (0.2) | 0.0 (0.0) | 6.4 (0.8) |
| 28/04 | 0.0 (0.0) | 12.1 (1.0) | 6.0 (1.2) | 48.1 (5.3) | 1.4 (0.7) | 1.6 (0.8) | 0.1 (0.1) | 0.1 (0.1) | 0.0 (0.0) | 17.0 (5.2) |
| 02/05 | 1.5 (0.4) | 41.5 (1.8) | 7.7 (1.1) | 12.9 (0.9) | 5.3 (0.7) | 2.4 (0.2) | 0.4 (0.1) | 0.4 (0.1) | 2.8 (0.4) | 4.6 (0.7) |
| 09/05 | 12.4 (5.2) | 0.0 (0.0) | 1.3 (0.4) | 54.1 (0.9) | 8.1 (1.6) | 1.8 (1.0) | 0.0 (0.0) | 0.0 (0.0) | 0.0 (0.0) | 11.5 (1.9) |
| 12/05 | 7.8 (1.8) | 8.1 (1.1) | 0.0 (0.0) | 57.3 (0.9) | 1.8 (1.5) | 0.0 (0.0) | 0.2 (0.1) | 0.1 (0.1) | 0.0 (0.0) | 6.6 (0.8) |
| 16/05 | 4.2 (1.9) | 18.7 (2.3) | 1.5 (0.3) | 46.7 (2.4) | 4.6 (2.6) | 1.1 (0.2) | 0.2 (0.1) | 0.1 (0.1) | 1.4 (1.3) | 7.8 (1.4) |
| 19/05 | 6.5 (4.9) | 34.7 (10.2) | 3.0 (0.6) | 26.9 (9.1) | 3.2 (0.1) | 1.6 (0.1) | 0.2 (0.0) | 0.1 (0.0) | 1.0 (1.7) | 6.6 (0.6) |
| 23/05 | 3.3 (1.2) | 5.1 (1.4) | 1.7 (1.4) | 52.6 (8.4) | 1.0 (0.4) | 1.8 (1.1) | 0.1 (0.1) | 0.1 (0.1) | 0.0 (0.0) | 20.1 (4.2) |
| 26/05 | 35.5 (4.4) | 0.0 (0.0) | 0.0 (0.0) | 26.1 (1.8) | 0.6 (0.2) | 4.4 (0.3) | 0.2 (0.2) | 0.3 (0.3) | 0.0 (0.0) | 15.5 (2.6) |
| 30/05 | 50.5 (8.9) | 2.3 (2.1) | 0.0 (0.0) | 14.9 (6.2) | 0.0 (0.0) | 3.7 (1.5) | 0.1 (0.2) | 0.2 (0.4) | 0.0 (0.0) | 14.8 (1.3) |
| 06/06 | 0.0 (0.0) | 5.2 (1.2) | 0.8 (0.7) | 52.6 (4.8) | 0.0 (0.0) | 0.0 (0.0) | 0.0 (0.0) | 0.0 (0.0) | 0.0 (0.0) | 26.6 (5.8) |
| 14/06 | 6.6 (1.6) | 7.4 (1.9) | 0.0 (0.0) | 39.6 (4.2) | 1.8 (1.7) | 1.3 (0.5) | 0.0 (0.0) | 0.7 (0.1) | 2.4 (0.8) | 20.2 (3.4) |
| 27/06 | 9.8 (0.9) | 7.4 (0.6) | 0.0 (0.0) | 12.6 (0.8) | 1.2 (0.1) | 0.4 (0.1) | 0.0 (0.0) | 7.9 (1.3) | 9.7 (0.5) | 19.7 (2.8) |
| 11/07 | 11.7 (0.6) | 8.8 (0.8) | 0.0 (0.0) | 14.8 (1.4) | 1.5 (0.3) | 0.5 (0.1) | 0.0 (0.0) | 9.2 (1.6) | 11.3 (0.5) | 21.6 (3.8) |
| 27/07 | 33.9 (3.8) | 0.0 (0.0) | 0.0 (0.0) | 26.5 (2.1) | 0.6 (0.2) | 4.5 (0.2) | 0.2 (0.2) | 0.3 (0.3) | 0.7 (0.6) | 15.7 (2.2) |
| 16/08 | 0.0 (0.0) | 16.0 (2.1) | 0.0 (0.0) | 23.5 (3.2) | 0.0 (0.0) | 0.0 (0.0) | 3.0 (1.4) | 10.2 (1.7) | 16.6 (2.7) | 9.3 (0.5) |
| 30/08 | 22.5 (7.3) | 12.7 (5.0) | 0.0 (0.0) | 22.4 (2.1) | 0.5 (0.5) | 3.6 (3.2) | 2.9 (2.2) | 1.1 (0.2) | 0.3 (0.4) | 9.2 (2.8) |
| 15/09 | 20.2 (8.5) | 9.2 (0.3) | 0.0 (0.0) | 22.5 (4.0) | 0.8 (0.1) | 4.9 (0.6) | 1.6 (0.1) | 1.2 (0.4) | 0.0 (0.0) | 19.1 (1.5) |
| 03/10 | 10.4 (4.0) | 3.8 (0.6) | 0.0 (0.0) | 48.0 (3.1) | 1.2 (0.0) | 2.1 (0.8) | 0.2 (0.3) | 0.1 (0.2) | 0.1 (0.1) | 14.7 (3.2) |
| 24/10 | 10.1 (4.8) | 5.3 (3.1) | 0.0 (0.0) | 40.2 (18.8) | 0.2 (0.1) | 3.3 (1.5) | 0.0 (0.0) | 0.0 (0.0) | 0.0 (0.0) | 5.9 (2.9) |

### 4.3.2 Pigment composition of the digestive contents

The pigment quantities measured in the stomach content were well correlated with the availability in the water column from June (polynomial regression: $r^2 = 0.64$, Fig. 4.3), whereas the correlation to water-sediment interface was very low ($r^2 = 0.03$). Fucoxanthin was the major pigment found both in stomach and rectum (up to 55 and 50 % respectively). Peridinin had a maximum occurrence at 43 % in the stomach and at 28 % in the rectum. The dynamics of these two predominant pigments varied in an opposite manner, as shown in Fig. 4.4.

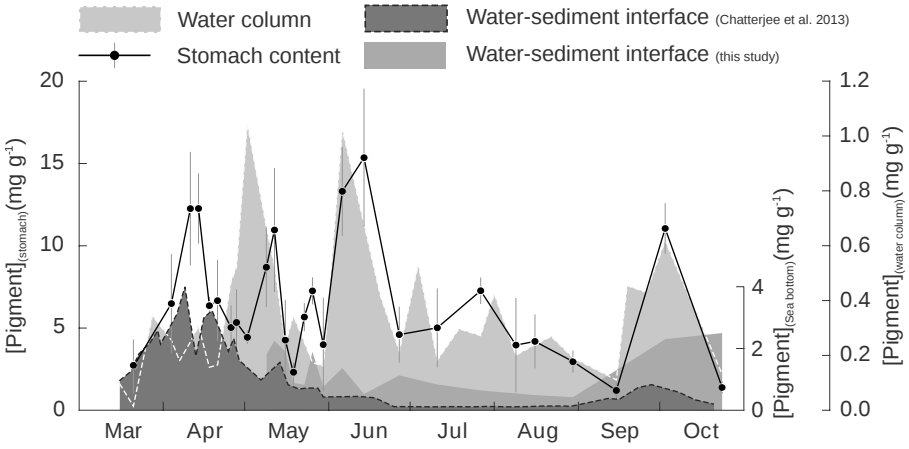


**Figure 4.3:** Total quantity of pigment measured in the water column (light gray area), at the water-sediment interface (gray area) and in the stomach content of *P. maximus* (dark line, full dots) in the Bay of Brest during year 2011. Standard deviations are presented as vertical gray lines. Data from the water-sediment interface from the study of Chatterjee et al. (2013) are also plotted (dark gray area) to complete the present data set.

Fucoxanthin in the stomach fluctuated strongly during spring (Fig. 4.2), with sharp increases from 10–20 % up to 50–55 % in late April, mid-May, late May and early June. The minimum was observed on May 30$^{th}$ (11.4 %) and the maximum in April 28$^{th}$ at 53.6 %. As observed in the water, a significant increase in autumn was registered. The proportion of fucoxanthin in the rectum was very similar to what was observed in the stomach, as shown by a linear regression coefficient of $r^2 = 0.78$ (Fig. 4.5). Peridinin showed a similar pattern, with a fluctuating spring period followed by low proportions in early summer and medium levels until autumn when it dropped to its minimum (2.4 %) on October 3$^{rd}$. The maximum was reached on May 2$^{nd}$ at 42.3 %. Compared to fucoxanthin, the linear regression between the proportion of peridinin in the rectum and in the stomach was less significant ($r^2 = 0.41$). For instance, at

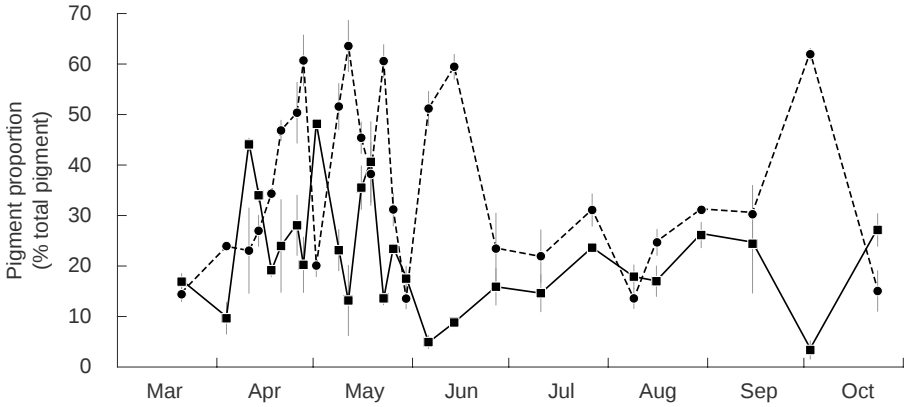


**Figure 4.4:** Proportions of fucoxanthin (solid line, full dots) and peridinin (dashed line, full squares) in the stomach content of *P. maximus* in the Bay of Brest during year 2011. Standard deviations are presented as vertical gray lines.

the end of May as well as in July and August, the discrepancy between the two compartments was 20 % between the entry and the exit of the digestive tract (Fig. 4.2).

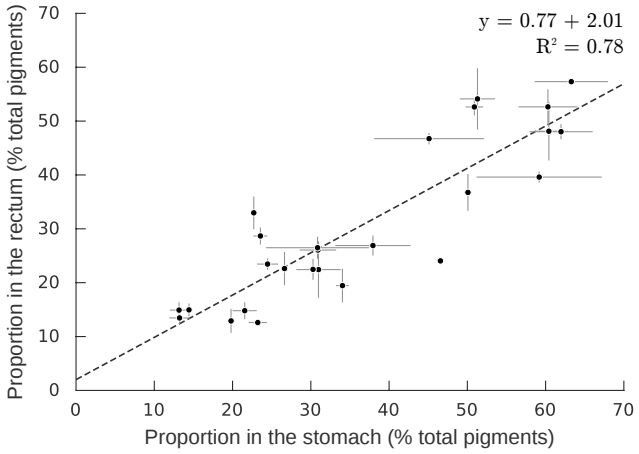


**Figure 4.5:** Linear regression ($r^2 = 0.78$) between the proportion of fucoxanthin measured in the stomach and in the rectum of *P. maximus* (expressed as pigment percentage of total) in the Bay of Brest, during the year 2011. Standard deviations are presented as vertical and horizontal gray lines.

The occurrence of chlorophyll-*b* was not observed in the gut of the scallops before an important peak of 13.5 % during June and July and a shorter one in mid-August (12 %). In the rectum, proportions of chlorophyll-*b* during the first increase were found to be lower (10.5 %) and higher during the second peak (16 %). Nevertheless, the correlation between the two compartments was rather elevated ($r^2 = 0.76$). To a lesser extent, two peaks of 19'HF were recorded, at 16 and 11 % respectively, in the stomach on April 11$^{th}$ and on May 2$^{nd}$ and another increase was reported during August, although only reaching 5 %. During the first peak and the late summer increase, the proportion of this pigment in the rectum did not change whereas it increased up to 8 % just after the second spring peak. Alloxanthin was more present in the rectum than in the stomach until mid-May (Fig. 4.2). Then the proportion of this pigment increased up to 5 % in the stomach in late May. A regular increase from June to October was registered in the gut of *P. maximus*. Finally, several events of increased proportion of 19'BF up to 5 % were observed in the stomach as well as in the rectum during April and the first week of May, whereas only one significant peak occurred in the seawater in the end of April.

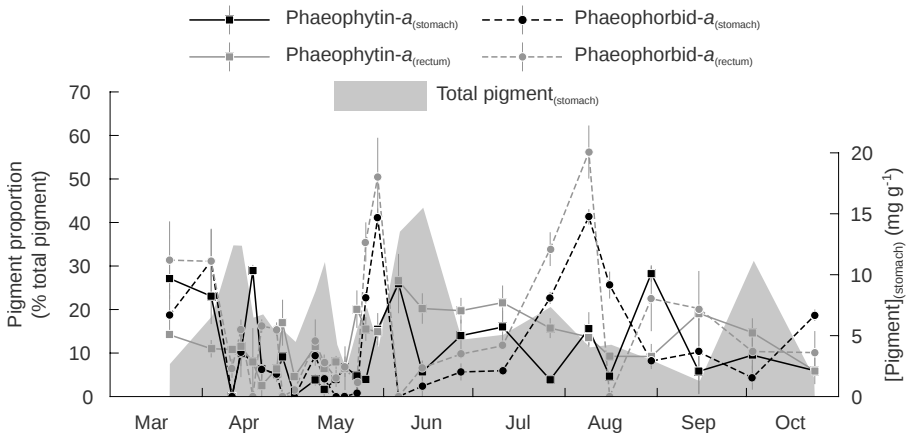


**Figure 4.6:** Total pigment concentration in the stomach content of *P. maximus* (gray area) and proportions of phaeophorbid-*a* (dashed lines, full dots) and phaeophytin-*a* (solid lines, full squares) in the stomach content (gray) and the rectum content (dark) of *P. maximus* in the Bay of Brest during year 2011. Standard deviations are presented as vertical gray lines.

Degraded pigments, namely phaeophorbid-*a* and phaeophytin-*a*, were also observed in both stomach and rectum (Fig. 4.6). High proportions (17–24 %) of these two pigments were already present in the stomach at the beginning of the study and dropped down to zero on April 11$^{th}$. A brief increase of phaeophytin-*a* to 24 % was noticed on April 18$^{th}$. A peak of degraded pigment was reached between May 26$^{th}$ and June 6$^{th}$ and a second event occurred be-

tween July 27$^{th}$ and August 30$^{th}$. In the rectum the level of degraded pigments followed very closely the pattern described for the stomach. Phaeophytin-*a*, however, fluctuated less from June and varied between 6 and 16 %. Moreover, when compared to the total pigment found in the stomach (Fig. 4.6), the proportions of degraded pigments seems rather disconnected from the periods of increased ingestion. During the four periods of high total pigment content in the gut, proportions of degraded pigments do not showed any strong dynamics. Conversely, the three periods of high levels of degraded pigments identified in the gut of scallops occurred after periods of low feeding activity and just before the ingestion peaks.

### 4.3.3 Fatty acid and sterol composition of the digestive gland

The total amount of FA and sterols in the DG of *P. maximus* showed particularly high variations during spring (Fig. 4.7f). Total FA content of the digestive gland (DG) increased from 45 to 75 mg g$^{-1}$ between the start and the end of the study, the highest value of 172 mg g$^{-1}$ being reached in mid-June (Fig. 4.7f). The main FA found in the polar fraction were 20:5(n-3) (EPA), 22:6(n-3) (DHA) and 16:0, each accounting for about 15 % of total FA (Table 4.2), 18:4(n-3), 20:4(n-6), around 5 % and to a lesser extent 18:2(n-6), 18:3(n-3), 18:1(n-9), 20:4(n-3) and iso 17:0, which accounted for less than 2 %. In the neutral fraction, 20:5(n-3) was the main FA (25 %, Table 4.3), 16:0 accounted for about 15 %, 14:0, 16:1(n-7) and 22:6(n-3) ranged between 6 and 12 %, 20:4(n-6) was found around 3.5 % and 18:1(n-9), 18:3(n-3), 18:4(n-3) and 18:5(n-3) were each accounting for about 2 %. Within the polar fraction, the ratio between EPA and DHA showed two periods of increase in late April–early May and at the beginning of June (Fig. 4.7e). Lower levels were observed at the beginning of April, at the end of May and in August. An analogous tendency was observed when comparing the proportions of 16:1(n-7) and 18:5(n-3) (in the neutral fraction). Fig. 4.7c shows a peak of 18:4(n-3) at the end of April, its proportion reaching 5 % of total FA, regularly increasing from June to October. Similar patterns were observed for 18:2(n-6) and 18:3(n-3) which also exhibited an important increase of twice their initial percentage in late May (4.7a). The proportion of 20:4(n-3) only varied between 0.3 and 0.7 %, but presented two important peaks in April and in late May and gradually increased throughout the summer until the end of the study (4.7c). Finally, iso 17:0 FA found in the polar lipids presented interesting dynamics as they were inversely related to other described FA. Indeed, highest proportions were observed in March and October. FA assimilated as reserve compounds (neutral fraction) were hardly related to the seasonal patterns observed through the analysis of pigments and polar lipids.

Sterol content in the DG increased from 35.9 to 105.3 µg g$^{-1}$ with a peak at 183.0 µg g$^{-1}$ on the 19$^{th}$ May (Table 4.4). Cholesta-5-e(n-3)$\beta$-ol (cholesterol) was, in average, the most present sterolic compound (24 %), followed by 5$\beta$-

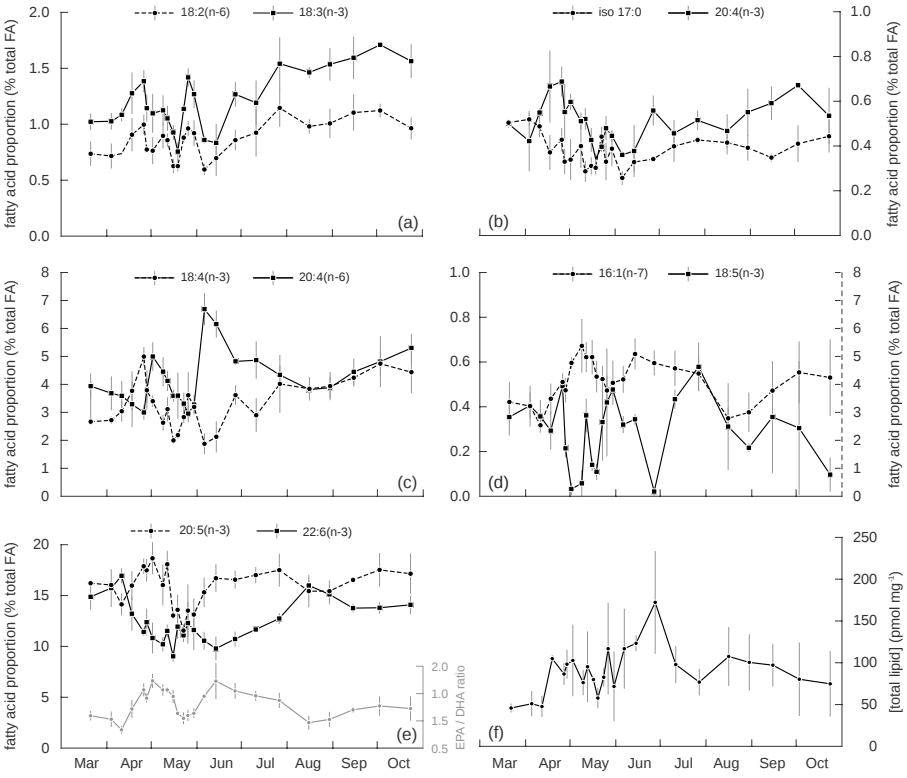


**Figure 4.7:** Proportions of ten major fatty acids in the digestive gland of *P. maximus* (expressed as fatty acid molar percentage of total) in the Bay of Brest, during the year 2011. (a): 18:2(n-6) (dashed line, full dots), 18:3(n-3) (solid line, full squares) in polar lipids; (b) iso 17:0 (dashed line, full dots), 20:4(n-3) (solid line, full squares) in polar lipids; (c) 18:4(n-3) (solid line, full dots) and 20:4(n-6) (solid line, full squares) in polar lipids; (d): 16:1(n-7) (dashed line, full dots) in polar lipids and 18:5(n-3) (solid line, full squares) in neutral lipids; (e): 20:5(n-3) (dashed line, full dots), 22:6(n-3) (solid line, full squares) in polar lipids and their ratio (gray line): 20:5(n-3)(EPA):22:6(n-3)(DHA); (f) total fatty acid concentration (polar plus neutral fractions, expressed in $\mu mol\, g^{-1}$). Standard deviations are presented as vertical gray lines.

**Table 4.2:** Fatty acids (FA) composition of the polar lipids in the digestive gland of *P. maximus* (expressed as FA molar percentage of total) in the Bay of Brest, during year 2011. Standard deviations are in brackets.

| *Date* | *TMTD* | *14:0* | *16:0* | *iso17:0* | *18:0* | *16:1(n-7)* | *18:1(n-9)* | *18:1(n-7)* | *18:2(n-6)* | *18:3(n-3)* |
|---|---|---|---|---|---|---|---|---|---|---|
| 21/03 | 8.3 (7.8) | 3.0 (0.1) | 11.5 (0.7) | 0.5(0.0) | 8.6 (1.1) | 3.4 (0.7) | 1.3 (0.1) | 1.0 (1.0) | 0.7 (0.1) | 1.0 (0.1) |
| 04/04 | 5.2 (9.0) | 3.2 (0.4) | 11.3 (0.7) | 0.5(0.0) | 8.7 (1.1) | 3.2 (0.7) | 1.2 (0.2) | 1.4 (1.2) | 0.7 (0.1) | 1.0 (0.1) |
| 11/04 | 1.9 (3.3) | 3.2 (0.3) | 13.3 (0.9) | 0.5(0.1) | 8.9 (0.6) | 2.5 (0.1) | 1.0 (0.1) | 2.0 (0.2) | 0.7 (0.0) | 1.1 (0.1) |
| 18/04 | 7.1 (6.4) | 3.9 (0.5) | 12.2 (1.0) | 0.4(0.1) | 7.8 (1.4) | 3.5 (0.5) | 1.3 (0.0) | 2.1 (0.2) | 0.9 (0.1) | 1.3 (0.2) |
| 26/04 | 8.0 (1.8) | 3.9 (0.1) | 14.0 (1.0) | 0.4(0.1) | 7.9 (0.3) | 4.1 (0.3) | 1.7 (0.1) | 2.5 (0.2) | 1.0 (0.1) | 1.4 (0.1) |
| 28/04 | 6.0 (5.3) | 4.0 (0.6) | 11.9 (0.8) | 0.3(0.1) | 8.2 (0.3) | 3.8 (0.4) | 1.2 (0.1) | 2.6 (0.2) | 0.8 (0.0) | 1.1 (0.1) |
| 02/05 | 6.6 (2.1) | 4.3 (0.3) | 13.0 (1.3) | 0.3(0.1) | 5.3 (4.6) | 4.8 (0.2) | 1.2 (0.2) | 3.5 (0.2) | 0.8 (0.1) | 1.1 (0.2) |
| 09/05 | 4.9 (2.1) | 4.0 (1.3) | 14.9 (1.6) | 0.4(0.1) | 9.0 (0.2) | 5.4 (0.9) | 1.5 (0.1) | 4.7 (0.3) | 0.9 (0.1) | 1.1 (0.1) |
| 12/05 | 5.9 (0.8) | 4.0 (0.5) | 14.3 (1.2) | 0.3(0.0) | 5.4 (4.7) | 5.0 (0.5) | 1.3 (0.1) | 5.3 (0.4) | 0.9 (0.1) | 1.1 (0.1) |
| 16/05 | 10.1 (0.6) | 4.5 (0.3) | 14.7 (0.2) | 0.3(0.0) | 10.6 (0.5) | 5.0 (0.6) | 1.4 (0.2) | 4.5 (0.3) | 0.6 (0.1) | 0.9 (0.1) |
| 19/05 | 7.0 (6.1) | 4.3 (0.5) | 15.2 (0.9) | 0.3(0.0) | 9.4 (0.5) | 4.3 (0.5) | 1.3 (0.1) | 4.2 (0.1) | 0.6 (0.0) | 0.8 (0.1) |
| 23/05 | 8.8 (1.3) | 4.6 (0.2) | 15.8 (0.5) | 0.4(0.0) | 9.8 (0.2) | 4.2 (0.4) | 1.8 (0.1) | 3.5 (0.2) | 0.9 (0.0) | 1.1 (0.0) |
| 26/05 | 6.9 (1.3) | 3.9 (0.8) | 15.3 (1.3) | 0.3(0.0) | 9.5 (0.6) | 3.8 (0.5) | 2.0 (0.2) | 3.1 (0.6) | 1.0 (0.1) | 1.4 (0.1) |
| 30/05 | 8.3 (1.4) | 4.6 (0.8) | 15.1 (0.9) | 0.4(0.1) | 8.9 (0.6) | 4.1 (0.8) | 1.8 (0.3) | 2.9 (0.4) | 0.9 (0.1) | 1.3 (0.1) |
| 06/06 | 7.6 (0.0) | 5.7 (0.4) | 12.4 (0.9) | 0.3(0.1) | 8.1 (0.6) | 4.2 (0.5) | 1.2 (0.1) | 2.5 (0.1) | 0.6 (0.0) | 0.9 (0.0) |
| 14/06 | 6.1 (1.5) | 5.4 (0.3) | 13.6 (1.4) | 0.3(0.0) | 8.4 (0.3) | 5.1 (0.5) | 1.4 (0.1) | 2.8 (0.2) | 0.7 (0.2) | 0.8 (0.2) |
| 27/06 | 6.0 (1.4) | 4.9 (0.6) | 14.1 (1.4) | 0.3(0.0) | 5.2 (4.5) | 4.8 (0.4) | 1.5 (0.1) | 2.9 (0.2) | 0.9 (0.1) | 1.3 (0.1) |
| 11/07 | 5.8 (1.7) | 4.7 (0.4) | 14.8 (0.7) | 0.4(0.0) | 8.5 (0.6) | 4.6 (0.6) | 1.7 (0.3) | 2.7 (0.2) | 0.9 (0.2) | 1.2 (0.2) |
| 27/07 | 4.7 (1.3) | 4.1 (0.1) | 15.5 (0.8) | 0.4(0.0) | 7.7 (0.5) | 4.4 (0.6) | 2.1 (0.4) | 2.7 (0.1) | 1.1 (0.2) | 1.5 (0.2) |
| 16/08 | 4.7 (0.3) | 3.2 (0.3) | 13.8 (0.2) | 0.4(0.1) | 7.7 (0.6) | 2.8 (0.4) | 1.4 (0.1) | 2.4 (0.1) | 1.0 (0.1) | 1.5 (0.0) |
| 30/08 | 4.4 (1.2) | 3.3 (0.5) | 14.2 (1.2) | 0.4(0.1) | 7.6 (0.4) | 3.0 (0.7) | 1.5 (0.2) | 2.5 (0.1) | 1.0 (0.1) | 1.5 (0.1) |
| 05/09 | 3.2 (0.3) | 3.8 (0.1) | 15.2 (1.1) | 0.4(0.0) | 7.7 (0.3) | 3.8 (0.1) | 1.6 (0.2) | 2.7 (0.1) | 1.1 (0.2) | 1.6 (0.2) |
| 03/10 | 3.3 (0.4) | 2.8 (1.9) | 15.6 (0.1) | 0.4(0.1) | 7.2 (1.4) | 4.4 (1.1) | 1.8 (0.2) | 2.7 (0.1) | 1.1 (0.1) | 1.7 (0.0) |
| 24/10 | 4.1 (0.5) | 2.7 (1.9) | 14.6 (1.2) | 0.4(0.1) | 7.2 (1.5) | 4.2 (1.4) | 1.8 (0.2) | 2.6 (0.2) | 1.0 (0.1) | 1.6 (0.1) |

| | *18:4(n-3)* | *20:4(n-6)* | *20:5(n-3)* | *22:6(n-3)* | *SAFA* | *MUFA* | *PUFA* | *DMA* | *(n-6)* | *(n-3)* |
|---|---|---|---|---|---|---|---|---|---|---|
| 21/03 | 2.7 (0.1) | 3.9 (0.4) | 16.2 (0.1) | 14.9 (1.2) | 24.9 (0.6) | 8.6 (1.0) | 47.3 (2.5) | 10.3 (3.8) | 2.4 (0.3) | 38.5 (2.6) |
| 04/04 | 2.7 (0.1) | 3.7 (0.6) | 16.0 (0.4) | 15.7 (1.8) | 25.0 (0.6) | 8.8 (1.0) | 48.1 (2.7) | 12.1 (4.5) | 2.4 (0.4) | 39.7 (3.2) |
| 11/04 | 3.0 (0.4) | 3.6 (0.5) | 14.1 (1.0) | 16.9 (0.7) | 27.6 (2.0) | 8.8 (0.3) | 49.5 (1.4) | 11.7 (1.3) | 2.9 (0.1) | 40.2 (1.8) |
| 18/04 | 3.8 (0.7) | 3.3 (0.8) | 16.0 (1.4) | 13.2 (1.6) | 25.7 (1.7) | 9.7 (1.0) | 47.3 (2.8) | 9.9 (1.7) | 2.6 (0.2) | 38.8 (2.4) |
| 26/04 | 5.0 (0.3) | 3.0 (0.2) | 17.9 (0.7) | 11.4 (0.3) | 26.7 (0.7) | 11.1 (0.8) | 47.5 (1.7) | 6.4 (0.3) | 2.5 (0.5) | 39.9 (0.8) |
| 28/04 | 3.8 (0.8) | 3.8 (0.7) | 17.5 (1.1) | 12.4 (1.3) | 25.6 (1.5) | 10.7 (0.5) | 47.7 (3.3) | 9.6 (0.2) | 2.3 (0.1) | 39.1 (3.3) |
| 02/05 | 3.4 (0.2) | 5.0 (0.5) | 18.7 (1.5) | 10.8 (1.5) | 23.7 (3.6) | 12.7 (0.8) | 48.2 (4.4) | 8.4 (0.7) | 2.6 (0.3) | 38.4 (3.8) |
| 09/05 | 2.6 (0.3) | 4.5 (0.5) | 16.0 (2.0) | 10.2 (0.7) | 29.1 (2.4) | 14.9 (0.9) | 42.9 (3.6) | 7.9 (1.2) | 2.7 (0.4) | 33.5 (2.5) |
| 12/05 | 3.1 (0.4) | 4.1 (0.3) | 18.1 (1.3) | 11.5 (0.6) | 25.3 (3.0) | 14.5 (1.2) | 46.6 (2.2) | 7.4 (0.2) | 2.6 (0.3) | 37.7 (2.3) |
| 16/05 | 2.0 (0.1) | 3.6 (0.2) | 13.0 (0.3) | 9.0 (0.5) | 31.7 (0.3) | 14.6 (0.8) | 36.2 (0.5) | 7.1 (0.8) | 2.1 (0.1) | 27.9 (0.3) |
| 19/05 | 2.2 (0.1) | 3.6 (0.8) | 13.6 (1.4) | 11.9 (1.1) | 31.2 (1.7) | 13.3 (0.5) | 40.8 (3.9) | 7.5 (1.6) | 2.2 (0.2) | 31.8 (2.9) |
| 23/05 | 2.8 (0.2) | 3.3 (0.4) | 11.6 (0.6) | 11.1 (0.6) | 32.3 (0.6) | 13.3 (0.7) | 38.4 (0.8) | 7.0 (0.3) | 2.3 (0.2) | 29.9 (0.4) |
| 26/05 | 3.6 (0.8) | 3.0 (0.3) | 13.5 (2.5) | 12.3 (2.0) | 30.6 (2.8) | 12.4 (1.9) | 41.9 (5.9) | 7.8 (0.2) | 2.4 (0.2) | 34.2 (5.7) |
| 30/05 | 3.2 (0.2) | 3.3 (0.3) | 13.1 (1.5) | 11.6 (1.9) | 30.6 (1.3) | 12.1 (1.8) | 40.9 (4.5) | 7.6 (0.6) | 2.3 (0.1) | 32.8 (3.6) |
| 06/06 | 1.9 (0.4) | 6.7 (0.6) | 15.3 (1.4) | 10.6 (0.8) | 27.5 (0.9) | 11.0 (0.6) | 47.5 (1.7) | 6.1 (0.6) | 2.6 (0.2) | 32.1 (2.6) |
| 14/06 | 2.1 (0.5) | 6.2 (0.5) | 16.7 (1.3) | 9.8 (1.1) | 29.2 (1.3) | 12.3 (0.9) | 44.1 (0.5) | 7.9 (1.1) | 2.5 (0.1) | 32.9 (0.8) |
| 27/06 | 3.6 (0.3) | 4.8 (0.1) | 16.6 (0.8) | 10.7 (0.7) | 26.0 (2.3) | 12.7 (1.1) | 47.1 (2.6) | 7.7 (0.5) | 2.8 (0.2) | 36.2 (1.7) |
| 11/07 | 2.9 (0.6) | 4.9 (0.6) | 17.0 (0.7) | 11.7 (0.2) | 29.3 (0.7) | 11.9 (0.9) | 46.3 (1.1) | 6.3 (0.9) | 2.8 (0.6) | 36.1 (1.7) |
| 27/07 | 4.0 (1.0) | 4.3 (0.3) | 17.5 (1.6) | 12.7 (0.5) | 28.7 (0.3) | 11.0 (0.8) | 49.4 (2.2) | 5.8 (1.2) | 2.7 (0.2) | 40.0 (2.9) |
| 16/08 | 3.8 (0.4) | 3.8 (0.1) | 15.4 (1.5) | 16.0 (0.5) | 25.9 (1.0) | 9.2 (0.9) | 53.0 (1.4) | 6.9 (0.2) | 2.5 (0.2) | 40.3 (2.0) |
| 30/08 | 3.9 (0.5) | 3.9 (0.4) | 15.4 (1.0) | 15.1 (0.9) | 26.3 (2.5) | 9.6 (0.9) | 52.6 (1.8) | 6.8 (0.4) | 2.7 (0.0) | 39.7 (1.1) |
| 05/09 | 4.2 (0.3) | 4.4 (0.5) | 16.5 (0.2) | 13.8 (0.4) | 28.5 (1.3) | 10.8 (0.3) | 50.1 (0.5) | 7.1 (0.9) | 2.7 (0.1) | 40.3 (0.6) |
| 03/10 | 4.7 (0.4) | 4.8 (0.9) | 17.5 (1.6) | 13.8 (0.5) | 27.4 (3.1) | 11.6 (1.8) | 51.7 (2.1) | 5.6 (1.4) | 2.8 (0.1) | 41.2 (0.5) |
| 24/10 | 4.4 (0.7) | 5.3 (0.5) | 17.1 (1.9) | 14.1 (0.9) | 26.3 (2.3) | 11.3 (2.2) | 51.8 (2.1) | 6.1 (1.8) | 2.9 (0.2) | 40.7 (1.0) |

**Table 4.3:** Fatty acids (FA) composition of the neutral lipids in the digestive gland of *P. maximus* (expressed as FA molar percentage of total) in the Bay of Brest, during year 2011. Standard deviations are in brackets.

| *Date* | *TMTD* | *14:0* | *16:0* | *16:1(n-7)* | *18:1(n-9)* | *18:1(n-7)* | *18:2(n-6)* | *18:3(n-3)* | *18:4(n-3)* | *18:5(n-3)* |
|---|---|---|---|---|---|---|---|---|---|---|
| 21/03 | 1.5 (0.2) | 2.1 (0.4) | 6.5 (2.5) | 8.8 (0.4) | 2.8 (0.0) | 3.8 (0.1) | 2.1 (0.0) | 2.2 (0.0) | 6.5 (0.0) | 0.4 (0.1) |
| 04/04 | 2.0 (0.4) | 2.1 (0.1) | 7.9 (2.3) | 8.0 (0.8) | 2.5 (0.0) | 4.0 (0.1) | 2.1 (0.0) | 2.5 (0.0) | 7.9 (0.0) | 0.4 (0.1) |
| 11/04 | 1.6 (0.4) | 2.3 (0.4) | 9.9 (0.9) | 7.5 (0.8) | 2.1 (0.3) | 3.3 (0.0) | 2.3 (0.2) | 2.8 (0.4) | 9.9 (2.3) | 0.4 (0.1) |
| 18/04 | 1.8 (0.2) | 7.5 (0.5) | 16.5 (0.2) | 8.1 (0.6) | 1.8 (1.3) | 3.6 (0.1) | 1.9 (0.4) | 2.1 (0.7) | 8.3 (1.2) | 0.3 (0.1) |
| 26/04 | 1.8 (0.2) | 8.1 (0.7) | 14.3 (4.2) | 8.2 (1.7) | 2.8 (0.2) | 2.9 (0.1) | 2.2 (0.2) | 2.8 (0.2) | 8.4 (0.8) | 0.5 (0.0) |
| 28/04 | 1.8 (0.3) | 7.6 (0.9) | 14.2 (2.2) | 9.4 (0.4) | 1.7 (1.0) | 3.8 (0.2) | 2.4 (0.3) | 2.3 (1.0) | 8.9 (2.9) | 0.2 (0.0) |
| 02/05 | 1.6 (1.4) | 10.4 (1.6) | 11.7 (4.8) | 7.2 (3.2) | 2.8 (0.2) | 3.6 (0.2) | 1.6 (0.2) | 2.6 (0.4) | 7.7 (1.4) | 0.0 (0.0) |
| 09/05 | 1.1 (1.0) | 10.5 (3.2) | 13.4 (3.4) | 9.8 (3.5) | 2.5 (0.5) | 3.3 (0.2) | 2.0 (1.0) | 2.0 (0.6) | 7.5 (1.8) | 0.1 (0.0) |
| 12/05 | 1.8 (0.0) | 8.3 (0.3) | 15.8 (0.6) | 11.2 (0.5) | 2.1 (0.1) | 4.4 (0.0) | 1.9 (0.2) | 2.4 (0.2) | 8.2 (0.4) | 0.4 (0.1) |
| 16/05 | 1.8 (0.1) | 8.6 (0.3) | 17.7 (0.2) | 10.5 (0.3) | 2.4 (0.1) | 4.7 (0.0) | 1.8 (0.1) | 2.1 (0.0) | 6.1 (0.3) | 0.1 (0.1) |
| 19/05 | 2.5 (0.2) | 9.3 (0.3) | 18.1 (0.3) | 10.3 (0.2) | 2.4 (0.2) | 5.0 (0.0) | 1.7 (0.2) | 1.9 (0.1) | 5.5 (0.6) | 0.1 (0.0) |
| 23/05 | 2.4 (0.6) | 7.0 (3.1) | 18.8 (2.8) | 12.0 (1.5) | 3.0 (1.1) | 1.5 (0.1) | 2.3 (0.0) | 2.4 (0.2) | 6.1 (0.2) | 0.3 (0.2) |
| 26/05 | 2.2 (0.3) | 6.4 (3.2) | 16.7 (3.2) | 13.2 (3.2) | 2.2 (0.8) | 4.9 (0.1) | 2.3 (0.4) | 2.0 (0.6) | 5.9 (1.4) | 0.4 (0.2) |
| 30/05 | 2.9 (0.8) | 9.3 (0.5) | 20.2 (3.3) | 9.2 (0.4) | 3.2 (0.9) | 4.0 (0.3) | 1.2 (1.3) | 1.7 (1.1) | 8.4 (3.8) | 0.5 (0.2) |
| 06/06 | 2.3 (0.6) | 10.1 (0.6) | 12.4 (4.1) | 8.8 (3.3) | 1.9 (0.8) | 4.0 (0.1) | 1.6 (0.1) | 1.9 (0.2) | 5.3 (1.2) | 0.3 (0.0) |
| 14/06 | 2.5 (0.5) | 10.0 (0.4) | 16.3 (1.9) | 11.3 (0.3) | 2.6 (0.3) | 1.5 (0.0) | 1.0 (0.3) | 2.4 (0.4) | 6.2 (0.9) | 0.3 (0.0) |
| 27/06 | 2.9 (0.3) | 10.4 (0.2) | 14.0 (0.7) | 10.4 (3.0) | 2.2 (0.6) | 2.2 (0.0) | 0.8 (0.5) | 2.2 (1.0) | 8.7 (0.6) | 0.0 (0.0) |
| 11/07 | 3.9 (3.3) | 9.3 (0.9) | 13.5 (2.4) | 9.6 (1.4) | 1.6 (0.8) | 3.2 (0.1) | 1.7 (0.4) | 2.3 (0.2) | 6.5 (0.4) | 0.4 (0.0) |
| 27/07 | 1.9 (0.4) | 5.8 (3.3) | 12.6 (3.2) | 10.0 (0.9) | 3.0 (0.4) | 3.9 (0.2) | 2.2 (0.3) | 2.6 (0.1) | 7.2 (0.5) | 0.6 (0.1) |
| 16/08 | 2.2 (0.5) | 8.3 (0.6) | 13.8 (0.9) | 9.4 (2.2) | 1.6 (0.1) | 3.0 (0.1) | 1.7 (0.9) | 2.9 (0.3) | 7.4 (0.2) | 0.3 (0.2) |
| 30/08 | 1.8 (0.1) | 8.5 (0.3) | 15.2 (2.6) | 8.0 (1.0) | 1.8 (0.5) | 4.0 (0.0) | 2.4 (0.4) | 2.9 (0.4) | 7.3 (0.2) | 0.2 (0.0) |
| 05/09 | 1.6 (0.3) | 7.9 (0.9) | 17.0 (4.2) | 7.9 (1.3) | 2.2 (1.1) | 2.7 (0.1) | 2.4 (0.5) | 2.9 (0.5) | 7.8 (1.3) | 0.4 (0.3) |
| 03/10 | 3.0 (2.5) | 7.1 (2.7) | 13.0 (1.6) | 5.5 (1.3) | 1.9 (1.3) | 2.6 (0.2) | 2.1 (1.1) | 2.5 (1.6) | 7.4 (3.0) | 0.3 (0.3) |
| 24/10 | 3.0 (2.2) | 6.8 (2.8) | 11.1 (3.2) | 6.3 (2.7) | 2.6 (1.3) | 1.9 (0.4) | 2.0 (1.1) | 2.5 (1.7) | 7.5 (3.3) | 0.1 (0.1) |

| | *20:4(n-6)* | *20:4(n-3)* | *20:5(n-3)* | *22:6(n-3)* | *SAFA* | *MUFA* | *PUFA* | *DMA* | *(n-6)* | *(n-3)* |
|---|---|---|---|---|---|---|---|---|---|---|
| 21/03 | 3.3 (0.0) | 1.0 (0.5) | 23.0 (0.0) | 6.8 (0.0) | 26.5 (0.0) | 18.4 (0.6) | 51.1 (0.0) | 1.5 (0.0) | 3.5 (0.1) | 41.7 (0.2) |
| 04/04 | 2.4 (0.0) | 1.1 (1.3) | 21.5 (0.0) | 6.6 (0.0) | 27.1 (0.0) | 18.1 (0.3) | 50.4 (0.1) | 1.4 (0.0) | 3.7 (0.2) | 41.9 (0.3) |
| 11/04 | 1.5 (1.1) | 1.2 (0.2) | 21.6 (0.8) | 6.6 (0.2) | 27.0 (1.5) | 15.7 (1.0) | 53.1 (2.1) | 2.2 (0.4) | 3.7 (0.3) | 44.9 (2.3) |
| 18/04 | 2.5 (0.3) | 1.3 (0.2) | 21.8 (1.3) | 6.6 (0.4) | 28.1 (0.9) | 17.2 (1.2) | 51.5 (0.9) | 0.7 (0.8) | 3.4 (0.5) | 42.9 (1.3) |
| 26/04 | 2.8 (0.4) | 1.0 (0.4) | 23.6 (3.2) | 6.2 (0.6) | 26.3 (4.0) | 17.5 (2.7) | 53.4 (6.2) | 0.2 (0.1) | 3.7 (0.3) | 44.7 (5.1) |
| 28/04 | 2.6 (1.1) | 1.3 (0.4) | 24.6 (0.7) | 6.6 (0.9) | 25.0 (2.6) | 18.2 (1.5) | 54.4 (4.0) | 0.1 (0.1) | 3.9 (0.5) | 46.2 (5.0) |
| 02/05 | 3.2 (0.4) | 0.7 (0.2) | 25.8 (5.5) | 6.4 (1.6) | 26.5 (3.8) | 16.8 (4.3) | 54.2 (7.6) | 0.5 (0.8) | 3.0 (0.1) | 45.3 (8.2) |
| 09/05 | 2.4 (0.7) | 1.0 (0.4) | 19.9 (3.2) | 6.7 (2.2) | 29.5 (4.3) | 19.7 (5.7) | 48.3 (1.8) | 0.7 (0.8) | 3.5 (1.6) | 39.5 (1.5) |
| 12/05 | 2.2 (0.2) | 1.2 (0.0) | 22.5 (1.3) | 4.9 (0.5) | 28.0 (0.9) | 20.7 (0.7) | 48.0 (1.6) | 0.2 (0.0) | 3.2 (0.1) | 41.4 (1.5) |
| 16/05 | 2.8 (0.1) | 1.0 (0.1) | 20.1 (0.1) | 5.0 (0.5) | 31.3 (0.1) | 21.3 (0.5) | 44.6 (0.5) | 0.2 (0.0) | 3.2 (0.1) | 36.2 (0.5) |
| 19/05 | 2.6 (0.6) | 0.9 (0.1) | 17.8 (0.4) | 5.7 (0.3) | 32.7 (0.2) | 21.7 (0.6) | 42.3 (0.8) | 0.2 (0.1) | 3.1 (0.3) | 34.0 (0.5) |
| 23/05 | 2.8 (1.0) | 0.9 (0.3) | 18.5 (4.3) | 5.9 (1.1) | 31.1 (5.5) | 21.7 (1.9) | 44.0 (6.4) | 0.1 (0.1) | 3.9 (0.3) | 35.8 (5.0) |
| 26/05 | 2.4 (0.8) | 1.1 (0.2) | 19.1 (7.0) | 7.2 (2.5) | 27.1 (7.1) | 23.5 (3.0) | 46.1 (10.0) | 0.1 (0.1) | 3.9 (0.8) | 37.8 (9.6) |
| 30/05 | 2.5 (1.0) | 0.7 (0.2) | 13.4 (0.4) | 6.6 (2.2) | 35.2 (4.2) | 21.2 (2.3) | 39.5 (5.0) | 0.4 (0.3) | 2.4 (1.0) | 32.5 (5.0) |
| 06/06 | 4.9 (0.9) | 0.7 (0.2) | 25.6 (2.7) | 5.6 (1.7) | 26.8 (4.0) | 18.1 (5.3) | 52.0 (4.5) | 0.1 (0.0) | 3.4 (0.3) | 41.6 (4.9) |
| 14/06 | 3.8 (0.5) | 0.9 (0.1) | 22.7 (1.2) | 5.4 (0.6) | 30.3 (2.1) | 17.7 (0.7) | 48.5 (1.1) | 0.2 (0.0) | 2.3 (0.3) | 39.7 (2.1) |
| 27/06 | 3.4 (0.4) | 0.7 (0.1) | 23.0 (0.5) | 6.8 (0.7) | 27.3 (0.8) | 18.0 (1.7) | 50.8 (2.3) | 0.2 (0.1) | 2.1 (0.5) | 43.4 (1.6) |
| 11/07 | 3.7 (0.6) | 1.0 (0.1) | 24.3 (2.1) | 6.8 (0.6) | 25.7 (3.0) | 17.4 (2.2) | 51.6 (2.6) | 0.5 (0.5) | 3.2 (0.4) | 42.6 (1.9) |
| 27/07 | 3.5 (0.6) | 0.9 (0.1) | 22.3 (2.2) | 7.7 (0.3) | 22.9 (6.3) | 20.8 (2.0) | 52.8 (4.1) | 0.3 (0.1) | 3.8 (0.5) | 43.3 (2.7) |
| 16/08 | 2.8 (1.0) | 1.2 (0.1) | 24.0 (1.2) | 7.4 (2.3) | 25.9 (0.7) | 18.0 (1.6) | 53.5 (2.6) | 0.1 (0.1) | 3.3 (0.7) | 44.9 (0.6) |
| 30/08 | 3.1 (0.2) | 1.0 (0.0) | 21.9 (1.2) | 7.3 (1.3) | 27.9 (3.2) | 17.3 (0.3) | 52.3 (3.7) | 0.2 (0.0) | 3.7 (0.4) | 42.4 (2.8) |
| 05/09 | 3.0 (0.3) | 1.1 (0.2) | 21.9 (3.0) | 7.5 (1.8) | 28.6 (4.6) | 15.9 (2.2) | 53.2 (7.2) | 0.2 (0.0) | 3.7 (0.5) | 43.7 (6.6) |
| 03/10 | 4.4 (1.7) | 0.8 (0.5) | 22.9 (3.5) | 11.0 (3.8) | 26.1 (3.5) | 12.3 (3.2) | 58.0 (3.6) | 0.3 (0.2) | 3.5 (0.9) | 47.3 (4.5) |
| 24/10 | 4.4 (1.3) | 0.7 (0.5) | 22.3 (4.0) | 10.5 (3.4) | 23.6 (5.2) | 14.3 (6.0) | 56.0 (4.6) | 2.8 (3.7) | 3.5 (1.1) | 46.0 (5.5) |

cholesta(n-3)$\beta$-ol (coprostanol, 21.6 %), 24$\beta$-methylenecholesta-5,24(28)-die(n-3)$\beta$-ol (24 methylene cholesterol, 15.8 %), 24$\beta$-methylcholesta-5,22-die(n-3)$\beta$-ol (brassicasterol, 11.8 %) and 24$\beta$-ethylenecholesta-5-e(n-3)$\beta$-ol ($\beta$-sitosterol, 5.4 %). Cholesterol decreased slowly from 29.5 to 20.5 % during the study period, without any strong variation (Fig. 4.8). The evolution of 24 methylene cholesterol followed the same dynamics as fucoxanthin in the stomach content and EPA or 16:1(n-7) in the stomach tissue. A first increase in May was observed, lasting for two weeks with a maximum at 22 %. It was followed by a second more intense peak, in early June, up to 24 %, and a final increase in late September to about the same level as the first spring peak. Brassicasterol showed an inverse dynamic: it decreased down to 10 % from mid-April to mid-May, then increased at the end of the month before reaching a plateau in summer and finally slightly decreased from mid-August until the end of the study.

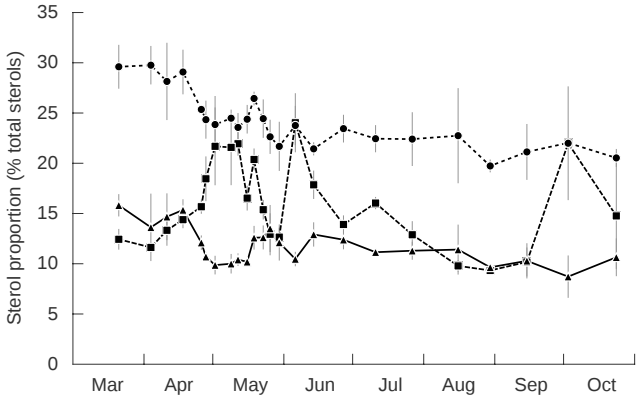


**Figure 4.8:** Proportion of cholesterol (dotted line, full dots), 24 methylene cholesterol (dashed line, full squares) and brassicasterol (solid line, full triangles) in the digestive gland of *P. maximus* (expressed as sterol percentage of total) in the Bay of Brest, during the year 2011. Standard deviations are presented as vertical gray lines.

**Table 4.4:** Sterol composition of the digestive gland of *P. maximus* (expressed as sterol percentage of total) in the Bay of Brest during year 2011. NOR: Norcholesterol, CHO: Cholesterol, BRA: Brassicasterol, DES: Desmosterol, CAM: Campesterol, 24M: 24 Methylene, STI: Stigmasterol, BSI: $\beta$-Sitosterol, FUS: Fucosterol, OTH: other sterols, TOT: total sterol concentration (in $\mu mol\, g^{-1}$). Standard deviations are in brackets.

| *Date* | *NOR* | *CHO* | *BRA* | *DES* | *CAM* | *24M* | *STI* | *BSI* | *FUC* | *OTH* | *TOT* |
|---|---|---|---|---|---|---|---|---|---|---|---|
| 21/03 | 4.0 (0.4) | 29.6 (2.1) | 15.8 (1.1) | 4.6 (0.3) | 2.5 (0.2) | 12.4 (1.0) | 3.3 (0.6) | 6.9 (0.4) | 1.7 (0.2) | 19.2 (1.3) | 46.77 (3.74) |
| 04/04 | 4.3 (0.2) | 29.8 (1.9) | 13.6 (3.3) | 4.0 (1.3) | 2.3 (0.5) | 11.6 (0.4) | 3.0 (1.0) | 5.9 (1.4) | 1.5 (0.4) | 23.9 (0.8) | 50.85 (10.28) |
| 11/04 | 4.1 (0.5) | 28.1 (3.8) | 14.7 (2.3) | 3.7 (0.3) | 2.5 (0.3) | 13.3 (1.5) | 2.9 (0.3) | 5.9 (0.8) | 1.7 (0.3) | 23.5 (1.3) | 35.92 (10.31) |
| 18/04 | 4.3 (0.2) | 29.1 (2.2) | 15.4 (1.0) | 2.9 (0.2) | 2.1 (0.1) | 14.4 (0.8) | 2.9 (0.4) | 6.1 (0.6) | 1.6 (0.2) | 21.8 (0.6) | 55.65 (5.89) |
| 26/04 | 3.6 (0.5) | 25.4 (0.4) | 12.1 (0.7) | 2.2 (0.8) | 1.9 (0.1) | 15.7 (0.7) | 2.1 (0.3) | 5.3 (0.8) | 1.9 (0.2) | 29.8 (0.4) | 58.81 (1.80) |
| 28/04 | 2.7 (0.1) | 24.3 (1.8) | 10.7 (0.4) | 2.8 (0.6) | 1.7 (0.1) | 18.5 (2.2) | 2.5 (0.3) | 5.6 (1.1) | 1.6 (0.2) | 30.1 (0.7) | 53.73 (6.10) |
| 02/05 | 3.3 (0.4) | 23.9 (2.8) | 9.9 (0.9) | 2.2 (0.2) | 1.9 (0.1) | 21.7 (3.8) | 2.5 (0.4) | 5.0 (0.9) | 1.3 (0.0) | 28.5 (0.4) | 50.75 (9.01) |
| 09/05 | 3.6 (0.3) | 24.5 (0.4) | 10.0 (0.9) | 1.8 (0.2) | 1.7 (0.2) | 21.6 (3.7) | 2.5 (0.5) | 5.0 (0.2) | 1.3 (0.1) | 27.9 (0.6) | 49.75 (3.02) |
| 12/05 | 3.2 (0.1) | 23.6 (1.4) | 10.4 (0.6) | 2.9 (0.3) | 1.8 (0.3) | 21.9 (1.1) | 3.0 (0.5) | 6.4 (0.3) | 1.3 (0.5) | 25.4 (0.3) | 47.28 (3.71) |
| 16/05 | 3.4 (0.3) | 24.4 (1.4) | 10.2 (0.1) | 2.9 (0.7) | 1.7 (0.5) | 16.5 (1.2) | 3.1 (0.3) | 6.2 (0.6) | 1.4 (0.1) | 30.1 (0.4) | 44.42 (3.44) |
| 19/05 | 0.0 (0.0) | 26.4 (0.6) | 12.6 (1.1) | 3.9 (0.5) | 2.3 (0.1) | 20.4 (1.0) | 4.1 (0.7) | 7.3 (0.8) | 2.0 (0.4) | 20.9 (1.2) | 41.18 (6.64) |
| 23/05 | 3.7 (0.2) | 24.4 (1.9) | 12.6 (1.1) | 2.9 (0.4) | 2.2 (0.1) | 15.4 (0.9) | 3.3 (0.2) | 6.2 (0.6) | 1.7 (0.3) | 27.6 (1.6) | 48.88 (7.28) |
| 26/05 | 3.6 (0.1) | 22.6 (1.7) | 13.5 (2.3) | 2.7 (0.5) | 2.3 (0.2) | 12.9 (2.0) | 3.4 (0.7) | 6.3 (1.0) | 2.0 (0.3) | 30.7 (0.7) | 52.73 (8.72) |
| 30/05 | 3.0 (0.4) | 21.7 (2.4) | 12.1 (1.7) | 3.2 (0.6) | 2.0 (0.2) | 12.6 (0.9) | 3.0 (1.0) | 5.7 (1.4) | 1.7 (0.4) | 34.9 (1.1) | 73.73 (9.28) |
| 06/06 | 3.4 (0.2) | 23.8 (1.9) | 10.5 (0.7) | 2.2 (0.1) | 2.4 (0.4) | 24.0 (2.9) | 2.5 (0.3) | 4.8 (0.6) | 1.1 (0.0) | 26.5 (0.5) | 183.08 (4.59) |
| 14/06 | 2.6 (0.1) | 21.4 (0.6) | 12.9 (1.2) | 2.8 (0.4) | 3.2 (0.4) | 17.9 (1.4) | 2.0 (0.4) | 4.9 (0.8) | 1.2 (0.2) | 31.1 (0.4) | 66.02 (5.00) |
| 27/06 | 3.3 (0.1) | 23.4 (1.3) | 12.4 (0.9) | 2.4 (0.1) | 2.2 (0.2) | 13.9 (0.9) | 2.7 (0.2) | 4.7 (0.1) | 1.4 (0.1) | 33.6 (0.8) | 62.34 (4.91) |
| 11/07 | 2.5 (0.3) | 22.4 (1.3) | 11.1 (0.3) | 3.5 (0.7) | 1.9 (0.2) | 16.0 (0.6) | 2.4 (0.3) | 4.9 (0.3) | 0.9 (0.5) | 34.3 (1.2) | 63.79 (2.78) |
| 27/07 | 2.4 (0.1) | 22.4 (2.6) | 11.3 (0.8) | 2.8 (1.2) | 2.3 (0.2) | 12.9 (1.3) | 2.6 (0.4) | 4.9 (0.5) | 1.8 (0.5) | 37.4 (1.7) | 54.35 (9.16) |
| 16/08 | 2.8 (0.6) | 22.7 (4.7) | 11.4 (2.4) | 2.3 (1.1) | 2.3 (0.1) | 9.8 (0.5) | 2.7 (0.2) | 6.4 (2.2) | 2.0 (0.1) | 42.4 (1.5) | 42.89 (4.49) |
| 30/08 | 2.4 (0.3) | 19.7 (0.6) | 9.6 (0.0) | 2.7 (0.3) | 2.1 (0.1) | 9.3 (0.1) | 2.6 (0.3) | 4.5 (0.3) | 1.6 (0.4) | 45.2 (0.5) | 91.12 (0.88) |
| 15/09 | 2.9 (0.2) | 21.1 (2.7) | 10.3 (1.7) | 1.5 (0.9) | 2.2 (0.4) | 10.2 (1.4) | 2.5 (0.7) | 3.2 (1.5) | 1.5 (0.4) | 44.7 (0.8) | 98.50 (6.42) |
| 03/10 | 1.9 (0.3) | 22.0 (0.4) | 8.7 (2.1) | 1.3 (0.9) | 1.8 (0.3) | 22.0 (5.6) | 2.3 (0.5) | 2.6 (1.7) | 1.3 (0.2) | 36.2 (1.4) | 65.43 (3.47) |
| 24/10 | 3.0 (0.4) | 20.5 (0.8) | 10.6 (1.8) | 2.0 (0.6) | 2.2 (0.3) | 14.8 (5.2) | 2.1 (0.1) | 4.4 (0.6) | 1.6 (0.2) | 39.5 (0.5) | 105.31 (8.02) |

## 4.4 Discussion

### 4.4.1 Validation of biomarkers

To our knowledge, the present study is the first one to combine the use of pigments, fatty acids (FA) and sterols as food source biomarkers in a seasonal trophic study of a marine suspension-feeding invertebrate. The only other study presenting similar data is the one of Hurtado et al. (2012), which focused on seasonal dynamics of pigments, FA and sterols in relation to the reproductive activity of female *Crassostrea corteziensis*. They concluded that these indicators were relevant when trying to infer energy reserve dynamics, because they are essential membrane components provided by diet and food availability.

There was a clear relationship between pigment concentration and composition in the water and the phytoplankton cell microscopic observations. The variation of fucoxanthin proportion well matched each diatom bloom in early May, early June and late September (Fig. 4.2). Indeed, this pigment has been reported to be a specific pigment of diatoms (Jeffrey, 1974, 1997; Lampert, 2001). Likewise, the highly variable dynamics of Dinophyceae blooms was very well reproduced by the proportion of peridinin in the water. Then, alloxanthin proportion recorded in the filtrates at the two sampled depths matched precisely the identification of Cryptophyceae, which is also in accordance with previous observations (Jeffrey, 1974, 1997; Lampert, 2001). The Prymnesiophyceae algae class has also been reported to especially contain 19'HF (Jeffrey, 1974, 1997; Lampert, 2001), which in the present study seemed to be well correlated to the development of this microalgae class. However, cell identification did not fit well with measurements of chlorophyll-*b*, a pigment usually linked to Chlorophyceae (Jeffrey, 1974, 1997; Lampert, 2001). Indeed, while the proportion of chlorophyll-*b* in the filtered water was rather high during the study (up to 15 % in the water column and 25 % at the bottom, especially during summer), only one bloom of Chlorophyceae was registered in late May (Chatterjee, 2014). Nevertheless, this pigment was also reported to be a major component of green macroalgae, which are often observed in the bay (Ménesguen et al., 2006). The important level registered in our filtrates could be then attributed to discarded pieces of macroalgae in the water (Lampert, 2001). The microalgae *Lepidodinium chlorophorum*, which bloomed between mid-July and mid-August (Chatterjee, 2014), is also the only known Dinophyceae to contain chlorophyll-*b* (Zapata et al., 2012), which is likely to explain the presence of this pigment in the water at this time.

Lipid dynamics in the digestive gland fluctuated less than pigments in the gut content. The incorporation of lipids in the tissues of the organism is a regulated process, smoothed by homeostatic processes and selective incorporation mechanisms (Soudant et al., 1996). On the other hand, pigments are not edible compounds to be assimilated by the scallops (Shuman and Lorenzen, 1975). For the majority, they are egested within faeces in a more or less de-

graded form. Considering the properties of these two biochemical compounds, the strong changes observed in both FA from the polar lipids and sterols were important and showed critical modifications of the cell membrane of the digestive gland tissue, notwithstanding the rather strong homeostasis that would be expected for these structural compounds.

### 4.4.2 Feeding ecology

#### Importance of Dinophyceae in the diet of *P. maximus*

The present study showed the complexity of the diet of *P. maximus*, which seemed to feed on the various algae classes available in the water. During the monitoring, the proportion of DHA, representative of Dinophyceae (Parrish et al., 1995; Dalsgaard et al., 2003; Parrish, 2013), in the polar lipids of the digestive gland showed rather important variations. Another FA already found in some Dinophyceae species is the 18:5(n-3) (Dijkman and Kromkamp, 2006), which displayed variations that were very similar to the dynamics of peridinin and DHA. The average level of peridinin, a specific pigment of the Dinophyceae (Jeffrey, 1974, 1997; Lampert, 2001), in the digestive tract of *P. maximus* reaches 18 % in the stomach, indicating a significant ingestion of this microalgae class. This is quite surprising as peridinin amount in the water did not exceed 13 %. Loret et al. (2000) observed similar results in *Pinctada margaritifera*, which actively selected Cryptophyceae despite their relatively low presence in the water. Dinophyceae were not the dominating phylum among the phytoplankton taxa identified in the water. Despite their relatively low occurrence in the water, biomarkers of this phylum were found in the scallop. This allows us to assume that *P. maximus* is actively selecting Dinophyceae. And yet, many of Dinophyceae species are known for their toxicity. Several studies have reported the negative consequences of such bloom events on the physiology of *P. maximus* (Erard-Le Denn et al., 1990; Lorrain et al., 2000; Chauvaud et al., 2001). Not all the species of Dinophyceae produce toxins but it has long been considered more as a threat than as a food source for the great scallop (Smolowitz and Shumway, 1997; Lorrain et al., 2000; Chauvaud et al., 2001; Bougrier et al., 2003). No harmful species were, however, observed during year 2011. Moreover, DHA as well as EPA are essential FA for bivalves (Soudant et al., 1996, 1998b) and DHA is known to be largely present in Dinophyceae yet also found in some Prymnesiophyceae (Parrish et al., 1995; Volkman et al., 1998; Dalsgaard et al., 2003; Mansour et al., 2005; Parrish, 2013). Thus, *P. maximus* seems to be able to select and sort ingested food on a qualitative basis. Suggestions have been made in this way to explain the active selection of food particles in suspension-feeding bivalves, involving ctenidia retention, labial palps sorting and physico-chemical interactions with aglal cell surface (Shumway et al., 1985; Ward and Shumway, 2004; Espinosa et al., 2010; Rosa et al., 2013).

Feeding activity seemed to be more correlated to the phytoplankton dynamics of bottom water in the beginning of spring, which goes along with the suggested ability of *P. maximus* to resuspend microphytobenthos and sedimented microalgae by clapping its shell valves (Lorrain et al., 2000; Chauvaud et al., 2001; MacDonald et al., 2006; Nerot et al., 2012). On the other hand, the scallop's diet followed more closely the seston dynamics of the water column for the rest of the study period, which is also in compliance with a well described benthic-pelagic coupling (Chauvaud et al., 2000; Cranford et al., 2005). Moreover, the great scallop seemed to be able to switch from one source to another depending on the season. Indeed, despite the predominant proportion of diatoms as food source for scallops, Fig. 4.4 shows that there is an alternation of two pigments in the stomach content between fucoxanthin, found mainly in diatoms; and peridinin, found exclusively in Dinophyceae. These shifts can also be observed in Fig. 4.7 which presents the proportion of 16:1(n-7) and EPA, representative of diatoms and DHA, representative of Dinophyceae. Furthermore, the ratio between EPA and DHA is often used as an indicator of a diatom- or flagellate-based diet (St. John and Lund, 1996; Auel et al., 2002). The variations of this index are in total accordance with the evolution of other biomarkers. Finally, Fig. 4.8 brings further evidence of this alternation by showing the evolution of 24 methylene cholesterol and brassicasterol in the digestive gland tissues, which have also been reported to be major sterols of these two algae classes respectively (Volkman, 1986). During the most important bloom in the water column in early May, proportions of fucoxanthin rapidly increased in the scallop's digestive gland before dropping on May 2$^{nd}$ and rise back to previous high level four days after. During this bloom the dominant species were the diatoms *Chaetoceros sp.*, *Dactiliosolen fragilissimus*, *Chaetoceros debilis* and *Cerataulina pelagica*. A temporary stop in diatom ingestion while cell concentrations are at their maximum in the water could result from an overload of sedimenting microalgae. This hypothesis was suggested by Lorrain et al. (2000), which claimed that overly elevated food particles of high quality in the surrounding of the scallop may have a negative effect on filtration and growth. Flocculation is well established as a dominant process in the transport of nutrients to the benthos (Alldredge and Gotschalk, 1989; Cranford et al., 2005) and is particularly significant in supplying food to species such as *P. maximus* that can reside on the continental shelf at depths of up to approximately 220 m (Nerot et al., 2012). However, the aggregation of blooming microalgae may have caused the scallop to close its valves to prevent/respond to gill clogging. Moreover, these blooming events might lead to oxygen depletion at the bottom, to which the scallop reacts by closing its valves (Taylor et al., 1985; Lorrain et al., 2000).

### Diet switches

*P. maximus*, as other suspension-feeding bivalves is known to feed mainly on microalgae, filtrated from the surrounding seawater (Le Pennec et al., 2003;

MacDonald et al., 2006). The "bottom-up" relationship between the great scallop and its food implies a feeding plasticity in response to the environmental availability. This study, conducted over eight months, during which food is abundant for *P. maximus*, shows that its diet is actually changing over time. Indeed, three contrasting periods can be observed. First, from the very beginning of the study until the first big bloom in the water column in early May, scallops seemed to feed on Dinophyceae, Prymnesiophyceae, Cryptophyceae and Chrysophyceae, given the respective proportions of peridinin, 19'HF, alloxanthin and 19'BF in their stomach. This is also supported by the evolution of DHA, found in high proportion in the Dinophyceae, 18:4(n-3), a common FA in Prymnesiophyceae and 20:4(n-3) rarely found in other microalgae classes than the Cryptophyceae (Volkman et al., 1998; Dalsgaard et al., 2003), even though the later can result from the elongation of 18:4(n-3). Then, during spring and the renewal of primary production in the water, *P. maximus* seems to feed mainly on diatoms and Dinophyceae, of which respective specific pigments account for more than 90 % of the total pigments found in the stomach content. At the end of May, the proportion of Prymnesiophyceae in the scallop's diet briefly increased, as shown by the ingestion of 19'HF-rich microalgae (Fig. 4.2) and the accumulation of 18:4(n-3) (Fig. 4.7). Later, the level of chlorophyll-*b* in the gut of the scallop, which remained under 2 % before the last spring bloom in early June, increased then up to 15 % during the first part of summer, indicating an ingestion of green micro- or macroalgae (Lampert, 2001). The FA composition of polar lipids 18:2(n-6) and 18:3(n-3), usually used as trophic signatures of green macroalgae or Chlorophyceae (Jamieson and Reid, 1972; Parrish et al., 1995; Zhukova and Aizdaicher, 1995; Volkman et al., 1998; Dalsgaard et al., 2003; Parrish, 2013), showed a rather smoothed increase from June until October. Finally at the end of the monitoring (late September-early October), sharp increases of 24 methylene cholesterol, fucoxanthin and EPA are evidence of a diatom based diet.

The dynamics of iso17:0 FA from the PL might indicate that bacteria took part into the diet of *P. maximus*. This FA is known to be very characteristic of marine bacteria (Perry et al., 1979; Vestal and White, 1989; Kharlamenko et al., 2001, 2008). Several studies proved that microorganisms could be ingested and assimilated by bivalves (McHenery and Birkbeck, 1985; Prieur et al., 1990; Alber and Valiela, 1994, 1995, 1996). In a review of the particle retention efficiency in Pectinidae, MacDonald et al. (2006) affirmed that free bacterioplankton, typically ranging in size from 0.3 to 1 µm, was not available as a food source for pectinids unless bound in aggregates. At certain times of the year, a large proportion (>70 %) of natural particulates of varying size and quality can form aggregates mixed with high molecular weight substances (flocs, marine snow; Alldredge et al., 1993, Crocker and Passow, 1995). Alber and Valiela (1995) and Alber and Valiela (1996) suggested that organic aggregates, or flocs, could potentially represent an important and nutritious food source for suspension-feeding bivalves. Therefore the proportions of iso 17:0 FA observed in the digestive gland of *P. maximus*, especially at the beginning

of the study (March), may be explained by an ingestion of bacteria. Finally, this diet might sustain to some extend the energetic requirements of the great scallop when microalgae are present in very low concentration in the water (i.e. during the bleak season).

### 4.4.3 Ingestion, digestion and assimilation

Some pigments detected in the water did not appear in the same proportions in the scallop's gut. Several experimental studies have pointed out the capacity of *P. maximus* to select different algae species on the basis of their size, nutritional value, physiological state or lipid content (Shumway et al., 1985; Soudant et al., 1998b; Ward and Shumway, 2004). The last findings revealed interactions between a protein of the mucus that covers oyster's gills and carbohydrate at the surface of microalgae cells Espinosa et al. (2010). These authors provided insights into the carbohydrate specificity of lectins that may be implicated in the selection of microalgal species. Rosa et al. (2013) also highlighted non-specific interactions involving surface-charge and wettability of particles in the particle discrimination process. During the second half of May, a surge of chlorophyll-*b* was observed in the seawater, both in the water column and in the water-sediment interface. The proportion of this pigment was nonetheless close to zero in the stomach content (Fig. 4.2). In contrast, the FA composition at this time showed a clear accumulation of 18:2(n-6) and 18:3(n-3) in the DG tissue. But this could possibly reflect an ingestion of Cryptophyceae or Prymnesiophyceae (observed in the seawater at this period), which can also present significant amounts of these FA (Viso and Marty, 1993; Soudant et al., 1996; Renaud et al., 2002). Moreover, zeaxanthin was measured at levels varying between 5 and 10 % in the water column as well as at the water-sediment interface during the whole duration of the study. However, except at the first sampling point, the contribution of zeaxanthin was close to zero for the rest of the time (Table 4.1). Zeaxanthin is a biomarker of cyanobacteria (Jeffrey, 1974, 1997; Lampert, 2001), the size of which is under 2 µm. The gill retention of most bivalve is not fine enough to capture such tiny particles (Møhlenberg and Riisgård, 1978; MacDonald et al., 2006; Strohmeier et al., 2012), but some studies have hypothesized that microalgae aggregates or adduction on bigger particle could permit an indirect ingestion of cyanobacteria by bivalves (Ward and Kach, 2009). This could explain the occurrence of zeaxanthin in relatively high amounts (3 %) in the first sample. Furthermore, their occurrence during the winter may sustain energy needs of *P. maximus* through this process, when no other trophic sources are available (Quéguiner and Tréguer, 1984; Strohmeier, 2009).

Beyond the matter of ingestion stands the question of the digestion and assimilation of the ingested products. Some pigments found in the stomach were found in the rectum in similar proportions, possibly meaning that they were not subject to digestion (Hawkins et al., 1986; Louda et al., 2008). This is the case for fucoxanthin during the month of May and at the end of July or

for peridinin in late May and in mid-July to mid-August. A strong correlation is also observed for chlorophyll-*b*, which could reflect a negative selectivity against this trophic source. Microalgae cell wall, varying in size, structure and composition among species, might affect the digestibility of phytoplankton.

Phaeophorbid-*a* and phaeophytin-*a* are two pigments resulting from the degradation of chlorophyll-*a* (Hawkins et al., 1986). Significant amounts (up to 36 % of phaeophorbid-*a* and 25 % of phaeophytin-*a*) were found in the stomach, suggesting a first step of food processing (Fig. 4.6). Digestion in *P. maximus* is both extra- and intracellular and occurs at several sites in the digestive tract (Beninger and Le Pennec, 2006). The first step of degradation occurs in the stomach with both a mechanical and chemical action of the crystalline style that breaks and releases enzymes attacking the microalgae frustule. Pigments contained in microalgae undergo different levels of degradation by the enzymatic activity of digestion (Bayne et al., 1987; Pastoureaud et al., 1995). Degradation peaks observed after periods of low ingestion could result from the degradation of the food remains in the stomach and the DG. Indeed, scallops have to cope with periods of low food availability, such as during the winter or between phytoplankton blooms. The degradation of the last food particles in the stomach could provide them with nutrients while awaiting a renewal of food supply. Another possible explanation could be the passive deterioration (not due to active digestion) of remaining products of digestion inside the stomach.

## Acknowledgements

This study has been supported in part by the following: CHIVAS ANR program (Agence Nationale de la Recherche, ANR-Blanc), the COMANCHE ANR program (Agence Nationale de la Recherche, ANR-2010-STRA-010) and the Yggdrasil scholarship (Research Council of Norway, grant 211173/F11). The authors gratefully acknowledge the IUEM dive team (Erwan Amice, Isabelle Bihannic, Julien Thébault, Joëlle Richard and Laurent Chauvaud) for deploying and collecting scallops and monitoring probes. We thank Charlotte Corporeau, Claudie Quéré and Gauthier Schall for the help in lipids analysis, result interpretation and fruitful discussions. We also thank Beatriz Beker, Aude Leynaert, Virginie Klein and Arnab Chatterjee for phytoplankton identification and Aurore Naegelen for providing water samples. We deeply acknowledge Ewan Harney for correction of English writing.

# Chapter 5

# Inversion of DEB model

**What the shell can tell about the scallop? Insights from inverted DEB model**

*Manuscript in preparation for submission to Ecological Modelling*

**Romain Lavaud**, Eric Rannou, Fred Jean and Jonathan Flye-Sainte-Marie.

**Abstract**
Dynamic Energy Budget (DEB) models describe the rates at which organisms assimilate and utilize energy from food for maintenance, growth, reproduction and development. We developed an inverted DEB model, relying on temperature and growth trajectories, in order to infer the functional response. It uses a single linear equation derived from DEB theory's set of equations that describes the dynamics of growth. It is thus possible to reconstruct the functional response to food availability. This formula gives also access to reserve state variable, reserve density, mobilization and somatic maintenance rates. Our approach addresses a difficulty of measuring food availability, often encountered in bioenergetics modeling. Many bivalves, such as the great scallop, *Pecten maximus*, provide high frequency archives of their past history thanks to the incremental growth of their shell. We thus explored the potential of the method to reconstruct the functional response from daily shell growth rate. Starting from a theoretical case, we explored the resolution and sensitivity limits of the method. Results were checked by using the reconstructed functional response in a back simulation of growth that was compared to the initial growth trajectory. Moreover, as growth data used in the reconstruction pro-

cess usually show high-frequency variability, we also developed a smoothing method, based on DEB theory assumptions, to filter growth data time series.

**Keywords:** modeling; Dynamic Energy Budget; growth; environmental reconstruction; functional response; physiological state; *Pecten maximus*; sclerochronology.

## 5.1 Introduction

All models are characterized by specific parameters that require input variables to produce a simulation (a prediction) of a computed process. Bioenergetic models rely on an energy input which will be determined by the formalization of various processes described within a given theory. The acquisition and thus the reliability of input variables are of the highest importance as it determines the confidence one should put in the model results. Nevertheless, a large number of bioenergetics modeling studies point to the difficulty of assessing the correct energy inputs (Furness, 1978; Stockwell and Johnson, 1997; Chipps and Wahl, 2008; Bourlès et al., 2009; Bartell et al., 1986).

Dynamic Energy Budget (DEB) models rely on a mechanistic theory that describes the quantitative organization of metabolism, accomplished within an organism thanks to the uptake and use of substrates (Kooijman, 2010). DEB models have been applied to a large number of species in order to describe and further understand the dynamics of their maintenance, growth, reproductive effort, maturation and many other biological traits (Pecquerie et al., 2009; Lorena et al., 2010; Jusup et al., 2011; Lavaud et al., 2013, e.g.). In the view of simulating such processes, DEB models require two fundamental inputs: temperature and food condition data. However, although the first one is generally easily obtained, food availability, as mentioned for other models, is more often problematic, especially for aquatic animals in natural environments. Indeed, the link between food availability and assimilation is a persistent issue, common to almost all bioenergetic models (Grant and Bacher, 1998; Flye-Sainte-Marie et al., 2007; Chipps and Wahl, 2008). Sometimes it is less difficult to measure the growth trajectory of organisms using longitudinal monitoring. This is the case for many shellfish, fish otoliths, some bones and tree rings, i.e. structures acting as archives of the organism's life history. The availability of such information, treated through sclerochronological techniques, theoretically allows the inversion of the model and to reconstruct the assimilated energy from observed growth trajectories and temperature.

Some promising attempts to reconstruct individual scaled food ingestion history have already been reported (Cardoso et al., 2006; Freitas et al., 2009; Troost et al., 2010; Pecquerie et al., 2012). Different approaches were used, from an empirical calibration of functional response (Cardoso et al., 2006) to a more formalized framework (Pecquerie et al., 2012). Recently, Rannou (2009) proposed a reformulation of DEB equations into a single simplified equation. This work has also provided the research community with a tool that can easily

be manipulated in order to simulate various processes. Among the possibilities revealed by this equation, the reconstruction of temporal food variation and of the dynamics of major DEB variables via growth trajectory is a crucial achievement.

The great scallop *Pecten maximus* has long been studied for its remarkable growth patterns, and more particularly with a focus on the shell microstructure. Resulting from the precipitation of calcium carbonate present in the surrounding environment, the calcified skeleton grows by tiny increments every day (Clark, 1968; Owen et al., 2002b; Clark, 2005). Incremental thickness is mainly controlled by temperature (Chauvaud et al., 1998) and food conditions (Chauvaud et al., 1998; Laing, 2000) but rapid changes of growth rate have also been suspected to be caused by salinity variations (Laing, 2002) and algae blooms (Chauvaud et al., 1998; Lorrain et al., 2000; Liu et al., 2008). Daily shell growth rate patterns provide such a high resolution that it is possible to assign calendar dates to each growth increment. This property has been exploited to use the shell of *P. maximus* as a biological archive for many different purposes including physiology (Lorrain et al., 2000), paleoclimate reconstructions through sclerochronology (Chauvaud et al., 2005), the study of growth influencing factors (Chauvaud et al., 1998; Laing, 2000, 2002) or elemental concentrations investigation, in order to try to infer ecosystem properties (Barats et al., 2008a,b, 2009; Thébault and Chauvaud, 2013).

In this study we explore the potential of using sclerochronological data for reconstruction of physiological variables, including the functional response using an inverted DEB model. The inversion procedure relies on the simplified growth equation of Rannou (2009), which gives access to various DEB variables from a single equation. We explored the accuracy and sensitivity limits of this method to reconstruct scaled food ingestion and other metabolic processes through a theoretical cases study. Moreover, as growth data used in the reconstruction process usually show high-frequency variability, we also developed a smoothing method to filter growth data time series based on DEB theory assumptions.

## 5.2 Material and methods

### 5.2.1 The DEB model

Dynamic Energy Budget theory (Kooijman, 2010) provides a generalized framework that permits one to quantitatively follow the bioenergetic dynamics of an individual by considering three state variables: reserves ($E$), structural volume ($V$) and reserves dedicated to reproduction ($E_R$). Two forcing variables are necessary to feed the model: the temperature and a food density proxy. According to DEB theory, ingested food is converted with a constant efficiency into assimilates added to the reserve compound. Energy from reserves is then used according to the $\kappa$-rule which states that a fixed fraction $\kappa$ of the mobilized reserves is allocated to somatic maintenance plus structural growth with

a priority to maintenance and the rest (1-$\kappa$) is directed to maturity maintenance plus maturation before puberty, and to maturity plus reproduction during the adult stage. Priority is here again given to maintenance costs. The implementation of energy fluxes within the organism and the estimation of a set of species-specific parameters allow the simulation of any metabolic process such as growth in length or in weight, reproductive activity, etc.

The simplest relationship between feeding and food density $X$ described in DEB theory is a scale hyperbolic functional response of the form $f = \frac{X}{X + X_K}$, where $X_K$ is the half saturation coefficient. The corresponding curve is a Holling type II function varying between 0 (no food uptake) and 1 (representing *ad libitum* food condition). According to DEB theory, growth is not directly connected to feeding as assimilates are not directly used to fuel metabolic functions but go into the reserve compartment, which is acting as a buffer. Assimilation flux varies as a function of environmental conditions while mobilization of energy from reserve depends on the state of the organism (i.e. its reserve density and body size). For practical reasons, we will directly use physical length (i.e. observed data) rather that structural length in the following part of this work.

### 5.2.2 A linear equation of growth in DEB theory

#### Assumptions

In the reconstruction process we will use a reformulation of DEB equations, developed by Rannou (2009), which is identical to the system of differential equations used in DEB theory to describe state variables dynamics. It gives access to DEB variables but requires only three compound parameters of the standard DEB model. This manipulation and the use of the "growth DEB equation" relies on the following assumptions:

1. The studied organism must have an isomorphic growth, which is likely to be the case for the great scallop, at least after metamorphosis, to which we restrict the analysis.

2. *P. maximus* produces daily shell growth increments (Clark, 1968; Antoine, 1978), which are considered as a means to evaluate the temporal dynamics of structural growth.

3. The dynamics of structural length must be positive. As we will use length increments, this assumption always hold in our case.

4. The use of the reformulated growth equation in its actual form is restricted to ectotherms and avoids any heating costs. As for standard DEB theory, temperature affects all rates in the same way and is formalized as a correction factor to each flux parameter on the basis of the commonly used Arrhenius relationship.

5. Maturity is not directly considered here but could be as it relates to growth through the $\kappa$-rule.

**"Growth DEB equation"**

The "growth DEB equation" is a second order equation expressed by a one-dimension parameter $L_w$ and contains only three DEB compound parameters ($\dot{k}_M$, $\dot{v}_\delta$ and $L_{wm}$) that are necessary to model growth within DEB theory in a synthetic form of a single equation. $\dot{k}_M$, a primary parameter from DEB theory, is the somatic maintenance rate coefficient ($\mathrm{d}^{-1}$). The two other parameters are corrected from shape differences as they both refer to structural measures divided by the shape coefficient. Thus $L_{wm}$ stands for the maximum physical length (cm) and $\dot{v}_\delta$ for the shape-corrected energy conductance ($\mathrm{cm\,d}^{-1}$). The "growth DEB equation" is built from a rewriting of the differential system of state variables dynamic in standard DEB theory (Rannou, 2009). The "growth DEB equation" is as follow:

$$\begin{aligned} &-9{L_w}'^2 + 3L_w{L_w}'' - f\dot{v}_\delta\dot{k}_M L_{wm} + 6fL_{wm}L'_w + 3\dot{v}_\delta L'_w + \dot{v}_\delta\dot{k}_M L_w - 2\dot{k}_M L_w L'_w \\ &-9f\frac{\dot{k}_M L_{wm}}{\dot{v}_\delta}{L_w}'^2 - 3\frac{\dot{k}_M}{\dot{v}_\delta}L_w{L_w}'^2 + 3\frac{\dot{k}_M}{\dot{v}_\delta}L_w^2{L_w}'' - 3\left(1+\frac{\dot{k}_M}{\dot{v}_\delta}\,L_w\right)L_wL'_w\frac{T_AT'}{T^2} = 0 \end{aligned} \tag{5.1}$$

where the three compound parameters are defined as follow:

- $\dot{k}_M = \frac{[\dot{p}_M]}{[E_G]}$
- $L_{wm} = \frac{L_m}{\delta_{\mathcal{M}}}$
- $\dot{v}_\delta = \frac{\dot{v}}{\delta_{\mathcal{M}}}$

The list of DEB primary parameters for *P. maximus* ($\delta_{\mathcal{M}}$, $[\dot{p}_M]$, $[E_G]$ and $\dot{v}$) are given in Table 5.1 and were taken from Lavaud et al. (2013). The last term of this equation corresponds to the temperature correction factor and is not strictly necessary. To get the functional response reconstruction, the $f$ term is eventually extracted from the "growth DEB equation" which gives:

$$\begin{aligned} f = \Bigg(&-9{L_w}'^2 + 3L_w{L_w}'' + 3\dot{v}_\delta L'_w + \dot{v}_\delta\dot{k}_M L_w - 2\dot{k}_M L_w L'_w - 3\frac{\dot{k}_M}{\dot{v}_\delta}L_w{L_w}'^2 + 3\frac{\dot{k}_M}{\dot{v}_\delta} \\ &L_w^2{L_w}'' - 3\left[1+\frac{\dot{k}_M}{\dot{v}_\delta}\,L_w\right]L_wL'_w\frac{T_AT'}{T^2}\Bigg) \Big/ \left(\left[\dot{v}_\delta - 6L'_w + \frac{9}{\dot{v}_\delta}{L_w}'^2\right]\dot{k}_M L_{wm}\right) \end{aligned} \tag{5.2}$$

**Table 5.1:** List of some primary DEB parameters for *P. maximus*, from Lavaud et al. (2013), used in the inverted DEB model. $\{\dot{p}_{Am}\}$ and $\dot{v}$ have been re-estimated with a corrected acceleration factor (see explanation in the text).

| *Parameter* | *Notation* | *Value* | *Unit* |
|---|---|---|---|
| Shape coefficient | $\delta_{\mathcal{M}}$ | 0.36 | – |
| Fraction of mobilised reserve allocated to soma | $\kappa$ | 0.86 | – |
| Energy conductance | $\dot{v}$ | 0.084 | $\mathrm{cm\,d^{-1}}$ |
| Volume–specific maintenance costs | $[\dot{p}_M]$ | 33.52 | $\mathrm{J\,cm^{-3}}$ |
| Volume–specific costs for structure | $[E_G]$ | 2959 | $\mathrm{J\,cm^{-3}}$ |
| Maximum surface–specific assimilation rate | $\{\dot{p}_{Am}\}$ | 376 | $\mathrm{J\,d^{-1}\,cm^{-2}}$ |
| Reference temperature (arbitrary) | $T_1$ | 293 | K |
| Arrhenius temperature | $T_A$ | 8990 | K |

Then, by letting $L_w$ be a solution of the "growth DEB equation", the following equations can be formulated, which makes it possible to reconstruct the dynamics of reserves, maintenance rate and mobilization rate:

$$\frac{\kappa}{\delta^3[E_G]}E = \frac{(\dot{k}_M L_w + 3{L_w}')L_w{}^3}{\dot{v}_\delta - 3{L_w}'} \tag{5.3}$$

$$\frac{\kappa}{E_G]}[E] = \frac{\dot{k}_M L_w + 3{L_w}'}{\dot{v}_\delta - 3{L_w}'} \tag{5.4}$$

$$\frac{1}{\delta^3[E_G]}\dot{p}_M = \dot{k}_M L_w{}^3 \tag{5.5}$$

$$\frac{\kappa}{\delta^3[E_G]}\dot{p}_C = 3L_w{}^2{L_w}' + \dot{k}_M L_w{}^3 \tag{5.6}$$

In these formulations the terms $\frac{\kappa}{\delta^3[E_G]}$ and $\frac{\kappa}{[E_G]}$ act as scaling factors and in this form we would have access to the dynamics of the physiological variables only (one can not assume the density of reserve without knowing these factors). But as soon as one know the specific values of $\kappa$, $\delta_{\mathcal{M}}$ and $[E_G]$ for the species of interest, these terms would disappear and the richness of the reconstructed variables would be considerably increased. In the case of *P. maximus*, Lavaud et al. (2013) gave estimates of all primary parameters (Table 5.1). Therefore, we were able to determine the dynamics of these variables without any scaling factor.

### 5.2.3 Theoretical investigations

#### Description of the investigation process

All computations were carried out in the GNU Octave environment (Eaton et al., 2008; Octave community, 2012). We assessed the capacities of the reconstruction procedure by setting up a theoretical study to investigate diverse cases (Fig. 5.1). First, we created artificial food and temperature conditions that fluctuate sinusoidally over one year. We choose commonly encountered environmental conditions for the scallop in the middle of its distribution range: temperature varied between 7 and 21 °C and the functional response to feeding ranged between 0.1 and 0.9. A growth data set of daily shell growth rate (named $L_w{}'$) was generated from these known food and temperature time series using a standard DEB model (Lavaud et al., 2013). The initial conditions of the DEB state variables for the modeled individual were as described in Lavaud et al. (2013), with initial length set at 1.5 cm, initial proportion of reserve set at 0.08 % and initial weight set at 0.25 g DW. Artificial noise was added to growth trajectories (according to a Gaussian law) to mimic the combined effect of observation of daily striae (Chauvaud et al., 1998), which entails measurement errors, and the natural inter-individual variability of daily growth (the latter effect being less important). Since real measurements of scallop shell striae cannot be carried out under a minimal incremental width of 50 µm, noise was added to growth trajectories above this threshold while remaining unchanged when below. As the major part of these artificial variations is caused by the measurement process, it must be smoothed to get closer to the real growth time series. The reconstruction process was thus as follow: (1) smoothing high frequency variations of growth trajectories, (2) calculating the corresponding functional response at each time step (i.e. at each growth value), using the "growth DEB equation", (3) calculating the DEB variables using the set of equations provided by the "growth DEB equation" and (4) taking the reconstructed $f$ time series as input in a backward simulation of growth trajectory in order to check the whole process of reconstruction.

#### Smoothing and interpolation of data

Several algorithms have been tested in order to smooth $L_w{}'$ time series: a simple moving average, a weighted moving average with linearly decreasing integer coefficients from the window center or an exponential moving average. As required variables for the reconstruction of $f$ consist of $L_w$, $L_w{}'$ and $L_w{}''$, we also tried to apply a low-pass filter: the Savitzky-Golay filter (Persson and Strang, 2003), as performed by an open source Octave package ("signal", function "sgolayfilt", Octave v. 3.6.4). This smoothing method uses a regression based on the minimization of least squares differences to estimate a third degree polynomial that better fit the data. The rationale for using this method is that in addition to smoothing the signal, it gives direct access to the derivative of $L_w{}'$ ($L_w{}''$), necessary to the run the reconstruction equation.

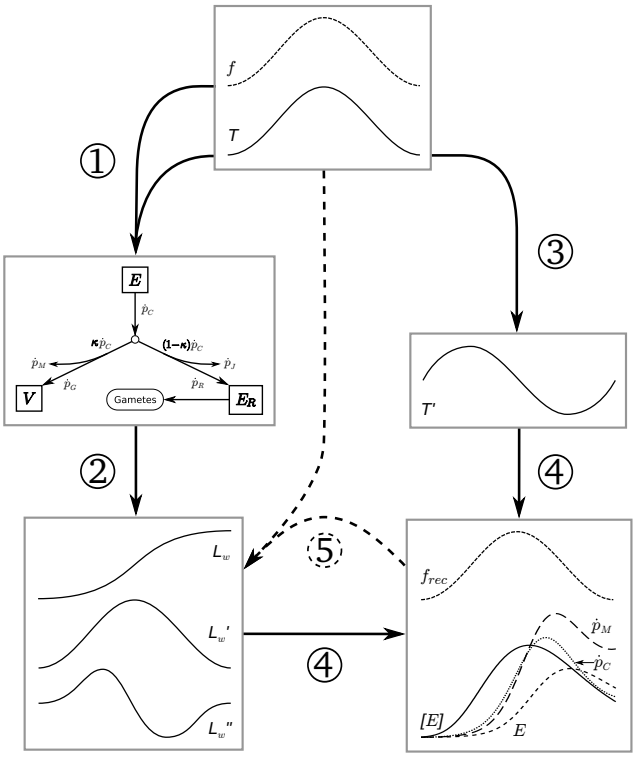


**Figure 5.1:** Conceptual scheme of the validation procedure of the reconstruction process. (1) Temperature and functional response time series are artificially created and used as input for a standard DEB model; (2) a growth trajectory is obtained as output from the DEB model; (3) the first derivative of temperature is calculated; (4) from temperature data and growth trajectories, functional response and dynamics of DEB variables are calculated using the "growth DEB equation" (Rannou, 2009); (5) reconstructed $f$ time series and temperature time series are used in a checking backward simulation to find the growth trajectory.

Another approach to smooth growth data was to consider the maximal and minimal growth laid down by predictions of the DEB model in order to bound possible outcomes to ensure reconstructed $f$ stays within its variation range. We thus calculated the possibilities of growth allowed by DEB theory at each time step of the growth time series: the maximal growth (when $f = 1$) and the minimal one (when $f = 0$). In this way, ${L_w}'$ at the next time step was constrained by "boundaries" and growth artifacts due to the observation method and some inter-individual variability were smoothed. This method will be hereafter referred as to the "DEB box" method.

Interpolation of data was tested both on growth data before and after the reconstruction procedure and on the reconstructed $f$, before the backward simulation. A cubic spline method, as first proposed by Kooijman (2010) was used but linear as well as polynomial Hermite interpolations were also tested. Hermite interpolation is often used as initial approach due to its simplicity.

Functional response and DEB variables were calculated from Eqn. 5.2 and Eqn. 5.3 to 5.6 respectively. The resulting functional response was highly variable, due to the method used here. Thus, reconstructed $f$ was smoothed using the different smoothing methods described earlier.

**Tests**

It has often been hypothesized that growth accidents in *P. maximus* shells could be due to feeding cessation, induced by toxic algae blooms or overloads of microalgae clogging scallop's gills (Chauvaud et al., 1998; Lorrain et al., 2000; Chauvaud et al., 2001). In order to investigate the potential of the daily shell growth rate to retrace feeding stops, we add artificial stops in the food input ($f$) in order to produce a growth data set showing decreases in growth. Different stop durations, which created more or less marked drops in the resulting growth time series, were applied to test the resolution of the smoothing method. Finally, simulations using different initial shell lengths were tested in order to check for any effect of initial conditions: the first (juvenile), second and third year of growth were simulated using initial conditions presented in Table 5.2.

## 5.3 Results

### 5.3.1 Growth time series smoothing tests

We first explored different averaging methods to smooth high frequency variations. Fig. 5.2a presents the different smoothing algorithms used to smooth a simple theoretical growth trajectory. The size of the averaging window was calibrated at 30 days when using moving averages and at 150 days for Savitzky-Golay method. In both cases, we chose to reduce the smoothing interval when approaching extremities of the growth time series to keep symmetric smoothing windows.

**Table 5.2:** Initial conditions of the simulations starting at age 1, 2 and 3: initial length $L_i$, initial weight $W_i$, initial reserves $E_i$ (percentage of the volume specific maximum energy density, $[E_m]V_i$).

| *Age* | $L_i$ | $W_i$ | $E_i$ (% $[E_m]V_i$) |
|---|---|---|---|
| 1 | 1.50 cm | 0.25 g DW | $5.65 \times 10^1$ J (0.08) |
| 2 | 5.60 cm | 2.30 g DW | $1.58 \times 10^4$ J (0.43) |
| 3 | 8.25 cm | 7.90 g DW | $6.46 \times 10^4$ J (0.55) |

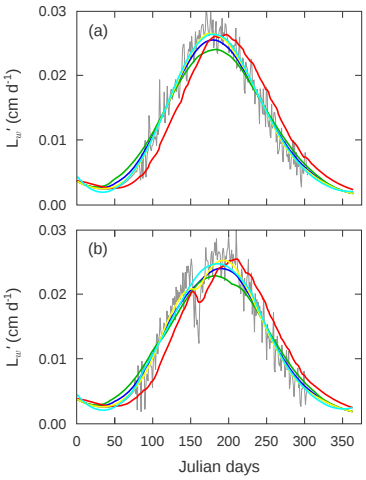


**Figure 5.2:** Different averaging methods to smooth artificially noised growth trajectories (gray line), with a simple seasonal growth time series as initial functional response (a) and with a forced stop in assimilation (b). The tested smoothing functions were: moving average (green line), weighted moving average with weighting coefficients linearly decreasing from the window center (blue line), exponential moving average (red line), polynomial moving average (yellow line) with a smoothing window of 30 d and Savitzky-Golay filter using a smoothing window of 150 d (cyan line).

The use of a simple moving average did not produce an acceptable smoothed curve as (1) tiny variations were still observed, likely due to the smoothing window size and (2) the smoothed curve was also under many points of the original growth trajectory in the central part of graph, which is actually caused by the rather large window length (30 d). Thus, other tests carried out with larger smoothing intervals (more than 150 d) in order to remove tiny variations observed would have worsened the second pattern observed. Therefore, this first

option was not considered for the rest of the study. Noticeable degradations occurred at start and ending boundaries of the smoothed curve when using an exponential moving average. Linearly decreasing weighting coefficients from the window center was the best option considering moving averages. Using a Savitzky-Golay filter was also conclusive, especially at the extremities (first and last twenty days) where the averaged curve is not as impacted by the last points as when using moving averages.

When producing an artificial stop of seven days in the functional response time series, leading to a decrease of growth rate, none of these methods was able to fit the growth accident, whatever the size of the smoothing window used (Fig. 5.2b). The "DEB box" method, to the contrary, succeeded in keeping this event in the resulting dynamics while constraining it to a variation range compatible DEB predictions (Fig. 5.3). The constrained growth curve then had a saw-tooth shape for the "DEB box" filter makes the signal to sharply vary between the two values 0 and 1 when observed growth overshoot DEB predictions. The reconstructed $f$ still showed fluctuating values. Nevertheless, when smoothing reconstructed data (using either a moving average or a Savitzky-Golay filter), we were able to simulate back the originally created $f$ time series (see further results in Fig. 5.4). As the "DEB box" method was the more reliable smoother, it was used for the rest of the study.

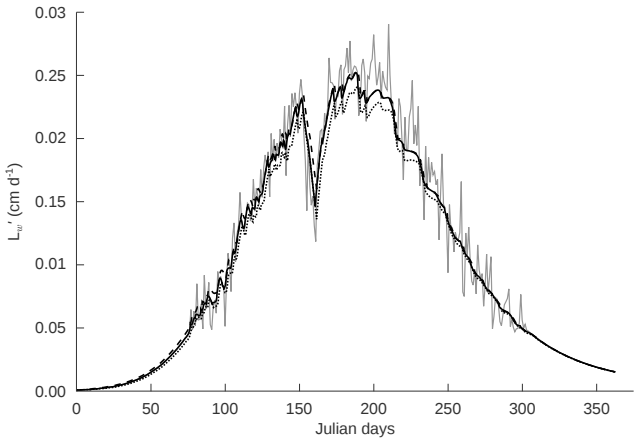


**Figure 5.3:** "DEB box" method used to smooth growth trajectory: for each point of the initial growth trajectory (gray line), predictions of growth for the next time step were made. Predicted growth was calculated for $f = 1$ (dashed dark line) and for $f = 0$ (dotted dark line), to set up the variation range of growth allowed by DEB theory. If initial growth trajectory was out of these bounds, the smoothed time series was set at the value given by the DEB model. If initial growth trajectory fitted inside DEB predictions, its value was kept unchanged.

### 5.3.2 Functional response reconstruction

Fig. 5.4a shows the results of the reconstruction process in the simplest case of a clean growth (without noise caused by observation). The functional response simulated from temperature and length increments exactly overlapped the original assimilation time series used to produce growth data.

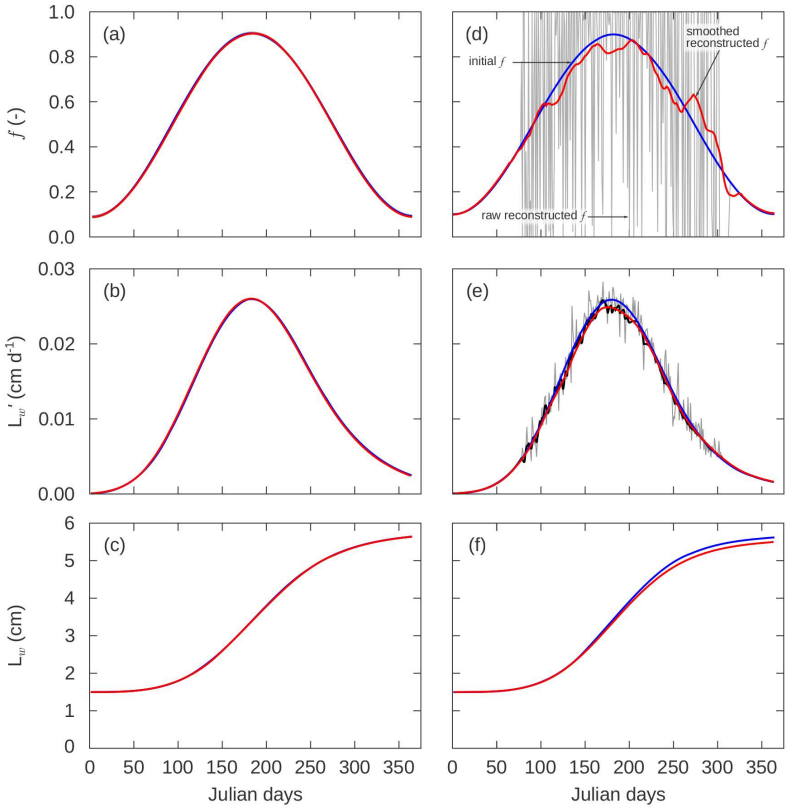


**Figure 5.4:** Reconstruction of assimilation trajectory from intact growth data (a, b, c) and artificially noisy growth data (d, e, f). (a, d) Initial $f$ trajectory is in blue line and raw reconstructed $f$ (gray line) was either smoothed using a weighted moving average with weighting coefficients linearly decreasing from the window center or by a Savitzky-Golay filter to produce a smoothed reconstructed $f$ (red line). (b, e) Intact growth trajectory (blue line) and artificially noisy growth trajectory (e, gray line) were smoothed using the "DEB box" method (b, e, dark line). (b, c, e, f) Backward simulation of daily shell growth rate (b, e, blue line) and shell length (c, f, blue line) using smoothed reconstructed $f$ are presented in red lines.

These good results were obtained whatever the smoothing method used. Backward simulation ran to check for inconsistency in the process, using smoothed reconstructed $f$, did not reveal any discrepancy from the original growth time series. When artificial noise was randomly added to the growth trajectory (Fig. 5.4b), results of both reconstruction and backward simulation, though not as faithful as in the clean case, were very satisfying.

### 5.3.3 Interpolation tests

The interpolation of growth data before to run the "growth DEB equation" in the model was not successful. The reason for this is because in the reconstruction process, the equation serves to calculate a value of $f$ corresponding to a given variation of $L_w$, $L_w\prime$ and $L_w\prime\prime$ between two time steps. However, while interpolating, we reduce the possibilities of adaptation of $f$ value to the next step values of these variables. In other words, $f$ value within long time steps can vary more freely than in short ones, as long as it produces the expected variable values at the next time step. As a result, the computed functional response sometimes showed extremely strong variations (more than ten times the initial values). Therefore, we abandoned this option.

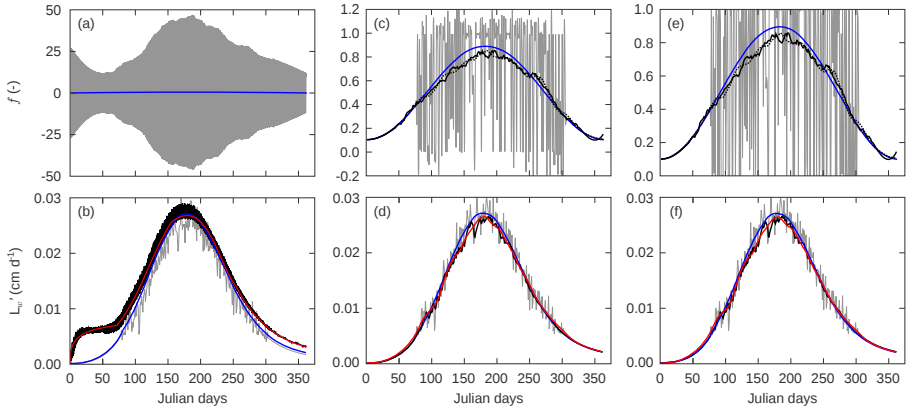


**Figure 5.5:** Reconstruction of assimilation trajectory using Hermite interpolation (a, b), cubic spline interpolation (c, d) or linear interpolation (e, f). (a, c, e) Initial $f$ trajectory is in blue line and raw reconstructed $f$ (gray line) was either smoothed using a weighted moving average with weighting coefficients linearly decreasing from the window center (dotted dark line) or by a Savitzky-Golay filter (strait dark line). (b, d, f) Artificial noise (gray line) was added to initial growth trajectories (blue line), which were smoothed using the "DEB box" method (dotted dark line). Backward simulation of growth rate (red line) used reconstructed $f$ smoothed with the Savitzky-Golay filter.

Fig. 5.5 presents results of cubic spline and Hermite interpolation of growth and reconstructed $f$ time series before the backward simulation. The Hermite procedure produced undesirable effects of instability (Fig. 5.5a). The use of cubic spline, although less unstable resulted in an interpolated reconstructed $f$ time series that went beyond its accepted range (between 0 and 1), mainly due to the fact the interpolant results from a piecewise polynomial. Finally, the better option was not to interpolate growth trajectories with a cubic spline but to interpolate the reconstructed $f$ with a simple linear interpolation, which was successful as both reconstructed functional response and backward simulation of length were in accordance with initially created time series.

### 5.3.4 Assimilation stops reconstruction

The duration of assimilation stops tested to get the resolution of the smoothing method showed that with a cessation of 24 h, growth time series did not present noticeable growth rate variation (Fig. 5.6b). Growth rate decreased when stops lasted for three and seven days, which was even more obvious in the latter case (Fig. 5.6d,f). In the reconstruction of $f$ dynamics, significant decreases were observed for three and seven days only.

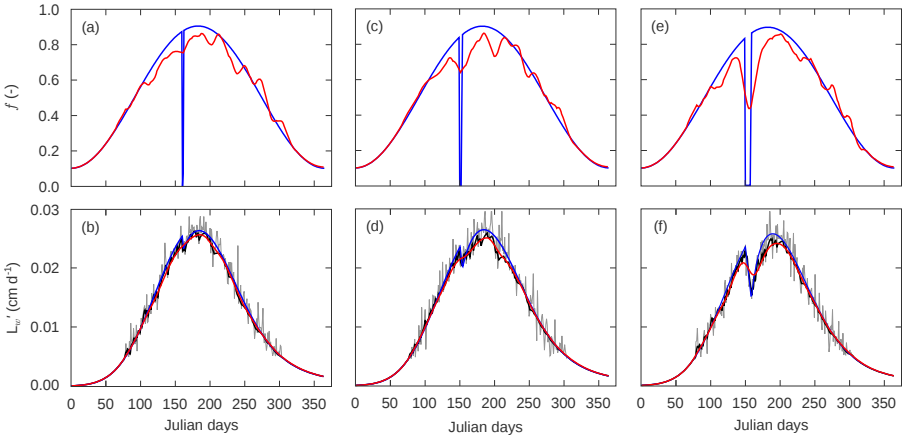


**Figure 5.6:** Reconstruction of assimilation trajectory presenting different cessation durations, from artificially noisy growth data: (a, b) one day, (c, d) three days, (e, f) seven days. (a, c, e) Initial $f$ trajectory is a blue line and reconstructed $f$ was smoothed using a Savitzky-Golay filter (red line). (b, d, f) Artificial noise (gray line) was added to initial growth trajectories (blue line), which were smoothed using the "DEB box" method (dark line). Backward simulation of growth rate (red line) used reconstructed $f$ smoothed with the Savitzky-Golay filter.

### 5.3.5 Physiological history reconstruction

The assessment of reserves $E$, reserve density $[E]$, mobilization rate $\dot{p}_C$ and maintenance rate $\dot{p}_M$ was then accomplished from a continuous sinusoidal $f$ time series and a noisy growth trajectory constrained by the "DEB box" filter. Fig. 5.7 shows that the high frequency variability of growth data impacts the simulation of $E$, $[E]$ and $\dot{p}_C$ but not of $\dot{p}_M$. As for the reconstruction of the functional response, equations 5.3 to 5.6 are based on growth trajectories constrained by the "DEB box" method which are not averages but dynamic time series, cleaned from variations of growth rate incompatible with a DEB model. Hence, they also need to be smoothed.

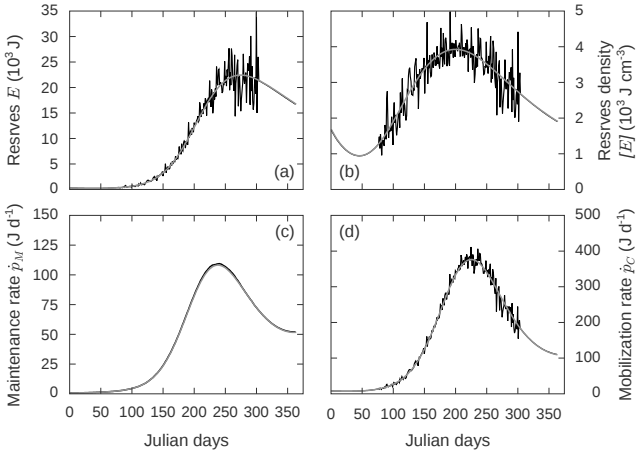


**Figure 5.7:** DEB variables calculated from the "growth DEB equation", using temperature and noised growth trajectory. In gray lines are the variables as predicted by the standard DEB model used to produce growth trajectory. In dark lines are the predictions made via the "growth DEB equation". (a) reserves E (J), (b) reserve density [E] ($\mathrm{J\,cm^{-3}}$), (c) maintenance rate $\dot{p}_M$ ($\mathrm{J\,d^{-1}}$), (d) mobilization rate $\dot{p}_C$ ($\mathrm{J\,d^{-1}}$).

This has been achieved by using a weighted moving average with weighting coefficients linearly decreasing from the window center (smoothing window: 30 d) and the Savitzky-Golay filter (smoothing window: 30 d, Fig. 5.8). Both methods showed very good results as the smoothed curves fitted well with the original dynamics of $E$, $[E]$ and $\dot{p}_C$. Maintenance rate was again well reconstructed, due to the fact that this variable is directly linked to structural growth, whereas the others are not.

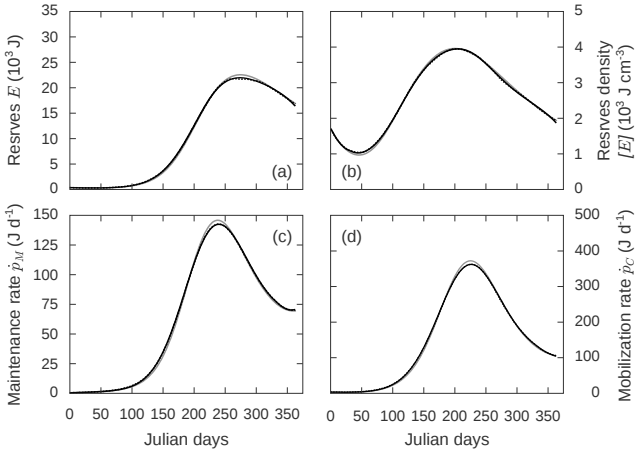


**Figure 5.8:** DEB variables calculated from the "growth DEB equation", using temperature and noisy growth trajectory. Growth was smoothed using a weighted moving average with weighting coefficients linearly decreasing from the window center (smoothing window: 30 d). In gray lines are the variables as predicted by the standard DEB model used to produce growth trajectory. In dark lines are the predictions made via the "growth DEB equation". (a) reserves $E$ (J), (b) reserve density $[E]$ ($\mathrm{J\,cm^{-3}}$), (c) maintenance rate $\dot{p}_M$ ($\mathrm{J\,d^{-1}}$), (d) mobilization rate $\dot{p}_C$ ($\mathrm{J\,d^{-1}}$).

### 5.3.6 Effect of shell size

Finally, we tested the potential effect of the initial shell size on the reconstruction process: initial conditions of the simulation were calibrated as if we were using the first, second or third year of growth of a given shell, leading to an increasing initial length with the age considered. Fig 5.9 shows results of reconstructed $f$ for a one year-old scallop's shell and for a three-year-old scallop's shell. The duration of growth was less important for the older individual, which resulted in a reduction of the reconstruction window. Moreover, its amplitude range was also lower, reaching $75\,\mu\mathrm{m\,d^{-1}}$, whereas the juvenile shell grew up to $300\,\mu\mathrm{m\,d^{-1}}$ at its maximum.

## 5.4 Discussion

### 5.4.1 Inverted DEB model to reconstruct food assimilation

Modeling of bioenergetics require energy input in the modeled system, which is often rather problematic to define. Within the Dynamic Energy Budget theory (Kooijman, 2010), it has been suggested to invert the argument and

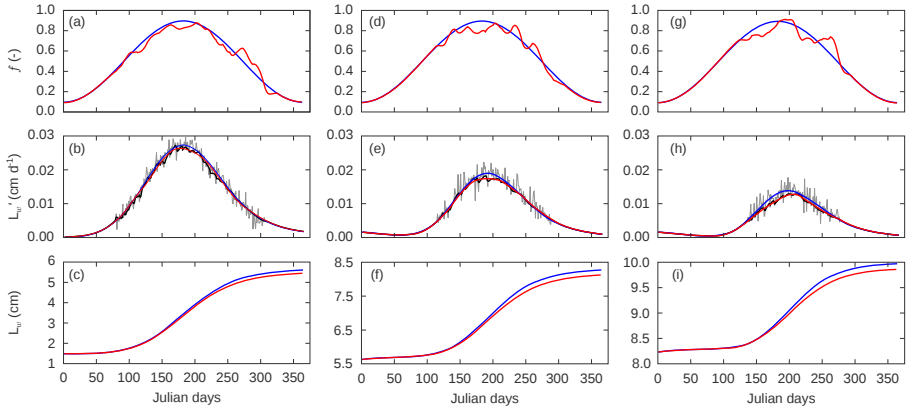


**Figure 5.9:** Reconstruction of functional response from theoretical growth rates of (a, b, c) one-year-old, (d, e, f) two-year-old and (g, h, i) three-year-old shells of *P. maximus*. Initial $f$ is presented in the upper graph (a, d, g, blue line) together with its reconstruction after applying a Savitzky-Golay filter (red line). (b, e, h) Artificial noise (gray line) was added to initial growth trajectories (blue line), which were smoothed using the "DEB box" method (dark line). (b, c, e, f, h, i) Backward simulation of daily shell growth rate (b, e, h, blue line) and shell length (c, f, i, blue line) using smoothed reconstructed $f$ are presented in red lines.

try to simulate the functional response of organisms when growth or reserve dynamics data together with temperature are available. In this study we presented a modeling method, based on the Dynamic Energy Budget theory, to reconstruct the assimilated energy from the trophic source of a bivalve from its shell.

Few studies have attempt to use DEB models in order to achieve such a goal. Cardoso et al. (2006) were the first to reconstruct mean functional responses of five bivalve species from annual growth data in Dutch coastal waters. In a simple empirical way, they manually calibrated the value of $f$ to match the monitored growth of these bivalves in different environments. Troost et al. (2010) adopted a similar concept of calibration of a more complex scaled food density. Then, Freitas et al. (2009) extended these investigations to a wider latitudinal range for a North-East Atlantic coastal bivalve species. Their approach was based on a regression routine (non-linear weighted least-squares regression using Nelder Mead's simplex method) to estimate the functional response given annual temperature cycles and observed length-at-age data. The assimilated capacities of studied species were all limited to a maximum of 60 %.

Pecquerie et al. (2012) developed a theoretical inverted model for reconstructing scaled food density trajectories and growth history of anchovy, using

opacity data of fish otoliths. Their approach relies on the determination of the feeding values minimizing the squared deviations between observed and predicted opacity values. These authors, while presenting promising results in theoretical cases, did report a low sensitivity of their method to temperature variations experienced by the organism. Compared to these four studies, our work presents a high resolution of the reconstruction of assimilation history. Moreover, it has the advantage of relying on an inversion of the model, with a mechanistic determination of the functional response, rather than on an empirical mean or on a regression method.

### 5.4.2 A mechanistic method using one DEB equation

This study is the first one to present an application of the "growth DEB equation" of Rannou (2009). It is a simplified method for working with DEB models as it fits in only one equation. Moreover, several variables can be derived from the core equation as shown in the reconstruction of the physiological state. Since many questions were unanswered as to the limits of the method, it was necessary to carry out various tests before any application to real data. In our testing procedure, we impose a supplementary difficulty adding noise to the theoretical data, in the view of producing "pseudo-real data". Yet, even then, the reconstruction process produced a more than satisfactory reconstruction of the initial assimilation time series. This scrambling step is not often encountered in the literature and theoretical studies usually settle for simpler cases.

A common issue encountered by sclerochronological researchers is the high variability of growth rate data in bivalves. Both due to individual variability and to the measurement method, difficulties remain. Despite a statistically rigorous procedure of growth trajectory treatment, the method proposed by Chauvaud et al. (1998), when based on too few individuals, can still result in data sets with high-frequency fluctuations. Though, most of the time these variations might not have any biological meaning. In the previously cited studies dealing with reconstruction of food assimilation trajectories from growth observations (Cardoso et al., 2006; Freitas et al., 2009; Troost et al., 2010; Pecquerie et al., 2012), the uncertainty or the variability of growth data measurement was a recurring issue. Cubic splines were globally used and advised for smoothing observed growth data variability (Freitas et al., 2009; Kooijman, 2010). However, this interpolation method used to smooth data has the disadvantage of producing highly variable derivative of growth rates, which causes the reconstructed trajectory to overshoot its accepted variation range (Freitas et al., 2009). In the current detailed method, the "growth DEB equation" makes use of the second derivative of length ($L_w{}''$) which then causes the reconstructed food assimilation to go beyond its accepted range (0–1). However, the cubic spline interpolation could be used after the reconstruction process, just before the backward simulation which only consists of a regular DEB simulation, not impacted by these considerations.

In the present work, however, the "DEB box" method was successfully implemented as a means to go beyond these pitfalls, for it allows one to constrain the evolution of observed growth trajectories (not necessarily biologically real), to a variation range compatible with DEB predictions at each time step. With the use of the "DEB box" approach, observed growth data did not require smoothing process any longer. The fact that raw reconstructed $f$ time series was highly variable is not aberrant as reconstruction was carried out at a short time step. Biologically, assimilation is a rather smoothed process at a daily scale compared to feeding activity. Therefore, the smoothing step implemented before the backward simulation is justified and permitted to get closer to a real assimilation time series. Both smoothing methods (linearly decreasing weighting coefficients from the window center or Savitzky-Golay filter) had their advantages and disadvantages: moving average produced smoother curves than a Savitzky-Golay filter but sometimes diverged at the extremities of the reconstruction, due to the reduction of the smoothing window size, while the Savitzky-Golay filter sometimes overshots the expected minimum and maximum values for $f$ (between 0 and 1), because it uses polynomial functions to fit the data. The discrepancies sometimes observed at the ending of the simulation may not be due to the averaging method alone. This effect could result from the addition of noise which might have imposed short increases of growth rate at a moment where less food is available and temperatures are decreasing, typically causing the growth to decrease. The functional response reconstructed from these artificial increases is then also rising. This might cause slight and temporary overestimations when using real data and one should be cautious in the interpretation of the reconstructed assimilation time series when approaching the extremity of growth trajectory.

From this perspective of temporal reconstruction, one might think that the older the archive the longer the reconstruction. It is, however, not the case in this situation. Indeed, after four (in southern populations) to six (in northern populations) years of life, individuals barely produce more than few millimeters of shell each year, while then can gain up to 4 cm during the second year of growth (Patry, 2009; Chauvaud et al., 2012). Thus, growth during the last years of life is dramatically reduced, both in duration and in amplitude, which makes it difficult to analyze through this method. Moreover, results presented in Fig. 5.9 also reveal that the reconstructed assimilation time series is less accurate when the third year of growth is used, compared to the first or the second. Therefore, one should rather use the first years of life to reconstruct the assimilation history.

### 5.4.3 Physiological state reconstruction

In addition to assimilation, the present approach allows the reconstruction of the physiological history of the studied organism. To our knowledge this has not been achieved so far through any kind of observation, proxy or model. This is of great interest for a number of fields of study: paleo-reconstruction (scle-

rochronology), assessment of pollutions, of diseases, creation of distribution maps, characterization of the carrying capacity of habitats, etc.

In this study we do not consider the reproductive aspect of metabolic processes achieved by an organism. To us, the validation of the method was a prerequisite to further exploitation of the "growth DEB equation". Dynamics of the reproduction buffer are simply related to growth due to the $\kappa$-rule. As we are now able to reconstruct reserve dynamics, access to the reconstruction of energy dynamics allocated to reproduction should be an easy step. Nevertheless, the reconstruction of spawning events would still depend on specific formulation, but this an issue encountered in DEB models in general.

### 5.4.4 Perspectives and further research

In this study we tested simple as well as less known filters to smooth the reconstructed $f$ trajectory. Possible improvements may be achieved (Eilers, 2003) through a deep investigation of numerical properties of the "growth DEB equation". These first tests have also revealed that predicted growth rate by the model were rather under expected growth rates for *P. maximus*. This has already been raised by Lavaud et al. (2013) and might be a source of under-estimation for further experiments, which could be corrected by the re-estimation of some parameters (particularly the surface area specific assimilation rate and the energy conductance).

This approach offers great perspectives, as scallop shell collections exist in many research centers along its geographical distribution range (in the University of Brest, France; the University of Bangor, Wales; the Institute of Marine Research of Bergen, Norway). Exploration of such monumental archives through the present method could aid comprehension of the physiology of this species and its remarkable growth and reproductive pattern throughout its distribution range. Moreover, it could help to study remote environments such as the edge of the continental shelf where scallop can also be found (Nerot et al., 2012).

So far, only the length of the shell has been used for the reconstruction of scaled food density. But one could think about combining our procedure with the approach of Pecquerie et al. (2012) in the reconstruction of feeding trajectory from opacity measurements of biogenic carbonates. In this way, two variables would be used rather than only one to reconstruct feeding history.

The shell of scallops as well as other bivalve species are now well recognized as biogenic archives of fluctuating environments (Chauvaud et al., 2005; Lavaud et al., 2012). The perspective of reconstructing environmental condition through sclerochronology together with the reconstruction of the organism's physiological history is an exiting scientific objective, especially in the context of environmental monitoring and climate change assessment.

# Chapter 6

# Reconstructing real physiological histories

**History of the great scallop by the mean of DEB theory, a study of ecological patterns along latitudinal and bathymetric gradients**

*Manuscript in preparation for submission to Ecological Modelling*

**Romain Lavaud**, Fred Jean, Aurélie Jolivet, Eric Rannou, Øivind Strand and Jonathan Flye-Sainte-Marie.

**Abstract**
The great scallop, *Pecten maximus*, presents a strong variability of growth and reproductive patterns in its distribution range. These differences in life history traits result from complex interactions between organisms and environmental conditions that can be apprehended through the study of energy dynamics. Numerical modeling has proven to be a relevant tool for answering these questions. As potential limitation for bioenergetic modeling lies in the determination of accurate food proxy, a recent study has provided with a new approach consisting of using temperature and growth time series to reconstruct the energy input from food, on the basis of DEB theory. In this study we coupled the use of sclerochronological data of the great scallop *Pecten maximus* with an inverted DEB model in order to reconstruct the temporal assimilation and physiological history of *P. maximus*. Required assimilated energy to support observed growth was reconstructed for different age classes of great scallops *P. maximus* in ten locations of its geographical distribution range. We especially explored the functional response ($f$) patterns along latitudinal and bathymetric gradients. The average reconstructed $f$ was found to increase with

latitude as well as its maximum value. Its variability, although increasing, did not show a significant relationship with the geographical position. Along the bathymetric gradient strong relationships were found between $f$ and depth. The mean functional response was thus more elevated in deep-sea scallops and also displayed much more variability. For a same year we observed similar patterns between year-classes, indicating low ontogenetic effect on $f$. Comparisons with field measurements of food indicators (chlorophyll-$a$ from the pelagic/benthic domains, phytoplankton cell counts, etc.) allow us to discuss the relevance of various food proxies in bioenergetic modeling of suspension-feeding bivalves. Chlorophyll-$a$ from water column was found to be the most related variable to functional response dynamics. Finally, as the inverted DEB model allows the reconstruction of physiological variables and energy fluxes, we also explored the potential differences in reserve and maintenance fluxes dynamics from scallops living in contrasting environments.

**Keywords:** modeling; Dynamic Energy Budget; environmental reconstruction; latitudinal gradient; bathymetric gradient; growth; reserve dynamics; maintenance flux; *Pecten maximus*; sclerochronology.

## 6.1 Introduction

Intra-specific variability in life history traits is a common feature of large distribution range species. It has been subject to numerous descriptions by ancient biologists who first observed that populations, within a given species, could achieve significantly different biological patterns of life span, growth or reproductive activity. The study of the variability in life history patterns can be apprehended by the description and the understanding of the energy fluxes. Modeling provides a useful tool to handle this question as it enables to test various hypotheses of metabolic organization and varying environment. The DEB theory (Kooijman, 2010) is a bioenergetic theory that quantitatively describes energy fluxes in a mechanistic framework relying on temperature and food concentration input variables. However, when studying marine suspension-feeding organisms, relevant food proxies able to describe the genuine energy input has long been an impediment in bioenergetic modeling (e.g. Bayne, 1998; Bourlès et al., 2009; Alunno-Bruscia et al., 2011).

Recently, some studies have tried to overturn this issue by inverting the model to reconstruct temporal assimilation time series from temperature and growth trajectories (Cardoso et al., 2006; Freitas et al., 2009; Troost et al., 2010; Pecquerie et al., 2012). Moreover, reconstruction of food condition from past and present aquatic species in their natural environment provides key ecological information for a better understanding of population dynamics (Pecquerie et al., 2012). While these studies have implemented reconstructions of functional response at an organism life time scale, Lavaud et al. (in prep.) showed that daily time series of the scaled functional response could be accurately reconstructed at a resolution of few days by using a single equation

derived from DEB theory: the "growth DEB equation" (Rannou, 2009), as well as various physiological variables such as maintenance rate, flux of mobilized energy from reserve or reserve quantity and density.

The great scallop *Pecten maximus* grows by sequential increments, producing growth striae on the shell surface that allow one to determine the age and the daily shell growth rate (DSGR) of an individual (Clark, 1968; Chauvaud et al., 1998; Lorrain et al., 2000; Owen et al., 2002b), providing a high resolution record of the growth dynamics. *P. maximus* is thus considered as a relevant and accurate biogenic archive used in paleo-environment reconstructions of seawater temperatures (Owen et al., 2002a,c; Chauvaud et al., 2005; Freitas et al., 2006), salinity (Chauvaud et al., 2005; Freitas et al., 2012), primary productivity (Thébault et al., 2009; Thébault and Chauvaud, 2013). The great scallop has a rather large distribution range, from the northern Norway south to the Iberian Peninsula and from just below the water mark in coastal waters to the edge of the continental shelf, which corresponds to a depth gradient of about 200 m (Antoine, 1979; Brand, 2006a). This distribution embraces highly contrasting environments, especially in terms of temperature and food availability, both in their absolute values and dynamics. These differential conditions might, thus, be responsible of the observed variability in the growth and reproductive patterns of this species (Buestel et al., 1987; Strand and Nylund, 1991; Mackie and Ansell, 1993; Chauvaud et al., 2012).

In this study, we present an application of the method described by Lavaud et al. (in prep.) for reconstructing physiological variables of great scallops from shell growth trajectories. We explored a collection of shells gathered from ten locations along latitudinal and bathymetric gradients. Different years of growth were tested and the reconstructed signals were then compared to potential trophic sources monitoring whenever possible. The aim was here to address whether the variability in life history traits could be explained by functional response patterns in relation to environmental conditions.

## 6.2 Material and methods

### 6.2.1 Study sites and shell collection

Ten study sites were analyzed along a latitudinal gradient with regard to their contrasting thermal and trophic conditions along the distribution range of *P. maximus* and the availability of data (Fig. 6.1): Traena in mid-Norway (1), Austevoll in southern Norway (2), Holyhead in the Irish Sea (3), Plymouth in the English Channel (4), the Bay of Brest in west France (5), Quiberon in the northeast part of the Golf of Biscay (6) and four sites along a bathymetric gradient off Brest in the Celtic Sea, at 98 m (7), 109 m (8), 150 m (9) and 162 m depth (10).

Scallop shells came from the multi-decadal archives of the EVECOS time series (maintained by the observatory of coastal domain in the University of

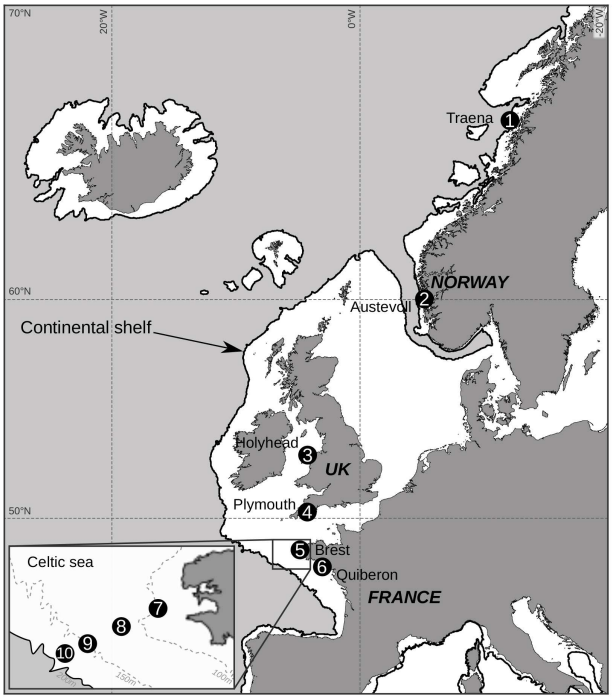


**Figure 6.1:** Geographic location of the ten study sites from which shells and temperature data were collected: Traena (1), Austevoll (2), Holyhead (3), Plymouth (4), Brest (5), Quiberon (6) and four deep sites in the Celtic Sea, at 98 m (7), 109 m (8), 150 m (9) and 162 m depth (10).

Brest), gathering shells from all around the distribution range of the great scallop. Depending on the site and their accessibility, individuals were collected by scuba diving or dredging. The number of shells used and their biometric data are presented in Table 6.1.

Seawater temperature time series were obtained from monitoring data sets acquired by various scientific institutions: SOMLIT (French acronym for Littoral Environment Observation Center) for the French locations, CEFAS (Centre for Environment, Fisheries and Aquaculture Science; Joyce, 2006) for the English locations. In the Norwegian locations, data were provided by Ø. Strand and L. Chauvaud (unpublished data). All these measurements corresponded to period of growth of the studied animals. In the deep locations field observations and hydrological models have shown that temperature slightly vary of only 0.5 to 1 °C along the year, for an average of 12 °C (Lazure et al., 2009). Moreover, the LPO (French acronym for Ocean Physics Laboratory) conducted a monitoring of deep sea temperatures (ASPEX mooring equipped with Mi-

**Table 6.1:** Geographical position of the ten sampled locations along the latitudinal and bathymetric gradients and number and age classes of individuals used.

| *Site* | *Latitude* | *Depth* | *Age classes* | *n shells* |
|---|---|---|---|---|
| Traena | 66°30'N | 18 m | 3 and 6 | 15 |
| Austevoll | 60°06'N | 15 m | 3 to 5 | 37 |
| Holyhead | 53°03'N | 46 m | 3 to 6 | 13 |
| Plymouth | 50°20'N | 12 m | 2 to 5 | 25 |
| Brest | 48°23'N | 20 m | 1 and 3 | 271 |
| Quiberon | 47°48'N | 15 m | 1 and 2 | 55 |
| Celtic Sea 98 m | 48°36'N | 98 m | 4 to 6 | 11 |
| Celtic Sea 109 m | 48°19'N | 109 m | 4 and 5 | 11 |
| Celtic Sea 150 m | 47°55'N | 150 m | 4 to 8 | 11 |
| Celtic Sea 162 m | 47°53'N | 162 m | 4 to 6 | 8 |

crocat T/S/P recorder) at 150 m over one year in 2010–2011 in the same area (47°12'643 N, 5°15'963 W), which confirmed that temperature varied less than 1 °C in these deep environments (Le Boyer et al., 2013 and L. Marié, unpublished data). Therefore, a constant temperature value of 12 °C was chosen for the reconstructions carried out in the Celtic Sea locations.

### 6.2.2 Measurement of growth trajectories

Different cohorts were studied in order to look at the potential effect of age on the reconstruction process, from age class one to age class six. The daily shell growth rate (DSGR) was determined individually on the external surface of the left valve by measuring the distance between two successive daily growth striae (Chauvaud et al., 2005, 2012), from the ventral margin towards the umbo. For each studied site, a mean growth trajectory was calculated by averaging the individual growth trajectory from a single cohort. As the growth of *P. maximus* stops in winter (Chauvaud et al., 1998, 2005; Lorrain et al., 2000), the procedure was performed for each year of growth. Calendar dates were assigned to each increment of the last year of growth (until catch) but not for previous years of life since winter slowdown duration cannot be known accurately. However, some observations of the relationship between temperature and DSGR time series over several decades within the EVECOS data set (Patry, 2009) revealed that one could resettle the growth trajectory in time, by aligning the highest DSGR value with the maximum value of temperature. Thus, we applied this method to the data sets of locations (1), (2) and (3), given their relative proximity.

### 6.2.3 Reconstruction method of physiological history

The reconstruction procedure used in this paper was described in Lavaud et al. (in prep.). Using an inverted DEB model, this method allows one to reconstruct temporal variations of the following physiological variables: the scaled functional response $f$, the reserve amount $E$, the reserve density $[E]$, the mobilization flux of energy from reserves $\dot{p}_C$ and the flux of energy allocated to somatic maintenance $\dot{p}_M$. This approach relies on the single "growth DEB equation" of Rannou (2009) in which DSGR is used as a proxy of the structural growth. The time axis of the reconstructed variables was expressed in Julian days (JD). We explored latitudinal and bathymetric patterns with linear regressions to establish relationships between average, maximum, minimum reconstructed $f$, its variability and the gradient parameters (latitude and depth).

As growth trajectories can present strong high frequency variability, partly due to the striae measurement method and also to a potentially high inter-individual variability, this approach includes a smoothing procedure (the "deb-box") based on a standard DEB model (Lavaud et al., in prep.): every day of the growth trajectory, the model calculate the possibilities of growth for the next day, for a maximum scaled functional response (1) and minimum one (0). When growth rate at the next day is to overshoot the modeled values, outcomes are bound and replaced by a DSGR value corresponding to the maximum value that $f$ can take at this time. The noisy growth trajectory is, hence, constrained to a "DEB-compatible" time series.

Lavaud et al. (2013) in their estimation of DEB parameters for *P. maximus* proposed a value of 3 for the post-metamorphosis metabolic acceleration coefficient, which increased the maximum surface-specific assimilation rate $\{\dot{p}_{Am}\}$ and the energy conductance $\dot{v}$ up to $282\,\mathrm{J\,d^{-1}\,cm^{-2}}$ and $0.063\,\mathrm{cm\,d^{-1}}$ respectively after metamorphosis. These relatively low values might have been responsible of the low average daily growth rate observed. We have thus re-estimated the value of this acceleration coefficient, using the same procedure as in Lavaud et al. (2013), to a value of 4, which consequently provided new values of $\{\dot{p}_{Am}\} = 376\,\mathrm{J\,d^{-1}\,cm^{-2}}$ and $\dot{v} = 0.084\,\mathrm{cm\,d^{-1}}$.

### 6.2.4 Food proxies

The reconstructed food assimilation dynamics carried out in the location of Brest were compared to independent field data. Different indicators of food availability were measured: chlorophyll-*a* from the pelagic or benthic compartment, phytoplankton cell counts and particulate organic matter (POM) provided by the monitoring network SOMLIT.

### 6.2.5 Statistical analysis

Reconstructed $f$ time series were averaged site by site in order to look at specific patterns along the studied gradients. Kruskal-Wallis one-way analyses were conducted to test the separation of data sets (from site to site). Linear

**Table 6.2:** Statistics of mean reconstructed functional response in the different studied locations.

| *Site* | *n* | *mean f* | *max f* | *min f* | *range f* | *var f* | *sd f* | *Days of growth* |
|---|---|---|---|---|---|---|---|---|
| Traena | 6 | 0.71 | 0.98 | 0.18 | 0.80 | 0.03 | 0.18 | 130.0 |
| Austevoll | 12 | 0.71 | 0.95 | 0.34 | 0.61 | 0.04 | 0.18 | 131.7 |
| Holyhead | 18 | 0.58 | 0.82 | 0.33 | 0.49 | 0.03 | 0.14 | 108.1 |
| Plymouth | 10 | 0.66 | 0.91 | 0.32 | 0.59 | 0.02 | 0.13 | 181.7 |
| Brest | 13 | 0.57 | 0.87 | 0.29 | 0.56 | 0.02 | 0.13 | 203.5 |
| Quiberon | 3 | 0.53 | 0.82 | 0.22 | 0.60 | 0.03 | 0.16 | 246.3 |
| Celtic Sea 98 m | 12 | 0.64 | 0.97 | 0.20 | 0.77 | 0.06 | 0.23 | 146.5 |
| Celtic Sea 109 m | 7 | 0.64 | 0.94 | 0.15 | 0.79 | 0.05 | 0.22 | 139.0 |
| Celtic Sea 150 m | 17 | 0.66 | 0.99 | 0.06 | 0.93 | 0.09 | 0.29 | 123.0 |
| Celtic Sea 162 m | 9 | 0.67 | 0.97 | 0.08 | 0.89 | 0.08 | 0.29 | 129.3 |

regressions were used to establish relationships between the observed patterns in reconstructed $f$ at the different locations and the two variables of interest (latitude and depth).

## 6.3 Results

### 6.3.1 Latitudinal gradient

The reconstruction of food assimilation was applied along the latitudinal gradient from Traena (66°30'N, Norway) south to Quiberon (47°48'N, France). Fig. 6.2 shows reconstructed $f$ time series along the gradient for age class one individuals. The average reconstructed functional response, as well as its maximum and minimum values, variance, standard deviation and variation range were calculated in each location (Table 6.2) and for each age class within each site (See details in Appendices: Table A.1). All descriptors were significantly different from one station to the other (Kruskal-Wallis tests, all $p\text{-}value < 0.002$). In both northernmost locations (Traena and Austevoll, Norway), the average $f$ among all age classes was of 0.71. However, in these habitats, growth trajectories sometimes seemed to be too much constrained by the "deb-box" smoothing method, which resulted in a reconstructed $f$ at its maximum value for rather long periods. In Holyhead and Plymouth locations, at the middle of the distribution range (UK), the average value of $f$ was of 0.58 (max = 0.82, min = 0.33) and 0.68 (max = 0.91, min = 0.32) respectively. Finally, in the southernmost studied locations of Brest and Quiberon $f$ reached an average value of 0.57 (max = 0.87, min = 0.29) and 0.53 (max = 0.82, min = 0.22) respectively.

We found a linear relationship between the latitude and the average $f$ (Table 6.3, $R^2 = 0.70$, $p\text{-}value < 0.05$). *P. maximus* growing in the Nordic

stations thus display a higher functional response in average than individuals in the southern stations. In the majority of the reconstructions carried out with shells from northern environments (11 over 18), $f$ reached a maximum value of 1 (Table A.1). In fact, the DEB model used within the "deb-box" to smooth growth rates variations at these locations was often very constraining the observed time series. This led to periods longer that a month when the reconstructed $f$ remained at 1. For half of these results the minimum $f$ was 0. To the contrary, reconstructed time series in the southern locations (Plymouth, Brest and Quiberon) never reached the maximum value.

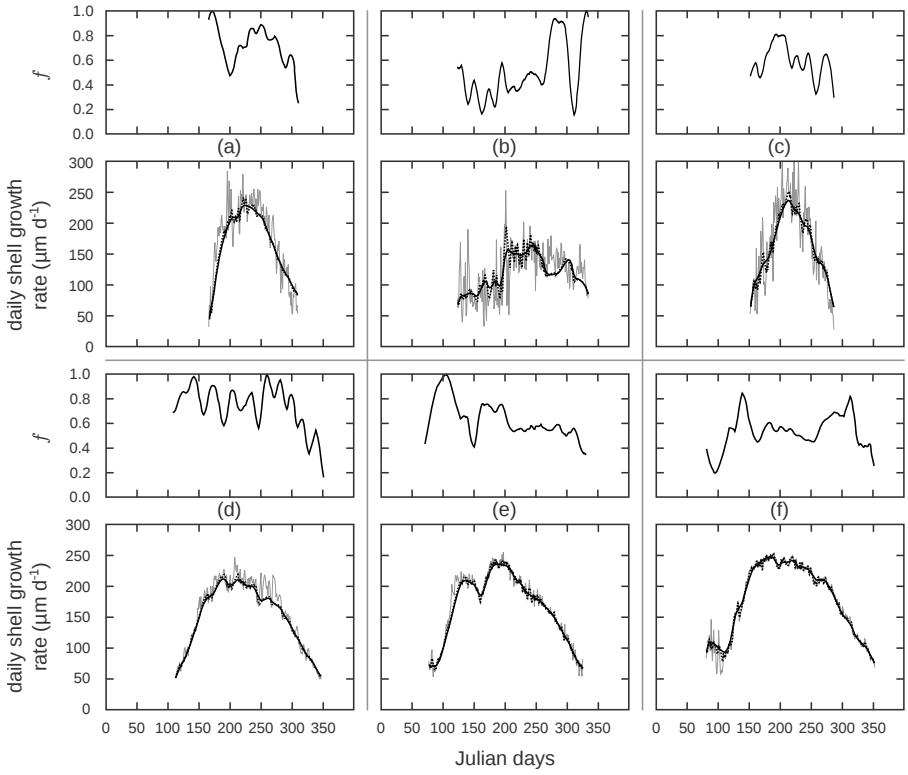


**Figure 6.2:** Reconstruction of the functional response obtained from growth trajectories of *P. maximus*, during the first year of growth, in the six studied locations of the latitudinal gradient: Traena (a), Austevoll (b), Holyhead (c), Plymouth (d), Brest (e) and Quiberon (f). In the upper graphs are the reconstructed functional response (strait dark line); in the lower ones are the growth trajectory (strait gray line), the growth time series after being smoothed by the "deb-box" (dashed dark line) and the back simulated growth trajectory using the reconstructed $f$ (strait dark line).

**Table 6.3:** Linear regression between reconstructed functional response patterns and latitude, depth and growth duration.

| | **Latitude** | | | **Depth** | | |
|---|---|---|---|---|---|---|
| | $R^2$ | *slope* | *p-value* | $R^2$ | *slope* | *p-value* |
| Mean $f$ | 0.70 | 0.008 60 | 0.04 | 0.98 | 0.000 65 | 0.00 |
| Maximum $f$ | 0.66 | 0.007 30 | 0.05 | 0.84 | 0.000 73 | 0.03 |
| Minimum $f$ | 0.09 | −0.002 60 | 0.56 | 0.94 | −0.001 50 | 0.01 |
| Amplitude $f$ | 0.56 | 0.010 00 | 0.09 | 0.97 | 0.002 40 | 0.00 |
| Variance $f$ | 0.32 | 0.000 57 | 0.24 | 0.91 | 0.000 44 | 0.01 |
| Std. Dev. $f$ | 0.61 | 0.002 40 | 0.07 | 0.98 | 0.001 10 | 0.00 |
| | **Days of Growth** | | | **Days of Growth** | | |
| | $R^2$ | *slope* | *p-value* | $R^2$ | *slope* | *p-value* |
| Mean $f$ | 0.38 | −0.000 90 | 0.19 | 0.96 | −0.001 20 | 0.00 |
| Maximum $f$ | 0.17 | −0.000 52 | 0.41 | 0.90 | −0.001 40 | 0.01 |
| Minimum $f$ | 0.09 | −0.000 37 | 0.56 | 0.88 | 0.002 70 | 0.02 |
| Amplitude $f$ | 0.01 | −0.000 21 | 0.84 | 0.96 | −0.004 40 | 0.00 |
| Variance $f$ | 0.19 | −0.000 06 | 0.39 | 0.85 | −0.000 79 | 0.03 |
| Std. Dev. $f$ | 0.09 | −0.000 13 | 0.57 | 0.91 | −0.002 00 | 0.01 |

The standard deviation of the reconstructed $f$ in each location also presented a clear positive relationship with the latitude (Table 6.3), with more variability of functional response observed in Nordic locations (Table 6.2).

### 6.3.2 Bathymetric gradient

Five locations were analyzed along the bathymetric gradient. Fig. 6.3 presents the reconstruction of the functional response from growth trajectories of individuals of different age class living at 98 m and 162 m depth compared to shallow coastal habitats. In some reconstructions in the deepest location (162 m), the growth trajectory often seemed to be very constrained by the "deb-box" smoothing method, resulting in maximum values of reconstructed $f$. The control procedure consisting of back simulate DSGR from the reconstructed functional response indicated that it was not successful (Fig. 6.3f). However for younger individuals and shallower environments, the reconstruction process was correctly achieved. The amplitude range of the reconstructed assimilation time series was greater in the two deep sites compared to the coastal one: in average the maximum value of $f$ was of 0.87 in Brest and 0.97 at both 98 m and 162 m depth and the minimum reached in these location was 0.29, 0.20 and 0.08 respectively (Table 6.2).

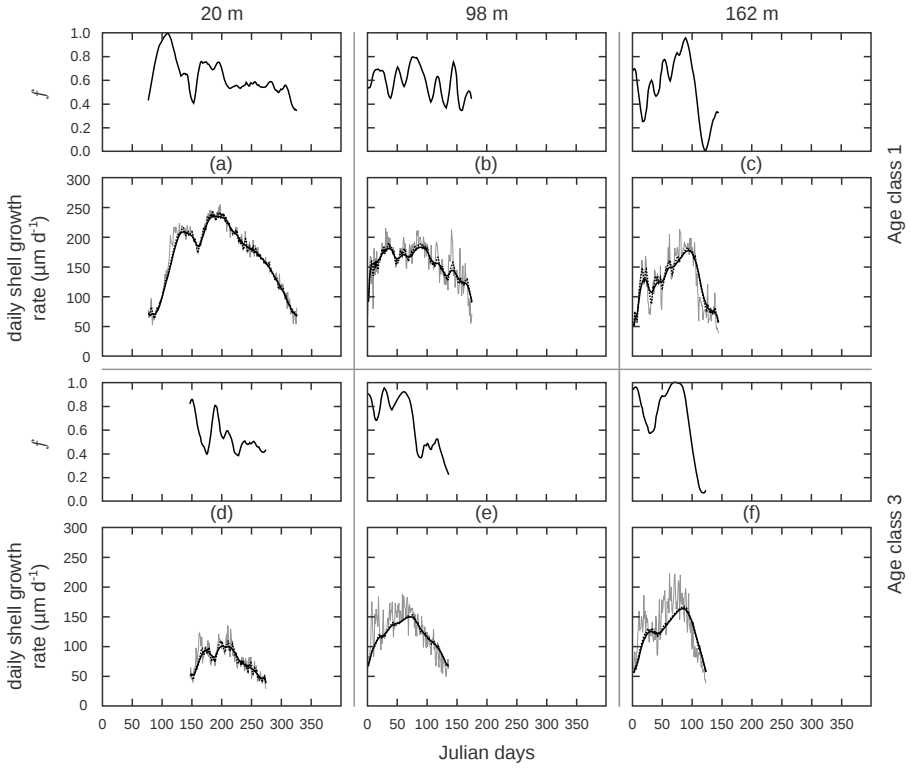


**Figure 6.3:** Reconstruction of the functional response obtained from growth trajectories of *P. maximus*, during the first (a, c, e) and third (b, d, f) year of growth, in three studied locations of the bathymetric gradient: at 20 m depth in a coastal site of Brest (a, b), at 98 m (c, d) and 162 m depth (e, f) in the Celtic Sea. In the upper graphs are the reconstructed functional response (strait dark line); in the lower ones are the growth trajectory (strait gray line), the growth time series after being smoothed by the "deb-box" (dashed dark line) and the back simulated growth trajectory using the reconstructed $f$ (strait dark line).

When considering the five locations along the bathymetric gradient, we found a linear relationship between the depth and the average $f$ (Table 6.3, $R^2 = 0.98$, $p\text{-}value < 0.001$). The average value of $f$ for all age classes in the location of Brest was 0.57 while it reached 0.64 at 98 m, 0.64 at 109 m, 0.66 at 150 m and up to 0.67 at 162 m depth.

Fig. 6.4 allows the comparison of patterns observed along the two studied gradients. While relationships between the reconstructed $f$ time series, especially in terms of variability, and depth was stronger than along the latitudinal gradient, one striking fact is the similarity between functional response patterns in northern locations (Traena and Austevoll) and the deep stations in the Celtic Sea. The average $f$ and its maximum value were very close in

these two types of environment. On the other hand, deep location seems to differ from the coastal stations in the minimum value of $f$, its variance and standard deviation. Indeed, while no significant linear relation was found in the coastal environments, a close relationship was found between depth and these patterns (Table 6.3).

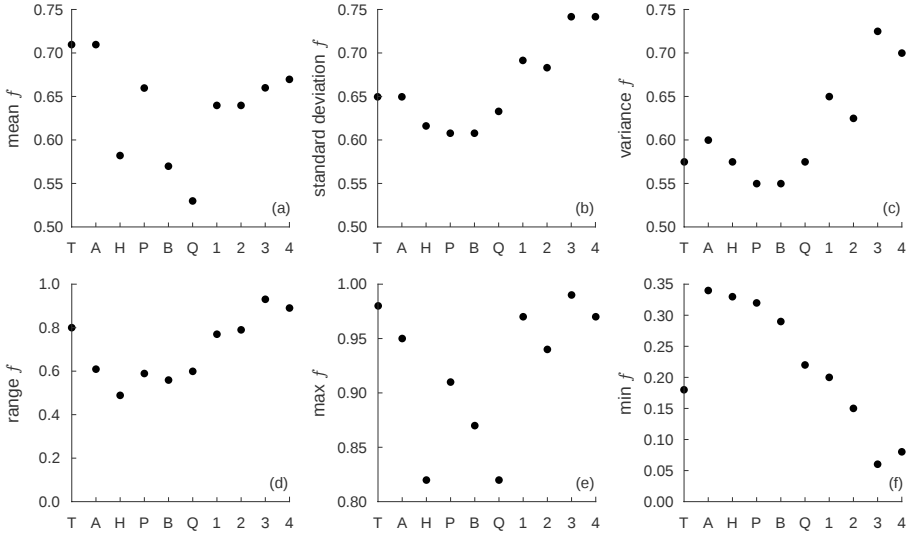


**Figure 6.4:** Description of reconstructed functional response patterns from the ten studied locations: T: Traena; A: Austevoll; H: Holyhead; P: Plymouth; B: Brest; Q: Quiberon; 1: 98 m 2: 109 m 3: 150 m 4: 162 m. (a) mean $f$; (b) standard deviation of $f$; (c) variance of $f$; (d) average range of variation of $f$; (e) average maximum value of $f$; (f) average minimum value of $f$.

### 6.3.3 Ontogenetic patterns?

In order to study the effect of age on the reconstruction process of the functional response, we analyzed different age classes during one year (Fig. 6.5). Four sites provided enough data to compare three to four cohorts: Austevoll (a), Holyhead (b), Plymouth (c) and the 98 m deep Celtic Sea location (d). In the first site, three age classes have been compared and showed very similar patterns in assimilation dynamics reconstruction. Indeed, the sharp decrease at the Julian Day (JD) 200 was present in every ages. In Holyhead location four age classes showed also a common decrease of the reconstructed functional response around JD 240, followed by a peak on JD 250. The rather elevated values at the beginning of the reconstruction showed more temporal variability between age classes, with a peak on JD 180 for the one-year-old time series, on JD 200 for the two-year-old's and on JD 210 for the two oldest age classes. Then, in Plymouth location, variability of the reconstructed $f$ between the

different age classes was more important and no clear tendency was deducted from this analysis. Finally, in the deep location of the Celtic Sea, at 98 m depth, the one- and three-year-old cohorts showed very similar variations of reconstructed $f$ whereas the two-year-old one was completely discordant with the two previous time series. In fact, on JD 190, the assimilation reconstruction for both youngest and oldest age classes presented a rapid drop of about 0.6 while the reconstructed $f$ from two-year-old scallops remained at 1 from JD 175 to 225.

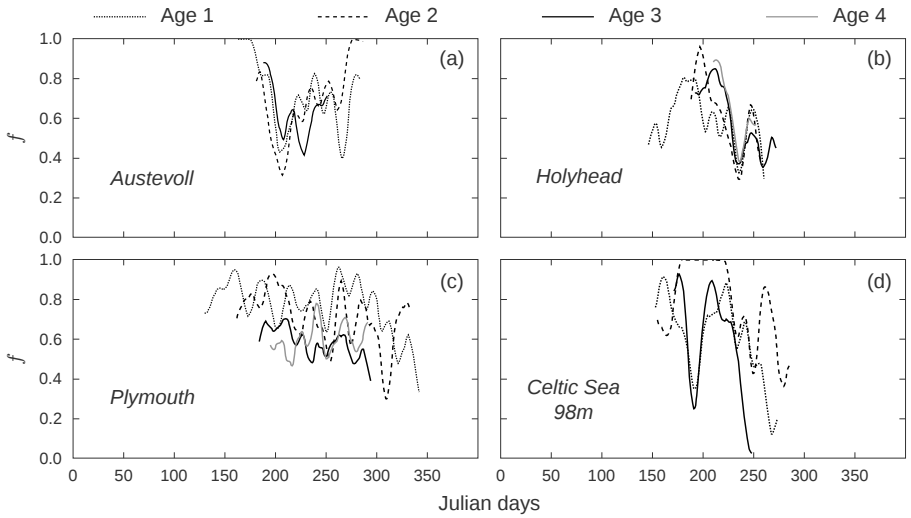


**Figure 6.5:** Reconstructed time series of the functional response of different age classes during a same year in the sites of Austevoll (a), Holyhead (b), Plymouth (c) and at 98 m depth in the Celtic Sea (d). Three ages classes were compared to each other in location (a) while four age classes were analyzed in locations (b), (c) and (d).

### 6.3.4 Comparing $f$ with observed food proxies

Fig. 6.6 presents a comparison between time series of reconstructed assimilation and some proxies of trophic availability for seven years in the Bay of Brest. We used growth trajectories obtained from age class one as they provide a more extended growing season than older animals in this area. Moreover, as many potential food descriptors were available for the period 2010–2011, more potential food indicators were compared to the reconstructed dynamics of assimilation (Fig. 6.6b). First of all it is clear that not only one food proxy is to explain the dynamics of $f$. The average value of $f$ in the Brest location is 0.57 (Table 6.2). Some sharp drops in the functional response of scallops were observed in 1998 (Fig. 6.6a, JD 150 to 155), 2001 (Fig. 6.6d, JD 130), in 2002 (Fig. 6.6e, JD 140 and 225) and in 2003 (Fig. 6.6f, JD 145).

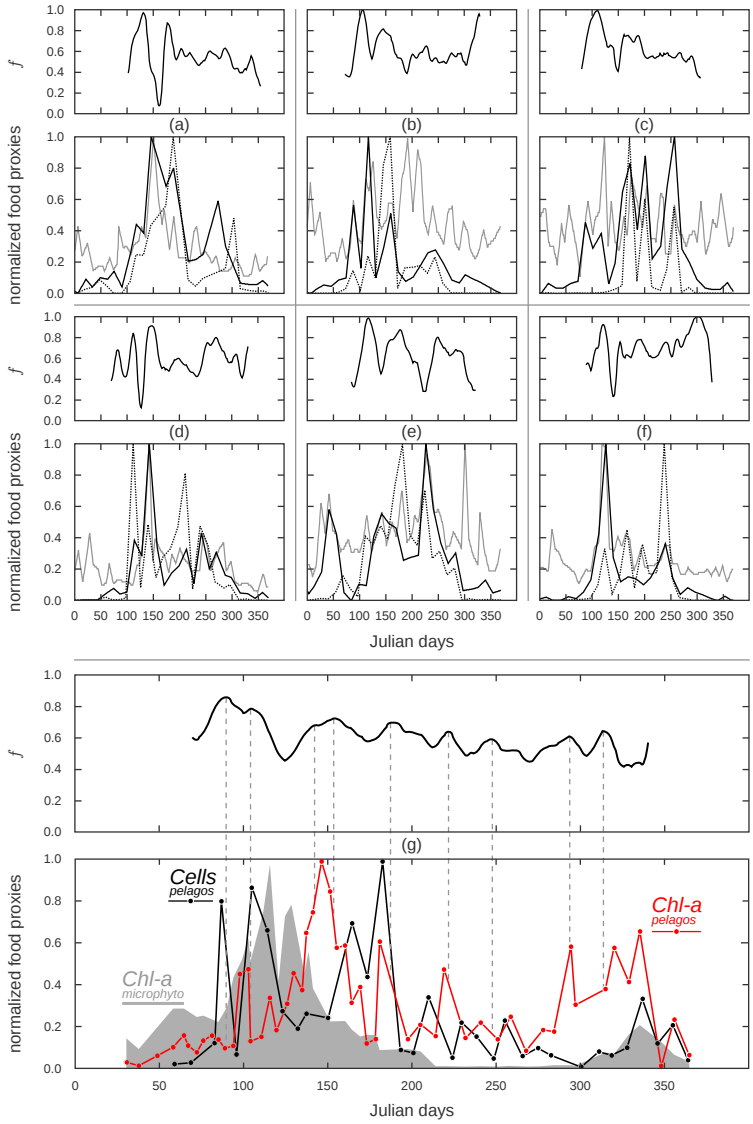


**Figure 6.6:** Comparison of reconstructed time series of functional response (upper graphs, strait dark line) with potential food proxies (normalized to 1) in the Bay of Brest (lower graphs). Age class one growth trajectories were used for two periods: 1998–2003 (a, b, c, d, e, f), for which comparisons were made with time series of chlorophyll-*a* (strait dark line), phytoplankton counts (dotted dark line) and POM concentration (strait gray line); 2011 (g), where chlorophyll-*a* concentration from the microphytobenthos (dotted line), from the pelagic seawater compartment (red line) and pelagic phytoplankton cell counts (dark line) were compared to the reconstructed $f$ time series.

Some of these depletions occurred while the studied food proxies were elevated and sometimes when, conversely, they also showed decreases. For instance, in 1998 all the trophic markers were close to their maximum when the drop in $f$ was observed. To the contrary, in 2000, the sharp reduction of assimilation happened between a peak of phytoplankton cell and a peak of chlorophyll-$a$. In 2011, the superposition of $f$ dynamics with chlorophyll-$a$ time series measured in the benthic and in the pelagic compartments revealed a tight relationship between the assimilation and chlorophyll-$a$ concentration from the pelagic domain. Interestingly, a decrease of $f$ in JD 120 was concomitant with a peak in chlorophyll-$a$ concentration at the water-sediment interface. This drop in functional response was concurrent with a bloom of two particular microalgae: *Amphora sp.* and *Pseudo-nitzschia cf delicatissima*, both of them producing the phycotoxin domoic acid.

### 6.3.5 Physiological variables

The approach developed by Lavaud et al. (in prep.) allows one to reconstruct not only the temporal dynamics of functional response but also various physiological variables. Reconstructed reserve amount $E$ was more important in scallops from the location of Brest (Fig. 6.7a, b). Interestingly, the amount of reserves in three-year-old scallops living in the Celtic Sea tended to get closer to the quantity observed in scallops from the inshore location of Brest. In terms of reserve density $[E]$, very similar dynamics were observed between the location of Traena and the Celtic Sea (98 m) while more stable time series resulted from the reconstruction in the location of Brest. The dynamics of reconstructed mobilsation flux of reserves $\dot{p}_C$, for further allocation to reproduction and growth plus their maintenance, were again very similar in Traena and at 98 m. Values observed for individuals from Brest were 2 to 5 times higher. Finally, the very same patterns were observed in the reconstruction of the maintenance rate coefficient $\dot{p}_M$.

## 6.4 Discussion

The approach developed in this study focuses on assimilation dynamics in order to describe and comprehend the life history traits of *Pecten maximus*. Focusing on the functional response patterns allows one to deal with the dynamics of energy input, which has long been a source of uncertainty in bioenergetic modeling, especially within bivalves (Bourlès et al., 2009; Alunno-Bruscia et al., 2011). In this context, the use of DEB theory is an advantage as it provides a mechanistic framework. In this study we achieved to use an inverted DEB model to reconstruct this functional response in various environments.

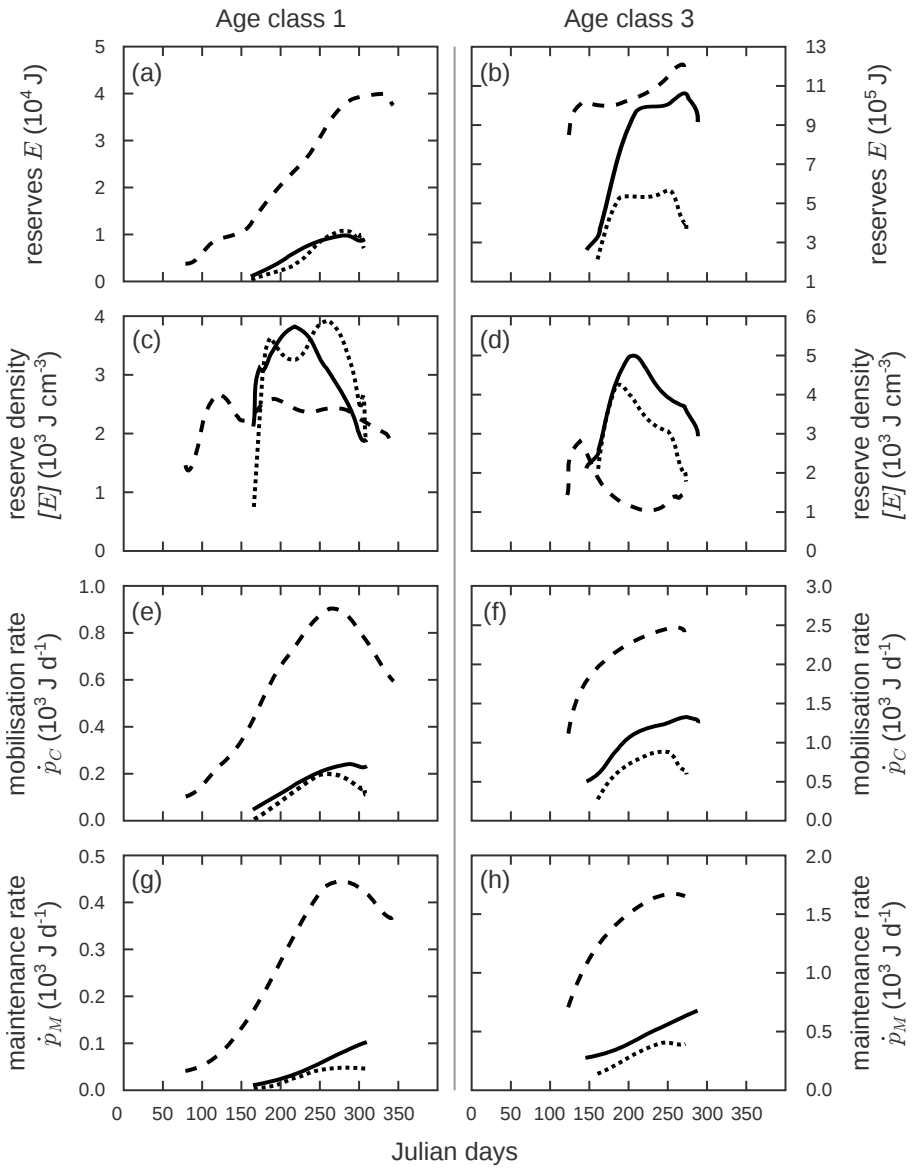


**Figure 6.7:** Reconstruction of physiological variables from growth trajectories of individuals from age class one (right) and three (left) living in Traena (dotted line), Brest (dashed line) and at 98 m deep in the Celtic Sea (strait line). Reserve amount $E$ (a, b) , reserve density $[E]$ (c, d), mobilization flux of energy from reserves $\dot{p}_C$ (e, f) and maintenance rate coefficient $\dot{p}_M$ (g, h).

### 6.4.1 Shell growth

The growth pattern of the great scallop have been extensively studied through sclerochronological studies (Chauvaud et al., 1998; Lorrain et al., 2000; Lorrain, 2002; Owen et al., 2002b; Patry, 2009; Guarini et al., 2011; Chauvaud et al., 2012). Generally, during the first years of life, there is a positive correlation between DSGR and the duration of the growing season in a year: a long growth period corresponds to high growth rates. When going northward or toward deep locations, the number of days of growth decreases (Patry, 2009; this study). However, when getting older, this number of days of growth declines more slowly than in other environments (Chauvaud et al., 2012). The oldest shell used in this study had more than eight winter marks. The potential of environmental reconstruction for a such long period is obviously interesting, however, one would get more accurate information from younger individuals as: (1) early years of growth allow for more extended reconstruction period as shell growth duration in juvenile and young adults spans longer than in older individuals (Patry, 2009; Chauvaud et al., 2012); (2) the variation range of DSGR values is higher in early years of growth, as shell can grow of about $0.3\,\mathrm{mm\,d^{-1}}$ which increases the resolution of growth rate variations — in comparison, the average maximum DSGR value of a four-year-old scallop in the middle of its distribution range would "only" reach $0.1\,\mathrm{mm\,d^{-1}}$; (3) the measurement of the increment width is easier in a young scallop because its shell has not been much damaged by the time (epibionths fixation, predators attacks, bumps and friction of sediment). The variation range of the reconstructed $f$ seems to be less important for older individuals. Nonetheless, this could be attributed to the fact that less extended time series can be reconstructed from three-year-old or older age classes as their growing period is shorter in time. In this way, the use of growth trajectories limits our interpretations to periods when animals achieve a certain growth rate (over $0.05\,\mathrm{mm\,d^{-1}}$).

### 6.4.2 Latitudinal gradient

It has been shown that *P. maximus* would regulate its clearance rate in response to relatively small changes in phytoplankton quantity (Strohmeier et al., 2009). Scallops inhabiting northern ecosystems, while facing extremely low seston conditions (Aure et al., 2007), do not seem to be limited by their ability to clear particles out of suspension (Strohmeier et al., 2009). The rather elevated values of $f$ reconstructed in the two northernmost locations (Traena and Austevoll, Norway) describe this biological pattern, with an increased assimilation rate. Transplant experiments have shown that scallops originating from various latitudinal locations did not display significant differences in growth when placed in the same conditions. Therefore, the high $f$ observed in northern sites might be considered as a local response to environmental conditions. We found that the variability of $f$ in higher latitudes was not significantly different from lower latitudes. Norwegian waters are often described

as oligotrophic (Aure et al., 2007) and experience large primary productivity during spring bloom periods (Erga and Heimdal, 1984; Dale et al., 1999; Bratbak et al., 2011; Erga et al., 2012). Nanoplankton communities dominate in winter and summer periods (Erga and Heimdal, 1984), while diatoms make up the main part of spring biomass. Thus, one could expect a more pronounced seasonality in functional response patterns at high latitudes.

In the center of its distribution range (UK, France), *P. maximus* showed lower functional responses in average, together with lower maximum values (Table 6.2). Waters of the English Channel and the Irish Sea are more eutrophic (Sathyendranath et al., 1995; Baan and van Buuren, 2003), which means that food availability is not likely to limit *P. maximus* energy acquisition, with the exception of the winter period. Moreover, the functional response of bivalves decreases when food availability increases (Widdows et al., 1979; MacDonald et al., 2006). Decrease of functional response in bivalves is also observed in overloaded environments (Bacon et al., 1998), mainly due to the production of not ingested pseudo-faeces. In the location of Plymouth and Quiberon, both close to estuaries (of the river Tamar and the Loire river respectively) and in the Bay of Brest, a semi-enclosed area, it is likely that the food quantity and inorganic inputs would cause sharp drops of the functional response. Even in higher latitudes of Norway, scallops were reported to cease filtrating during the periods of high chlorophyll-*a* quantities in late winter and spring blooms (Strohmeier et al., 2009).

### 6.4.3 Bathymetric gradient

Reconstructed $f$ patterns along the bathymetric gradient were highly correlated to depth: mean, maximum, minimum values of $f$, its variance, standard deviation and variation range (Table 6.3). The deeper the location, the higher the average $f$ and its variability. Little is known about the ecological pattern of great scallops living on the continental shelf. Physical parameters such as the cold and constant temperature of bottom water (12 °C in the Celtic Sea and the Bay of Biscay) and the low food quantity and quality may be responsible for major metabolic changes in deep water organisms, such as reduced growth rate (Buick and Ivany, 2004), respiration (Smith and Teal, 1973), and reproduction (Rokop, 1974). As no light penetrate deep enough to sustain primary production at the bottom, organic matter inputs rely on the vertical export of phytodetritus from the upper photic layers (Bunt, 1975; Pingree et al., 1982; Duineveld et al., 1997; Nerot et al., 2012). Therefore, the functional response might follow the seasonal pattern of open ocean pelagic primary production.

### 6.4.4 Local adaptations

DEB theory aims at providing a common mechanistic framework that allows one to model energy dynamics in variable environments. The species specific set of parameters estimated for a given species are theoretically able to describe

energetics of any individual of the same species. However, the parameter set is likely to evolve as more and more data set are tested. The use of the DEB parameters estimated by Lavaud et al. (2013) in this application urged us to revise the value of some parameters linked to the metabolic acceleration experienced by scallops after their metamorphosis, which was already supposed to cause the slight under-estimation of DSGR in the study of Lavaud et al. (2013). Although it improved most of our simulations, in some reconstructions in the northern (Traena and Austevoll) and the deepest locations (162 m), results were not completely satisfying. The difficulties encountered in the reconstruction of functional response in these locations might account for potentially high physiological and metabolical differences within animals living in such extreme environment when compared to inshore individuals. Indeed, plasticity of physiological mechanisms are very likely to occur to permit the survival of scallops in deep-seas and polar environments (Buick and Ivany, 2004). Such a plasticity has been reported concerning reproduction and growth patterns between European coastal populations of *P. maximus* (Antoine et al., 1979; Beaumont et al., 1993; Cochard and Devauchelle, 1993; Mackie and Ansell, 1993; Magnesen and Christophersen, 2008). However these studies showed that the existence of separated stocks is still under debate.

### 6.4.5 Linking functional response to food proxies

The search for energy input proxies in bioenergetic modeling of bivalves is a recurrent issue that is likely to determine the goodness of fit and the reliability of simulations. The comparison that we made between the different food proxies and the reconstructed functional response highlights the complexity of the linkage between food availability, ingestion and assimilation as shown by many authors (Lorrain et al., 2002; MacDonald and Ward, 2009; Ward and Kach, 2009; Nerot et al., 2012). Moreover, the discrepancy of time scales between the high frequency modeled time series of $f$ and the daily to weekly time scale of environmental conditions monitoring.

Nevertheless, we showed that in the Bay of Brest, during seven years of study, the dynamics of the reconstructed functional response was more related to chlorophyll-$a$ variations than to any other food proxy. More precisely, chlorophyll-$a$ concentrations measured in the water column (and not at the bottom) showed the better match to $f$ time series. Chlorophyll-$a$ has long been used as the food proxy for filter feeding organisms (e.g. Bacher et al., 1997; Pouvreau et al., 2006; Sarà et al., 2012) for this pigment is present in every phytoplankton species. In coastal locations from the middle of *P. maximus*' distribution range, such as in France and UK, phytoplankton is abundant during more than half of the year (from March to October). Therefore, chlorophyll-$a$ might be enough to represent the dynamics of food availability in these ecosystems, during the period of growth of the great scallop.

This study revealed that the particulate organic matter was not likely to explain the variations of $f$. however, Lavaud et al. (2013) showed that this

potential food source for the great scallop sustained energy inputs especially during late autumn, winter and early spring, i.e. outside blooming periods of phytoplankton (Chapter 2). The present method reaches here one of its limits as growth slows down or even stop during this period, which do not allow us to reconstruct $f$. Studies comparing the use of other markers of food availability (Bourlès et al., 2009; Handå et al., 2011; Hawkins et al., 2014; Chapter 2), such as POM, SPM or phytoplankton cell counts, came to similar conclusions: the relevance of other seston variables than chlorophyll-$a$ is likely to increase along with decreasing phytoplankton densities.

### 6.4.6 Limits

It is not possible to assign calendar dates to growth increments deposited before the last winter stop experienced by the animal. The method used to resettle older growth trajectory in time thanks to the temperature relies on the fact that temperature is the main factor that influencing DSGR variation. However, strong uncertainty persists and this is yet to be confirmed. Other factors such as irradiance would probably display a more tight relationship with growth maximum (C. Le Goff, pers. comm.). This approach relies on the growth data provided by the incremental width of growth striae. In turn, it is possible to apply the reconstruction process only to periods of significant growth. Indeed, the measurement of DSGR can not be conducted below a threshold of $0.05\,\mathrm{mm\,d^{-1}}$. Therefore, no information can be extracted from the winter period when growth is extremely slowed which, instead of producing clearly visible striae, results in a dense accumulation of tiny increment appearing as a large mark in macroscopic observation.

### 6.4.7 Perspectives and prospects

#### Coupling DEB reconstruction to geochemical analysis of the shell

The use of bivalve shells as biogenic archives of past environmental conditions provides a remarkable source of information for the understanding of paleoclimate and paleoenvironments (Jones, 1983; Grossman and Ku, 1986; Goodwin et al., 2001; Schöne et al., 2011). Indeed, the analysis of various geochemical proxies from sequential sampling along the shell growth axis provides high-resolution records of spatial and temporal patterns in temperature, flood, primary production or large scale climatic events (Jones et al., 1984; Chauvaud et al., 2005; Thébault et al., 2009; Thébault and Chauvaud, 2013; Lavaud et al., 2012; Royer et al., 2013). Very few potential proxies of the trophic availability have been reported into the carbonated skeleton of marine bivalve, which are still being debated (Barats et al., 2009; Thébault et al., 2009; Thébault and Chauvaud, 2013). The present work provides a new perspective in the reconstruction of past environmental conditions. The possibility of studying the variability of assimilation patterns and its seasonality over the long term could help understanding present and past ecological mechanisms of the great

scallop. Since the study of oxygen isotopes ratios allows the reconstruction of temperatures at the moment of growth (Chauvaud et al., 2005), an extremely attractive perspective would be to use this reconstructed temperature time series extracted from the shell to reconstruct the dynamics of food assimilation and physiological variables. Therefore, one might be able to determine past environmental (thermal and trophic) conditions from a shell, without any field measurement.

**Reconstruction of reproduction**

The current knowledge on the reproductive physiology of *P. maximus* is detailed concerning the process itself but less understood is the overall physiology of organisms during reproduction. For instance, there are still questioning about assimilation being affected by spawning? The development of our knowledge on these processes might allow us to decipher such activity from assimilation time series in the past. Moreover, it would be interesting to know the evolution of reproduction activity dynamics in the past. Nevertheless, validation of the estimation of the physiological variables ($E$, $[E]$, $\dot{p}_C$ and $\dot{p}_M$) is still required, which could be achieved through the seasonal biochemical analysis of scallops (Pazos et al., 1997; Strohmeier et al., 2000) from various locations of the distribution range of *P. maximus*.

## Acknowledgements

The authors want to acknowledge the SOMLIT and the CEFAS monitoring networks. The author especially acknowledge the maintainers of the EVECOS data base (L. Chauvaud, A. Jolivet, Y.-M. Paulet). We deeply acknowledge Ewan Harney for correction of English writing.

# Chapter 7

# General discussion

## 7.1 A Dynamic model of the Energy Budget of *P. maximus*

This work has been developed around a modeling approach of the bioenergetics of the great scallop, *Pecten maximus*, in order to address the description and the understanding of the variability of life history traits of this species. The modeling of energy fluxes allows one to describe the variability in physiological patterns such as growth, reproduction, respiration and feeding. Dynamic Energy Budget (DEB) theory provides a mechanistic formalization of such metabolic processes, which is increasingly used to study individual bioenergetics and investigate the relationship between organisms and their environment. Chapter 2 presents the first DEB parameter set estimated for the great scallop.

### 7.1.1 Parameter estimation

The list of primary parameters estimated through the covariation method of Lika et al. (2011a) is very close to other bivalves already modeled in DEB theory (Add_my_pet library: `http://www.bio.vu.nl/thb/deblab`). Among them, the value of surface specific assimilation rate, $\{\dot{p}_{Am}\}$, the fraction $\kappa$ for allocation to soma and energy conductance, $\dot{v}$, are particularly close to the parameters estimated for the blue mussel *Mytilus edulis*. The similarity in $\{\dot{p}_{Am}\}$ comes from the fact that parameters for a species are given for a newly born individual. During the larval stage, the development of these two species is very similar and both will develop filibranch gills (gill filaments independent from each other). Before metamorphosis, an acceleration of metabolism is likely to occur (Kooijman et al., 2011), which causes the surface specific assimilation rate of *P. maximus* to increase up to $374\,\mathrm{J\,d^{-1}\,cm^{-2}}$. This change in metabolism has indeed been suggested by MacDonald et al. (2006) and is supported by several facts: (1) the change in shape during metamorphosis (from larva to young scallop), which implies a reorganization of tissues and metabolic strategies; (2) some data sets of larval and juvenile growth (Beau-

mont and Budd, 1982; Beaumont and Barnes, 1992; Laing, 2000; Christophersen et al., 2006); (3) this seems to be a common observation in bivalves (Kooijman et al., 2011; Kooijman, subm.). In combination with genetic control on parameter values, these epigenetic processes help to understand the causes of variation amongst individuals which are vital to evolutionary change (Kooijman et al., 2011). Age at metamorphosis was the only empirical data not well fitted with this set of parameters (Chapter 2). This critical event has been extensively studied in the laboratory (Gruffydd and Beaumont, 1972; Beaumont and Budd, 1982; Cochard and Devauchelle, 1993) but little is known on development in natural conditions (except that it is a principal cause of mortality for young scallops). Furthermore, while numerous data sets describe the evolution of length until metamorphosis, very few concern the following steps of development of spat (Robert and Nicolas, 2000; Nicolas and Robert, 2001). This lack of data might be responsible for the difficulty in fitting these biometric values after metamorphosis.

Lika et al. (2011b) explored parameter patterns in the covariation method for estimation of DEB parameters. They observed that the prior parameter estimates (pseudo-data) used as a basis for the estimation process had very little influence if the real data contain enough information about the parameter values. The effect of pseudo data for the energy conductance would be reduced when information on age at birth and puberty is given. This stresses the lack of data used in the estimation of parameters (length over time data, Chapter 2, Fig. 2.11). This kind of data is indeed relatively easy to obtain but does not give enough information, especially on the reserve dynamics of the species. Moreover, no accurate data is available about puberty of *P. maximus*; articles on this subject mention only that sexual maturity is reached during the second year (Tang, 1941; Mason, 1958; Pazos et al., 1997). This also contributes to uncertainty in the parameter set.

### 7.1.2 The growth challenge

The set of parameters estimated in the first part of this work allowed the accurate simulations of growth in weight and length. A slight underestimation of the daily shell growth rate was identified in the simulation of bioenergetics of scallops from the Bay of Brest. Relatively low values of $\{\dot{p}_{Am}\}$ and $\dot{v}$ after metamorphosis were suspected to explain this inaccuracy. The fact that small deviations from observations occur when testing the model on real data is not completely surprising for a first attempt to estimate DEB parameters. If growth alone was to be modeled, only a few parameters would probably be sufficient to achieve such a simulation. Moreover, in that case, several parameter sets might lead to successful results. However, if other physiological functions are desired (e.g. growth rate, weight, reproductive activity), less combinations of parameters would allow good results to be obtained. The changing of scales from season (in Chapter 2) to day (in Chapter 6) was another constraint. In other words, when more tests are carried out and different types of data

are used in various environments, the constraint on the parameter estimates increases.

During first trials with the inversion of the DEB model carried out in Chapter 6, under-estimation of growth rate was encountered. In fact, a miscalculation of the acceleration factor resulted in the low value of $\{\dot{p}_{Am}\}$ and $\dot{v}$. Therefore, a re-calculation of this acceleration factor was conducted to result in more reliable values of these parameters, without changing the other estimates. The goodness of fit was then slightly reduced from 8.72 to 8.60 which is still satisfying. The simulations carried out in Chapter 2 with the previous parameter values were run again using this new parameter set. Providing adjustments in the value of the filtration rates for food particles of type $X$ and $Y$ (already calibrated in the model described in Chapter 2) gave even better fit to observed data (see Appendix B, Fig. B.1, B.2 and B.3). Modeling of daily shell growth rate especially showed a better fit.

DEB parameters are likely to evolve when based on more (or other) data in the estimation process. In bivalves particularly, it has been the case for the Pacific oyster *Crassostrea gigas*, for which the first set of parameters was estimated by van der Veer et al. (2006). These were re-estimated in order to fit applications in other geographical areas (Pouvreau et al., 2006; Alunno-Bruscia et al., 2011) and after a reconsideration of the handling rule for the reproduction buffer (Bernard et al., 2011). The same applied to the blue mussel, *M. edulis* (van der Veer et al., 2006; Rosland et al., 2009; Saraiva et al., 2011b) and the cockle *Cerastoderma edule* (van der Veer et al., 2006; Wijsman and Smaal, 2011). This illustrates the evolution of DEB parameters estimates, which is likely to apply for the great scallop in coming years.

### 7.1.3 Feeding preference implemented through Synthesizing Units

The test of the selection capacity implemented in the DEB model of *P. maximus* (Chapter 2) relies on the Synthesizing Units (SUs) concept of Kooijman (2010). SUs are in the core of DEB theory. They allow for a mechanistic interpretation of energy flows and particularly of the feeding process. As SUs act like generalized enzymes, several types of interaction with substrate(s) can be considered (complementarity, preference, inhibition, etc.). The explicit implementation of SUs in the feeding process has already been carried out by Saraiva et al. (2011a) on the blue mussel *M. edulis*. These authors also included the effect of inorganic suspended matter on filtration and feeding, by adding a third substrate (silts) to the potentially processed particles. Therefore they tried to understand and assess how bivalve growth rates were affected by food quantity and quality. The great scallop can be found in coastal waters where several processes might impact its filtration activity: river discharges (Guillaud et al., 2008), resuspension of deposited material due to waves and currents (De Jonge and Van Beusekom, 1995), phytoplankton bloom sedimentation (Bienfang, 1981; Smetacek, 1985; Chauvaud et al., 2001) and human

activities (e.g. dredging). All of these processes may result in broad fluctuations in both quality and quantity of suspended particulate matter. Therefore, it would be interesting to test the effect of silt on *P. maximus* filtration, especially in comparison with deep-sea population which may not experience such processes and also with scallops from northern systems, where water turbidity in coastal areas is lower (Nair, 1962). This might also help to explain the brief periods of growth reduction often observed in coastal areas despite the availability of food.

### 7.1.4 From the individual to the population

A first step in the transition from the individual level to the population scale has been achieved in Chapter 3 through the modeling of the distribution of *P. maximus* at a regional scale. In this approach, the individual DEB model was integrated into a modeling system providing inputs for the bioenergetic simulations, which in turn determined the trajectory of an average individual. This approach gives information on the evolution of an average individual and thus differs from real population models. As there are no interactions between individuals it also differs from Individual Based Models (IBM). Population modeling can be achieved through DEB theory (e.g. Diekmann and Metz, 2010; Nisbet et al., 2010; Pethybridge et al., 2013) and it would be interesting to investigate this question of the distribution of *P. maximus* by changing the scale from individual to population, which is closer to the definition of a stock. Recent advances in population modeling also gave promising perspectives through the coupling of individual DEB models with IBM models (Bacher and Gangnery, 2006; Duarte et al., 2012; Martin, 2013).

## 7.2 Feeding ecology

### 7.2.1 Living on the bottom, feeding on what comes from above

Many authors showed through physiological and biochemical studies that the diet of the suspension-feeding bivalves was likely composed of other food sources than phytoplankton only (e.g. Heral, 1989; Langdon and Newell, 1990; MacDonald et al., 2006). Lorrain et al. (2002) and Nerot et al. (2012) demonstrated through isotopic and fatty acid analysis of the digestive gland that *P. maximus* also had diversified food sources. Results acquired in Chapter 2 support this hypothesis as particulate organic matter (POM; except living phytoplankton) from the water considerably enhanced growth and reproduction of the great scallop. Many benthic filter feeders has long been suspected to feed on the resuspended microphytobenthos, i.e. microalgae (mainly diatoms) developing on bottom substrates. Behavioral theories have hypothesized that *P. maximus* could actively resuspend benthic microalgae by clapping their

valves (Davis and Marshall, 1961; Chauvaud et al., 2001; Lorrain et al., 2002). Nerot (2011) investigated trophic patterns along bathymetric gradients in west France and concluded: (1) from the isotopic study of muscles that microphytobenthos might account for an important part of the diet of coastal individuals; (2) from fatty acid analysis of digestive gland that diatoms were the main food source for *P. maximus*; (3) that bacteria might be a significant trophic source for deep-sea individuals. Results from the high frequency seasonal monitoring (Chapter 4) tend to confirm these hypotheses, at least for a certain period of the study. Microphytobenthos, which bloomed earlier than pelagic microalgae, was ingested and assimilated by the scallop. But as soon as the pelagic biomass of phytoplankton bloomed, pigments and fatty acids dynamics measured in the digestive gland of *P. maximus* rather indicate a dominance of the pelagic phytoplankton in its diet. The pelagic chlorophyll-*a* marker also presented the more tight relationship to the reconstructed functional response of the scallops (Chapter 6). These results highlight the importance of coupling between the pelagic and benthic compartment. Nevertheless, in northern environments, high phytoplankton development is limited to spring (Erga and Heimdal, 1984; Strohmeier et al., 2009; Erga et al., 2012) and might not be sufficient to provide energy for benthic suspension-feeders. Although temperature is lower, more light penetrates to the sea bottom as a result of their low turbidity (Nair, 1962). In coastal areas of Norway, shallow sandy habitats with limited impact from riverine input are common (Erga et al., 2012). These conditions might enhance microphytobenthos development (Taasen and Høisæter, 1981), which could provide scallops with a more sustainable food source after the high but short spring pelagic blooms.

### 7.2.2 Food availability - What to eat, what to reject?

In the light of the results obtained in the trophic study (Chapter 4), previous knowledge of the feeding activity of *P. maximus* has been partly confirmed and new insights arose. It has long been suggested that *P. maximus*, as a filter-feeder, would be likely to ingest several types of food particle: phytoplankton, microphytobenthos, detrital material, nanoplankton, bacteria and macro-algae detritus (Heral, 1989; Langdon and Newell, 1990; Alber and Valiela, 1996; MacDonald et al., 2006; Bachok et al., 2009; Yokoyama et al., 2009; Cranford et al., 2011; Nerot et al., 2012). The study was conducted in a well known coastal environment, the Bay of Brest. The results of the multi-proxy approach used to track potential food sources for the great scallop confirmed that microphytobenthos is actually a significant part of its diet, as mentioned above, mostly during the first weeks of spring. The alternation of ingestion and assimilation of diatoms and dinoflagellates is a newly observed pattern in feeding of filter feeders. The majority of literature on dinoflagellate ingestion in bivalves deals with microalgae species that are potentially toxic for consumers (e.g. Abbott and Ballantine, 1957; Shumway and Cucci, 1987; Erard-Le Denn et al., 1990; Bricelj et al., 2004; Hégaret et al., 2007, 2012). Our results show

that dinoflagellates strongly contribute to the diet of *P. maximus*. In northern ecosystems phytoplankton communities are often dominated by taxonomic groups of small microalgae (<10 µm; Murphy and Haugen, 1985; Reid et al., 1990) such as many dinoflagellates species (Erga and Heimdal, 1984; Reid et al., 1990; Erga et al., 2012; Strohmeier et al., 2012). They might, thus, account for an even more important part of the diet of northern great scallops.

A short break in ingestion was monitored during a large spring bloom of diatoms, a phenomenon that has already been reported by Strohmeier et al. (2009) who found a negative correlation of clearance rate to chlorophyll-*a* during large spring blooms. Lorrain et al. (2000) and Chauvaud et al. (2001) related drops in growth rate to these events and suggested that *P. maximus* might experience gill clogging (Dame, 2011) caused by post-bloom sedimentation of senescent phytoplankton (Smetacek, 1985; Riebesell, 1991; Ragueneau et al., 1994).

Despite the presence of green macro- and/or microalgae in the environment, only small amounts were found in the digestive tract of the great scallop, suggesting pre-ingestive selection processes against these algae. Cranford and Grant (1990) found similar experimental results with *Placopecten magellanicus* fed with phytoplankton, fresh and aged macroalgal detritus. Moreover, Utting and Millican (1998) in a review of diet in hatchery conditioning of scallops emphasized the low food value of green microalgae such as *Dunaliella tertiolecta*, *Phaeodactylum tricornutum*, *Tetraselmis chuii* or *Chlorella autotrophica* for *Argopecten irradians concentricus*.

This study also suggested that cyanobacteria and other bacteria might be considered as a food source for the great scallop. Several studies proved that microorganisms could be ingested and assimilated by bivalves (McHenery and Birkbeck, 1985; Prieur et al., 1990; Alber and Valiela, 1994, 1995, 1996). In a review of the particle retention efficiency in Pectinidae, MacDonald et al. (2006) affirmed that free bacterioplankton, typically ranging in size from 0.3 to 1 µm, was available as a food source for pectinids if bound in aggregates. Moreover, Alber and Valiela (1995, 1996) suggested that organic aggregates, or flocs, could potentially represent an important and nutritious food source for suspension-feeding bivalves. Additionally, more than thirty bivalve species have been found to contain lysozyme-like enzymes that could digest the cell walls of bacteria (McHenery et al., 1979, 1986; Alber and Valiela, 1994). The highest values of iso 17:0 (fatty acid marker of bacteria; Vestal and White, 1989; Kharlamenko et al., 2001), observed at the beginning of March may be explained by an ingestion of bacteria during winter in this coastal area. In a study of Fatty Acid signature of scallop tissues, Nerot et al. (2012) highlighted a strong contribution of bacteria, especially in deep-sea individuals (190 m in the Celtic Sea). Thus, bacteria may sustain to some extent the energetic requirements of *P. maximus* when microalgae are present in very low concentration in the water during wintertime.

This close investigation of the seasonal feeding ecology of *P. maximus* confirms its ability to switch from one trophic source to another. Moreover, some

food sources seem to be neglected by the great scallop (green algae), in favor of diatoms and dinoflagellates, supporting the hypothesis of food preference (Møhlenberg and Riisgård, 1978; Stuart and Klumpp, 1984; Shumway et al., 1985; Ward et al., 1997; Bacon et al., 1998; Baker et al., 1998; Ward et al., 1998; Levinton et al., 2002; Beninger et al., 2004; Ward and Shumway, 2004; MacDonald et al., 2006; Ward and Kach, 2009; Espinosa et al., 2010; Rosa et al., 2013). Mechanisms for food selection have been proposed and are still under debate. Recent findings of Espinosa et al. (2010) and Rosa et al. (2013) provide more evidence for this theory of food particle selection. Espinosa et al. (2010) revealed interactions between a protein of the mucus that covers oyster's gills, and carbohydrates at the surface of microalgae cells. They provided insights into the carbohydrate specificity of lectins that may be implicated in the selection of microalgal species. Rosa et al. (2013) highlighted non-specific interactions involving surface-charge and wettability of particles in the particle discrimination process.

### 7.2.3 Feeding behaviour

Apart from chemical and physical mechanisms for food ingestion, scallops also show interesting behaviour in feeding. In addition to the hypothesized active resuspension of microphytobenthos by valve clapping already mentioned, some studies have reported the capacity of scallops to control their orientation with regard to the direction the shell is facing (Brand, 2006a). Hartnoll (1967) and Mathers (1976) showed that *P. maximus* modifies its orientation depending on the direction of water currents. In locations where tidal flow reverse, Mathers (1976) found a tendency for *P. maximus* to orientate to either of two directions, so that half of the population would face ebb currents while the other half face the flood current. A phenomenon also shared by many taxa is that food intake after a period of starvation is substantially higher during a short period. Hyperphagia has also been reported for migrant and wintering/summering species (Nebel, 2012). After at least three months of low food conditions during winter, a rapid change occurs in spring thanks to increased irradiance and nutrient availability, enhancing microalgae development. The blooming of microalgae in spring provides large food concentrations, allowing the resumption of growth in the great scallop. Variations of food availability can stimulate growth (Gurney and Nisbet, 2004; Morel, 1987), which can be implemented through DEB theory (Kooijman, 2010). Large seasonal changes in the rates and efficiencies of feeding and absorption have been reported for *P. magellanicus* (Cranford and Hill, 1999). These authors showed that the highest ingestion and absorption rates, observed in spring and autumn, might not be explained solely by seasonal food quality and temperature fluctuations. The sea scallop may also display a large capacity for controlling clearance and absorption rates. The same pattern has been highlighted for the blue mussel (Strohmeier et al., 2009). Physiological and behavioural compensations for change in the food environment are thus important elements for a full

understanding of suspension-feeding (Bayne, 1998). These mechanisms might complicate modeling studies but must be kept in mind when interpreting data.

## 7.3 Feeding the scallop, feeding the model

### 7.3.1 The almighty chlorophyll-*a*

In modeling in general, model inputs are subject to sources of uncertainty, including errors of measurement, absence or lack of information and poor or partial understanding of the driving forces and mechanisms. In the first part of this thesis (Chapter 2), both the second and third points were addressed by dividing the model input into two sources and proposing a mechanistic and simple approach for selection. Indeed, several studies had previously revealed the need for more accurate and developed food proxies (Rosland et al., 2009; Bernard et al., 2011; Alunno-Bruscia et al., 2011; Handå et al., 2011; Saraiva et al., 2011a). The use of chlorophyll-*a* concentrations as food proxy is not always erroneous and may lead to accurate predictions during spring. However, important deviations from observations would occur especially at the end of the simulations, probably due to the high seasonality of this proxy, present in very low amount during several months (Chauvaud et al., 2000; Erga et al., 2012; Chatterjee et al., 2013). The potential lack of information in the use of chlorophyll-*a* comes from four observations: (1) chlorophyll-*a* concentration in phytoplankton can dramatically vary depending on the physiological state of the microalgae (Llewellyn et al., 2005). This is especially true in deep water where food quality is usually poor, due to the origin of microalgae cells, sinking from the upper euphotic layers (McCave, 1975; Billett et al., 1983), which are degraded (and chlorophyll-*a* as well) during their sedimentation. (2) *P. maximus* also feeds on food sources that do not contain chlorophyll-*a* (e.g. bacteria, POM). (3) chlorophyll-*a*, while being a good biomass indicator, is not a good qualitative proxy for food availability and do not allow for the discrimination of different algae groups. Indeed, as it is present in every micro- and macro-algae, it can trace non ingested particles for the great scallop, such as green algae (Chapter 4). In Chapter 6, the reconstructed functional response was found to follow many but not all of chlorophyll-*a* peaks monitored in the pelagic domain in the Bay of Brest. Furthermore, some microalgae species, such as *Gymnodinium cf. nagasakiense*, might cause valve closure and filtration stops in the great scallop (Lorrain et al., 2000; Chauvaud et al., 2001). (4) Even edible phytoplankton species can be considered as harmful in certain conditions, thus turning chlorophyll-*a* into a bad food proxy. Indeed, Lorrain et al. (2000) and Chauvaud et al. (2001) suggested that hyper-productive blooms of *Cerataulina pelagica* and *Rhizosolenia delicatula* caused growth anomalies resulting in a decrease or a cessation of filtering activity for few days. Above a threshold of 0.4 µg Chl-*a* $L^{-1}$, Strohmeier et al. (2009) documented a decline of clearance rate in low seston acclimated scallops.

### 7.3.2 Other food proxies

Bourlès et al. (2009) and Handå et al. (2011) investigated the potential of using other food proxies in the prediction of mussel and oyster growth. Their results indicated that chlorophyll-*a* concentration may not always represent the absolute food availability for mussels, which suggests that other organic matter, such as total suspended/particulate matter, particulate organic matter (POM) and carbon (POC), may also be an important part of the diet (Handå et al., 2011). Bourlès et al. (2009) found that the use of POM, POC and/or cell enumeration as food proxies produced the most reliable simulations compared to observed data for the pacific oyster *C. gigas*. Since microalgae are selected by bivalves prior to ingestion (Kiørboe and Møhlenberg, 1981; Ward et al., 1997, 1998; Beninger et al., 2004), the relevance of other seston variables than chlorophyll-*a* is likely to increase along with decreasing phytoplankton densities. This is also suggested by results from Chapter 2, indicating the need for a second food source marker. In Chapter 4 we also pointed out the possible ingestion of bacteria during the winter period, which is not taken into account by the single use of a chlorophyll-*a* proxy.

In Chapter 6, different food proxies were compared to the reconstructed functional response from growth trajectories of juvenile scallops in the Bay of Brest. They were: chlorophyll-*a* measured in the water column and at the water-sediment interface, phytoplankton counts in the same two compartments plus in the microphytobenthos (collected from scratched artificial substrates), particulate organic matter and carbon measured in the water column and particulate suspended matter. Despite the remarks made previously on chlorophyll-*a*, the best relationship between the reconstructed $f$ and available food proxies was found for chlorophyll-*a* in the water column. However, no significant correlation could be obtained, suggesting that a single food proxy might not be sufficient to explain variations in functional response, which is in accordance with previous studies on *P. maximus*' diet (Lorrain et al., 2002). Moreover, as chlorophyll-*a* would covary with some studied descriptors (phytoplankton cells, POM to a lesser extend), the other proxies might be of importance for a certain period of time, thus expressing the high seasonality of food sources in this environment. Furthermore, as already deducted from the field monitoring (Chapter 4), phytoplankton biomass from the water column was found to be more related to *P. maximus*' ingestion and assimilation, confirming the observations made from modeling results.

### 7.3.3 Towards a multi-proxy approach

Solid observations of selection of dietary items have been made in bivalves (Ward et al., 1997, 1998; Ward and Shumway, 2004; Beninger et al., 2004, 2007; Espinosa et al., 2010). Few bioenergetic models have considered different particle types, present in the surroundings of bivalves, as potential food sources (Grant and Bacher, 1998; Scholten and Smaal, 1998; Saraiva et al., 2011a;

Hawkins et al., 2013). The preference hypothesis implemented in the DEB model of *P. maximus* (Chapter 2) allows the integration of several food quantifiers in order to model more accurately bivalve feeding, especially in variable environments presenting a strong seasonality of food availability. Variation in growth performance and survival of scallops (adults and larvae) has been investigated under different microalgal diets (Delaunay et al., 1993; Utting and Millican, 1998; Navarro et al., 2000; Caers et al., 2003) but these studies targeted just a few microalgae species. In addition, controlled experiments on bivalves fed with monocultures or mixed diets tend to display different feeding behavior to those given natural food (Strohmeier, 2009; Cranford et al., 2011). On the other hand, relating in situ growth performance to food quantity and quality is not always easy (Chauvaud et al., 1998, 2001; Lorrain et al., 2000; Patry, 2009; Strohmeier et al., 2009; Handå et al., 2011; this study, Chapter 6). Both approaches are necessary: there is a need for experimental studies to fully validate the hypotheses invoked in the light of the results gathered in this study, concerning the importance of food sources other than diatoms in the diet of the great scallop (Dinophyceae, cyanobacteria, other bacteria). One could investigate whether there is a differential selectivity in favor or against these groups when in presence of various concentrations of diatoms. Natural food supplies might be considered as well in lab experiments, which quantity and quality can still be controlled (Strohmeier, 2009; Strohmeier et al., 2009).

## 7.4 Effect of variable environments on life history

### 7.4.1 Inter-individual variability

Although genetic divergence in body size among populations is not uncommon, phenotypic plasticity is likely to be a major contributor to geographic clines in body size because lab studies have shown that a reduction in environmental temperature causes an increase in adult size in the majority of ectotherms (Angilletta et al., 2004). The great scallop has shown an important inter-individual variability in almost every ecological trait that have been studied: growth rate variability from one individual to another can be significant even when both live in close proximity (Patry, 2009), which might be due to biotic interaction with competitors for food or space and with predators. The variation of growth patterns within the distribution range of *P. maximus* has been thoroughly described (Buestel et al., 1987; Patry, 2009; Chauvaud et al., 2012) and show that plasticity in growth rate and body size in response to environmental heterogeneity is clearly present in scallops. Many authors also demonstrated considerable variability in the timing and synchronization of spawning over both small and large spatial scales (Mason, 1958; Lubet et al., 1987; Paulet et al., 1988; Strand and Nylund, 1991; Cochard and Devauchelle, 1993; Mackie and Ansell, 1993). Plasticity in physiological traits

has been reported concerning reproduction and growth patterns between European coastal populations of *P. maximus* (Antoine et al., 1979; Beaumont et al., 1993; Cochard and Devauchelle, 1993; Mackie and Ansell, 1993; Magnesen and Christophersen, 2008). However, these studies showed that the existence of separated stocks is still under debate. The difficulties encountered in reconstructing the functional response of great scallops originating from various locations of its distribution range may be attributed to such plasticity.

### 7.4.2 Reproduction

In Chapter 2 the implementation of reproduction through a DEB model has been achieved. It includes three environmental parameters: temperature, food concentration and photoperiod, and one internal parameter, the filling state of the gonad (here expressed as a gonado-somatic weight index). This combination of triggering factors includes the most recognized parameters from the literature and the model fairly well fitted real measurements over the six years of the study. Additionally, in Chapter 3 a simulation of the reproductive activity of the great scallop in the English Channel was performed. Results showed that the number of eggs spawned was highly determined by depth. It is still unclear how deep-sea population can maintain themselves, especially for newly born larvae, but some hypotheses can be made. Indeed, Nerot (2011) reported extremely atrophied gonad from deep-sea scallops collected off Brittany coasts (western France), which probably would not allow for these individuals to sustain a deep-sea stock. Moreover, in coastal environments, the success of larval development and survival are drastically constrained by environmental factors such as temperature, food availability, current transport, predation, etc. (Paulet et al., 1988; Paulet and Fifas, 1989; Beaumont and Barnes, 1992; Cragg, 2006). Temperature and currents might not be the most important parameters in deep environment as they display a relative stability. However, food conditions (very low and fluctuating) would probably not permit the development of young scallops, in which survival is already rather low in coastal waters which display higher temperature and food supplies. One possible explanation for the presence of great scallop as far as to the edge of the continental shelf might be the transport of larvae from inshore to offshore areas. Le Boyer et al. (2013) described the seasonality of currents in the northern Bay of Biscay. They showed that during spring and summer, northwest winds tend to create surface currents towards the southwest (due to the Coriolis force). So there is a possibility for coastal waters to drift offshore. This is also observed when looking at the riverine discharges during summer which are dispersed seaward. Therefore, as young *P. maximus* larvae are known to accumulate at the surface during the first part of their development, they might be transported by these upper layer currents over the continental shelf. Moreover, Nicolle et al. (2013) modeled larval dispersal in two basins of the English Channel and suggested that according to a planktonic life duration of 36 days, *P. maximus* larvae could be transported over more than 200 km,

which is about the distance from the Atlantic coast of France and Ireland to the continental slope. They also stressed that swimming behaviour of older larvae had little influence on their dispersal in these areas under strong currents influence. Nevertheless, one question remains: how do larvae cross the thermocline present in summer? This frontier between two water masses of contrasting physico-chemical conditions might indeed stop the sinking of larvae down to the sea bottom. The use of the numerical model developed by Nicolle et al. (2013), which relies on hydrodynamical implementations, might help our understanding of the dispersion of *P. maximus* larvae up to the western Europe continental slope.

### 7.4.3 Origin of spatialized growth variations: Physiological plasticity?

Ultimate sizes are frequently found to decrease with increasing temperature (Bergmann, 1847) and were long explained as an effect of temperature. Large body size goes with small surface area/volume ratios, which makes endotherms more efficient per unit body volume. However, this tendency of increasing size when going northward is also observed in ectotherms such as *P. maximus*. Some authors invoked the simple consequence of developmental processes that cause cells to grow larger in lower temperatures (Van Voorhies, 1996), but this is rarely supported (Angilletta et al., 2004). Kooijman (2010) proposed the following reason: the feeding rate increases with temperature, so, at higher temperatures, food supplies are likely to become limited, which reduces ultimate size. In *P. maximus* however, while temperature actually increases clearance rate (Laing, 2004), the relative homogeneity of aquatic environments compared to terrestrial ones and the high food concentrations observed in the southern part of its distribution range are not likely to result in a limitation of food. Moreover, Chauvaud et al. (2012) did not find a clear relationship between food quantity along the geographical gradient and size and growth patterns of the great scallop. In Chapter 6, the variability of trophic conditions was, however, related to functional response variations. This points to the same conclusions as Muller and Nisbet (2000), suggesting that organisms become bigger with increasing latitude due to increasing seasonal variability in food. Climatic and physical conditions such as irradiance, turbidity, together with genetic plasticity may also play an important role in the explanation of these patterns.

Muller and Nisbet (2000) studied the dynamic behavior of a simple DEB model in fluctuating environments. They showed that scaled energy density (i.e. the ratio between the reserve density $[E]$ and its maximum value $[E_m]$) not only increases with the highest food density, but also depends on the frequency of food density oscillations. Thus, organisms (which would have survived to this alternation of high and low food densities) might grow bigger if food fluctuations are more intense. In continental seas low food levels occur throughout the year, punctuated by seasonal inputs of degraded organic matter

from upper water layers (McCave, 1975; Oliver, 1979; Allen, 1983; Billett et al., 1983). Little is known about the periodicity and magnitude of sedimenting organic matter that may be ingested by benthic animals. Nevertheless, due to the remoteness of these habitats, hydrodynamism, stratification, grazing on phytoplankton, microbial remineralization and climate oscillations, one can assume a rather strong seasonality in food supplies and a high variability in the quality of the sedimenting organic matter. Therefore, the small size of deep-sea individuals might be explained by the combined low, irregular and magnitude limited food densities encountered at these depths compared to coastal environments.

The approach developed in Chapter 5 allows for the reconstruction of various physiological variables and energy fluxes. It permitted a comparison of *P. maximus* energetics from different locations within its distribution range in Chapter 6. The very low values of the reconstructed maintenance rate coefficient $\dot{p}_M$ in Traena and at the continental shelf have long been suggested to explain the low growth rates observed in these ecosystems (Palmer, 1994; Parsons, 1997) and might result from environmental conditions. The reconstructed reserve amount $E$ (in J) was more important in scallops from the location of Brest (west France) than in some from Traena (middle of Norway). Interestingly, the amount of reserves in three-year-old scallops living in the Celtic Sea tended to get closer to the quantity observed in scallops from the inshore location of Brest. The lower reserve density $[E]$ (reserve to structure ratio) observed in the Bay of Brest compared to the location of Traena and the Celtic Sea (98 m) might reflect the relative small size of northern and offshore individuals compared to southern ones in a given cohort. Indeed, as these two populations present lower growth rates during the first years of growth, young scallops are smaller than the fast growing ones from the southern location (Patry, 2009). In fact, DEB theory shows that the smaller the individual, the faster reserve density follows fluctuations in food density. Reproduction buffer dynamics might not help explain this discrepancy as atrophied gonad have been observed in deep-sea animals (Nerot, 2011). There might be also a dilution effect of growth as more structure (in the scallops from Brest) reduces the reserve to structure ratio ($E/V$). Moreover, the high variability detected in higher latitudes and at greater depths might emphasize the high variability of food inputs in these areas (McCave, 1975; Erga and Heimdal, 1984).

A potential explanation for the functional response variability among contrasting environments is the dimensions of the feeding organs. Flexibility in the size of gills and palps to natural turbidity has been demonstrated for suspension-feeding bivalves (Theisen, 1982; Jones et al., 1992; Payne et al., 1995a,b; Dutertre et al., 2007). These previous researches on several species of oysters and mussels indicated smaller gills and larger palps at turbid sites, with thereby reduced feeding rates. Dutertre et al. (2007) showed that oysters with small gills displayed an increased selection efficiency and that clearance rate was positively related to palp area. On the other hand, large gills processed the particles without an effect of palps but with a decrease in clearance rate.

Therefore, the functional responses associated with pallial organ variations showed that the pre-ingestive particle processing in oysters is an integrated mechanism dependent on the gill and labial palp areas. To what extent this would apply to the great scallop has not been observed yet, but would be worth investigating.

While the sedimentation of some phytoplankton cells has been suspected to be harmful in coastal environments as suggested by the stop in growth and filtration during sinking bloom events (Chauvaud et al., 1998, 2001; Lorrain et al., 2000), it is recognized as an essential food input for deep-sea populations of suspension-feeders (McCave, 1975; Oliver, 1979; Allen, 1983; Billett et al., 1983). According to Knudsen (1970) and Gage and Tyler (1992), bivalves become less abundant with increasing depth as the amount and quality of suspended particulate matter decreases. Nevertheless, Oliver (1979) identified two strategies of deep-sea filter-feeding bivalves to cope with these harsh conditions: (1) increased efficiency of food capture and (2) reduction of the amount of food required. Allen (1983) noticed an increased size of labial palps with depth which might sustain the first hypothesis. The deep-sea Limidae *Acesta excavata* also has been reported to have the second largest bivalve gill area (Järnegren and Altin, 2006), which may allow it to be more efficient in particle retention. It is very unlikely that such an "adaptation" would occur in the case of *P. maximus*, for the reasons related to the connectivity of coastal and deep-sea stocks detailed earlier. Nevertheless, as mentioned above, plasticity phenomenon could affect labial palps and gills dimensions, which might explain the observations of relatively high clearance rate in low seston concentration (Strohmeier et al., 2009). There is no published evidence for such plasticity in the size of *P. maximus* feeding organs, but measurements of gill area through photography analysis have been carried out on scallops collected in 2008 during two scientific cruises on the continental shelf (sampling depth: up to 200 m). Results do not support this assumption as no significant difference in surface area was observed (C. Nerot, unpublished data).

One argument in favor of the second proposition lies in the observation of the small size of deep-sea individuals. Given the relatively low knowledge about the trophic conditions on the continental shelf, modeling might help understand what happens in terms of energy fluxes in deep-sea scallops. A theoretical case can be investigated using a simplified form of the DEB model described in Chapter 2, i.e. set $f$ as a forcing variable and thus skipping the implementation of ingestion, in order to test hypothetical environmental conditions. Fig. 7.1 shows a set of simulations of various energy fluxes for theoretical coastal and deep-sea individuals. Environmental conditions in coastal locations are highly influenced by seasons (temperature, food availability and photoperiod), whereas at 150 m there is no more light and temperatures are almost constant. Determining the trajectory of $f$ is speculative for the deep-sea area, but given that the major source of organic matter seems to be sedimenting phytoplankton, one can assume the following patterns of functional response: a sinusoidal signal during the productive seasons (spring and sum-

mer), varying between 0 and 1, while remaining at 0 the rest of the time, resulting in an average value of 0.25 over the year in the deep site; a sinusoidal trajectory varying between 0.2 and 0.8 throughout the year, with a mean value of 0.5 in the coastal site. The simulations cover the second year of growth, when growth rates are high and sexual maturity is reached (Initial length: 5.6 cm; initial dry weight: 2.3 g; initial reserves: $1.8 \times 10^4$ J). Somatic maintenance costs are very much lower for deep-sea individuals than for coastal ones (Fig. 7.1f), which might sustain the second hypothesis of Oliver (1979). This might be a consequence of low temperatures, which maintain a relatively low metabolism, and to the lower reserve amounts in the deep-sea individual (Fig. 7.1e), leading to a limited mobilization of energy. If temperature would vary, at this depth, it might lead to even more depleted reserves which would hardly sustain maintenance costs (results not shown).

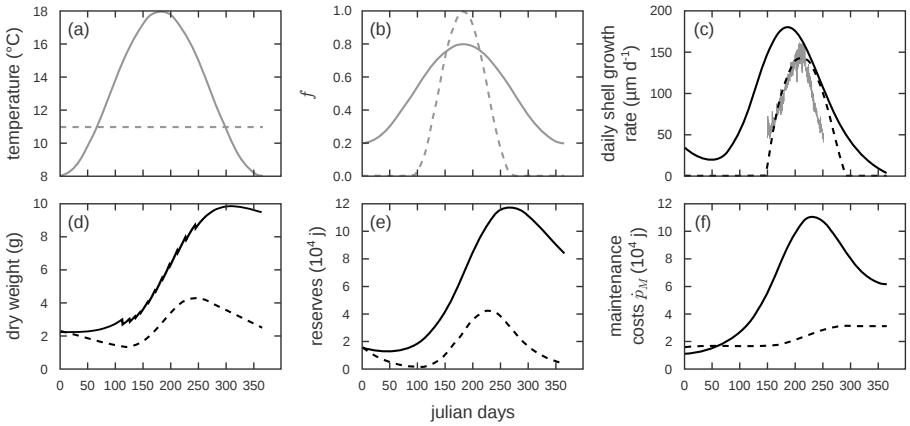


**Figure 7.1:** Simulations of energy fluxes in theoretical coastal (strait line) and deep-sea (dashed line) individuals of *P. maximus* using a DEB model with $f$ arbitrarily determined. (a) temperature; (b) functional response; (c) daily shell growth rate (in gray: observations from Patry, 2009); (d) dry weight; (e) reserve amount; (f) somatic maintenance costs.

Therefore, great scallops living on the continental shelf might be smaller because of both low food conditions and low temperatures. Posgay and Merrill (1979) and Schick et al. (1988) showed a decrease in mean size at age with depth in *Placopecten magellanicus*. They both suggested that environmental conditions of temperature and food quality and quantity were likely to explain these patterns. As minimum food level to cover maintenance costs increases with (structural) body length, smaller individuals are likely to be favored in low food conditions and mild temperatures. A selection phenomenon might occur here (Cowen and Sponaugle, 2009): the only individuals that survive may have slightly different physiological (genetic) characteristics allowing them to

recruit in deep-sea population. Fast growing individuals might not be provided enough energy to sustain their increasing maintenance requirements.

### 7.4.4 Bioenergetic cycle

Several studies have described the seasonality in biochemical composition of the different organs of *P. maximus* in coastal environments (López-Benito, 1956; Comely, 1974; Lucas, 1993; Pazos et al., 1997; Saout, 2000; Strohmeier et al., 2000). The knowledge gathered since the first work of López-Benito (1956) led to the definition of a seasonal cycle in energy allocation between three organs of the great scallop (muscle, digestive gland and gonad) that are implied in energetic metabolism functions (Paulet et al., 1988; Saout et al., 1999; Saout, 2000; Strohmeier et al., 2000; Lorrain et al., 2002; Paulet et al., 2006). According to these studies, a year of life of *P. maximus* could be divided into either two or three parts (Fig. 7.2): (1) a metabolic "translocation" from somatic to reproductive tissues during winter (mid-October until mid-March); (2) a transitory period (not present in Strohmeier et al., 2000) of simultaneous production of somatic and reproductive tissues sustained mainly by food at spring (from April to May); (3) the building of reserves from food until autumn (from June to mid-October).

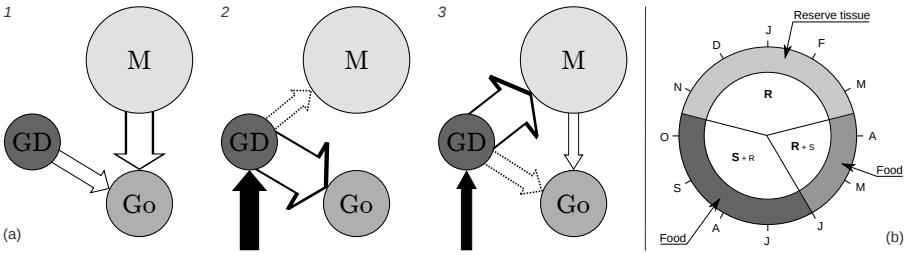


**Figure 7.2:** Hypothetical models of seasonal energy allocation for *P. maximus*: (a) from Lorrain et al. (2002), (b) from Paulet et al. (2006). M: muscle; GD: digestive gland; Go: gonad. R: gonadic growth; S: somatic growth.

This allocation theory does not fit completely with the DEB concept of reserves. DEB theory partitions biomass into structure and reserves compartments that differ in their dynamics. Only structure needs maintenance, while reserve is synthesized from substrates taken from the environment and used for metabolic purposes (Kooijman, 2010). This contrasts with the previous empirical vision of the above cited authors who invoked an energy input for somatic growth and reproduction coming directly from food in spring and summer and from reserves in late autumn and winter. According to DEB theory, all the assimilated energy passes through the reserve compartment. Nevertheless, reserve compounds are usually stored scattered throughout the body and are measured as an integral part of the structural body mass. In Pectinidae,

proteins are stored in unspecialized cells of the adductor muscle (Barber and Blake, 1981). Muscle cells themselves are part of the structural mass, but the lipid and carbohydrate content of their vesicles are part of the reserves. Moreover, atretic recycling is a well known phenomenon that provides energy and metabolites to the formation of novel gametic cells from the recovery of lytic material (resulting from senescent gamete atresia) (Le Pennec et al., 1991; Beninger et al., 2003). Under extreme starvation conditions, individuals can use the reproduction buffer to cover maintenance costs and avoid shrinking (Pecquerie, 2007; Kooijman, 2010; Bernard et al., 2011; this study, Chapter 2). This can produce complex seasonal patterns in the reserve density. The distinction made between reserve storage and gonadal tissue also differs from the concepts of DEB theory, which considers a reproduction buffer, i.e. a pool of reserves dedicated to the production of gametes in the adult stage, and to development in juveniles. Thus, part of the energy stored in the digestive gland and the muscle that will be mobilized to fuel reproduction might be considered as part of the reproduction buffer. An important point is also that gonad weight or condition index can, thus, only be implemented through the reproduction buffer, which might lead to inconsistencies between predictions and observations.

It remains unclear how the great scallop copes with winter environmental conditions. In adults, shell growth is stopped or strongly reduced during this period, while gametogenesis has been reported to be initiated at this time (Devauchelle and Mingant, 1991; Strand and Nylund, 1991; Paulet et al., 1995; Strohmeier et al., 2000; Lorrain et al., 2002; Paulet et al., 2006). According to DEB theory the growth slowdown suggests that not enough energy is mobilized from reserves to sustain both somatic growth and maintenance costs, with priority in allocation being given to maintenance. The DEB model developed in this thesis allows one to look at these maintenance costs. On the basis of the same studied period as in Chapter 2, an average time series of each flux and variable can be achieved (Fig. 7.3). The average maintenance costs for structure vary over this six-year period between 100 and 1100 $\mathrm{J\,d^{-1}}$ while those for maturity only range from 1 to 6 $\mathrm{J\,d^{-1}}$ (Fig. 7.3d). As the energy mobilized from reserves is fractioned at a constant proportion between soma and germinal compartments (due to the $\kappa$-rule), the low amount of energy that can flow from reserves during the winter would not limit the energy accumulation in the reproduction buffer (and thus the maturation of gametes) whereas structural growth would be not provided enough energy to sustain both maintenance and biomass increase. During spring, both thermal and food availability conditions improve, leading to an increase of energy input through microalgae blooms. All metabolic functions might thus be accomplished: structural growth, gamete production (from mobilization of energy in the reproduction buffer) and of course maintenance. After the main spawning events in late spring and early summer, reserves levels have been reported to increase (Strohmeier et al., 2000; Lorrain et al., 2002; Paulet et al., 2006). This is also observed in the simulations (Fig. 7.3c). Moreover, with the present dynamic modeling of energy budgets,

it is possible to distinguish the two reserves pools: while reserve compartment $E$ starts to decrease as lower food concentrations occur, the energy allocated to the reproduction buffer $E_R$ continues to rise throughout the end of the year.

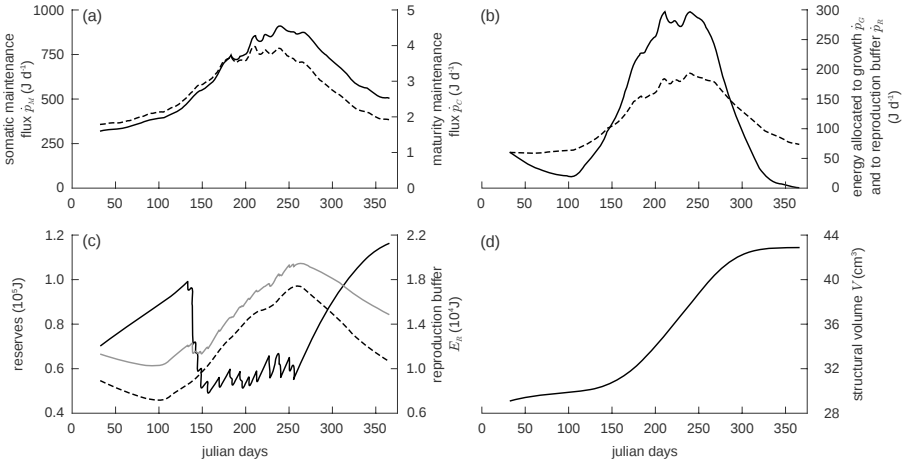


**Figure 7.3:** Average energy fluxes and state variable dynamics over the six years of study in the Bay of Brest (see Chapter 2). (a) somatic (strait line) and maturity (dashed line) maintenance fluxes; (b) energy fluxes allocated to growth (strait line) and to the reproduction buffer (dashed line); (c) reproduction buffer energy content (strait dark line), reserve content (dashed dark line) and sum of energy in the reserve compartment and in the reproduction buffer (strait gray line); (d) structural volume.

Therefore, the change in allocation strategy described by Strand and Nylund (1991), Strohmeier et al. (2000), Lorrain et al. (2002) and Paulet et al. (2006) can be seen, from the point of view of DEB theory, as a consequence of metabolic properties (the DEB parameters) together with environmental seasonality which lead to the following interpretation of reserve dynamics: (1) low energy inputs in winter cause a decrease in allocation to somatic growth due to requirements of somatic maintenance costs and mobilization of reserve toward the reproduction buffer (mid-October until mid-March); (2) resumption of allocation to structural growth with the onset of microalgae spring bloom is accompanied by a continuous allocation to reproduction buffer and its conversion into gametes (from April to May); (3) reaching of a maximum reserve density and rebuilding of the reproduction buffer. This does not formally contradict the previous hypotheses but offers a mechanistic explanation of energy fluxes and body biomass partition.

## 7.5 Concluding remarks and perspectives

This study has shown that modeling of energy fluxes is a powerful tool to explore and interpret the variability of life history traits (Chapter 2, 3, 5 and 6). The complex linkage between the great scallop and the contrasting environments where it lives has been partly revealed. Food availability and quality appear as major sources of variability in the energetic response of the organism (Chapter 2, 3 and 6). Together with temperature, we have showed that a mechanistic description of bioenergetics could explain the differential growth patterns observed along the distribution range of this species (Chapter 6). The emphasis put on food source determination adds to the description of feeding dynamics and provides a valuable high frequency monitoring of food input for filter feeding bivalves (Chapter 4). It allowed us to show that *P. maximus* is highly dependent on pelagic organic inputs to the sea floor and highlighted the rapid and seasonal changes that occur in the selection of food sources. We showed that a multi-proxy approach to describe food availability is more efficient in predicting mass and energy fluctuations (Chapter 2). The study of physiological capacities carried out in Chapters 3 and 6 and the development of a population scale approach will be integrated to further studies on the management of *P. maximus* exploited stocks in the English Channel. Nevertheless, much remains to be explored: the reproduction activity of *P. maximus*, although well described in the literature, still shows some challenges. While many environmental triggers have been described, genetic factors are almost always implied, though they remain undiscovered. DEB models do not explicitly formalize the handling rules for reproduction and the present study still requires improvement. Moreover, a plasticity of filtration functions in relation to the habitat is probably of high importance and confirms previous findings on this topic.

### 7.5.1 Better, faster, stronger...

In order to improve the set of DEB parameters more physiological data should be used in the estimation process. Filtration rate, respiration rate and growth rate measurements have been conducted on juvenile individuals of *Pecten maximus* during a three-month study under controlled conditions. Scallops were conditioned at several temperatures and subjected to a period of starvation during the last month of the experiment. This extensive data set would certainly improve the current parameter estimates, especially in the assessment of the metabolic costs that might be observed throughout the starvation period (Kooijman, 2010, p.297). Another way to simply increase the constraint imposed to the parameter estimation is to provide the estimation procedure with length plus weight over time. Indeed, length data over time provide strong information on the dynamics of structure, whereas weight data is more informative about both structure and reserve. The joint evolution of weights and volume (cubic length) thus constrains the possibilities of parameter values in

the simulation of the hidden variables of structure and reserve. In order to get as much extended time series as possible this kind of data could be acquired more easily in collaboration with scallop hatcheries that are well developed in France and Norway (Norman et al., 2006). Moreover, as shown in Chapter 2, the post-metamorphosis stage of development requires more thorough investigations, most importantly, in the acquisition of more accurate experimental and field data of transition to puberty in terms of weight and physiological functions (such as filtration) that would help in estimating a stronger parameter set.

The modeling system presented in Chapter 3 is a promising step towards the spatialization of physiological processes at wider scales. Further studies on population modeling might benefit from the development of coupled DEB-IBM models, as described by Martin (2013). The simulations carried out with this approach should be less time consuming.

### 7.5.2 Winter is coming

In further development of these investigations, an important step would be achieved in the understanding of *P. maximus* bioenergetics annual cycle by focusing on the winter period. Indeed, when temperature decreases and food availability drops, the great scallop enters what has been called by some authors a dormancy time (Guarini et al., 2011). As in other ectotherms, its metabolic activity is reduced by the lowered temperatures, which may contribute to the reduction of its growth rate, clearly identified on the shell by large rings every year. Phytoplankton biomass is drastically reduced during this period and the great scallop is suspected to rely on its energy reserves accumulated during summer and autumn (Paulet et al., 2006). However, it is also during winter that gametogenesis is activated, which has been interpreted as a means for scallops to be ready to spawn when late spring conditions are favorable for offspring development. In this study some hypotheses have been suggested to explain observed growth reduction and gametogenesis during wintertime (importance of maintenance fluxes of both structure and maturity). In a context of global warming one could ask what effect would warmer winters have on great scallop energetics? Indeed, milder temperatures would keep the energy fluxes at a relatively more elevated state than during cold winters, which may induce a faster reserve depletion. As the state of reserve density at the end of winter is likely to impact the resumption of growth and the termination of gamete maturation before spawning during spring, investigating this question would also bring insights to the energetic cycle model discussed above (Strohmeier et al., 2000; Lorrain et al., 2002; Paulet et al., 2006). This might be accomplished through a controlled experiment starting in December with two thermal conditions (field temperature and a five-degree increased temperature level for instance). The study presented in Strohmeier (2009, paper 2), on the seasonal investigation of clearance rates of *P. maximus* in natural low

seston conditions could be used as a basis for a similar experiment in high seston environments (e.g. western France).

### 7.5.3 Paleo-reconstructions

In addition to the study of actual links between organisms and their environment, DEB theory allows one to look at past biological patterns through the inversion of the model, permitting the reconstruction of ancient energy dynamics from growth trajectories. The use of bivalve shells as biogenic archives of past environmental conditions provides a remarkable source of information for the understanding of paleoclimate and paleoenvironments (Jones, 1983; Grossman and Ku, 1986; Goodwin et al., 2001; Schöne et al., 2011). Very few potential proxies of the trophic availability have been reported from the carbonated skeleton of marine bivalves, which relevance is still being debated: lithium to calcium ratio (Thébault and Chauvaud, 2013) and barium to calcium ratio (Barats et al., 2009; Thébault et al., 2009). The approach developed here provides a new perspective in the reconstruction of past environmental conditions. The possibility of studying the variability of assimilation patterns and its seasonality at a high frequency (daily resolution) and over the long term could help understand present and past ecological mechanisms in the great scallop. Moreover, as oxygen isotope ratios of the shell is a temperature proxy (Owen et al., 2002c; Chauvaud et al., 2005), an extremely attractive perspective would be to use this reconstructed temperature time series extracted from the shell to reconstruct the dynamics of food assimilation and physiological variables.

### 7.5.4 Climate change consequences

In the actual context of increasing uptake of carbon from the atmosphere, physico-chemical conditions of the surrounding environment of the great scallop are likely to undergo critical changes. Two major modifications are of particular interest to the scientific community: the increase of seawater temperatures and ocean acidification (OA) (Caldeira and Wickett, 2003). Indeed, while an increase of temperature may boost primary production (Polovina et al., 2008; Doney et al., 2009) and thus enhance growth and recruitment efficiency (Shephard et al., 2010), scallop populations from northern areas might be impacted by hotter winter conditions, as explained above.

Moreover, a thorough understanding of the mechanisms behind shell production is also advised in order to understand the effect of OA. Lowered pH might, in fact, lead to dissolution of the precipitated $CaCO_3$ (Fabry et al., 2008; Doney et al., 2009; Andersen et al., 2013). Some recent investigations modeling calcification of such structures within DEB theory might help address this question: Pecquerie et al. (2012) provided a very promising implementation of fish otolith calcification processes and Muller and Nisbet (2014) started to explore the impact of OA on coccolithophores, both within the DEB theory

framework. An application to the great scallop is very tempting and should be investigated as this species provides an easily studied growth structure (size, growth and composition patterns) compared to other bivalves.

Furthermore, the frequency of hypoxic events, as well as the extension of hypoxic areas, are also suspected to occur (Stramma et al., 2008; Vaquer-Sunyer and Duarte, 2008). Recent work by Artigaud (2013) explored the physiological response of *P. maximus* to combined temperature rise and oxygen depletion. Results showed a decrease in regulation capacity when temperature increase together with a reduction of aerobic performances (Artigaud et al., subm.). It would be interesting to look at the energetic consequences of such phenomenon through DEB theory, which might also give insights on the respiration capacity, the maintenance costs and the physiological plasticity of individual response to environmental stresses.

### 7.5.5 Linking external and internal forcing

Finally, it is of great importance to develop studies coupling genetic analysis and physiological response together with environmental monitoring in order to disentangle the effect of environmental variables and genetic history on metabolism (corresponding to a phenotype). This would allow the investigation of the potential variability of DEB parameters within the species and might address some difficulties in modeling the bioenergetics of animals living in very contrasting conditions such as the northern waters of Europe and the sea bottom of the continental shelf. This kind of study is necessary if we want to understand the effect of climate change on these different populations.

# Appendix A

# Reconstruction of functional response in all study sites

**Table A.1:** Statistics of the functional response reconstructions for each year of the different age-classes in the ten studied locations. *AC*: Age Class; *YL*: Year of Life; $L_i$: initial length of the shell; *mean*: average reconstructed $f$ over the reconstructed period; *max*: maximum value of $f$; *min*: minimum value of $f$; *range*: amplitude range of $f$; *var*: variance of f; *sd*: standard deviation of $f$; *DG*: Days of growth.

| *n* | *AC* | *YL* | $L_i$ | *mean* | *max* | *min* | *range* | *var* | *sd* | *DG* |
|---|---|---|---|---|---|---|---|---|---|---|
| *Traena* | | | | | | | | | | |
| 9 | 3 | 1 (1999) | 1.8 | 0.77 | 0.99 | 0.02 | 0.97 | 0.06 | 0.24 | 178 |
| 4 | 6 | 1 (1994) | 1.8 | 0.72 | 1.00 | 0.25 | 0.75 | 0.05 | 0.23 | 144 |
| | | 2 (1995) | 3.7 | 0.83 | 1.00 | 0.18 | 0.82 | 0.01 | 0.09 | 152 |
| | | 3 (1996) | 6.0 | 0.71 | 1.00 | 0.00 | 1.00 | 0.04 | 0.21 | 114 |
| | | 4 (1997) | 8.3 | 0.59 | 0.98 | 0.21 | 0.77 | 0.01 | 0.11 | 98 |
| | | 5 (1998) | 9.8 | 0.65 | 0.93 | 0.42 | 0.51 | 0.03 | 0.18 | 94 |
| *Austevoll* | | | | | | | | | | |
| 5 | 3 | 1 (1986) | 1.9 | 0.55 | 0.89 | 0.04 | 0.85 | 0.11 | 0.33 | 132 |
| | | 2 (1987) | 4.5 | 0.83 | 1.00 | 0.46 | 0.54 | 0.03 | 0.16 | 141 |
| | | 3 (1988) | 6.5 | 0.71 | 1.00 | 0.40 | 0.60 | 0.03 | 0.17 | 142 |
| 11 | 4 | 1 (1985) | 1.9 | 0.49 | 1.00 | 0.16 | 0.84 | 0.05 | 0.23 | 212 |
| | | 2 (1986) | 4.5 | 0.76 | 0.96 | 0.33 | 0.63 | 0.02 | 0.14 | 134 |
| | | 3 (1987) | 6.5 | 0.85 | 1.00 | 0.60 | 0.40 | 0.02 | 0.13 | 127 |
| | | 4 (1988) | 8.2 | 0.68 | 1.00 | 0.31 | 0.69 | 0.03 | 0.19 | 127 |
| 23 | 5 | 1 (1984) | 1.9 | 0.45 | 0.70 | 0.18 | 0.52 | 0.03 | 0.16 | 85 |
| | | 2 (1985) | 4.5 | 0.75 | 1.00 | 0.00 | 1.00 | 0.06 | 0.25 | 165 |
| | | 3 (1986) | 6.5 | 0.83 | 1.00 | 0.35 | 0.65 | 0.05 | 0.22 | 140 |
| | | 4 (1987) | 8.2 | 0.95 | 1.00 | 0.83 | 0.17 | 0.00 | 0.05 | 90 |
| | | 5 (1988) | 9.6 | 0.62 | 0.88 | 0.41 | 0.47 | 0.02 | 0.13 | 85 |
| *Holyhead* | | | | | | | | | | |
| 2 | 3 | 1 (2000) | 2.3 | 0.31 | 0.39 | 0.25 | 0.14 | 0.00 | 0.05 | 85 |
| | | 2 (2001) | 4.4 | 0.59 | 0.81 | 0.29 | 0.52 | 0.02 | 0.15 | 136 |
| | | 3 (2002) | 7.1 | 0.72 | 1.00 | 0.50 | 0.50 | 0.03 | 0.16 | 97 |
| 5 | 4 | 1 (1999) | 2.2 | 0.36 | 0.60 | 0.21 | 0.39 | 0.01 | 0.10 | 140 |
| | | 2 (2000) | 4.4 | 0.60 | 0.86 | 0.30 | 0.56 | 0.02 | 0.14 | 146 |
| | | 3 (2001) | 7.0 | 0.59 | 0.85 | 0.35 | 0.50 | 0.03 | 0.17 | 102 |
| | | 4 (2002) | 8.7 | 0.69 | 0.92 | 0.34 | 0.58 | 0.02 | 0.14 | 76 |
| 3 | 5 | 1 (1998) | 2.0 | 0.40 | 0.67 | 0.25 | 0.42 | 0.02 | 0.13 | 130 |
| | | 2 (1999) | 4.3 | 0.62 | 0.77 | 0.16 | 0.61 | 0.02 | 0.14 | 154 |

*Continued on next page*

Table A.1 – *Continued from previous page*

| *n* | *AC* | *YL* | $L_i$ | *mean* | *max* | *min* | *range* | *var* | *sd* | *DG* |
|---|---|---|---|---|---|---|---|---|---|---|
| | | 3 (2000) | 7.0 | 0.67 | 0.98 | 0.36 | 0.62 | 0.03 | 0.16 | 134 |
| | | 4 (2001) | 8.6 | 0.61 | 0.96 | 0.29 | 0.67 | 0.03 | 0.18 | 91 |
| | | 5 (2002) | 9.7 | 0.70 | 0.88 | 0.57 | 0.31 | 0.01 | 0.10 | 73 |
| 3 | 6 | 1 (1997) | 2.3 | 0.38 | 0.57 | 0.25 | 0.32 | 0.01 | 0.08 | 101 |
| | | 2 (1998) | 4.6 | 0.59 | 0.90 | 0.12 | 0.78 | 0.03 | 0.18 | 144 |
| | | 3 (1999) | 7.5 | 0.69 | 0.94 | 0.30 | 0.64 | 0.03 | 0.17 | 118 |
| | | 4 (2000) | 9.4 | 0.69 | 1.00 | 0.46 | 0.54 | 0.04 | 0.20 | 102 |
| | | 5 (2001) | 10.1 | 0.63 | 0.89 | 0.37 | 0.52 | 0.03 | 0.16 | 64 |
| | | 6 (2002) | 10.7 | 0.64 | 0.74 | 0.51 | 0.23 | 0.01 | 0.07 | 52 |
| *Plymouth* | | | | | | | | | | |
| 8 | 2 | 2 (2005) | 6.5 | 0.74 | 1.00 | 0.16 | 0.84 | 0.02 | 0.15 | 234 |
| 7 | 3 | 2 (2004) | 6.5 | 0.78 | 0.98 | 0.05 | 0.93 | 0.04 | 0.19 | 236 |
| | | 3 (2005) | 8.6 | 0.71 | 0.93 | 0.30 | 0.63 | 0.02 | 0.12 | 193 |
| 8 | 4 | 2 (2003) | 6.5 | 0.73 | 1.00 | 0.19 | 0.81 | 0.03 | 0.18 | 263 |
| | | 3 (2004) | 8.6 | 0.75 | 1.00 | 0.46 | 0.54 | 0.02 | 0.15 | 176 |
| | | 4 (2005) | 9.6 | 0.59 | 0.71 | 0.40 | 0.31 | 0.00 | 0.06 | 132 |
| 2 | 5 | 2 (2002) | 6.5 | 0.73 | 1.00 | 0.40 | 0.60 | 0.03 | 0.18 | 198 |
| | | 3 (2003) | 8.6 | 0.64 | 0.94 | 0.37 | 0.57 | 0.02 | 0.13 | 170 |
| | | 4 (2004) | 9.6 | 0.57 | 0.76 | 0.38 | 0.38 | 0.01 | 0.08 | 97 |
| | | 5 (2005) | 10.1 | 0.60 | 0.78 | 0.46 | 0.32 | 0.01 | 0.07 | 118 |
| *Brest* | | | | | | | | | | |
| 55 | 1 | 1 (1998) | 3.6 | 0.54 | 0.97 | 0.07 | 0.90 | 0.03 | 0.18 | 275 |
| 39 | 1 | 1 (1999) | 3.4 | 0.61 | 1.00 | 0.35 | 0.65 | 0.02 | 0.15 | 279 |
| 39 | 1 | 1 (2000) | 3.3 | 0.63 | 0.99 | 0.34 | 0.65 | 0.02 | 0.15 | 249 |
| 27 | 1 | 1 (2001) | 3.0 | 0.59 | 0.91 | 0.13 | 0.78 | 0.02 | 0.15 | 283 |
| 19 | 1 | 1 (2002) | 3.0 | 0.63 | 0.99 | 0.28 | 0.71 | 0.03 | 0.18 | 259 |
| 31 | 1 | 1 (2003) | 2.6 | 0.71 | 1.00 | 0.23 | 0.77 | 0.03 | 0.17 | 262 |
| 32 | 1 | 1 (2011) | 2.8 | 0.60 | 0.86 | 0.41 | 0.45 | 0.01 | 0.10 | 282 |
| 10 | 3 | 3 (1998) | 9.1 | 0.52 | 0.83 | 0.24 | 0.59 | 0.01 | 0.12 | 149 |
| 10 | 3 | 3 (1999) | 9.1 | 0.53 | 0.80 | 0.29 | 0.51 | 0.01 | 0.12 | 144 |
| 10 | 3 | 3 (2000) | 9.4 | 0.54 | 0.86 | 0.38 | 0.48 | 0.02 | 0.13 | 128 |
| 10 | 3 | 3 (2001) | 9.2 | 0.47 | 0.67 | 0.32 | 0.35 | 0.01 | 0.10 | 129 |
| 11 | 3 | 3 (2002) | 8.7 | 0.54 | 0.71 | 0.41 | 0.30 | 0.01 | 0.09 | 83 |
| 10 | 3 | 3 (2003) | 8.8 | 0.50 | 0.70 | 0.38 | 0.32 | 0.01 | 0.08 | 123 |
| *Quiberon* | | | | | | | | | | |
| 20 | 1 | 1 (2001) | 2.4 | 0.59 | 0.98 | 0.18 | 0.80 | 0.07 | 0.26 | 258 |
| 35 | 2 | 1 (2000) | 2.2 | 0.53 | 0.84 | 0.20 | 0.64 | 0.02 | 0.15 | 272 |
| | | 2 (2001) | 6.1 | 0.46 | 0.65 | 0.27 | 0.38 | 0.01 | 0.07 | 209 |
| *Celtic Sea* 98 m | | | | | | | | | | |
| 3 | 4 | 1 (1995) | 2.0 | 0.60 | 1.00 | 0.13 | 0.87 | 0.07 | 0.26 | 187 |
| | | 2 (1996) | 4.5 | 0.61 | 0.92 | 0.12 | 0.80 | 0.04 | 0.21 | 142 |
| | | 3 (1997) | 6.4 | 0.66 | 0.95 | 0.23 | 0.72 | 0.05 | 0.23 | 136 |
| 2 | 5 | 1 (1994) | 2.0 | 0.61 | 0.85 | 0.26 | 0.59 | 0.04 | 0.19 | 155 |
| | | 2 (1995) | 4.5 | 0.71 | 0.97 | 0.23 | 0.74 | 0.06 | 0.25 | 155 |
| | | 3 (1996) | 6.4 | 0.78 | 1.00 | 0.36 | 0.64 | 0.04 | 0.21 | 152 |
| | | 4 (1997) | 7.8 | 0.65 | 1.00 | 0.32 | 0.68 | 0.04 | 0.20 | 157 |
| 6 | 6 | 1 (1993) | 2.0 | 0.58 | 1.00 | 0.13 | 0.87 | 0.02 | 0.13 | 175 |
| | | 2 (1994) | 4.5 | 0.68 | 1.00 | 0.19 | 0.81 | 0.07 | 0.27 | 160 |
| | | 3 (1995) | 6.4 | 0.61 | 1.00 | 0.18 | 0.82 | 0.07 | 0.27 | 133 |
| | | 4 (1996) | 7.8 | 0.60 | 0.93 | 0.02 | 0.91 | 0.08 | 0.29 | 99 |
| | | 5 (1997) | 8.9 | 0.61 | 1.00 | 0.18 | 0.82 | 0.08 | 0.29 | 107 |
| *Celtic Sea* 109 m | | | | | | | | | | |
| 2 | 4 | 2 (1996) | 4.0 | 0.68 | 1.00 | 0.26 | 0.74 | 0.03 | 0.18 | 181 |
| | | 3 (1997) | 6.3 | 0.67 | 1.00 | 0.07 | 0.93 | 0.09 | 0.30 | 132 |
| 2 | 5 | 1 (1994) | 2.1 | 0.45 | 0.67 | 0.08 | 0.59 | 0.02 | 0.13 | 113 |
| | | 2 (1995) | 4.0 | 0.70 | 1.00 | 0.05 | 0.95 | 0.07 | 0.26 | 175 |
| | | 3 (1996) | 6.3 | 0.71 | 1.00 | 0.15 | 0.85 | 0.07 | 0.26 | 167 |
| | | 4 (1997) | 8.2 | 0.68 | 0.98 | 0.13 | 0.85 | 0.07 | 0.27 | 92 |
| | | 5 (1998) | 9.2 | 0.62 | 0.91 | 0.33 | 0.58 | 0.03 | 0.16 | 113 |
| *Celtic Sea* 150 m | | | | | | | | | | |
| 3 | 4 | 1 (1995) | 2.5 | 0.56 | 1.00 | 0.04 | 0.96 | 0.10 | 0.31 | 129 |
| | | 2 (1996) | 4.3 | 0.74 | 1.00 | 0.18 | 0.82 | 0.07 | 0.26 | 126 |
| | | 3 (1997) | 6.2 | 0.73 | 1.00 | 0.00 | 1.00 | 0.13 | 0.36 | 128 |
| 3 | 6 | 1 (1993) | 2.5 | 0.62 | 1.00 | 0.00 | 1.00 | 0.11 | 0.32 | 116 |
| | | 2 (1994) | 4.3 | 0.69 | 1.00 | 0.10 | 0.90 | 0.10 | 0.32 | 137 |

*Continued on next page*

Table A.1 – *Continued from previous page*

| *n* | *AC* | *YL* | $L_i$ | *mean* | *max* | *min* | *range* | *var* | *sd* | *DG* |
|---|---|---|---|---|---|---|---|---|---|---|
| | | 3 (1995) | 6.2 | 0.71 | 1.00 | 0.00 | 1.00 | 0.08 | 0.29 | 132 |
| | | 4 (1996) | 7.9 | 0.63 | 1.00 | 0.02 | 0.98 | 0.13 | 0.35 | 123 |
| | | 5 (1997) | 8.8 | 0.65 | 0.99 | 0.00 | 0.99 | 0.05 | 0.22 | 89 |
| 4 | 7 | 1 (1992) | 2.5 | 0.56 | 1.00 | 0.15 | 0.85 | 0.04 | 0.21 | 163 |
| | | 2 (1993) | 4.3 | 0.71 | 1.00 | 0.10 | 0.90 | 0.08 | 0.28 | 145 |
| | | 3 (1994) | 6.2 | 0.70 | 1.00 | 0.00 | 1.00 | 0.11 | 0.34 | 118 |
| | | 4 (1995) | 7.9 | 0.65 | 1.00 | 0.08 | 0.92 | 0.07 | 0.26 | 132 |
| | | 5 (1996) | 8.8 | 0.62 | 1.00 | 0.01 | 0.99 | 0.10 | 0.32 | 87 |
| 2 | 8 | 1 (1991) | 2.5 | 0.50 | 0.87 | 0.05 | 0.82 | 0.06 | 0.24 | 119 |
| | | 2 (1992) | 4.3 | 0.65 | 1.00 | 0.30 | 0.70 | 0.06 | 0.24 | 154 |
| | | 3 (1993) | 6.2 | 0.79 | 1.00 | 0.01 | 0.99 | 0.06 | 0.25 | 112 |
| | | 4 (1994) | 7.9 | 0.64 | 1.00 | 0.05 | 0.95 | 0.10 | 0.32 | 81 |
| *Celtic Sea* 162 m | | | | | | | | | | |
| 3 | 4 | 2 (1996) | 4.2 | 0.60 | 0.98 | 0.07 | 0.91 | 0.06 | 0.24 | 192 |
| | | 3 (1997) | 5.8 | 0.64 | 1.00 | 0.00 | 1.00 | 0.10 | 0.31 | 137 |
| 3 | 5 | 1 (1994) | 2.0 | 0.61 | 0.85 | 0.26 | 0.59 | 0.06 | 0.25 | 144 |
| | | 2 (1995) | 4.2 | 0.68 | 1.00 | 0.16 | 0.84 | 0.10 | 0.32 | 124 |
| | | 3 (1996) | 5.8 | 0.74 | 1.00 | 0.00 | 1.00 | 0.10 | 0.32 | 134 |
| | | 4 (1997) | 7.1 | 0.72 | 0.95 | 0.07 | 0.88 | 0.09 | 0.31 | 96 |
| 2 | 6 | 2 (1994) | 4.2 | 0.69 | 1.00 | 0.05 | 0.95 | 0.07 | 0.27 | 115 |
| | | 3 (1995) | 5.8 | 0.71 | 1.00 | 0.08 | 0.92 | 0.10 | 0.31 | 123 |
| | | 4 (1996) | 7.1 | 0.60 | 0.93 | 0.02 | 0.91 | 0.08 | 0.29 | 99 |

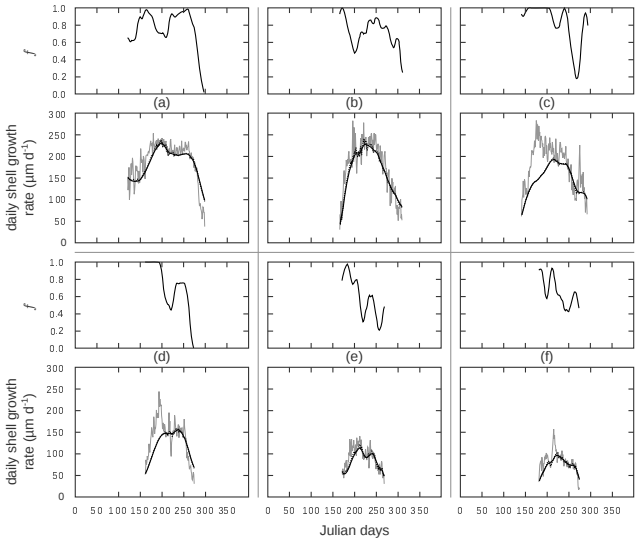


**Figure A.1:** Reconstruction of the functional response obtained from growth trajectories of *P. maximus*, in the location of Traena. Age class one (a) to six (f) were analyzed from animals born in 1998 (a) and 1993 (b–f). In the upper graph are the reconstructed functional response (strait dark line); in the lower one are the growth trajectory (strait gray line), the same growth time series after being smoothed by the "deb-box" (dashed dark line) and the back simulated growth trajectory using the reconstructed $f$ (strait dark line).

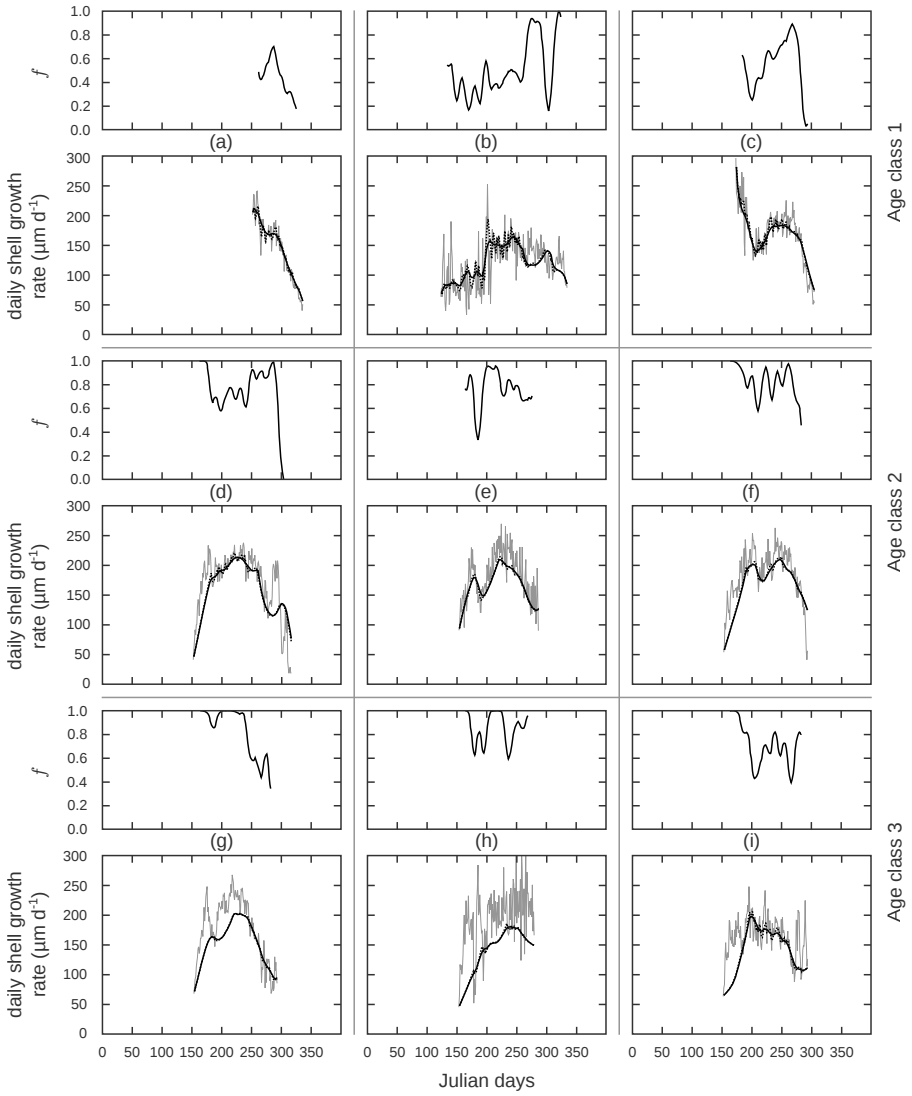


**Figure A.2:** Reconstruction of the functional response obtained from growth trajectories of *P. maximus*, in the location of Austevoll. Age class one (a, b, c), two (d, e, f) and three (g, h, i) were analyzed from animals born in 1983 (left column), 1984 (middle column) and 1985 (right column). In the upper graph are the reconstructed functional response (strait dark line); in the lower one are the growth trajectory (strait gray line), the same growth time series after being smoothed by the "deb-box" (dashed dark line) and the back simulated growth trajectory using the reconstructed $f$ (strait dark line).

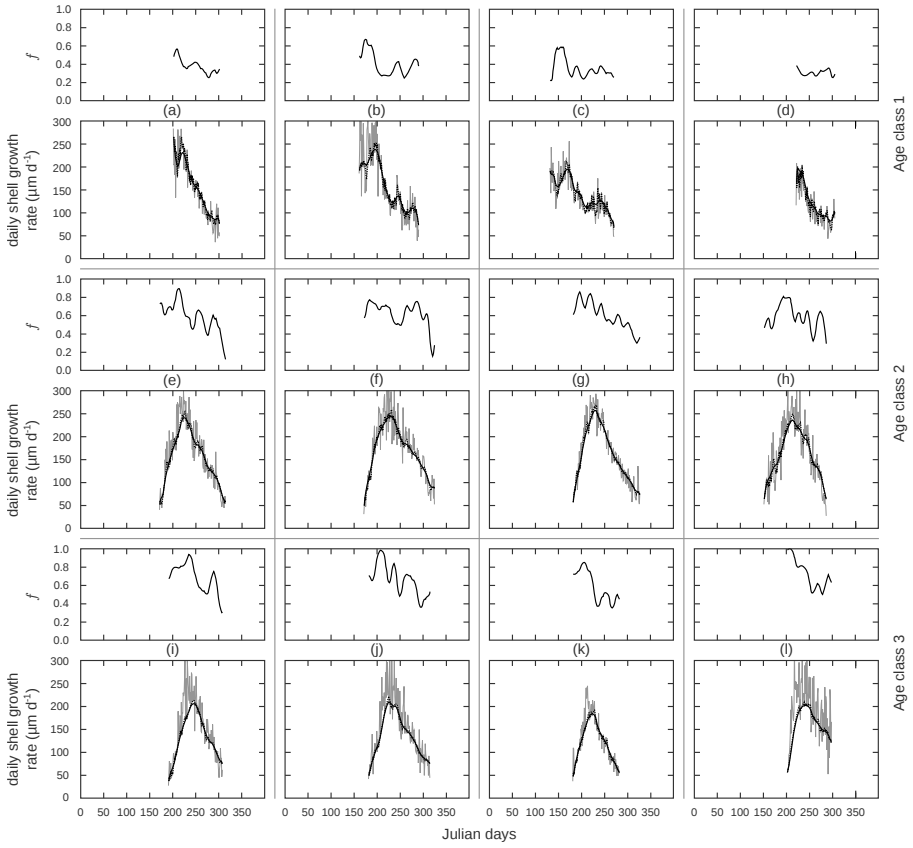


**Figure A.3:** Reconstruction of the functional response obtained from growth trajectories of *P. maximus*, in the location of Holyhead. Age class one (a, b, c, d), two (e, f, g, h) and three (i, j, k, l) were analyzed from animals born in 1999 (first left column), 1998 (second column) 1997 (thrid column) and 1996 (fourth column). In the upper graph are the reconstructed functional response (strait dark line); in the lower one are the growth trajectory (strait gray line), the same growth time series after being smoothed by the "deb-box" (dashed dark line) and the back simulated growth trajectory using the reconstructed $f$ (strait dark line).

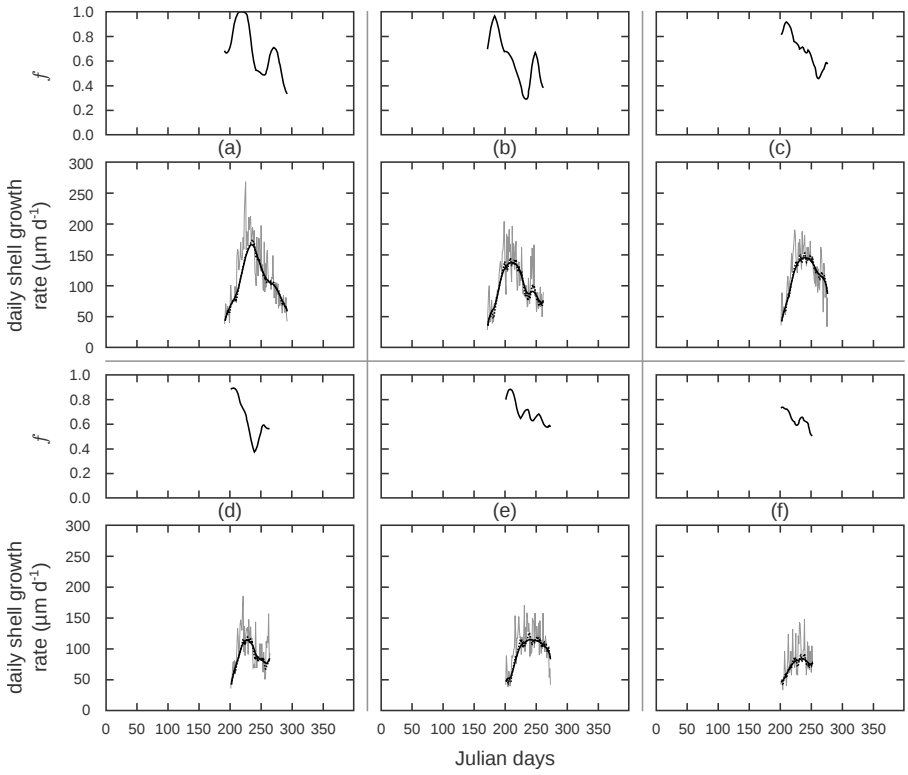


**Figure A.4:** Reconstruction of the functional response obtained from growth trajectories of *P. maximus*, in the location of Holyhead. Age class four (a, b, c), five (d, e) and six (f) were analyzed from animals born in 1996 (a, d), 1997 (b, e, f) and 1998 (c). In the upper graph are the reconstructed functional response (strait dark line); in the lower one are the growth trajectory (strait gray line), the same growth time series after being smoothed by the "deb-box" (dashed dark line) and the back simulated growth trajectory using the reconstructed $f$ (strait dark line).

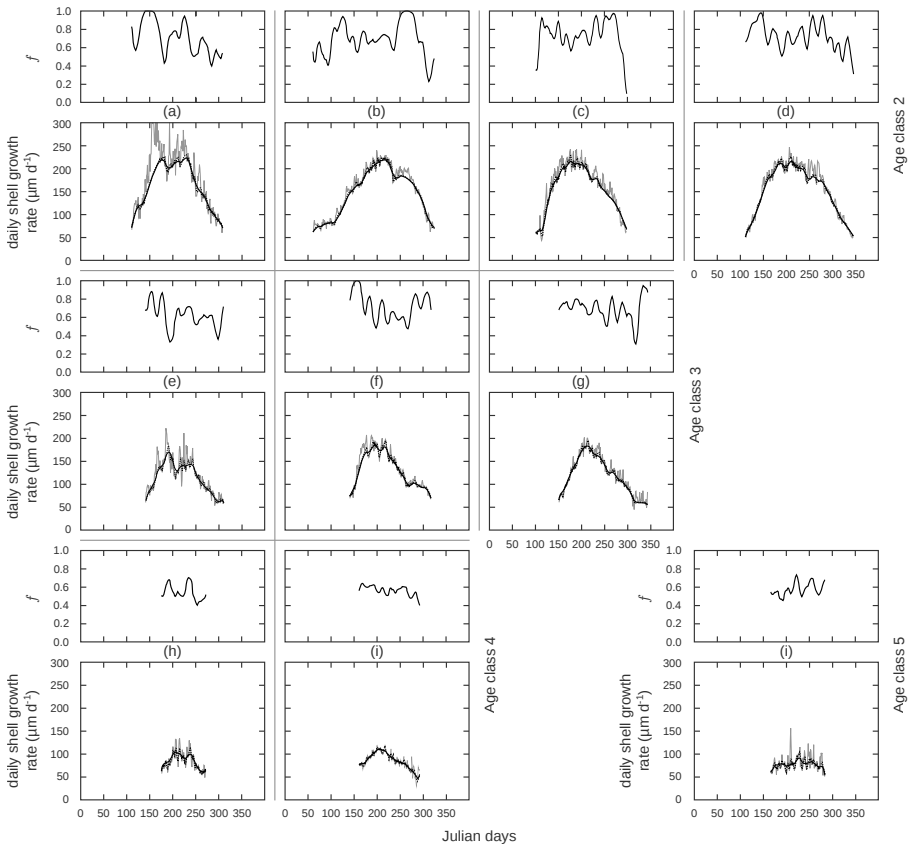


**Figure A.5:** Reconstruction of the functional response obtained from growth trajectories of *P. maximus*, in the location of Plymouth. Age class two (a, b, c, d), three (e, f, g), four (h, i) and five (j) were analyzed from animals born in 2001 (a, e, h, j), 2002 (b, f, i), 2003 (c, g) and 2004 (d). In the upper graph are the reconstructed functional response (strait dark line); in the lower one are the growth trajectory (strait gray line), the same growth time series after being smoothed by the "deb-box" (dashed dark line) and the back simulated growth trajectory using the reconstructed $f$ (strait dark line).

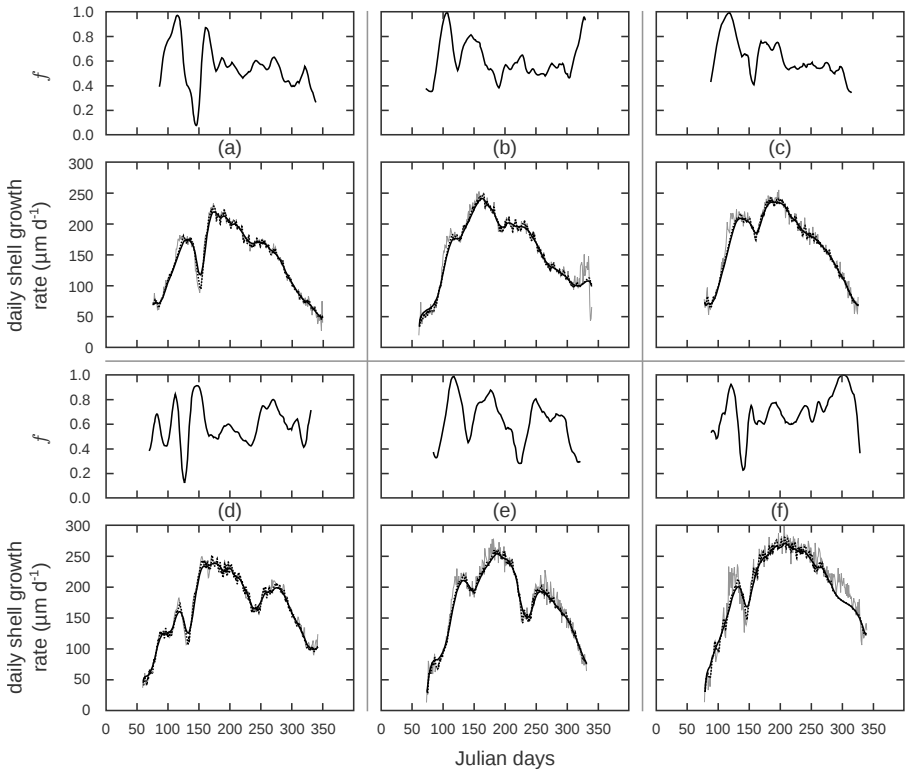


**Figure A.6:** Reconstruction of the functional response obtained from growth trajectories of *P. maximus*, in the location of Brest. Age class one were analyzed from animals born in 1997 (a), 1998 (b) 1999 (c), 2000 (d), 2001 (e) and 2002 (f). In the upper graph are the reconstructed functional response (strait dark line); in the lower one are the growth trajectory (strait gray line), the same growth time series after being smoothed by the "deb-box" (dashed dark line) and the back simulated growth trajectory using the reconstructed $f$ (strait dark line).

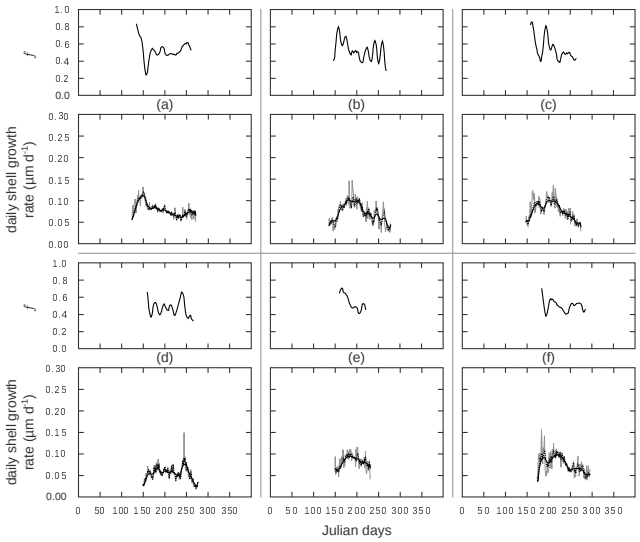


**Figure A.7:** Reconstruction of the functional response obtained from growth trajectories of *P. maximus*, in the location of Brest. Age class three were analyzed from animals born in 1995 (a), 1996 (b) 1997 (c), 1998 (d), 1999 (e) and 2000 (f). In the upper graph are the reconstructed functional response (strait dark line); in the lower one are the growth trajectory (strait gray line), the same growth time series after being smoothed by the "deb-box" (dashed dark line) and the back simulated growth trajectory using the reconstructed $f$ (strait dark line).

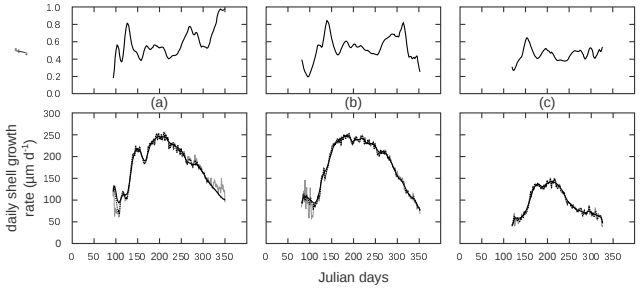


**Figure A.8:** Reconstruction of the functional response obtained from growth trajectories of *P. maximus*, in the location of Quiberon. Age class one (a, b) and two (c) were analyzed from animals born in 2000 (a) and 1999 (b, c). In the upper graph are the reconstructed functional response (strait dark line); in the lower one are the growth trajectory (strait gray line), the same growth time series after being smoothed by the "deb-box" (dashed dark line) and the back simulated growth trajectory using the reconstructed $f$ (strait dark line).

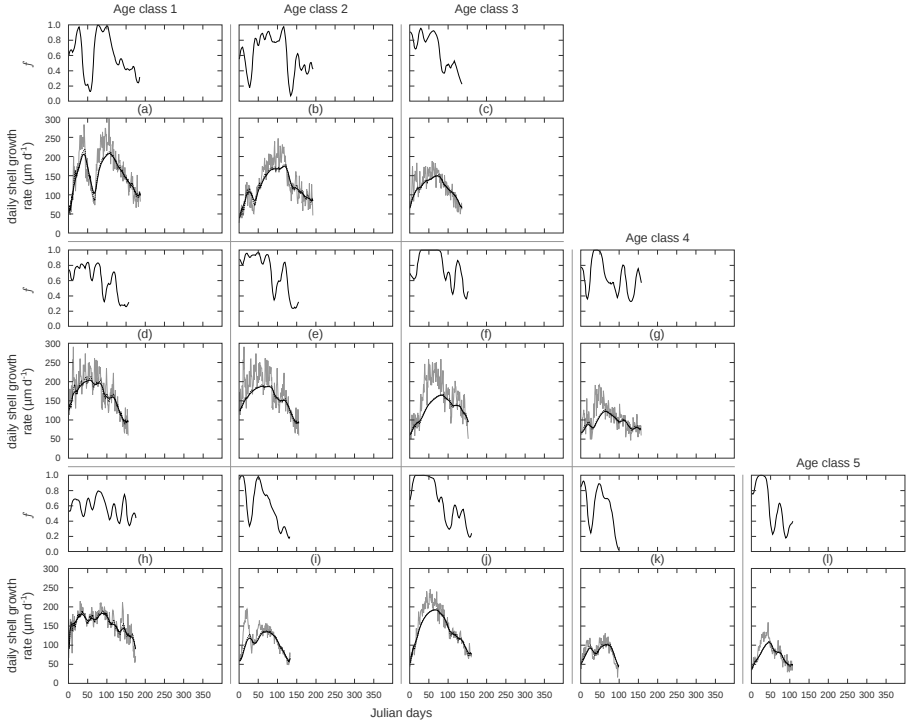


**Figure A.9:** Reconstruction of the functional response obtained from growth trajectories of *P. maximus*, from 98 m deep in Celtic Sea. Age class one (left column) to five (right column) were analyzed from animals born in 1994 (a, b, c), 1993 (d, e, f, g) and 1992 (h, i, j, k, l). In the upper graph are the reconstructed functional response (strait dark line); in the lower one are the growth trajectory (strait gray line), the same growth time series after being smoothed by the "deb-box" (dashed dark line) and the back simulated growth trajectory using the reconstructed $f$ (strait dark line).

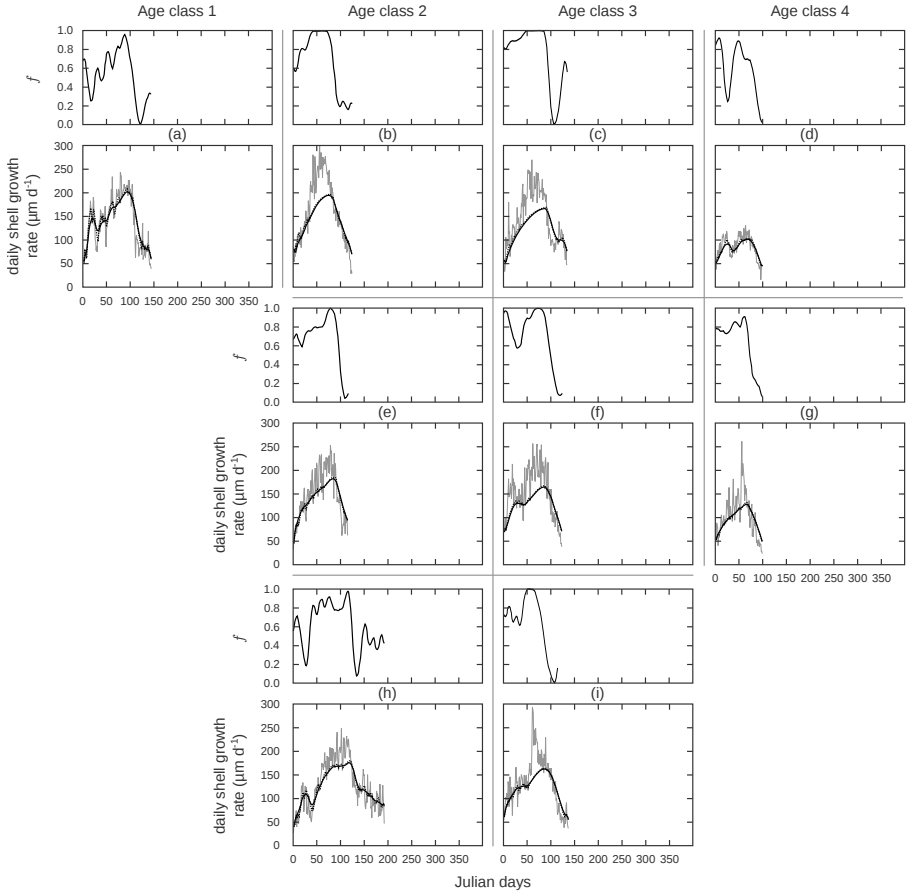


**Figure A.10:** Reconstruction of the functional response obtained from growth trajectories of *P. maximus*, from 162 m deep in Celtic Sea. Age class one (left column) to five (right column) were analyzed from animals born in 1993 (a, b, c, d), 1992 (e, f, g) and 1994 (h, i). In the upper graph are the reconstructed functional response (strait dark line); in the lower one are the growth trajectory (strait gray line), the same growth time series after being smoothed by the "deb-box" (dashed dark line) and the back simulated growth trajectory using the reconstructed $f$ (strait dark line).

# Appendix B

# Simulations using the two parameter sets

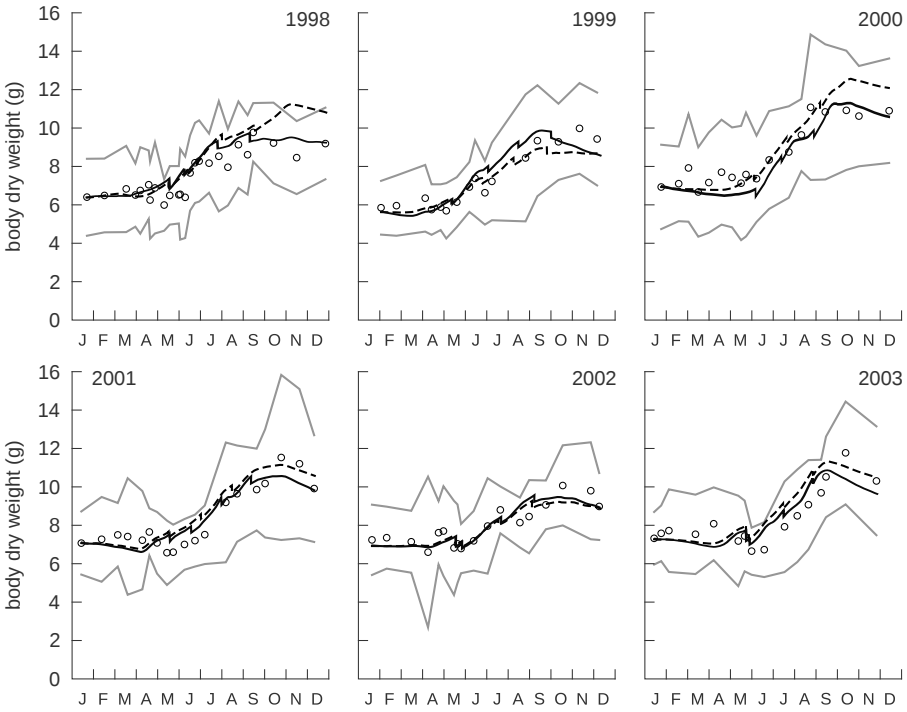


**Figure B.1:** Comparison between dry weight simulations carried out in Chapter 2 with the parameter set described therein (dotted dark line), and simulations carried out using the re-estimated acceleration coefficient (Chapter 6, strait dark line). Dots represent observed data, with upper and lower limits of the confidence interval of measurements for p = 0.05 (strait gray lines).

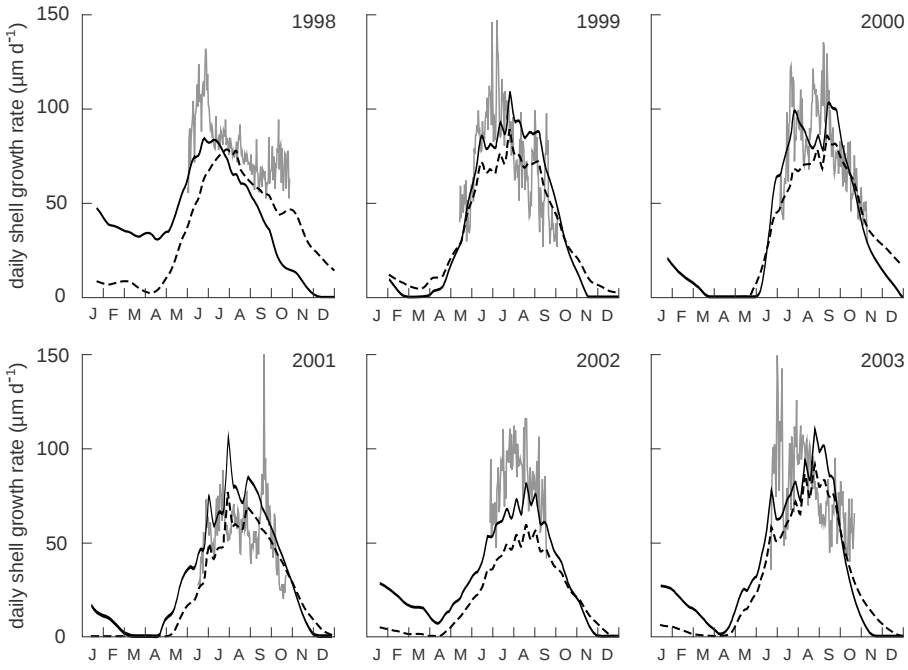


**Figure B.2:** Comparison between DSGR simulations carried out in Chapter 2 with the parameter set described therein (dotted dark line), and simulations carried out using the re-estimated acceleration coefficient (Chapter 6, strait dark line). Dots represent observed data, with upper and lower limits of the confidence interval of measurements for p = 0.05 (strait gray lines).

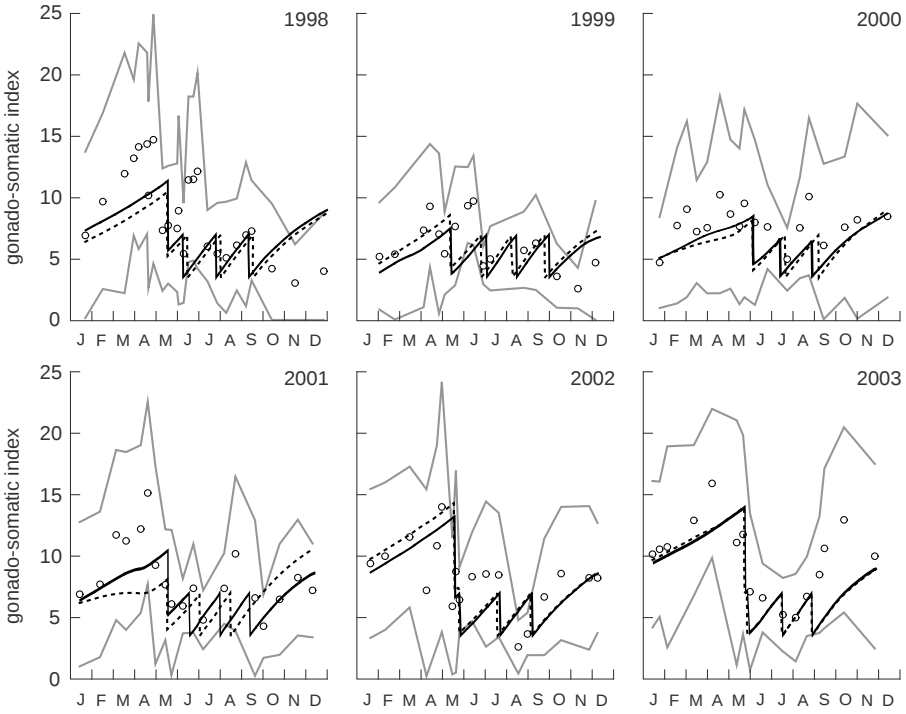


**Figure B.3:** Comparison between GSI simulations carried out in Chapter 2 with the parameter set described therein (dotted dark line), and simulations carried out using the re-estimated acceleration coefficient (Chapter 6, strait dark line). Dots represent observed data, with upper and lower limits of the confidence interval of measurements for p = 0.05 (strait gray lines).

# Bibliography


Abbes, R., 1991. Atlas des ressources et des pêches françaises dans les mers européennes. Ifremer, Ouest-France eds.

Abbott, B. C., Ballantine, D., 1957. The toxin from *Gymnodinium veneficum* Ballantine. Journal of the Marine Biological Association of the United Kingdom 36 (1), 169–189.

Aguire, A., 2010. Etude de la variabilité à long terme des paramètres de croissance de la coquille saint-jacques (*Pecten maximus*) en rade de Brest. Study of the long term variability of growth parameters of the great scallop's shell (*Pecten maximus*) in the bay of Brest. Master's thesis, University of Brest.

Alber, M., Valiela, I., 1994. Incorporation of organic aggregates by marine mussels. Marine Biology 121 (2), 259–265.

Alber, M., Valiela, I., 1995. Organic aggregates in detrital food webs: incorporation by bay scallops *Argopecten irradians*. Marine Ecology Progress Series 121 (1), 117–124.

Alber, M., Valiela, I., 1996. Utilization of microbial organic aggregates by bay scallops, *Argopecten irradians* (Lamarck). Journal of Experimental Marine Biology and Ecology 195 (1), 71–89.

Alldredge, A. L., Gotschalk, C. C., 1989. Direct observations of the mass flocculation of diatom blooms: characteristics, settling velocities and formation of diatom aggregates. Deep Sea Research Part I: Oceanographic Research Papers 36 (2), 159–171.

Alldredge, A. L., Passow, U., Logan, B. E., 1993. The abundance and significance of a class of large, transparent organic particles in the ocean. Deep Sea Research Part I: Oceanographic Research Papers 40 (6), 1131–1140.

Allen, J. A., 1983. The ecology of deep-sea molluscs. The Mollusca, volume 6. Ecology, 29–75.

Alunno-Bruscia, M., Bourlès, Y., Maurer, D., Robert, S., Mazurié, J., Gangnery, A., Goulletquer, P., Pouvreau, S., 2011. A single bio-energetics growth and reproduction model for the oyster *Crassostrea gigas* in six Atlantic ecosystems. Journal of Sea Research 66 (4), 340–348.

Andersen, S., Christophersen, G., Magnesen, T., 2011. Spat production of the great scallop (*Pecten maximus*): a roller coaster. Canadian Journal of Zoology 89 (7), 579–598.

Andersen, S., Grefsrud, E. S., Harboe, T., 2013. Effect of increased $pCO_2$ level on early shell development in great scallop (*Pecten maximus* Lamarck) larvae. Biogeosciences 10 (10), 6161–6184.

Angilletta, M. J., Sears, M. W., 2011. Coordinating theoretical and empirical efforts to understand the linkages between organisms and environments. Integrative and Comparative Biology 51 (5), 653–661.

Angilletta, M. J., Steury, T. D., Sears, M. W., 2004. Temperature, growth rate, and body size in ectotherms: fitting pieces of a life-history puzzle. Integrative and Comparative Biology 44 (6), 498–509.

Ansell, A. D., Dao, J. C., Mason, J., 1991. Three European scallops: *Pecten maximus*, *Chlamys (Aequipecten) opercularis* and *C. (Chlamys) varia*. Scallops: Biology, Ecology and Aquaculture 2, 715–751.

Antoine, L., 1978. La croissance journaliere chez *Pecten maximus* (L.)(Pectinidae, Bivalvia). daily growth of *Pecten maximus* (L.)(Pectinidae, Bivalvia). Haliotis 9, 627–636.

Antoine, L., 1979. La croissance de la coquille Saint-Jacques *Pecten maximus* (L.) et ses variations en mer Celtique et en Manche. The growth of the great scallop *Pecten maximus* (L.) and its variations in the Celtic sea and the English Channel. Ph.D. thesis, University of Brest.

Antoine, L., Garen, P., Lubet, P., 1979. Conséquences sur la maturation et la croissance d'une transplantation de naissain de *Pecten maximus* (L.). consequences of spat transplantation on maturation and growth of *Pecten maximus* (L.). Cahiers de Biologie Marine (Station Biologique de Roscoff) 20 (2), 139–150.

Arrhenius, S., 1889. über die reaktionsgeschwindigkeit bei der Inversion von Rohrzucker durch Säuren. Zeitschrift für physikalische Chemie 4, 226–248.

Artigaud, S., 2013. Approche intégrative de la réponse d'un organisme marin face au changement climatique : la coquille Saint-Jacques *Pecten maximus* et les stress thermique et hypoxique. integrative approach of the response of a marine organism to climate change: the great scallop *Pecten maximus* facing thermal and hypoxic stresses. Ph.D. thesis, University of Brest, Brest.

Artigaud, S., Lavaud, R., Thébault, J., Jean, F., Strand, Ø., Strohmeier, T., Milan, M., Pichereau, V., subm. Proteomic-based comparison of *Pecten maximus* populations along a latitudinal gradient. Journal of Proteome Research.

Auel, H., Harjes, M., da Rocha, R., Stübing, D., Hagen, W., 2002. Lipid biomarkers indicate different ecological niches and trophic relationships of the Arctic hyperiid amphipods *Themisto abyssorum* and *T. libellula*. Polar Biology 25 (5), 374–383.

Aure, J., Strand, Ø., Erga, S. R., Strohmeier, T., 2007. Primary production enhancement by artificial upwelling in a western Norwegian fjord. Marine Ecology Progress Series 352, 39.

Baan, P. J. A., van Buuren, J. T., 2003. Testing of indicators for the marine and coastal environment in Europe. Part 3: Present state and development of indicators for eutrophication, hazardous substances, oil and ecological quality. European Environment Agency, Copenhagen. Technical Report 86.

Bacher, C., Duarte, P., Ferreira, J. G., Héral, M., Raillard, O., 1997. Assessment and comparison of the Marennes-Oléron Bay (France) and Carlingford Lough (Ireland) carrying capacity with ecosystem models. Aquatic Ecology 31 (4), 379–394.

Bacher, C., Gangnery, A., 2006. Use of dynamic energy budget and individual based models to simulate the dynamics of cultivated oyster populations. Journal of Sea Research 56 (2), 140–155.

Bachok, Z., Meziane, T., Mfilinge, P. L., Tsuchiya, M., 2009. Fatty acid markers as an indicator for temporal changes in food sources of the bivalve *Quidnipagus palatum*. Aquatic Ecosystem Health & Management 12 (4), 390–400.

Bachok, Z., Mfilinge, P. L., Tsuchiya, M., 2003. The diet of the mud clam *Geloina coaxans* (Mollusca, Bivalvia) as indicated by fatty acid markers in a subtropical mangrove forest of Okinawa, Japan. Journal of Experimental Marine Biology and Ecology 292 (2), 187–197.

Bacon, G. S., MacDonald, B. A., Ward, J. E., 1998. Physiological responses of infaunal (*Mya arenaria*) and epifaunal (*Placopecten magellanicus*) bivalves to variations in the concentration and quality of suspended particles: I. Feeding activity and selection. Journal of Experimental Marine Biology and Ecology 219 (1), 105–125.

Baker, S. M., Levinton, J. S., Kurdziel, J. P., Shumway, S. E., 1998. Selective feeding and biodeposition by zebra mussels and their relation to changes in phytoplankton composition and seston load. Journal of Shellfish Research 17 (4), 1207–1214.

Barats, A., Amouroux, D., Chauvaud, L., Pécheyran, C., Lorrain, A., Thébault, J., Church, T. M., Donard, O. F. X., 2008a. High frequency Barium profiles in shells of the great scallop *Pecten maximus*: a methodical long-term and multi-site survey in Western Europe. Biogeosciences 6 (2), 157–170.

Barats, A., Amouroux, D., Pécheyran, C., Chauvaud, L., Donard, O. F. X., 2008b. High-Frequency archives of manganese inputs to coastal waters (Bay of seine, France) resolved by the LA-ICP-MS analysis of calcitic growth layers along scallop shells (*Pecten maximus*). Environmental Science & Technology 42 (1), 86–92.

Barats, A., Amouroux, D., Pécheyran, C., Chauvaud, L., Thébault, J., Donard, O. F. X., 2009. Spring molybdenum enrichment in scallop shells: a potential tracer of diatom productivity in coastal temperate environments (Brittany, NW France)? Biogeosciences Discussions 6 (4), 8041–8074.

Barber, B. J., Blake, N. J., 1981. Energy storage and utilization in relation to gametogenesis in *Argopecten irradians concentricus* (Say). Journal of Experimental Marine Biology and Ecology 52 (2), 121–134.

Barber, B. J., Blake, N. J., 2006. Reproductive physiology. In Scallops: Biology, Ecology and Aquaculture. Vol. 35. Sandra E. Shumway and G. Jay Parsons, Editors. Elsevier, Developments in aquaculture and fisheries science, Ch. 8, pp. 357–416.

Barillé, L., Héral, M., Barillé-Boyer, A.-L., 1997. Modélisation de l'écophysiologie de l'huître *Crassostrea gigas* dans un environnement estuarien. ecophysiological modeling of the oyster *Crassostrea gigas* in an estuarine environment. Aquatic Living Resources 10 (1), 31–48.

Barillé, L., Prou, J., Héral, M., Bourgrier, S., 1993. No influence of food quality, but ration-dependent retention efficiencies in the Japanese oyster *Crassostrea gigas*. Journal of Experimental Marine Biology and Ecology 171 (1), 91–106.

Bartell, S. M., Breck, J. E., Gardner, R. H., Brenkert, A. L., 1986. Individual parameter perturbation and error analysis of fish bioenergetics models. Canadian Journal of Fisheries and Aquatic Sciences 43 (1), 160–168.

Batchelder, H. P., Edwards, C. A., Powell, T. M., 2002. Individual-based models of copepod populations in coastal upwelling regions: implications of physiologically and environmentally influenced diel vertical migration on demographic success and nearshore retention. Progress in Oceanography 53 (2), 307–333.

Bayne, B. L., 1976. Marine mussels: their ecology and physiology. Vol. 10. Cambridge University Press.

Bayne, B. L., 1998. The physiology of suspension feeding by bivalve molluscs: an introduction to the Plymouth "TROPHEE" workshop. Journal of Experimental Marine Biology and Ecology 219 (1), 1–19.

Bayne, B. L., Hawkins, A. J. S., Navarro, E., 1987. Feeding and digestion by the mussel *Mytilus edulis* L. (Bivalvia: Mollusca) in mixtures of silt and algal cells at low concentrations. Journal of Experimental Marine Biology and Ecology 111 (1), 1–22.

Bayne, B. L., Newell, R. C., 1983. Physiological energetics of marine molluscs. In The Mollusca: Physiology part 1. Vol. 5. Saleuddin A.S.M. and K.M. Wilbur, Editors. Academic Press, New York, pp. 407–415.

Bayne, B. L., Salkeld, P. N., Worrall, C. M., 1983. Reproductive effort and value in different populations of the marine mussel, *Mytilus edulis* L. Oecologia 59 (1), 18–26.

Bayne, B. L., Worrall, C. M., 1980. Growth and production of mussels *Mytilus edulis* from two populations. Marine Ecology Progress Series 3, 317–328.

Beaumont, A. R., 2006. Genetics. In Scallops: Biology, Ecology and Aquaculture. Vol. 35. Sandra E. Shumway and G. Jay Parsons, Editors. Elsevier, Developments in aquaculture and fisheries science, Ch. 10, pp. 543–594.

Beaumont, A. R., Barnes, D. A., 1992. Aspects of veliger larval growth and byssus drifting of the spat of *Pecten maximus* and *Aequipecten* (*Chlamys*) *opercularis*. ICES Journal of Marine Science: Journal du Conseil 49 (4), 417 –423.

Beaumont, A. R., Budd, M. D., 1982. Delayed growth of mussel (*Mytilus edulis*) and scallop (*Pecten maximus*) veligers at low temperatures. Marine Biology 71 (1), 97–100.

Beaumont, A. R., Morvan, C., Huelvan, S., Lucas, A., Ansell, A. D., 1993. Genetics of indigenous and transplanted populations of *Pecten maximus*: no evidence for the existence of separate stocks. Journal of Experimental Marine Biology and Ecology 169 (1), 77–88.

Bellon-Humbert, C., 1972. Inventaire des mollusques marins vivants recueillis sur la cote de la province de Tarfaya par le professeur J.B. Panouse. inventary of living marine mollusks collected on the coast of the Tarfaya province by professor J.B. Panouse. Bulletin de la Société des Sciences naturelles et physiques du Maroc 52 (3–4), 85–105.

Beninger, P. G., Decottignies, P., Guiheneuf, F., Barille, L., Rince, Y., 2007. Comparison of particle processing by two introduced suspension feeders: selection in *Crepidula fornicata* and *Crassostrea gigas*. Marine Ecology Progress Series 334, 165–177.

Beninger, P. G., Decottignies, P., Rincé, Y., 2004. Localization of qualitative particle selection sites in the heterorhabdic filibranch *Pecten maximus* (Bivalvia: Pectinidae). Marine Ecology Progress Series 275, 163–173.

Beninger, P. G., Le Pennec, G., Le Pennec, M., 2003. Demonstration of nutrient pathway from the digestive system to oocytes in the gonad intestinal loop of the scallop *Pecten maximus* (L.). Biology Bulletin 205 (1), 83–92.

Beninger, P. G., Le Pennec, M., 2006. Structure and function in scallop. In Scallops: Biology, Ecology and Aquaculture. Vol. 35. Sandra E. Shumway and G. Jay Parsons, Editors. Elsevier, Developments in aquaculture and fisheries science, Ch. 3, pp. 123–228.

Bergmann, C., 1847. Über die Verhältnisse der Wärmeökonomie der Thiere zu ihrer Grösse. Vol. 1. Götinger Studien.

Bernard, I., de Kermoysan, G., Pouvreau, S., 2011. Effect of phytoplankton and temperature on the reproduction of the Pacific oyster *Crassostrea gigas*: Investigation through DEB theory. Journal of Sea Research 66 (4), 349–360.

Bienfang, P. K., 1981. Sinking rates of heterogeneous, temperate phytoplankton populations. Journal of Plankton Research 3 (2), 235–253.

Billett, D. S. M., Lampitt, R. S., Rice, A. L., Mantoura, R. F. C., 1983. Seasonal sedimentation of phytoplankton to the deep-sea benthos. Nature 302 (5908), 520–522.

Bode, A., Alvarez-Ossorio, M. T., Varela, M., 2006. Phytoplankton and macrophyte contributions to littoral food webs in the Galician upwelling estimated from stable isotopes. Marine Ecology Progress Series 318, 89–102.

Bougrier, S., Lassus, P., Bardouil, M., Masselin, P., Truquet, P., 2003. Paralytic shellfish poison accumulation yields and feeding time activity in the Pacific oyster (*Crassostrea gigas*) and king scallop (*Pecten maximus*). Aquatic Living Resources 16 (4), 347–352.

Bourlès, Y., Alunno-Bruscia, M., Pouvreau, S., Tollu, G., Leguay, D., Arnaud, C., Goulletquer, P., Kooijman, S. A. L. M., 2009. Modelling growth and reproduction of the Pacific oyster *Crassostrea gigas*: Advances in the oyster-DEB model through application to a coastal pond. Journal of Sea Research 62 (2–3), 62–71.

Brand, A. R., 2006a. Scallop ecology: distributions and behaviour. In Scallops: Biology, Ecology and Aquaculture. Vol. 35. Sandra E. Shumway and G. Jay Parsons, Editors. Elsevier, Developments in aquaculture and fisheries science, Ch. 12, pp. 651–744.

Brand, A. R., 2006b. The European scallop fisheries for *Pecten maximus*, *Aequipecten opercularis* and *Mimachlamys varia*. Vol. 35. Sandra E. Shumway and G. Jay Parsons, Editors. Elsevier, Developments in aquaculture and fisheries science, Ch. 19, pp. 991–1058.

Brandt, S. B., Hartman, K. J., 1993. Innovative approaches with bioenergetics models: future applications to fish ecology and management. Transactions of the American Fisheries Society 122 (5), 731–735.

Bratbak, G., Jacquet, S., Larsen, A., Pettersson, L. H., Sazhin, A. F., Thyrhaug, R., 2011. The plankton community in Norwegian coastal waters – abundance, composition, spatial distribution and diel variation. Continental Shelf Research 31 (14), 1500–1514.

Bricelj, V. M., Krause, M. K., 1992. Resource allocation and population genetics of the bay scallop, *Argopecten irradians irradians*: effects of age and allozyme heterozygosity on reproductive output. Marine Biology 113 (2), 253–261.

Bricelj, V. M., MacQuarrie, S. P., Smolowitz, R., 2004. Concentration-dependent effects of toxic and non-toxic isolates of the brown tide alga *Aureococcus anophagefferens* on growth of juvenile bivalves. Marine Ecology Progress Series 282, 101–114.

Buestel, D., Cochard, J.-C., Dao, J.-C., Gérard, A., 1982. Production artificielle de naissain de coquilles Saint-Jacques *Pecten maximus* (L.). Premiers résultats en rade de Brest. artificial spat production of great scallop *Pecten maximus* (L.). First results in the Bay of Brest. Vie Marine – Annales de la Fondation océanographique Ricard 4, 24–28.

Buestel, D., Gérard, A., Guénolé, A., 1987. Croissance de différents lots de coquilles Saint-Jacques *Pecten maximus* en culture sur le fond dans la rade de Brest. growth of different batch of great scallop *Pecten maximus* cultivated in the bottom of the Bay of Brest. Haliotis 16, 173–177.

Buick, D. P., Ivany, L. C., 2004. 100 years in the dark: Extreme longevity of Eocene bivalves from Antarctica. Geology 32 (10), 921–924.

Bunt, J. S., 1975. Primary productivity of marine ecosystems. In Primary productivity of the biosphere, Ecological Studies. Vol. 14. H. Lieth & R.H. Whittaker, Berlin, pp. 169–183.

Buxton, C. D., Newell, R. C., Field, J. G., 1981. Response surface analysis of the combined effects of exposure and acclimation temperatures on filtration, oxygen consumption and scope for growth in the oyster *Ostrea edulis*. Marine Ecology Progress Series 6, 73–82.

Caers, M., Coutteau, P., Sorgeloos, P., Gajardo, G., 2003. Impact of algal diets and emulsions on the fatty acid composition and content of selected tissues of adult broodstock of the Chilean scallop *Argopecten purpuratus* (Lamarck, 1819). Aquaculture 217 (1–4), 437–452.

Caldeira, K., Wickett, M. E., 2003. Oceanography: anthropogenic carbon and ocean pH. Nature 425 (6956), 365–365.

Calow, P., 1983. Life-cycle patterns and evolution. In The Mollusca. Ecology. Vol. 6. Russell-Hunter, W. D., Editor. London: Academic Press., pp. 649–678.

Cardoso, J. F. M. F., Witte, J. I. J., van der Veer, H. W., 2006. Intra- and interspecies comparison of energy flow in bivalve species in Dutch coastal waters by means of the Dynamic Energy Budget (DEB) theory. Journal of Sea Research 56 (2), 182–197.

Casse, N., 1995. Embryonic development of *Pecten maximus* (L.) (Bivalve, Mollusc). Ph.D. thesis, University of Brest.

Chaparro, O. R., Montory, J. A., Segura, C. J., Pechenik, J. A., 2009. Effect of reduced pH on shells of brooded veligers in the estuarine bivalve *Ostrea chilensis* Philippi 1845. Journal of Experimental Marine Biology and Ecology 377 (2), 107–112.

Chatterjee, A., 2014. Rôle des micro-algues benthiques dans la zone côtière : biodiversité, productivité, toxicité. Role of benthic microalgae in the coastal area: biodiversity, productivity, toxicity. Ph.D. thesis, University of Brest.

Chatterjee, A., Klein, C., Naegelen, A., Claquin, P., Masson, A., Legoff, M., Amice, E., L'Helguen, S., Chauvaud, L., Leynaert, A., 2013. Comparative dynamics of pelagic and benthic micro-algae in a coastal ecosystem. Estuarine, Coastal and Shelf Science 133, 67–77.

Chauvaud, L., Donval, A., Thouzeau, G., Paulet, Y.-M., Nézan, E., 2001. Variations in food intake of *Pecten maximus* (L.) from the Bay of Brest (France): Influence of environmental factors and phytoplankton species composition. Comptes Rendus de l'Académie des Sciences – Series III – Sciences de la Vie 324 (8), 743–755.

Chauvaud, L., Jean, F., Ragueneau, O., Thouzeau, G., 2000. Long-term variation of the Bay of Brest ecosystem: benthic-pelagic coupling revisited. Marine Ecology Progress Series 200, 35–48.

Chauvaud, L., Lorrain, A., Dunbar, R. B., Paulet, Y.-M., Thouzeau, G., Jean, F., Guarini, J.-M., Mucciarone, D., 2005. Shell of the great scallop *Pecten maximus* as a high-frequency archive of paleoenvironmental changes. Geochemistry Geophysics Geosystems 6, Q08001.

Chauvaud, L., Patry, Y., Jolivet, A., Cam, E., Le Goff, C., Strand, Ø., Charrier, G., Thébault, J., Lazure, P., Gotthard, K., Clavier, J., 2012. Variation in size and growth of the great scallop *Pecten maximus* along a latitudinal gradient. PLoS ONE 7 (5), e37717.

Chauvaud, L., Thouzeau, G., Paulet, Y.-M., 1998. Effects of environmental factors on the daily growth rate of *Pecten maximus* juveniles in the Bay of Brest (France). Journal of Experimental Marine Biology and Ecology 227 (1), 83–111.

Chipps, S. R., Wahl, D. H., 2008. Bioenergetics modeling in the 21st century: reviewing new insights and revisiting old constraints. Transactions of the American Fisheries Society 137 (1), 298–313.

Christophersen, G., 2000. Effects of air emersion on survival and growth of hatchery reared great scallop spat. Aquaculture International 8, 159–168.

Christophersen, G., Torkildsen, L., van der Meeren, T., 2006. Effect of increased water recirculation rate on algal supply and post-larval performance of scallop (*Pecten maximus*) reared in a partial open and continuous feeding system. Aquacultural Engineering 35 (3), 271–282.

Clark, G. R., 1968. Mollusk shell: daily growth lines. Science 161 (3843), 800–802.

Clark, G. R., 2005. Daily growth lines in some living Pectens (Mollusca: Bivalvia), and some applications in a fossil relative: Time and tide will tell. Palaeogeography, Palaeoclimatology, Palaeoecology 228 (1–2), 26–42.

Clarke, A., 2003. Costs and consequences of evolutionary temperature adaptation. Trends in Ecology & Evolution 18 (11), 573–581.

Claustre, H., Ras, J., 2009. The third seawifs HPLC analysis round-robin experiment (seaharre-3), Chap. 6: The LOV method. NASA technical Memorandum 215849.

Cloern, J. E., Nichols, F. H., 1978. A von Bertalanffy growth model with a seasonally varying coefficient. Journal of the Fisheries Board of Canada 35 (11), 1479–1482.

Cochard, J.-C., Devauchelle, N., 1993. Spawning, fecundity and larval survival and growth in relation to controlled conditioning in native and transplanted populations of *Pecten maximus* (L.): evidence for the existence of separate stocks. Journal of Experimental Marine Biology and Ecology 169 (1), 41–56.

Comely, C. A., 1974. Seasonal variations in the flesh weights and biochemical content of the scallop *Pecten maximus* (L.) in the Clyde Sea area. Journal du Conseil 35 (3), 281–295.

Cowen, R. K., Sponaugle, S., 2009. Larval dispersal and marine population connectivity. Annual Review of Marine Science 1, 443–466.

Cragg, S. M., 2006. Development, physiology, behaviour and ecology of scallop larvae. In Scallops: Biology, Ecology and Aquaculture. Vol. 35. Sandra E. Shumway and G. Jay Parsons, Editors. Elsevier, Developments in aquaculture and fisheries science, Ch. 2, pp. 45–122.

Cranford, P. J., Armsworthy, S. L., Mikkelsen, O. A., Milligan, T. G., 2005. Food acquisition responses of the suspension-feeding bivalve *Placopecten magellanicus* to the flocculation and settlement of a phytoplankton bloom. Journal of Experimental Marine Biology and Ecology 326 (2), 128–143.

Cranford, P. J., Grant, J., 1990. Particle clearance and absorption of phytoplankton and detritus by the sea scallop *Placopecten magellanicus* (Gmelin). Journal of Experimental Marine Biology and Ecology 137 (2), 105–121.

Cranford, P. J., Hill, P. S., 1999. Seasonal variation in food utilization by the suspension-feeding bivalve molluscs *Mytilus edulis* and *Placopecten magellanicus*. Marine Ecology Progress Series 190, 223–239.

Cranford, P. J., Ward, J. E., Shumway, S. E., 2011. Bivalve filter feeding: variability and limits of the aquaculture biofilter. In Shellfish Aquaculture and the Environment, First Edition. Sandra E. Shumway ed. John Wiley & Sons, Inc., pp. 81–124.

Crocker, K. M., Passow, U., 1995. Differential aggregation of diatoms. Marine Ecology Progress Series 117 (1), 249–257.

Cucci, T. L., Shumway, S. E., Newell, R. C., Selvin, R., Guillard, R. R. L., Yentsch, C. M., 1985. Flow cytometry: a new method for characterization of differential ingestion, digestion and egestion by suspension feeders. Marine Ecology Progress Series 24 (1), 201–204.

Cugier, P., Struski, C., Blanchard, M., Mazurié, J., Pouvreau, S., Olivier, F., Trigui, J. R., Thiébaut, E., 2010. Assessing the role of benthic filter feeders on phytoplankton production in a shellfish farming site: Mont Saint Michel Bay, France. Journal of Marine Systems 82 (1), 21–34.

Cushing, D. H., 1990. Plankton production and year-class strength in fish populations: an update of the match/mismatch hypothesis. Advances in Marine Biology 26, 249–293.

Dabrowski, T., Lyons, K., Curé, M., Berry, A., Nolan, G., 2012. Numerical modelling of spatio-temporal variability of growth of *Mytilus edulis* (L.) and influence of its cultivation on ecosystem functioning. Journal of Sea Research 76, 5–21.

Dale, T., Rey, F., Heimdal, B., 1999. Seasonal development of phytoplankton at a high latitude oceanic site. Sarsia 84 (5–6), 419–436.

Dalsgaard, J., St. John, M., Kattner, G., Müller-Navarra, D., Hagen, W., 2003. Fatty acid trophic markers in the pelagic marine environment. Advances in Marine Biology 46, 225–340.

Dame, R. F., 2011. Ecology of marine bivalves: an ecosystem approach. Second edition. Taylor & Francis Group, LLC. CRC Press.

Davis, R. L., Marshall, N., 1961. The feeding of the bay scallop, *Aequipecten irradians*. Proceedings of the National Shellfisheries Association 52, 25–29.

De Jonge, V. N., Van Beusekom, J. E. E., 1995. Wind- and tide-induced resuspension of sediment and microphytobenthos from tidal flats in the Ems estuary. Limnology and oceanography 40 (4), 766–778.

Delaunay, F., Marty, Y., Moal, J., Samain, J.-F., 1993. The effect of monospecific algal diets on growth and fatty acid composition of *Pecten maximus* (L.) larvae. Journal of Experimental Marine Biology and Ecology 173 (2), 163–179.

Devauchelle, N., Mingant, C., 1991. Review of the reproductive physiology of the scallop, *Pecten maximus*, applicable to intensive aquaculture. Aquatic Living Resources 4 (1), 41–51.

Diekmann, O., Metz, J. A. J., 2010. How to lift a model for individual behaviour to the population level? Philosophical Transactions of the Royal Society B: Biological Sciences 365 (1557), 3523–3530.

Dijkman, N. A., Kromkamp, J. C., 2006. Phospholipid-derived fatty acids as chemotaxonomic markers for phytoplankton: application for inferring phytoplankton composition. Marine Ecology Progress Series 324 (1), 113–125.

Doney, S. C., Fabry, V. J., Feely, R. A., Kleypas, J. A., 2009. Ocean acidification: the other $CO_2$ problem. Marine Science 1, 169–192.

Dowd, M., 1997. On predicting the growth of cultured bivalves. Ecological Modelling 104 (2), 113–131.

Duarte, P., Fernández-Reiriz, M. J., Labarta, U., 2012. Modelling mussel growth in ecosystems with low suspended matter loads using a Dynamic Energy Budget approach. Journal of Sea Research 67 (1), 44–57.

Dufour, S. C., Beninger, P. G., 2001. A functional interpretation of cilia and mucocyte distributions on the abfrontal surface of bivalve gills. Marine Biology 138 (2), 295–309.

Duineveld, G. C. A., Lavaleye, M. S. S., Berghuis, E. M., De Wilde, P. A. W. J., van Der Weele, J., Kok, A., Batten, S. D., De Leeuw, J. W., 1997. Patterns of benthic fauna and benthic respiration on the Celtic continental margin in relation to the distribution of phytodetritus. Internationale Revue der gesamten Hydrobiologie und Hydrographie 82 (3), 395–424.

Duinker, A., Saout, C., Paulet, Y.-M., 1999. Effect of photoperiod on conditioning of the great scallop. Aquaculture International 7 (6), 449–457.

Dupuy, C., Vaquer, A., Lam Hoai, T., Rougier, C., Mazouni, N., Lautier, J., Collos, Y., Le Gall, S., 2000. Feeding rate of the oyster *Crassostrea gigas* in a natural planktonic community of the Mediterranean Thau Lagoon. Marine Ecology Progress Series 205, 171–184.

Dutertre, M., Barillé, L., Haure, J., Cognie, B., 2007. Functional responses associated with pallial organ variations in the Pacific oyster *Crassostrea gigas* (Thunberg, 1793). Journal of Experimental Marine Biology and Ecology 352 (1), 139–151.

Eaton, J. W., Bateman, D., Hauberg, S., 2008. GNU Octave Manual Version 3. Network Theory Limited.

Eilers, P. H. C., 2003. A perfect smoother. Analytical Chemistry 75 (14), 3631–3636.

Emmery, A., Lefebvre, S., Alunno-Bruscia, M., Kooijman, S. A. L. M., 2011. Understanding the dynamics of $\delta^{13}$C and $\delta^{15}$N in soft tissues of the bivalve *Crassostrea gigas* facing environmental fluctuations in the context of Dynamic Energy Budgets (DEB). Journal of Sea Research 66 (4), 361–371.

Erard-Le Denn, E., Morlaix, M., Dao, J.-C., 1990. Effects of *Gyrodinium cf. aureolum* on *Pecten maximus* (post larvae, juveniles and adults). In Toxic marine phytoplankton. Granéli, E., B. Sundström, L. Edler, D.M. Anderson, Elsevier, New York, pp. 132–136.

Erga, S. R., 1989. Ecological studies on the phytoplankton of Boknafjorden, western Norway. 1. The effect of water exchange processes and environmental factors on temporal and vertical variability of biomass. Sarsia 74 (3), 161–176.

Erga, S. R., Heimdal, B. R., 1984. Ecological studies on the phytoplankton of Korsfjorden, western Norway. The dynamics of a spring bloom seen in relation to hydrographical conditions and light regime. Journal of Plankton Research 6 (1), 67–90.

Erga, S. R., Ssebiyonga, N., Frette, Ø., Hamre, B., Aure, J., Strand, Ø., Strohmeier, T., 2012. Dynamics of phytoplankton distribution and photosynthetic capacity in a western Norwegian fjord during coastal upwelling: Effects on optical properties. Estuarine, Coastal and Shelf Science 97, 91–103.

Espinosa, E. P., Perrigault, M., Ward, J. E., Shumway, S. E., Allam, B., 2010. Microalgal cell surface carbohydrates as recognition sites for particle sorting in suspension-feeding bivalves. The Biological Bulletin 218 (1), 75–86.

Fabry, V. J., Seibel, B. A., Feely, R. A., Orr, J. C., 2008. Impacts of ocean acidification on marine fauna and ecosystem processes. ICES Journal of Marine Science: Journal du Conseil 65 (3), 414–432.

Faure, L., 1956. The scallop *Pecten maximus* from the Brest Bay (Brittany). Revue des Travaux de l'Institut des Pêches Maritimes 20 (2).

Fifas, S., 1993. Analyse et modelisation des parametres d'exploitation du stock de coquilles saint-jacques (*Pecten maximus*, L.) en baie de Saint-Brieuc (Manche ouest, France). Analyze and modeling of the operating parameters of the scallop stock (*Pecten maximus*, L.) of Saint-Brieuc (Western English Channel, France). Ph.D. thesis, University of Brest.

Fifas, S., 2004. La coquille Saint-Jacques en Bretagne. Tech. rep., Ifremer.

Filgueira, R., Grant, J., Strand, Ø., Asplin, L., Aure, J., 2010. A simulation model of carrying capacity for mussel culture in a Norwegian fjord: Role of induced upwelling. Aquaculture 308 (1–2), 20–27.

Filgueira, R., Rosland, R., Grant, J., 2011. A comparison of scope for growth (SFG) and dynamic energy budget (DEB) models applied to the blue mussel (*Mytilus edulis*). Journal of Sea Research 66 (4), 403–410.

Flye-Sainte-Marie, J., Jean, F., Paillard, C., Ford, S. E., Powell, E., Hofmann, E., Klinck, J., 2007. Ecophysiological dynamic model of individual growth of *Ruditapes philippinarum*. Aquaculture 266 (1–4), 130–143.

Flye-Sainte-Marie, J., Jean, F., Paillard, C., Kooijman, S. A. L. M., 2009. A quantitative estimation of the energetic cost of Brown Ring Disease in the Manila clam using Dynamic Energy Budget theory. Journal of Sea Research 62 (2–3), 114–123.

Fouillaron, P., 2001. Modélisation des flux d'énergie entre les différents compartiments de la coquille saint-jacques (*Pecten maximus*) : cas de la population brestoise (1989–2000). modeling of energy fluxes between the different compartment of the great scallop (*Pecten maximus*): the case of the brest population (1989–2000). Master's thesis, University of Brest.

Freitas, P. S., Clarke, L. J., Kennedy, H., Richardson, C. A., 2012. The potential of combined Mg/Ca and $\delta^{18}$O measurements within the shell of the bivalve *Pecten maximus* to estimate seawater $\delta^{18}$O composition. Chemical Geology 291, 286–293.

Freitas, P. S., Clarke, L. J., Kennedy, H., Richardson, C. A., Abrantes, F., 2006. Environmental and biological controls on elemental (Mg/Ca, Sr/Ca and Mn/Ca) ratios in shells of the king scallop *Pecten maximus*. Geochimica et Cosmochimica Acta 70 (20), 5119–5133.

Freitas, V., Cardoso, J. F. M. F., Santos, S., Campos, J., Drent, J., Saraiva, S., Witte, J. I. J., Kooijman, S. A. L. M., van der Veer, H. W., 2009. Reconstruction of food conditions for northeast atlantic bivalve species based on dynamic energy budgets. Journal of Sea Research 62 (2–3), 75–82.

Furness, R. W., 1978. Energy requirements of seabird communities: a bioenergetics model. The Journal of Animal Ecology 47, 39–53.

Gage, J. D., Tyler, P. A., 1992. Deep-sea biology: a natural history of organisms at the deep-sea floor. Cambridge University Press.

Gaylord, B., Hill, T. M., Sanford, E., Lenz, E. A., Jacobs, L. A., Sato, K. N., Russell, A. D., Hettinger, A., 2011. Functional impacts of ocean acidification in an ecologically critical foundation species. The Journal of Experimental Biology 214 (15), 2586–2594.

Gazeau, F., Gattuso, J.-P., Greaves, M., Elderfield, H., Peene, J., Heip, C. H. R., Middelburg, J. J., 2011. Effect of carbonate chemistry alteration on the early embryonic development of the Pacific oyster (*Crassostrea gigas*). PLoS ONE 6 (8), e23010.

Goodwin, D. H., Flessa, K. W., Schöne, B. R., Dettman, D. L., 2001. Cross-calibration of daily growth increments, stable isotope variation, and temperature in the Gulf of California bivalve mollusk *Chione cortezi*: implications for paleoenvironmental analysis. Palaios 16 (4), 387–398.

Grangeré, K., Lefebvre, S., Bacher, C., Cugier, P., Ménesguen, A., 2010. Modelling the spatial heterogeneity of ecological processes in an intertidal estuarine bay: dynamic interactions between bivalves and phytoplankton. Marine Ecology Progress Series 415, 141–158.

Grant, B. W., Porter, W. P., 1992. Modeling global macroclimatic constraints on ectotherm energy budgets. American Zoologist 32 (2), 154–178.

Grant, J., 1996. The relationship of bioenergetics and the environment to the field growth of cultured bivalves. Journal of Experimental Marine Biology and Ecology 200 (1), 239–256.

Grant, J., Bacher, C., 1998. Comparative models of mussel bioenergetics and their validation at field culture sites. Journal of Experimental Marine Biology and Ecology 219 (1–2), 21–44.

Grant, J., Bacher, C., 2001. A numerical model of flow modification induced by suspended aquaculture in a Chinese bay. Journal of Experimental Marine Biology and Ecology 58 (5), 1003–1011.

Grant, J., Bacher, C., Cranford, P. J., Guyondet, T., Carreau, M., 2008. A spatially explicit ecosystem model of seston depletion in dense mussel culture. Journal of Marine Systems 73 (1), 155–168.

Grant, J., Curran, K. J., Guyondet, T. L., Tita, G., Bacher, C., Koutitonsky, V., Dowd, M., 2007. A box model of carrying capacity for suspended mussel aquaculture in lagune de la Grande-Entrée, Iles-de-la-Madeleine, Québec. Ecological Modelling 200 (1), 193–206.

Grant, J., Dowd, M., Thompson, K., Emerson, C., Hatcher, A., Dame, R. F., 1993. Perspectives on field studies and related biological models of bivalve growth and carrying capacity. Nato Asi Series G: Ecological Sciences 33, 371–371.

Grossman, E. L., Ku, T. L., 1986. Oxygen and carbon isotope fractionation in biogenic aragonite: temperature effects. Chemical Geology: Isotope Geoscience Section 59, 59–74.

Gruffydd, L. D., Beaumont, A. R., 1972. A method for rearing *Pecten maximus* larvae in the laboratory. Marine Biology 15 (4), 350–355.

Guarini, J. M., Chauvaud, L., Cloern, J. E., Clavier, J., Coston-Guarini, J., Patry, Y., 2011. Seasonal variations in ectotherm growth rates: Quantifying growth as an intermittent non steady state compensatory process. Journal of Sea Research 65 (3), 355–361.

Guillaud, J.-F., Aminot, A., Delmas, D., Gohin, F., Lunven, M., Labry, C., Herbland, A., 2008. Seasonal variation of riverine nutrient inputs in the northern Bay of Biscay (France), and patterns of marine phytoplankton response. Journal of Marine Systems 72 (1), 309–319.

Gurney, W. S. C., Nisbet, R. M., 2004. Resource allocation, hyperphagia and compensatory growth. Bulletin of mathematical biology 66 (6), 1731–1753.

Guyondet, T., Roy, S., Koutitonsky, V. G., Grant, J., Tita, G., 2010. Integrating multiple spatial scales in the carrying capacity assessment of a coastal ecosystem for bivalve aquaculture. Journal of Sea Research 64 (3), 341–359.

Guzmán-Agüero, J., Nieves-Soto, M., Hurtado, M., Piña Valdez, P., Garza-Aguirre, M. D. C., 2012. Feeding physiology and scope for growth of the oyster *Crassostrea corteziensis* (Hertlein, 1951) acclimated to different conditions of temperature and salinity. Aquaculture International 36 (14), 1–15.

Handå, A., Alver, M., Edvardsen, C. V., Halstensen, S., Olsen, A. J., Øie, G., Reitan, K. I., Olsen, Y., Reinertsen, H., 2011. Growth of farmed blue mussels (*Mytilus edulis* L.) in a Norwegian coastal area; comparison of food proxies by DEB modeling. Journal of Sea Research 66 (4), 297–307.

Hartnoll, R. G., 1967. An investigation of the movement of the scallop, *Pecten maximus*. Helgoländer wissenschaftliche Meeresuntersuchungen 15 (1-4), 523–533.

Hawkins, A. J. S., Bayne, B. L., Mantoura, R. F. C., Llewellyn, C. A., Navarro, E., 1986. Chlorophyll degradation and absorption throughout the digestive system of the blue mussel *Mytilus edulis* L. Journal of Experimental Marine Biology and Ecology 96 (3), 213–223.

Hawkins, A. J. S., Duarte, P., Fang, J. G., Pascoe, P. L., Zhang, J. H., Zhang, X. L., Zhu, M. Y., 2002. A functional model of responsive suspension-feeding and growth in bivalve shellfish, configured and validated for the scallop *Chlamys farreri* during culture in China. Journal of Experimental Marine Biology and Ecology 281 (1–2), 13–40.

Hawkins, A. J. S., Pascoe, P. L., Parry, H., Brinsley, M., Black, K. D., McGonigle, C., Moore, H., Newell, C. R., O'Boyle, N., Ocarroll, T., O'Loan, B., Service, M., Smaal, A. C., Zhang, X. L., Zhu, M. Y., 2013. Shellsim: a generic model of growth and environmental effects validated across contrasting habitats in bivalve shellfish. Journal of Shellfish Research 32 (2), 237–253.

Hawkins, A. J. S., Pascoe, P. L., Parry, H., Brinsley, M., Cacciatore, F., Black, K. D., Fang, J. G., Jiao, H., Mcgonigle, C., Moore, H., O'Boyle, N., O'Carroll, T., O'Loan, B., Service, M., Smaal, A. C., Yan, X., Zhang, J. H., Zhang, X. L., Zhu, M. Y., 2014. Comparative feeding on chlorophyll-rich versus remaining organic matter in bivalve shellfish. Journal of Shellfish Research 32 (3), 883–897.

Hégaret, H., Brokordt, K. B., Gaymer, C. F., Lohrmann, K. B., García, C., Varela, D., 2012. Effects of the toxic dinoflagellate *Alexandrium catenella* on histopathogical and escape responses of the Northern scallop *Argopecten purpuratus*. Harmful Algae 18, 74–83.

Hégaret, H., Wikfords, G. H., Shumway, S. E., 2007. Diverse feeding responses of five species of bivalve mollusc when exposed to three species of harmful algae. Journal of Shellfish Research 26 (2), 549–559.

Heipel, D. A., Bishop, J. D. D., Brand, A. R., Thorpe, J. P., 1998. Population genetic differentiation of the great scallop *Pecten maximus* in western Britain investigated by randomly amplified polymorphic DNA. Marine Ecology Progress Series 162, 163–171.

Heral, M., 1989. Traditional oyster culture in France. In Barnabe Aquaculture. Ellis Horwood, pp. 342–387.

Hochachka, P. W., Somero, G. N., 2002. Biochemical adaptation: mechanism and process in physiological evolution. Vol. 480. Oxford University Press, New York.

Høisæter, T., 1986. An annotated check-list of marine molluscs of the Norwegian coast and adjacent waters. Sarsia 71 (2), 73–145.

Hold, N., Murray, L. G., Hinz, H., Neill, S. P., Lass, S., Lo, M., Kaiser, M. J., 2013. Environmental drivers of small scale spatial variation in the reproductive schedule of a commercially important bivalve mollusc. Marine Environmental Research 92, 144–153.

Huret, M., Petitgas, P., Struski, C., Leger, F., Sourisseau, M., Lazure, P., 2010. A 37 years hindcast of a coupled physical-biogeochemical model and its use for fisheries oceanography in the Bay of Biscay. ICES-CIEM Annual Science Conference ICES CM 2010/A06, Nantes, 20–24 September 2010.

Hurtado, M. A., Racotta, I., Arcos, F., Morales-Bojórquez, E., Moal, J., Soudant, P., Palacios, E., 2012. Seasonal variations of biochemical, pigment, fatty acid, and sterol compositions in female (*Crassostrea corteziensis*) oysters in relation to the reproductive cycle. Comparative Biochemistry and Physiology Part B: Biochemistry and Molecular Biology 163 (2), 172–183.

Ibarra, D. A., Fennel, K., Cullen, J. J., 2014. Coupling 3-D Eulerian bio-physics (ROMS) with individual-based shellfish ecophysiology (SHELL-E): A hybrid model for carrying capacity and environmental impacts of bivalve aquaculture. Ecological Modelling 273, 63–78.

IPCC, 2013. Climate Change 2013: The Physical Science Basis. Working Group 1 (WG1). Contribution to the Intergovernmental Panel on Climate Change (IPCC), fifth Assessment Report (AR5). Tech. rep.

Iverson, S. J., Field, C., Don Bowen, W., Blanchard, W., 2004. Quantitative fatty acid signature analysis: a new method of estimating predator diets. Ecological Monographs 74 (2), 211–235.

Jager, T., Heugens, E. H. W., Kooijman, S. A. L. M., 2006. Making sense of ecotoxicological test results: towards application of process-based models. Ecotoxicology 15 (3), 305–314.

Jamieson, G. R., Reid, E. H., 1972. The component fatty acids of some marine algal lipids. Phytochemistry 11 (4), 1423–1432.

Järnegren, J., Altin, D., 2006. Filtration and respiration of the deep living bivalve *Acesta excavata* (J.C. Fabricius, 1779) (Bivalvia; Limidae). Journal of Experimental Marine Biology and Ecology 334 (1), 122–129.

Jeffrey, S. W., 1968. Quantitative thin-layer chromatography of chlorophylls and carotenoids from marine algae. Biochimica et Biophysica Acta – Bioenergetics 162 (2), 271–285.

Jeffrey, S. W., 1974. Profiles of photosynthetic pigments in the ocean using thin-layer chromatography. Marine Biology 26 (2), 101–110.

Jeffrey, S. W., 1997. Phytoplankton Pigments in Oceanography: Guidelines to Modern Methods. S.W. Jeffrey, R.F.C. Mantoura and S.W. Wright, Editors. UNESCO, Paris.

Jones, D. S., 1983. Sclerochronology: Reading the record of the molluscan shell: Annual growth increments in the shells of bivalve molluscs record marine climatic changes and reveal surprising longevity. American Scientist 71 (4), 384–391.

Jones, D. S., Williams, D. F., Arthur, M. A., Krantz, D. E., 1984. Interpreting the paleoenvironmental, paleoclimatic and life history records in mollusc shells. Geobios 17, 333–339.

Jones, H. D., Richards, O. G., Southern, T. A., 1992. Gill dimensions, water pumping rate and body size in the mussel *Mytilus edulis* (L.). Journal of Experimental Marine Biology and Ecology 155 (2), 213–237.

Jørgensen, C. B., 1983. Fluid mechanical aspects of suspension feeding. Marine Ecology Progress Series 11, 89–103.

Joyce, A. E., 2006. The coastal temperature network and ferry route programme: long-term temperature and salinity observations. Science Series Data Report 43, pp. 129.

Jusup, M., Klanjscek, T., Matsuda, H., Kooijman, S. A. L. M., 2011. A full lifecycle bioenergetic model for Bluefin tuna. PLoS ONE 6 (7), e21903.

Kamermans, P., 1994. Similarity in food source and timing of feeding in deposit- and suspension-feeding bivalves. Marine Ecology Progress Series 104, 63–75.

Kang, C. K., Sauriau, P.-G., Richard, P., Blanchard, G. F., 1999. Food sources of the infaunal suspension-feeding bivalve *Cerastoderma edule* in a muddy sandflat of Marennes-Oléron Bay, as determined by analyses of carbon and nitrogen stable isotopes. Marine Ecology Progress Series 187, 147–158.

Kharlamenko, V. I., Kiyashko, S. I., Imbs, A. B., Vyshkvartzev, D. I., 2001. Identification of food sources of invertebrates from the seagrass *Zostera marina* community using carbon and sulfur stable isotope ratio and fatty acid analyses. Marine Ecology Progress Series 220, 103–117.

Kharlamenko, V. I., Kiyashko, S. I., Rodkina, S. A., Imbs, A. B., 2008. Determination of food sources of marine invertebrates from a subtidal sand community using analyses of fatty acids and stable isotopes. Russian Journal of Marine Biology 34 (2), 101–109.

Kiørboe, T., Møhlenberg, F., 1981. Particle selection in suspension-feeding bivalves. Marine Ecology Progress Series 5, 291–296.

Knudsen, J., 1970. The systematics and biology of abyssal and hadal Bivalvia. Galathea Report 11, 7–241.

Kooijman, S. A. L. M., 1998. The Synthesizing Unit as model for the stoichiometric fusion and branching of metabolic fluxes. Biophysical Chemistry 7 (1–2), 179–188.

Kooijman, S. A. L. M., 2006. Pseudo-faeces production in bivalves. Journal of Sea Research 56 (2), 103–106.

Kooijman, S. A. L. M., 2010. Dynamic Energy Budget theory for metabolic organization. Cambridge, UK, third edition. University Press.

Kooijman, S. A. L. M., subm. Metabolic acceleration in animal ontogeny: an evolutionary perspective. Submitted to Journal of Sea Research.

Kooijman, S. A. L. M., Pecquerie, L., Augustine, S., Jusup, M., 2011. Scenarios for acceleration in fish development and the role of metamorphosis. Journal of Sea Research 66 (4), 419–423.

Kroeker, K. J., Kordas, R. L., Crim, R. N., Singh, G. G., 2010. Meta-analysis reveals negative yet variable effects of ocean acidification on marine organisms. Ecology Letters 13 (11), 1419–1434.

LaBarbera, M., 1984. Feeding currents and particle capture mechanisms in suspension feeding animals. American Zoologist 24 (1), 71–84.

Laing, I., 2000. Effect of temperature and ration on growth and condition of king scallop *Pecten maximus* spat. Aquaculture 183 (3–4), 325–334.

Laing, I., 2002. Effect of salinity on growth and survival of king scallop spat *Pecten maximus*. Aquaculture 205 (1–2), 171–181.

Laing, I., 2004. Filtration of king scallops *Pecten maximus*. Aquaculture 240 (1–4), 369–384.

Lampert, L., 2001. Dynamique saisonnière et variabilité pigmentaire des populations phytoplanctoniques dans l'Atlantique Nord (Golfe de Gascogne). Seasonal dynamics and pigmentary variability of phytoplanktonic populations in the Northern Atlantic (bay of Biscay). Ph.D. thesis, University of Brest.

Langdon, C. J., Newell, R. I. E., 1990. Utilization of detritus and bacteria as food sources by two bivalve suspension-feeders, the oyster *Crassostrea virginica* and the mussel *Geukensia demissa*. Marine Ecology Progress Series 58, 299–310.

Larsen, P. S., Filgueira, R., Riisgård, H. U., 2014. Somatic growth of mussels *Mytilus edulis* in field studies compared to predictions using BEG, DEB, and SFG models. Journal of Sea Research (in press).

Lavaud, R., Flye-Sainte-Marie, J., Jean, F., Emmery, A., Strand, Ø., Kooijman, S. A. L. M., 2013. Feeding and energetics of the great scallop, *Pecten maximus*, through a DEB model. Journal of Sea Research (in press).

Lavaud, R., Rannou, E., Jean, F., Flye-Sainte-Marie, J., in prep. What the shell can tell about the scallop? insights from inverted deb model. Submitted for publication in Ecological Modelling.

Lavaud, R., Thébault, J., Lorrain, A., van der Geest, M., Chauvaud, L., 2012. *Senilia senilis* (Linnaeus, 1758), a biogenic archive of environmental conditions on the Banc d'Arguin (Mauritania). Journal of Sea Research 76, 61–72.

Lawrence, A. J., Soame, J. M., 2004. The effects of climate change on the reproduction of coastal invertebrates. Ibis 146 (s1), 29–39.

Lazure, P., Dumas, F., 2008. An external-internal mode coupling for a 3D hydrodynamical model for applications at regional scale (MARS). Advances in Water Resources 31 (2), 233–250.

Lazure, P., Garnier, V., Dumas, F., Herry, C., Chifflet, M., 2009. Development of a hydrodynamic model of the Bay of Biscay. Validation of hydrology. Continental Shelf Research 29 (8), 985–997.

Le Boyer, A., Charria, G., Le Cann, B., Lazure, P., Marié, L., 2013. Circulation on the shelf and the upper slope of the Bay of Biscay. Continental Shelf Research 55, 97–107.

Le Pennec, M., Beninger, P. G., Dorange, G., Paulet, Y.-M., 1991. Trophic sources and pathways to the developing gametes of *Pecten maximus* (Bivalvia: Pectinidae). Journal of the Marine Biological Association of the United Kingdom 71, 451–463.

Le Pennec, M., Paugam, A., Le Pennec, G., 2003. The pelagic life of the pectinid *Pecten maximus* – a review. ICES Journal of Marine Science: Journal du Conseil 60 (2), 211–233.

Lefort, S., Aumont, O., Bopp, L., Maury, O., Gehlen, M., 2013. Response of marine living resources to global climate change. ICES CM B:77.

Lett, C., Ayata, S.-D., Huret, M., Irisson, J.-O., 2010. Biophysical modelling to investigate the effects of climate change on marine population dispersal and connectivity. Progress in Oceanography 87 (1), 106–113.

Levinton, J., Ward, J. E., Shumway, S. E., 2002. Feeding responses of the bivalves *Crassostrea gigas* and *Mytilus trossulus* to chemical composition of fresh and aged kelp detritus. Marine Biology 141 (2), 367–376.

Lika, K., Kearney, M. R., Kooijman, S. A. L. M., 2011b. The "covariation method" for estimating the parameters of the standard Dynamic Energy Budget model II: Properties and preliminary patterns. Journal of Sea Research 66 (4), 278–288.

Lika, K., Kearney, M. R. Freitas, V., van der Veer, H. W., van der Meer, J., Wijsman, J. W. M., Pecquerie, L., , Kooijman, S. A. L. M., 2011a. The "covariation method" for estimating the parameters of the standard Dynamic Energy Budget model I: Philosophy and approach. Journal of Sea Research 66 (4), 270–277.

Liu, H., Kelly, M. S., Campbell, D. A., Fang, J., Zhu, J., 2008. Accumulation of domoic acid and its effect on juvenile king scallop *Pecten maximus* (Linnaeus, 1758). Aquaculture 284 (1–4), 224–230.

Llewellyn, C. A., Fishwick, J. R., Blackford, J. C., 2005. Phytoplankton community assemblage in the English Channel: a comparison using chlorophyll-*a* derived from HPLC-CHEMTAX and carbon derived from microscopy cell counts. Journal of Plankton Research 27 (1), 103–119.

López-Benito, M., 1956. Composición química de algunos moluscos y crustáceos de la ría de Vigo. Invest. Pesq. 4, 127–132.

Lorena, A., Marques, G. M., Kooijman, S. A. L. M., Sousa, T., 2010. Stylized facts in microalgal growth: interpretation in a dynamic energy budget context. Philosophical Transactions of the Royal Society B: Biological Sciences 365 (1557), 3509–3521.

Loret, P., Pastoureaud, A., Bacher, B., Delesallel, B., 2000. Phytoplankton composition and selective feeding of the pearl oyster *Pinctada margaritifera* in the Takapoto lagoon (Tuamotu Archipelago, French Polynesia): in situ study using optical microscopy and HPLC pigment analysis. Marine Ecology Progress Series 199, 55–67.

Lorrain, A., 2002. Utilisation de la coquille Saint-Jacques comme traceur environnemental: approches biologique et biogéochimique. The use of the great scallop's shell as an environmental tracer: biological and biochemical approaches. Ph.D. thesis, University of Brest.

Lorrain, A., Paulet, Y.-M., Chauvaud, L., Savoye, N., Donval, A., Saout, C., 2002. Differential $\delta^{13}$C and $\delta^{15}$N signatures among scallop tissues: implications for ecology and physiology. Journal of Experimental Marine Biology and Ecology 275 (1), 47–61.

Lorrain, A., Paulet, Y.-M., Chauvaud, L., Savoye, N., Nézan, E., Guérin, L., 2000. Growth anomalies in *Pecten maximus* from coastal waters (Bay of Brest, France): relationship with diatom blooms. Journal of the Marine Biological Association of the UK 80 (4), 667–673.

Louda, J. W., Neto, R. R., Magalhaes, A. R. M., Schneider, V. F., 2008. Pigment alterations in the brown mussel *Perna perna*. Comparative Biochemistry and Physiology Part B: Biochemistry and Molecular Biology 150 (4), 385–394.

Lubet, P., Besnard, J.-Y., Faveris, R., Robbins, I., 1987. Physiologie de la reproduction de la coquille Saint-Jacques (*Pecten maximus*, L.). Reproductive physiology of the scallop (*Pecten maximus*, L.). Oceanis 13 (3), 265–290.

Lucas, A., 1993. Bioénergétique des animaux aquatiques. Masson, Paris.

Maar, M., Bolding, K., Petersen, J. K., Hansen, J. L. S., Timmermann, K., 2009. Local effects of blue mussels around turbine foundations in an ecosystem model of Nysted off-shore wind farm, Denmark. Journal of Sea Research 62 (2), 159–174.

MacDonald, B. A., Bricelj, M. V., Shumway, S. E., 2006. Physiology: Energy acquisition and utilisation. In Scallops: Biology, Ecology and Aquaculture. Vol. 35. Sandra E. Shumway and G. Jay Parsons, Editors. Elsevier, Developments in aquaculture and fisheries science, Ch. 7, pp. 417–492.

MacDonald, B. A., Thompson, R. J., 1986. Influence of temperature and food availability on the ecological energetics of the giant scallop *Placopecten magellanicus*. Marine Biology 93 (1), 37–48.

MacDonald, B. A., Ward, J. E., 2009. Feeding activity of scallops and mussels measured simultaneously in the field: Repeated measures sampling and implications for modelling. Journal of Experimental Marine Biology and Ecology 371 (1), 42–50.

Mackey, M. D., Mackey, D. J., Higgins, H. W., Wright, S. W., 1996. CHEMTAX a program for estimating class abundances from chemical markers: application to HPLC measurements of phytoplankton. Marine Ecology Progress Series 14 (1), 265–283.

Mackie, L. A., Ansell, A. D., 1993. Differences in reproductive ecology in natural and transplanted populations of *Pecten maximus*: evidence for the existence of separate stocks. Journal of Experimental Marine Biology and Ecology 169 (1), 57–75.

Magnesen, T., Christophersen, G., 2008. Reproductive cycle and conditioning of translocated scallops *Pecten maximus* from five broodstock populations in Norway. Aquaculture 285 (1–4), 109–116.

Mansour, M. P., Frampton, D. M. F., Nichols, P. D., Volkman, J. K., Blackburn, S. I., 2005. Lipid and fatty acid yield of nine stationary-phase microalgae: Applications and unusual C24-C28 polyunsaturated fatty acids. Journal of Applied Phycology 17 (4), 287–300.

Marín Leal, J. C., Dubois, S., Orvain, F., Galois, R., Blin, J.-L., Ropert, M., Bataillé, M.-P., Ourry, A., Lefebvre, S., 2008. Stable isotopes ($\delta^{13}$C, $\delta^{15}$N) and modelling as tools to estimate the trophic ecology of cultivated oysters in two contrasting environments. Marine Biology 153 (4), 673–688.

Martin, B. T., 2013. Linking individual-based models and Dynamic Energy Budget Theory: lessons for ecology and ecotoxicology. Ph.D. thesis, Vrije Universitet Amsterdam and University of Potsdam.

Mason, J., 1957. The age and growth of the scallop, *Pecten maximus* (L.), in Manx waters. Journal of the Marine Biological Association of the United Kingdom 36 (3), 473–492.

Mason, J., 1958. The breeding of the scallop, *Pecten maximus* (L.), in Manx waters. Journal of the Marine Biological Association of the United Kingdom 37 (3), 653–671.

Mason, J., 1983. Scallop and queen fisheries in the British Isles. Fishing News Books Ltd (Buckland Foundation), Farnham, UK.

Mathers, N. F., 1976. The effects of tidal currents on the rhythm of feeding and digestion in *Pecten maximus* (L.). Journal of Experimental Marine Biology and Ecology 24 (3), 271–283.

Maury, O., Shin, Y.-J., Faugeras, B., Ben Ari, T., Marsac, F., 2007. Modeling environmental effects on the size-structured energy flow through marine ecosystems. Part 2: Simulations. Progress in Oceanography 74 (4), 500–514.

McCarthy, H. R., Luo, Y., Wullschleger, S. D., 2012. Integrating empirical-modeling approaches to improve understanding of terrestrial ecology processes. New Phytologist 195 (3), 523–525.

McCave, I., 1975. Vertical flux of particles in the ocean. Deep Sea Research and Oceanographic Abstracts 22 (7), 491–502.

McHenery, J. G., Allen, J. A., Birkbeck, T. H., 1986. Distribution of lysozyme-like activity in 30 bivalve species. Comparative Biochemistry and Physiology Part B: Comparative Biochemistry 85 (3), 581–584.

McHenery, J. G., Birkbeck, T. H., 1985. Uptake and processing of cultured microorganisms by bivalves. Journal of Experimental Marine Biology and Ecology 90 (2), 145–163.

McHenery, J. G., Birkbeck, T. H., Allen, J. A., 1979. The occurrence of lysozyme in marine bivalves. Comparative Biochemistry and Physiology Part B: Comparative Biochemistry 63 (1), 25–28.

Ménesguen, A., Cugier, P., Leblond, I., 2006. A new numerical technique for tracking chemical species in a multi-source, coastal ecosystem, applied to nitrogen causing Ulva blooms in the Bay of Brest (France). Limnology and oceanography 51 (1), 591–601.

Møhlenberg, F., Riisgård, H. U., 1978. Efficiency of particle retention in 13 species of suspension feeding bivalves. Ophelia 17, 239–246.

Morel, F. M. M., 1987. Kinetics of nutrients uptake and growth in phytoplankton. Journal of Phycology 23 (1), 137–150.

Mueller, E. N., Wainwright, J., Parsons, A. J., Turnbull, L., Millington, J. D. A., Papanastasis, V. P., 2014. Land degradation in drylands: Reevaluating pattern-process interrelationships and the role of ecogeomorphology. In Patterns of Land Degradation in Drylands. Mueller, E. N., Wainwright, J., Parsons, A. J. and Turnbull, L. ed., pp. 367–383.

Muller, E. B., Nisbet, R. M., 2000. Survival and production in variable resource environments. Bulletin of Mathematical Biology 62 (6), 1163–1189.

Muller, E. B., Nisbet, R. M., 2014. Dynamic Energy Budget modeling reveals the potential of future growth and calcification for the coccolithophore *Emiliania huxleyi* in an acidified ocean. Global Change Biology (in press).

Murphy, L. S., Haugen, E. M., 1985. The distribution and abundance of phototrophic ultraplankton in the North Atlantic. Limnology and oceanography 30 (1), 47–58.

Nair, N. B., 1962. Ecology of marine fouling and wood-boring organisms of western Norway. Sarsia 8 (1), 1–88.

Napolitano, G. E., Ackman, R. G., Silva-Serra, M. A., 1993. Incorporation of dietary sterols by the sea scallop *Placopecten magellanicus* (Gmelin) fed on microalgae. Marine Biology 117, 647–654.

Navarro, J. M., Leiva, G. E., Martinez, G., Aguilera, C., 2000. Interactive effects of diet and temperature on the scope for growth of the scallop *Argopecten purpuratus* during reproductive conditioning. Journal of Experimental Marine Biology and Ecology 247 (1), 67–83.

Nebel, S., 2012. Animal migration. Nature Education Knowledge 10 (29), 17.

Nerot, C., 2011. Invertébrés benthiques et biomarqueurs: témoins du fonctionnement trophique de l'écosystème côtier. Benthic invertebrates and biomarkers: whitnesses of coastal ecosystem trophic functionning. Ph.D. thesis, University of Brest.

Nerot, C., Lorrain, A., Grall, J., Gillikin, D. P., Munaron, J.-M., Le Bris, H., Paulet, Y.-M., 2012. Stable isotope variations in benthic filter feeders across a large depth gradient on the continental shelf. Estuarine, Coastal and Shelf Science 96, 228–235.

Neville, A. C., 1967. Daily growth layers in animals and plants. Biological Reviews 42 (3), 421–439.

Nicolas, L., Robert, R., 2001. The effect of food supply on metamorphosis and post-larval development in hatchery-reared *Pecten maximus*. Aquaculture 192 (2), 347–359.

Nicolle, A., Dumas, F., Foveau, A., Foucher, E., Thiébaut, E., 2013. Modelling larval dispersal of the king scallop (*Pecten maximus*) in the English Channel: examples from the bay of Saint-Brieuc and the bay of Seine. Ocean Dynamics 63 (6), 661–678.

Nisbet, R. M., McCauley, E., Johnson, L. R., 2010. Dynamic energy budget theory and population ecology: lessons from Daphnia. Philosophical Transactions of the Royal Society B: Biological Sciences 365 (1557), 3541–3552.

Nisbet, R. M., Muller, E. B., Lika, K., Kooijman, S. A. L. M., 2000. From molecules to ecosystems through dynamic energy budget models. Journal of Animal Ecology 69 (6), 913–926.

Norman, M., Román, G., Strand, Ø., 2006. European aquaculture. In Scallops: Biology, Ecology and Aquaculture. Vol. 35. Sandra E. Shumway and G. Jay Parsons, Editors. Elsevier, Developments in aquaculture and fisheries science, Ch. 20, pp. 1059–1066.

Octave community, 2012. GNU/Octave. www.gnu.org/software/octave/.

Olive, P. J. W., Clark, S., Lawrence, A., 1990. Global warming and seasonal reproduction: perception and transduction of environmental information. Advances in Invertebrate Reproduction 5, 265–270.

Oliver, P. G., 1979. Adaptations of some deep-sea suspension-feeding bivalves (Limopsis and Bathyarca). Sarsia 64 (1-2), 33–36.

Owen, R., Kennedy, H., Richardson, C., 2002a. Isotopic partitioning between scallop shell calcite and seawater: Effect of shell growth rate. Geochimica et Cosmochimica Acta 66 (10), 1727–1737.

Owen, R., Kennedy, H., Richardson, C., 2002b. Experimental investigation into partitioning of stable isotopes between scallop (*Pecten maximus*) shell calcite and sea water. Palaeogeography, Palaeoclimatology, Palaeoecology 185 (1), 163–174.

Owen, R., Richardson, C., Kennedy, H., 2002c. The influence of shell growth rate on striae deposition in the scallop *Pecten maximus*. Journal of the Marine Biological Association of the United Kingdom 82 (4), 621–623.

Palmer, A. R., 1994. Temperature sensitivity, rate of development, and time to maturity: geographic variation in laboratory-reared *Nucella* and a cross-phyletic overview. In Reproduction and development of marine invertebrates. W.H. Wilson, S.A. Stricker and G.L. Shinn, Editors. Johns Hopkins University Press, Baltimore, Md, pp. 177–194.

Parrish, C. C., 2013. Lipids in marine ecosystems. ISRN Oceanography 2013, 16.

Parrish, C. C., McKenzie, C. H., MacDonald, B. A., Hatfield, E. A., 1995. Seasonal studies of seston lipids in relation to microplankton species composition and scallop growth in South Broad Cove, Newfoundland. Marine Ecology Progress Series 129, 151–164.

Parsons, K. E., 1997. Contrasting patterns of heritable geographic variation in shell morphology and growth potential in the marine gastropod *Bembicium vittatum*: evidence from field experiments. Evolution, 784–796.

Pastoureaud, A., Heral, M., Prou, J., Razet, D., Russu, P., 1995. Particle selection in the oyster *Crassostrea gigas* (Thunberg) studied by pigment HPLC analysis under natural food conditions. Aquaculture 19 (1), 79–88.

Patry, Y., 2009. Variation de la croissance journalière et de la forme chez *Pecten maximus*: impact de l'environnement, depuis l'échelle saisonnière à celle de la vie, le long de gradients latitudinaux et bathymétriques. Daily growth and shape variations in *Pecten maximus*: environmental impact, from seasonal to life scale, along latitudinal and bathymetric gradients. Ph.D. thesis, University of Brest.

Paulet, Y.-M., Bekhadra, F., Devauchelle, N., Donval, A., Dorange, G., 1995. Cycles saisonniers, reproduction et qualité des ovocytes chez *Pecten maximus* en rade de Brest. Seasonal cycles, reproduction and oocytes quality of *Pecten maximus* in the Bay of Brest. 3e Rencontres Scientifiques Internationales du contrat de baie de la rade de Brest, Brest, 14–16 March 1995.

Paulet, Y.-M., Bekhadra, F., Devauchelle, N., Donval, A., Dorange, G., 1997. Seasonal cycles, reproduction and oocyte quality in *Pecten maximus* from the Bay of Brest. Annales de l'Institut océanographique 73 (1), 101–112.

Paulet, Y.-M., Fifas, S., 1989. Etude de la fécondité potentielle de la coquille Saint-Jacques *Pecten maximus*, en baie de Saint-Brieuc. Study of the potential fecundity of the great scallop *Pecten maximus*, in the Bay of Saint-Brieuc. Haliotis (19), 275–285.

Paulet, Y.-M., Lorrain, A., Richard, J., Pouvreau, S., 2006. Experimental shift in diet $\delta^{13}$C: A potential tool for ecophysiological studies in marine bivalves. Organic Geochemistry 37 (10), 1359–1370.

Paulet, Y.-M., Lucas, A., Gérard, A., 1988. Reproduction and larval development in two *Pecten maximus* (L.) populations from Brittany. Journal of Experimental Marine Biology and Ecology 119 (2), 145–156.

Payne, B. S., Miller, A. C., Hubertz, E. D., Lei, J., 1995a. Adaptive variation in palp and gill size of the zebra mussel (*Dreissena polymorpha*) and Asian clam (*Corbicula fluminea*). Canadian Journal of Fisheries and Aquatic Sciences 52 (5), 1130–1134.

Payne, B. S., Miller, A. C., Lei, J., 1995b. Palp to gill area ratio of bivalves: a sensitive indicator of elevated suspended solids. Regulated Rivers: Research & Management 11 (2), 193–200.

Pazos, A. J., Román, G., Acosta, C. P., Abad, M., Sánchez, J. L., 1997. Seasonal changes in condition and biochemical composition of the scallop *Pecten maximus* (L.) from suspended culture in the Ria de Arousa (Galicia, N.W. Spain) in relation to environmental conditions. Journal of Experimental Marine Biology and Ecology 211 (2), 169–193.

Peña, J. B., 2001. Taxonomía, morfología, distribución y hábitat de los pectínidos iberoamericanos. Los moluscos pectínidos de Iberoamérica: Ciencia y Acuicultura, 1–25.

Pecquerie, L., 2007. Modélisation bioénergétique de la croissance, du développement et de la reproduction d'un petit pélagique: l'anchois du golfe de Gascogne. Bioenergetic modelling of the growth, development and reproduction of a small pelagic fish: the bay of Biscay anchovy. Ph.D. thesis, Agrocampus Rennes.

Pecquerie, L., Fablet, R., De Pontual, H., Bonhommeau, S., Alunno-Bruscia, M., Petitgas, P., Kooijman, S. A. L. M., 2012. Reconstructing individual food and growth histories from biogenic carbonates. Marine Ecology Progress Series 447, 151–164.

Pecquerie, L., Petitgas, P., Kooijman, S. A. L. M., 2009. Modeling fish growth and reproduction in the context of the Dynamic Energy Budget theory to predict environmental impact on anchovy spawning duration. Journal of Sea Research 62 (2–3), 93–105.

Peirson, W. M., 1983. Utilization of eight algal species by the bay scallop, *Argopecten irradians concentricus* (Say). Journal of Experimental Marine Biology and Ecology 68 (1), 1–11.

Perry, G. J., Volkman, J. K., Johns, R. B., Bavor Jr, H. J., 1979. Fatty acids of bacterial origin in contemporary marine sediments. Geochimica et Cosmochimica Acta 43 (11), 1715–1725.

Persson, P.-O., Strang, G., 2003. Smoothing by Savitzky-Golay and Legendre filters. In Mathematical Systems Theory in Biology, Communications, Computation, and Finance. Joachim Rosenthal and David S. Gilliam eds., pp. 301–315.

Peters, R. H., 1986. The ecological implications of body size. Vol. 2. Cambridge University Press.

Pethybridge, H., Roos, D., Loizeau, V., Pecquerie, L., Bacher, C., 2013. Responses of European anchovy vital rates and population growth to environmental fluctuations: An individual-based modeling approach. Ecological Modelling 250, 370–383.

Piersma, T., Drent, J., 2003. Phenotypic flexibility and the evolution of organismal design. Trends in Ecology & Evolution 18 (5), 228–233.

Pingree, R. D., Mardell, G. T., Holligan, P. M., Griffiths, D. K., Smithers, J., 1982. Celtic Sea and Armorican current structure and the vertical distributions of temperature and chlorophyll. Continental Shelf Research 1 (1), 99–116.

Pitel, M., Berthou, P., Fifas, S., 2001. Dredge designs and fisheries. Report from the ECODREDGE program.

Pittendrigh, C. S., 1993. Temporal organization: reflections of a darwinian clock-watcher. Annual Review of Physiology 55 (1), 17–54.

Polovina, J. J., Howell, E. A., Abecassis, M., 2008. Ocean's least productive waters are expanding. Geophysical Research Letters 35 (3), L03618.

Posgay, J. A., Merrill, A. S., 1979. Age and growth data for the Atlantic coast sea scallop, *Placopecten magellanicus*. National Marine Fisheries Service-North East Fishery Center (NMFS-NEFC). Laboratory Reference Document, 58–79.

Pouvreau, S., Bacher, C., Héral, M., 2000. Ecophysiological model of growth and reproduction of the black pearl oyster, *Pinctada margaritifera*: potential applications for pearl farming in French Polynesia. Aquaculture 186 (1), 117–144.

Pouvreau, S., Bourlès, Y., Lefebvre, S., Gangnery, A., Alunno-Bruscia, M., 2006. Application of a dynamic energy budget model to the Pacific oyster, *Crassostrea gigas*, reared under various environmental conditions. Journal of Sea Research 56 (2), 156–167.

Powell, E. N., Hofmann, E. E., Klinck, J. M., Ray, S. M., 1992. Modeling oyster populations: I. A commentary on filtration rate. Is faster always better? Journal of Shellfish Research 11 (2), 387–398.

Prieur, D., Mevel, G., Nicolas, J. L., Plusquellec, A., Vigneulle, M., 1990. Interactions between bivalve molluscs and bacteria in the marine environment. Oceanography Marine Biology Annual Revue 28, 277–352.

Quéguiner, B., Tréguer, P., 1984. Studies on the phytoplankton in the Bay of Brest (western Europe). Seasonal variations in composition, biomass and production in relation to hydrological and chemical features (1981–1982). Botanica Marina 27, 449–459.

Raby, D., Mingelbier, M., Dodson, J. J., Klein, B., Lagadeuc, Y., Legendre, L., 1997. Food-particle size and selection by bivalve larvae in a temperate embayment. Marine Biology 127, 665–672.

Ragueneau, O., De Blas Varela, E., Treguer, P., Quéguiner, B., Del Amo, Y., 1994. Phytoplankton dynamics in relation to the biogeochemical cycle of silicon in a coastal ecosystem of western Europe. Marine Ecology Progress Series 106, 157–157.

Raikow, D. F., Hamilton, S. K., 2001. Bivalve diets in a midwestern US stream: a stable isotope enrichment study. Limnology and Oceanography 46 (3), 514–522.

Rannou, E., 2009. Discovering and learning DEB theory through the Growth DEB equation. DEB Theory Symposium 2009: 30 years of research for metabolic organization. Brest, France, 19–22 April 2009.

Reid, P. C., Lancelot, C., Gieskes, W. W. C., Hagmeier, E., Weichart, G., 1990. Phytoplankton of the North Sea and its dynamics: a review. Netherlands Journal of Sea Research 26 (2), 295–331.

Ren, J. S., Ross, A. H., 2005. Environmental influence on mussel growth: A dynamic energy budget model and its application to the greenshell mussel *Perna canaliculus*. Ecological Modelling 189 (3–4), 347–362.

Renaud, S. M., Thinh, L.-V., Lambrinidis, G., Parry, D. L., 2002. Effect of temperature on growth, chemical composition and fatty acid composition of tropical Australian microalgae grown in batch cultures. Aquaculture 211 (1), 195–214.

Richard, J., 2005. *Crepidula fornicata*: un modèle biologique pour l'étude du rôle de la variabilité des caractères phénotypiques (reproduction, croissance et nutrition) sur les processus de colonisation en milieu marin. *Crepidula fornicata*: a biological model to study the role of phenotypic variability (reproduction, growth, nutrition) on the colonisation processes in the marine environment. Ph.D. thesis, Université de Genève.

Ricker, W., 1975. Computation and interpretation of biological statistics of fish populations. Bulletin of the Fisheries Research Board of Canada 191, 382.

Riebesell, U., 1991. Particle aggregation during a diatom bloom. II. Biological aspects. Marine Ecology Progress Series 69, 281–291.

Ries, J. B., Cohen, A. L., McCorkle, D. C., 2009. Marine calcifiers exhibit mixed responses to $CO_2$-induced ocean acidification. Geology 37 (12), 1131–1134.

Riisgård, H. U., 2001. On measurement of filtration rates in bivalves – the stony road to reliable data: review and interpretation. Marine Ecology Progress Series 211, 275–291.

Robert, R., Moal, J., Campillo, M.-J., Daniel, J.-Y., 1994. The food value of starch rich flagellates for *Pecten maximus* (L.) larvae. Preliminary results. Haliotis 23, 169–710.

Robert, R., Nicolas, L., 2000. The effect of seawater flow and temperature on metamorphosis and postlarval development in great scallop. Aquaculture International 8 (6), 513–530.

Roditi, H. A., Fisher, N. S., Sañudo-Wilhelmy, S. A., 2000. Uptake of dissolved organic carbon and trace elements by zebra mussels. Nature 407 (6800), 78–80.

Rokop, F. J., 1974. Reproductive patterns in the deep-sea benthos. Science 186 (4165), 743–745.

Ropes, J. W., Murawski, S. A., 1983. Maximum shell length and longevity in ocean quahogs, *Arctica islandica* Linne. ICES CM 1983, 8.

Rosa, M., Ward, J. E., Shumway, S. E., Wikfors, G. H., Pales-Espinosa, E., Allam, B., 2013. Effects of particle surface properties on feeding selectivity in the eastern oyster *Crassostrea virginica* and the blue mussel *Mytilus edulis*. Journal of Experimental Marine Biology and Ecology 446, 320–327.

Rosland, R., Strand, Ø., Alunno-Bruscia, M., Bacher, C., Strohmeier, T., 2009. Applying Dynamic Energy Budget (DEB) theory to simulate growth and bioenergetics of blue mussels under low seston conditions. Journal of Sea Research 62 (2–3), 49–61.

Ross, A. H., Nisbet, R. M., 1990. Dynamic models of growth and reproduction of the mussel *Mytilus edulis* L. Functional Ecology 4, 777–787.

Rossi, F., Herman, P. M. J., Middelburg, J. J., 2004. Interspecific and intraspecific variation of $\delta^{13}$C and $\delta^{15}$N in deposit- and suspension-feeding bivalves (*Macoma balthica* and *Cerastoderma edule*): Evidence of ontogenetic changes in feeding mode of *Macoma balthica*. Limnology and Oceanography 49 (2), 408–414.

Royer, C., Thébault, J., Chauvaud, L., Olivier, F., 2013. Structural analysis and palaeoenvironmental potential of dog cockle shells *Glycymeris glycymeris* in Brittany, northwest France. Palaeogeography, Palaeoclimatology, Palaeoecology 373, 123–132.

Rubenstein, D. I., Koehl, M. A. R., 1977. The mechanisms of filter feeding: some theoretical considerations. American Naturalist 111 (981), 981–994.

Samain, J. F., Cochard, J. C., Chevolot, L., Daniel, J. Y., Jeanthon, C., Le Coz, J. R., Marty, Y., Moal, J., Prieur, D., Salaun, M., 1986. Effect of sea water quality on larval growth of *Pecten maximus* in a hatchery: preliminary results. Haliotis (16), 363–381.

Saout, C., 2000. Contrôle de la reproduction chez *Pecten maximus* (L.): Etudes in situ et expérimentales. The control of reproduction in *Pecten maximus* (L.): in situ and experimental studies. Ph.D. thesis, University of Brest.

Saout, C., Quéré, C., Donval, A., Paulet, Y.-M., Samain, J.-F., 1999. An experimental study of the combined effects of temperature and photoperiod on reproductive physiology of *Pecten maximus* from the Bay of Brest (France). Aquaculture 172 (3–4), 301–314.

Sarà, G., Reid, G. K., Rinaldi, A., Palmeri, V., Troell, M., Kooijman, S. A. L. M., 2012. Growth and reproductive simulation of candidate shellfish species at fish cages in the Southern Mediterranean: Dynamic Energy Budget (DEB) modelling for integrated multi-trophic aquaculture. Aquaculture 324–325, 259–266.

Saraiva, S., van der Meer, J., Kooijman, S. A. L. M., Sousa, T., 2011a. Modelling feeding processes in bivalves: A mechanistic approach. Ecological Modelling 222 (3), 514–523.

Saraiva, S., van der Meer, J., Kooijman, S. A. L. M., Sousa, T., 2011b. DEB parameters estimation for *Mytilus edulis*. Journal of Sea Research 66 (4), 289–296.

Sathyendranath, S., Longhurst, A., Caverhill, C. M., Platt, T., 1995. Regionally and seasonally differentiated primary production in the North Atlantic. Deep Sea Research Part I: Oceanographic Research Papers 42 (10), 1773–1802.

Savina, M., Ménesguen, A., 2008. A deterministic population dynamics model to study the distribution of a benthic bivalve with planktonic larvae (*Paphia rhomboïdes*) in the English Channel (NW Europe). Journal of Marine Systems 70 (1–2), 63–76.

Schick, D. F., Shumway, S. E., Hunter, M. A., 1988. A comparison of growth rate between shallow water and deep water populations of scallops, *Placopecten magellanicus* (Gmelin, 1791), in the Gulf of Maine. American Malacological Bulletin 6 (1), 1–8.

Schmidt-Nielsen, K., 1997. Animal physiology: adaptation and environment. Cambridge University Press.

Scholten, H., Smaal, A. C., 1998. Responses of *Mytilus edulis* L. to varying food concentrations: testing EMMY, an ecophysiological model. Journal of Experimental Marine Biology and Ecology 219 (1), 217–239.

Schöne, B. R., Wanamaker Jr., A. D., Fiebig, J., Thébault, J., Kreutz, K., 2011. Annually resolved $\delta^{13}$C shell chronologies of long-lived bivalve mollusks (*Arctica islandica*) reveal oceanic carbon dynamics in the temperate North Atlantic during recent centuries. Palaeogeography, Palaeoclimatology, Palaeoecology 302 (1-2), 31–42.

Shephard, S., Beukers-Stewart, B., Hiddink, J. G., Brand, A. R., Kaiser, M. J., 2010. Strengthening recruitment of exploited scallops *Pecten maximus* with ocean warming. Marine Biology 157 (1), 91–97.

Shuman, F. R., Lorenzen, C. J., 1975. Quantitative degradation of chlorophyll by a marine herbivore. Limnology and Oceanography 20 (4), 580–586.

Shumway, S. E., Cucci, T. L., 1987. The effects of the toxic dinoflagellate *Protogonyaulax tamarensis* on the feeding and behaviour of bivalve molluscs. Aquatic toxicology 10 (1), 9–27.

Shumway, S. E., Cucci, T. L., Newell, R. C., Yentsch, C. M., 1985. Particle selection, ingestion, and absorption in filter-feeding bivalves. Journal of Experimental Marine Biology and Ecology 91 (1), 77–92.

Shumway, S. E., Parsons, G. J., 2006. Scallops: Biology, Ecology and Aquaculture. Vol. 35. Sandra E. Shumway and G. Jay Parsons, Editors. Elsevier, Developments in Aquaculture and Fisheries Science.

Shumway, S. E., Selvin, R., Schick, D. F., 1987. Food resources related to habitat in the scallop *Placopecten magellanicus* (Gmelin, 1791): a qualitative study. Journal of Shellfish Research 6 (2), 89–95.

Silvester, N. R., Sleigh, M. A., 1984. Hydrodynamic aspects of particle capture by *Mytilus*. Journal of the Marine Biological Association of the United Kingdom 64 (4), 859–879.

Smaal, A. C., Prins, T. C., Dankers, N. M. J. A., Ball, B., 1997. Minimum requirements for modelling bivalve carrying capacity. Aquatic Ecology 31 (4), 423–428.

Smetacek, V. S., 1985. Role of sinking in diatom life-history cycles: ecological, evolutionary and geological significance. Marine Biology 84 (3), 239–251.

Smith, K. L., Teal, J. M., 1973. Deep-sea benthic community respiration: an in situ study at 1850 meters. Science 179 (4070), 282–283.

Smith, T. M., Reynolds, R. W., 2003. Extended reconstruction of global sea surface temperatures based on COADS data (1854–1997). Journal of Climate 16 (10), 1495–1510.

Smith, T. M., Reynolds, R. W., Livezey, R. E., Stokes, D. C., 1996. Reconstruction of historical sea surface temperatures using empirical orthogonal functions. Journal of Climate 9 (6), 1403–1420.

Smolowitz, R., Shumway, S. E., 1997. Possible cytotoxic effects of the dinoflagellate, *Gyrodinium aureolum*, on juvenile bivalve molluscs. Aquaculture International 5 (4), 291–300.

Solidoro, C., Pastres, R., Melaku Canu, D., Pellizzato, M., Rossi, R., 2000. Modelling the growth of *Tapes philippinarum* in northern Adriatic lagoons. Marine Ecology Progress Series 199, 137–148.

Soudant, P., Le Coz, J.-R., Marty, Y., Moal, J., Robert, R., Samain, J.-F., 1998a. Incorporation of microalgae sterols by scallop *Pecten maximus* (L.) larvae. Comparative Biochemistry and Physiology Part A: Molecular & Integrative Physiology 119 (2), 451–457.

Soudant, P., Marty, Y., Moal, J., Masski, H., Samain, J.-F., 1998b. Fatty acid composition of polar lipid classes during larval development of scallop *Pecten maximus* (L.). Comparative Biochemistry and Physiology Part A: Molecular & Integrative Physiology 121 (3), 279–288.

Soudant, P., Marty, Y., Moal, J., Robert, R., Quéré, C., Le Coz, J.-R., Samain, J.-F., 1996. Effect of food fatty acid and sterol quality on *Pecten maximus* gonad composition and reproduction process. Aquaculture 143 (3–4), 361–378.

Soudant, P., Marty, Y., Moal, J., Samain, J.-F., 1995. Separation of major polar lipids in *Pecten maximus* by high-performance liquid chromatography and subsequent determination of their fatty acids using gas chromatography. Journal of Chromatography B: Biomedical Sciences and Applications 673 (1), 15–26.

St. John, M., Lund, T., 1996. Lipid biomarkers: linking the utilization of frontal plankton biomass to enhanced condition of juvenile North Sea cod. Marine Ecology Progress Series 131 (1–3), 75–85.

Stockwell, J. D., Johnson, B. M., 1997. Refinement and calibration of a bioenergetics-based foraging model for kokanee (*Oncorhynchus nerka*). Canadian Journal of Fisheries and Aquatic Sciences 54 (11), 2659–2676.

Stramma, L., Johnson, G. C., Sprintall, J., Mohrholz, V., 2008. Expanding oxygen-minimum zones in the tropical oceans. science 320 (5876), 655–658.

Strand, Ø., Brynjeldsen, E., 2003. On the relationship between low winter temperatures and mortality of juvenile scallops, *Pecten maximus* (L.), cultured in western Norway. Aquaculture Research 34 (15), 1417–1422.

Strand, Ø., Nylund, A., 1991. The reproductive cycle of the scallop *Pecten maximus* (Linnaeus, 1758) from two populations in western Norway, 60N and 64N. In An International Compendium of Scallop Biology and Culture. Special Publication. World Aquaculture Society, 95–105.

Strand, Ø., Parsons, G. J., 2006. Scandinavia. In Scallops: Biology, Ecology and Aquaculture. Vol. 35. Sandra E. Shumway and G. Jay Parsons, Editors. Elsevier, Developments in aquaculture and fisheries science, Ch. 21, pp. 1067–1092.

Strohmeier, T., 2009. Feeding behavior and bioenergetic balance of the great scallop *Pecten maximus* and the blue mussel *Mytilus edulis* in a low seston environment and relevance to suspended shellfish aquaculture. Ph.D. thesis, University of Bergen, Bergen.

Strohmeier, T., Duinker, A., Lie, Ø., 2000. Seasonal variation in chemical composition of the female gonad and storage organs in *Pecten maximus* (L.) suggesting that somatic and reproductive growth are separated in time. Journal of Shellfish Research 19 (2), 741–747.

Strohmeier, T., Strand, Ø., Alunno-Bruscia, M., Duinker, A., Cranford, P. J., 2012. Variability in particle retention efficiency by the mussel *Mytilus edulis*. Journal of Experimental Marine Biology and Ecology 412, 96–102.

Strohmeier, T., Strand, Ø., Cranford, P., 2009. Clearance rates of the great scallop *Pecten maximus* and blue mussel *Mytilus edulis* at low natural seston concentrations. Marine Biology 156 (9), 1781–1795.

Stuart, V., Klumpp, D. W., 1984. Evidence for food-resource partitioning by kelp-bed filter feeders. Marine Ecology Progress Series 16 (1), 27–37.

Suquet, M., Cosson, J., Donval, A., Labbe, C., Boulais, M., Haffray, P., Bernard, I., Fauvel, C., 2012. Marathon vs sprint racers: an adaptation of sperm characteristics to the reproductive strategy of pacific oyster, turbot and seabass. Journal of Applied Ichthyology 28 (6), 956–960.

Taasen, J. P., Høisæter, T., 1981. The shallow-water soft-bottom benthos in Lindåspollene, western Norway: 4. Benthic marine diatoms, seasonal density fluctuations. Sarsia 66 (4), 293–316.

Tang, S.-F., 1941. The breeding of the scallop (*Pecten maximus* L.) with a note on the growth rate. Proceedings of the Liverpool Biological Society, Liverpool 54, 9–28.

Taylor, F. J., Taylor, N. J., Walsby, J. R., 1985. A bloom of the planktonic diatom, *Cerataulina pelagica*, off the coast of northeastern New Zealand in 1983, and its contribution to an associated mortality of fish and benthic fauna. Internationale Revue der gesamten Hydrobiologie und Hydrographie 70 (6), 773–795.

Tebble, N., 1966. British bivalve seashells. A handbook for identification. Trustees of the British Museum (Natural History) London. Alden Press, Oxford.

Thébault, J., Chauvaud, L., 2013. Li/Ca enrichments in great scallop shells (*Pecten maximus*) and their relationship with phytoplankton blooms. Palaeogeography, Palaeoclimatology, Palaeoecology 373, 108–122.

Thébault, J., Chauvaud, L., L'Helguen, S., Clavier, J., Barats, A., Jacquet, S., Pécheyran, C., Amouroux, D., 2009. Barium and molybdenum records in bivalve shells: Geochemical proxies for phytoplankton dynamics in coastal environments? Limnology and Oceanography 54 (3), 1002–1014.

Theisen, B. F., 1973. The growth of *Mytilus edulis* L. (Bivalvia) from Disko and Thule district, Greenland. Ophelia 12 (1–2), 59–77.

Theisen, B. F., 1982. Variation in size of gills, labial palps, and adductor muscle in *Mytilus edulis* L. (Bivalvia) from Danish waters. Ophelia 21 (1), 49–63.

Thiel, H., Pörtner, H.-O., Arntz, W. E., 1996. Marine life at low temperatures – a comparison of polar and deep-sea characteristics. Deep-sea and extreme shallow-water habitats: affinities and adaptations. Biosystematics and Ecology Series 11, 183–219.

Thomas, Y., Garen, P., Pouvreau, S., 2011a. Application of a bioenergetic growth model to larvae of the pearl oyster *Pinctada margaritifera* L. Journal of Sea Research 66 (4), 331–339.

Thomas, Y., Mazurié, J., Alunno-Bruscia, M., Bacher, C., Bouget, J.-F., Gohin, F., Pouvreau, S., Struski, C., 2011b. Modelling spatio-temporal variability of *Mytilus edulis* (L.) growth by forcing a dynamic energy budget model with satellite-derived environmental data. Journal of Sea Research 66 (4), 308–317.

Thompson, R. J., MacDonald, B. A., 2006. Physiological integrations and energy partitioning. In Scallops: Biology, Ecology and Aquaculture. Vol. 35. Sandra E. Shumway and G. Jay Parsons, Editors. Elsevier, Developments in aquaculture and fisheries science, Ch. 8, pp. 493–520.

Thouzeau, G., 1991. Experimental collection of postlarvae of *Pecten maximus* (L.) and other benthic macrofaunal species in the Bay of Saint-Brieuc, France. II. Reproduction patterns and postlarval growth of five mollusc species. Journal of Experimental Marine Biology and Ecology 148 (2), 181–200.

Thouzeau, G., Chauvaud, L., Clavier, J., Donval, A., Guerin, L., Jean, F., Le Hir, M., Lorrain, A., Marc, R., Paulet, Y.-M., Raffin, C., Richard, J., Richard, M., 2002. La crépidule: identifier les mécanismes de sa prolifération et caractériser ses effets sur le milieu pour envisager sa gestion (Chantier: Rade de Brest). The slipper limpet: identifying the mechanisms of its proliferation and describe its effects on the environment in order to consider its management (Bay of Brest). Tech. rep.

Tomanek, L., 2010. Variation in the heat shock response and its implication for predicting the effect of global climate change on species' biogeographical distribution ranges and metabolic costs. The Journal of Experimental Biology 213 (6), 971–979.

Toupoint, N., Gilmore-Solomon, L., Bourque, F., Myrand, B., Pernet, F., Olivier, F., Tremblay, R., 2012. Match/mismatch between the *Mytilus edulis* larval supply and seston quality: effect on recruitment. Ecology 93 (8), 1922–1934.

Troost, T. A., Wijsman, J. W. M., Saraiva, S., Freitas, V., 2010. Modelling shellfish growth with dynamic energy budget models: an application for cockles and mussels in the Oosterschelde (Southwest Netherlands). Philosophical Transactions of the Royal Society B: Biological Sciences 365 (1557), 3567–3577.

Tully, O., Hervas, A., Berry, A., Hartnett, M., Sutton, G., O'Keeffe, E., Hickey, J., 2006. Monitoring and assessment of scallops off the south east coast of Ireland. Fisheries Resource Series (3).

Utting, S. D., Millican, P. F., 1998. The role of diet in hatchery conditioning of *Pecten maximus* (L.): a review. Aquaculture 165 (3–4), 167–178.

Vahl, O., 1985. Size-specific reproductive effort in *Chlamys islandica*: reproductive senility or stabilizing selection? Proceedings of the 19th European Marine Biology Symposium, Plymouth, Devon, UK, 16–21 September 1984.

van der Veer, H. W., Cardoso, J. F. M. F., van der Meer, J., 2006. The estimation of DEB parameters for various Northeast Atlantic bivalve species. Journal of Sea Research 56 (2), 107–124.

Van Voorhies, W. A., 1996. Bergmann size clines: a simple explanation for their occurrence in ectotherms. Evolution, 1259–1264.

Van Wynsberge, S., Andréfouët, S., Gilbert, A., Stein, A., Remoissenet, G., 2013. Best management strategies for sustainable giant clam fishery in French Polynesia islands: answers from a spatial modeling approach. PLoS ONE 8 (5), e64641.

Vaquer-Sunyer, R., Duarte, C. M., 2008. Thresholds of hypoxia for marine biodiversity. Proceedings of the National Academy of Sciences 105 (40), 15452–15457.

Vestal, J. R., White, D. C., 1989. Lipid analysis in microbial ecology. Bioscience 39 (8), 535–541.

Viso, A.-C., Marty, J.-C., 1993. Fatty acids from 28 marine microalgae. Phytochemistry 34 (6), 1521–1533.

Volkman, J. K., 1986. A review of sterol markers for marine and terrigenous organic matter. Organic Geochemistry 9 (2), 83–99.

Volkman, J. K., Barrett, S. M., Blackburn, S. I., Mansour, M. P., Sikes, E. L., Gelin, F., 1998. Microalgal biomarkers: A review of recent research developments. Organic Geochemistry 29 (5–7), 1163–1179.

Walker, R. L., Heffernan, P. B., 1996. Adult age-specific embryonic viability of the northern quahog. North American Journal of Fisheries Management 16 (3), 633–639.

Ward, J. E., Kach, D. J., 2009. Marine aggregates facilitate ingestion of nanoparticles by suspension-feeding bivalves. Marine Environmental Research 68 (3), 137–142.

Ward, J. E., Levinton, J. S., Shumway, S. E., Cucci, T., 1997. Site of particle selection in a bivalve mollusc. Nature 390 (6656), 131–132.

Ward, J. E., Levinton, J. S., Shumway, S. E., Cucci, T., 1998. Particle sorting in bivalves: in vivo determination of the pallial organs of selection. Marine Biology 131 (2), 283–292.

Ward, J. E., Shumway, S. E., 2004. Separating the grain from the chaff: particle selection in suspension- and deposit-feeding bivalves. Journal of Experimental Marine Biology and Ecology 300 (1–2), 83–130.

Warren, C. E., Davies, G. E., 1967. Laboratory studies on the feeding bioenergetics and growth of fishes. In The biological basis of freshwater fish production. S. D. Gerking, ed. Blackwell, Oxford, pp. 175–214.

Welladsen, H. M., Southgate, P. C., Heimann, K., 2010. The effects of exposure to near-future levels of ocean acidification on shell characteristics of *Pinctada fucata* (Bivalvia: Pteriidae). Molluscan Research 30 (3), 125–130.

West-Eberhard, M. J., 2003. Developmental plasticity and evolution. Oxford University Press.

Whitman, D. W., Agrawal, A. A., 2009. What is phenotypic plasticity and why is it important? In Phenotypic plasticity of insects: Mechanism and Consequences. Whitman, D. W. and T. N. Ananthakrishnan, Editors. Science Publishers. Enfield, NH, USA., pp. 1–63.

Widdows, J., Fieth, P., Worrall, C. M., 1979. Relationships between seston, available food and feeding activity in the common mussel *Mytilus edulis*. Marine Biology 50 (3), 195–207.

Wijsman, J. W. M., Smaal, A. C., 2011. Growth of cockles (*Cerastoderma edule*) in the Oosterschelde described by a Dynamic Energy Budget model. Journal of Sea Research 66 (4), 372–380.

Wijsman, J. W. M., Smaal, A. C., 2013. Growth of cockles (*Cerastoderma edule*) in the Oosterschelde described by a Dynamic Energy Budget model. Journal of Sea Research 66, 372–380.

Wilding, C. S., Beaumont, A. R., Latchford, J. W., 1997. Mitochondrial DNA variation in the scallop *Pecten maximus* (L.) assessed by a PCR-RFLP method. Heredity 79 (2), 178–189.

Wilding, C. S., Latchford, J. W., Beaumont, A. R., 1998. An investigation of possible stock structure in *Pecten maximus* (L.) using multivariate morphometrics, allozyme electrophoresis and mitochondrial DNA polymerase chain reaction-restriction fragment length polymorphism. Journal of Shellfish Research 17 (1), 131–140.

Woodin, S. A., Hilbish, T. J., Helmuth, B., Jones, S. J., Wethey, D. S., 2013. Climate change, species distribution models, and physiological performance metrics: predicting when biogeographic models are likely to fail. Ecology and Evolution 3 (10), 3334–3346.

Yokoyama, H., Sakami, T., Ishihi, Y., 2009. Food sources of benthic animals on intertidal and subtidal bottoms in inner Ariake Sound, southern Japan, determined by stable isotopes. Estuarine, Coastal and Shelf Science 82 (2), 243–253.

Zapata, M., Fraga, S., Rodríguez, F., Garrido, J. L., 2012. Pigment-based chloroplast types in dinoflagellates. Marine Ecology Progress Series 465, 33–52.

Zhukova, N. V., Aizdaicher, N. A., 1995. Fatty acid composition of 15 species of marine microalgae. Phytochemistry 39 (2), 351–356.

# List of publications

This thesis is based on the following publications and manuscripts:

**I. Lavaud R.**, Flye-Sainte-Marie J., Jean F., Emmery A., Strand Ø. and Kooijman S.A.L.M. (2013) Feeding and energetics of the great scallop, *Pecten maximus*, through a DEB model. Journal of Sea Research, *in Press*.

**II.** Le Goff C., **Lavaud R.**, Cugier P., Flye-Sainte-Marie J., Foucher E. and Jean F. (manuscript) Modelling the distribution of the Great scallop *Pecten maximus* in the English Channel: linking physical and biological processes to define scallop habitat. In preparation for submission to publication in Journal of Marine Systems.

**III. Lavaud R.**, Artigaud S., Donval A., Le Grand F., Soudant P., Strohmeier T., Strand Ø., Flye-Sainte-Marie J. and Jean F. (submitted) New insights of the seasonal feeding ecology of *Pecten maximus* using pigments, fatty acids and sterols analyses. Submitted to publication in Comparative Biochemistry and Physiology - Part B.

**IV. Lavaud R.**, Rannou E., Jean F., Kooijman S.A.L.M., Flye-Sainte-Marie J. (manuscript) What the shell can tell about the scallop? Insights from inverted DEB model. In preparation for submission to publication in Ecological modeling.

**V. Lavaud R.**, Flye-Sainte-Marie J., Rannou E., Kooijman S.A.L.M. and Jean F. (manuscript) History of the great scallop by the mean of DEB theory, a study of ecological patterns along latitudinal and bathymetric gradients. In preparation for submission to publication in Ecological modeling.

Other publications:

**Lavaud R.**, Thébault J., Lorrain A., van der Geest M. and Chauvaud, L. (2012) *Senilia senilis* (Linnaeus, 1758), a biogenic archive of environmental conditions on the Banc d'Arguin (Mauritania). Journal of Sea Research 76, 61–72.

Cuvelier D., De Busserolles F., **Lavaud R.**, Floc'h E., Fabri M.-C., Sarradin P.-M. and Sarrazin, J. (2012) Biological data extraction from imagery-how far can we go? A case study from the Mid-Atlantic Ridge. Marine Environmental Research 82, 15–27.

Artigaud S., **Lavaud R.**, Thébault J., Jean F., Strand Ø., Strohmeier T., Milan M. and Pichereau V. (submitted) Proteomic-based comparison of *Pecten maximus* populations along a latitudinal gradient. Submitted to publication in Journal of Proteome Research.

# Summary

The relationship between environmental conditions and life history has intrigued biologists for centuries. This thesis aims to better understand the variability of life history traits of the great scallop, *Pecten maximus*, facing environmental variability. This economically important species for French, English and Norwegian fisheries has a wide distribution range (from the Azores to Lofoten Islands). Growth and reproduction patterns are very variable within this area, potentially due to the environmental variability. Great scallops living at the head of Norway's fjords are the biggest but grow slowly whereas individuals from lower latitudes have faster growth rates and reach a smaller ultimate size and those from the continental shelf display both low growth rates and a reduced size. The variability in biological traits might be attributed to a plasticity or genetic adaptation of the physiological response of individuals to the environment, to mechanistic causes related to energy fluxes that fuel the metabolism again with regard to environmental forcings or to a combination of these two mechanisms.

The approach considered here to study the causes of this variability focuses on the dynamics of energy fluxes which allow us to deal with all the metabolic functions of the individual. The Dynamic Energy Budget (DEB) theory provides a mechanistic framework that allows a quantitative description of feeding, assimilation, growth, reproduction, maturation and maintenance over the full life cycle, in relation to thermal and trophic conditions. The first part of this thesis is dedicated to the development of a DEB model for *P. maximus*, with an emphasis on feeding implementation. The model makes use of the Synthesizing Units to provide the system with two substrates which quantifies food selection by the animal. We tested the model on the great scallop population from the Bay of Brest (France), with two proxies of trophic resource: phytoplankton cell counts and suspended organic particles.

The second chapter expands on the integration of this individual bioenergetic model to a 3D biogeochemical model in the English Channel. This modeling system allows the mapping of growth and reproduction capacities according to environmental conditions. The individual model simulations enabled us to improve a spatialized model of population dynamics divided in age-classes and including the planktonic larval stage. We carried out predictions over a period of 30 years, thus providing a potential tool for exploited stock forecasting in the English Channel.

In the third part of this thesis, we investigated the seasonality and diversity of the diet of this suspension-feeding bivalve in a coastal environment, with the aim to improve our knowledge on the seasonal dynamics of feeding in this species and better understand how we feed the bioenergetic model. We used the combination of three trophic markers (pigments, fatty acids and sterols), measured in the seawater and in two parts of the digestive tract. This study revealed five important pieces of information: (i) the unexpected importance of dinoflagellates in the diet of *P. maximus*; (ii) the recurrent switch between ingestion of diatoms and dinoflagellates along with the succession of algae blooms; (iii) the probable ingestion and assimilation of cyanobacteria and other bacteria, in particular during low microalgae densities; (iv) the selection capacity of the great scallop, which can preferentially select some algae classes and neglect some others; (v) trophic inputs from the water column proved to be more important than from the benthos except in early spring.

In the two last chapters, we developed and applied a modeling approach consisting of the inversion of the DEB model in order to reconstruct the functional response of food assimilation from growth data (obtained from the sclerochronological study of the shell) and temperature. Indeed, it is generally difficult to simply link the dynamics of trophic availability with the dynamics of assimilation and the method proposed here overcomes this issue. The process relies on a simplified equation of growth as described in DEB theory. This, therefore, facilitates the inversion of the model while also allowing the reconstruction of state variables and some energy fluxes (reserve dynamics, maintenance costs). As for many organisms producing a carbonated skeleton, *P. maximus*' shell grows by sequential increments. The analysis of the striae allows an accurate measurement of daily growth dynamics. We exploited these high frequency data in order to reconstruct the history of functional response along the growth trajectory. This method was applied in a study of the variability of growth patterns along latitudinal and bathymetric gradients. The highly fluctuating pattern of food availability seems to be a key factor in understanding the energy fluxes dynamics in northern and deep-sea populations. The combination of mild temperatures and low and varying food conditions on the continental shelf might lead to a local selection of smaller individuals which require limited maintenance costs. Moreover, this approach allowed us to explore the relationship between the functional response and various markers of trophic availability. It showed that chlorophyll-*a* measurements in the water column did well and truly explain the major part of the variability of assimilation, at least when phytoplanktonic production in the water column is important.

This work shows that the modeling of energy fluxes provides a tool that helps understanding the origin and fate of various energy sources as well as the distribution patterns of individuals. This tool also provides a mechanistic explanation to intra-specific variability patterns. Nevertheless, some physiological traits such as the filtration rate are very likely to show some plasticity. Indeed, the simulation carried out in northern and deep-water populations us-

ing the parameter set that was estimated in the Bay of Brest provided less relevant results. Further investigations should be conducted on data from early stages and in contrasting environments, in order to better integrate the variability within this species, which would help refine the DEB parameter set. The study of *P. maximus* physiological capacities, carried out on a spatial scale in this thesis, and the stepping to the population level could be useful tools for a better assessment and management of scallop fisheries (which fluctuating recruitment is still poorly understood). Finally, while the effects of global change are being investigated, the use of DEB theory in this work could provide a powerful framework to evaluate the impact of changing environments on the energetics of the great scallop.

# Résumé

Ces travaux de thèse ont été mené dans le but de mieux comprendre la variabilité des traits d'histoire de vie de la coquille Saint-Jacques, *Pecten maximus*, face à la variabilité de son environnement. Cette espèce d'importance économique en France, au Royaume-Uni et en Norvège a une aire de répartition étendue (des Açores aux Lofoten). La croissance et la reproduction sont des caractéristiques très variables au sein de cette aire, potentiellement du fait de la variabilité environnementale. Les coquilles Saint-Jacques vivant à la sortie des fjords de Norvège sont les plus grandes mais grandissent lentement alors que des individus présent à des latitudes moins élevées montrent des taux de croissance rapides et atteignent une taille maximale plus réduite. Les coquilles provenant du plateau continental au large de la France et de l'Irlande, quant à elles, ont à la fois une croissance lente et une petite taille. La variabilité de ces trait biologiques peut être attribuée à des adaptations ou une plasticité génétique dans la réponse physiologique des individus face à leur environnement, à des cause mécanistes liées aux flux d'énergie alimentant son métabolisme en lien également avec les forçages environnementaux ou à une combinaison de ces deux mécanismes.

L'approche adoptée pour traiter cette question de la variabilité des traits biologiques se focalise sur la dynamique des flux d'énergie qui permet d'appréhender l'ensemble des fonctions métaboliques de l'individu. Le théorie des bilans d'énergie dynamiques (Dynamic Energy Budget, DEB) fourni un cadre mécaniste pour décrire de façon quantitative l'ingestion, l'assimilation, la croissance, la reproduction, la maturation et la maintenance sur l'ensemble du cycle de vie, en fonction des conditions thermiques et trophiques. Dans la première partie de cette thèse, nous avons développé un modèle DEB pour *P. maximus* en mettant l'accent sur un élément déterminant dans la modélisation des flux d'énergie: l'apport d'énergie par la nourriture. Ainsi, le modèle intègre, via les *Synthesizing Units*, la possibilité pour l'animal de sélectionner sa nourriture parmi deux substrats. Nous avons testé ce modèle sur des coquilles Saint-Jacques de la rade de Brest (France) avec comme marqueurs des ressources trophiques des comptages de cellules phytoplanctoniques et des particules organiques en suspension.

Le second chapitre de ce manuscrit détaille l'intégration de ce modèle de bioénergétique individuelle à un modèle biogéochimique 3D à l'échelle de la Manche. Ce système de modélisation permet d'établir une cartographie des capacités de croissance et de reproduction en fonction des conditions du milieu.

Les simulations du modèle individuel ont permis d'affiner un modèle spatialisé de dynamique de population divisé en classes d'ages et tenant compte du stade de vie larvaire planctonique. Nous avons réalisé des prédictions sur une période de 30 ans, procurant un outil potentiel pour la prédiction de l'évolution des stocks exploités dans cette zone.

Dans la troisième partie de ce travail, sont examinés la saisonnalité et la diversité du régime alimentaire de ce bivalve suspensivore en environnement côtier, ceci dans le but d'améliorer nos connaissances de la dynamique saisonnière de l'alimentation de la coquille Saint-Jacques et aussi de mieux appréhender la façon dont nous alimentons le modèle bioénergétique. Grâce à la combinaison de marqueurs trophiques regroupant les pigments, les acides gras et les stérols, mesurés dans le milieu et dans différents compartiments du tractus digestif de l'animal, nous avons mis en évidence cinq résultats majeurs: (i) l'importance inattendue du groupe des dinoflagellées dans son alimentation; (ii) l'alternance entre l'ingestion de diatomées et de dinoflagellées au fil des efflorescences microalgales; (iii) la probable ingestion et assimilation de cyanobactéries et autres bactéries en particulier en période de faible abondance de microalgues; (iv) la capacité de sélection de certaines classes d'algues au détriment d'autres groupes et enfin (v) l'importance des apports de nourriture d'origine pélagique vers le compartiment benthique durant la majeure partie de l'année.

Dans les deux derniers chapitres nous avons développé puis appliqué une approche consistant à inverser le modèle DEB afin de reconstruire la réponse fonctionnelle de l'assimilation d'énergie provenant de la nourriture à partir de données de croissance (issues de l'étude sclérochronologique de la coquille) et de température. Il est en effet généralement difficile de relier simplement la dynamique de la disponibilité trophique avec la dynamique de l'assimilation et le procédé développé permet de contourner cette difficulté. Pour cela nous avons utilisé une équation simplifiée de la croissance telle qu'elle est décrite dans la théorie DEB. Ceci rend l'inversion du modèle plus aisée tout en permettant, de surcroît, la reconstruction des variables d'états et certains flux d'énergie du modèle (dynamique des réserves, coûts de maintenance). Comme pour de nombreux organismes à squelette carbonaté, la coquille de *P. maximus* a cette particularité de croître par incréments. L'analyse de ces stries permet une mesure précise des variations de la croissance journalière. Il est donc possible d'exploiter ces données afin de reconstruire à haute fréquence l'historique de la réponse fonctionnelle et ce tout au long de la trajectoire de croissance de l'animal. Cette méthode a été utilisée pour étudier la variabilité des caractéristiques de croissance le long d'un gradient latitudinal et bathymétrique. Le caractère variable de la disponibilité en nourriture semble être un facteur clé pour comprendre la dynamique des flux d'énergie chez les populations nordiques et profondes. La combinaison de températures douces à de faibles et variables apports trophiques sur le plateau continental pourraient conduire à une sélection locale d'individus plus petits, présentant des coûts de maintenance limités. De plus, cette approche a permis d'explorer

la relation entre la réponse fonctionnelle reconstruite et différents marqueurs de disponibilité trophique. Ainsi les mesures de chlorophyll-*a* dans la colonne d'eau semblent bel et bien expliquer une part importante de la variabilité de l'assimilation observée, du moins lorsque la production phytoplanctonnique est importante dans la colonne d'eau.

Ce travail montre que la modélisation des flux d'énergie fournit un outil permettant de mieux comprendre l'origine et l'importance de diverses source d'énergie ainsi que la répartition géographique des individus. Cet outil apporte aussi une explication mécaniste aux phénomènes de variabilité intra-spécifique. Toutefois, une plasticité de certains traits physiologiques tels que la filtration est très probable dans la mesure où les paramètres du modèle, calibrés pour la rade de Brest, ne permettent pas de simuler avec autant d'efficacité la dynamique énergétique des populations nordiques et profondes. Des efforts doivent donc être portés sur la prise en compte de données provenant des premiers stades de développement et d'environnements contrastés pour de mieux tenir compte de cette variabilité au sein de l'espèce afin d'affiner le jeu de paramètres DEB pour cette espèce. L'étude des potentiels physiologiques de *P. maximus*, réalisée au cours de cette thèse, ainsi que le passage à l'échelle de la population devraient s'avérer utiles à une meilleure estimation et gestion des stocks exploités de coquilles Saint-Jacques (dont les fluctuations de recrutement commencent à être mieux comprises). Enfin, alors que les effets du changement global sur ces populations côtières sont en train d'être évalués, l'utilisation de la théorie DEB au sein de ce travail fournit des outils intéressants afin d'évaluer l'impact des changements environnementaux sur les flux d'énergie de la coquille Saint-Jacques.